Department of Energy
Washington, DC 20585

March 20, 2017

WM-00058

U.S. Nuclear Regulatory Commission
Attn: Document Control Desk
Deputy Director
Mail Stop T8-F5
Washington, DC 20555-0001

Subject: U.S. Department of Energy Office of Legacy Management Position paper regarding Flow Processes in the Floodplain Alluvial Aquifer at the Shiprock, New Mexico, Disposal Site

To Whom It May Concern:

Enclosed, for the U.S. Nuclear Regulatory Commission (NRC) review, is a Position Paper prepared by the U.S. Department of Energy, Office of Legacy Management (DOE-LM) entitled *Flow Processes in the Floodplain Alluvial Aquifer at the Shiprock, New Mexico, Disposal Site.*

The findings presented are based primarily on analyses of data from wells in the floodplain groundwater system and investigations by DOE-LM's Environmental Sciences Laboratory (ESL). A large portion of this study examines how groundwater flow in the alluvial aquifer is influenced by the San Juan River, which borders the entire length of the aquifer on its east and north sides.

Please call me at (970) 248-6018 if you have any questions. Please address any correspondence to:

U.S. Department of Energy
Office of Legacy Management
2597 Legacy Way
Grand Junction, CO 81503

Sincerely,

Mark Kautsky

Mark Kautsky
Site Manager

Enclosure

NMSSZO

cc w/enclosure:
D. Orlando, NRC
S. Austin, NNEPA
M. Roanhorse, NN AML/UMTRA
J. Tallbull, NN AML/UMTRA

cc w/o enclosure:
J. Carman, Navarro (e)
B. Cook, Navarro (e)
S. Marutzky, Navarro (e)
D. Miller, Navarro (e)
File: SHP 0410.10 (records)

Sites\Shiprock\3-15-17 SHP Floodplain Alluvial Aquifer Rpt Final (NRC).docx

LMS/SHP/S07318

Flow Processes in the Floodplain Alluvial Aquifer at the Shiprock, New Mexico, Disposal Site

November 2016

U.S. DEPARTMENT OF ENERGY | Legacy Management

This page intentionally left blank

Contents

Abbreviations vi
Executive Summary vii
1.0 Introduction 1
2.0 Study Scope 7
2.1 Project Focus Topics 8
2.2 Project Objectives 9
3.0 Site Description 11
3.1 Relevant Site History 11
3.2 Sources of Groundwater Contamination in the Floodplain 16
3.3 Historical Water Monitoring 18
3.4 Floodplain Remediation System 23
3.4.1 Extraction Wells Remediation System 23
3.4.2 Trench 1 Remediation System 26
3.4.3 Trench 2 Remediation System 28
3.4.4 Seep Collection Sump 30
3.5 SOARS Monitoring 31
3.6 River Gaging Station 31
4.0 Existing Conceptual Model 37
4.1 General Hydrogeology 37
4.2 River–Aquifer Exchange 39
4.3 Baseline Flow Conditions 40
4.4 Water Budget 45
4.5 Historical Contaminant Plumes 47
4.5.1 Sulfate and Uranium 48
4.5.2 Groundwater Salinity and Density 51
4.5.3 Nitrate 51
4.6 Remediation Flow Patterns 52
5.0 Field Activities in 2011 59
5.1 Monitoring Wells 59
5.2 New SOARS Wells 59
5.3 River Elevation Surveys 63
5.3.1 Low-Flow Survey 63
5.3.1.1 River Gage Elevation 64
5.3.1.2 Pool and Riffle Slopes 69
5.3.2 High-Flow Survey 70
6.0 Updated Assessment of the Alluvial Aquifer 71
6.1 Bedrock Elevations 71
6.2 Well Hydrographs 71
6.2.1 Group 1—Wells Close to the San Juan River 72
6.2.2 Group 2—Wells West and South of the River Gaging Station 77
6.2.3 Group 3—Wells in the Trench 1 Area 80
6.3 Seasonal Changes in Groundwater Elevation 82
6.3.1 Assessment of Semiannual Monitoring Data 82
6.3.2 Hydrographs for Wells West and South of the USGS Gaging Station 83
6.3.3 Significance of Evapotranspiration Losses 89

6.4 Contaminant Plumes in 2011 89
6.4.1 Sulfate and Uranium 90
6.4.2 Nitrate 95
6.4.3 Reductions in Plume Mass 95
6.5 Contaminant Sources in Terrace Groundwater 96
6.5.1 Discharge to the Alluvial Aquifer 99
6.5.2 Quantifying Mancos Shale Flows 100
6.6 Evidence of Bedrock Inflow 101
6.6.1 Groundwater Levels at Wells Near the Escarpment 101
6.6.2 Multivariate Statistics Study 102
6.6.3 Rebound of Specific Conductance near Trench 1 103
6.6.4 Concentration Histories in Wells at the Base of the Escarpment 107
6.7 Further Evaluation of Contaminant Discharge to the Floodplain 107
7.0 Groundwater Flow Modeling 111
7.1 Model Construction 111
7.2 Boundary Conditions 112
7.3 Model Calibration 115
7.3.1 Nonpumping Conditions in March 2011 115
7.3.1.1 Flow Patterns 117
7.3.1.2 Calibration Measures 117
7.3.1.3 Water Budget 118
7.3.1.4 Groundwater Velocities 124
7.3.2 Transient Flow Model 124
7.3.2.1 Changing River Profiles 125
7.3.2.2 Aquifer Specific Yield 127
7.3.2.3 Simulated Hydrographs at Group 2 Wells (West and South of the USGS Gaging Station) 127
7.3.2.4 Accounting for Evapotranspiration Effects 131
7.3.2.5 Simulated Hydrographs at Wells in the Group 3 (Trench 1) Area 132
7.3.2.6 Transient Flow Patterns in the High-Runoff Period 133
7.4 Pumping Conditions in March 2010 139
7.4.1 Flow Patterns 139
7.4.2 Hydraulic Head Residuals 140
7.4.3 Water Budget 149
7.5 Pumping Conditions in September 2010 149
8.0 Updated Conceptual Model 155
8.1 Naturally Dynamic Groundwater System 155
8.1.1 Winter and Spring (November–April) 156
8.1.2 Early Summer (May–June) 156
8.1.3 Midsummer to Fall (July–October) 157
8.2 Contaminant Movement and Distribution 158
8.2.1 Contaminant Migration Under Baseline (Nonpumping) Conditions 158
8.2.1.1 Influence of Transient Groundwater Flow 158
8.2.1.2 Additional Contributions to Plume Spreading and Variable Flow Patterns 161
8.2.1.3 Well 618 Area 162

8.2.2 Effects of Remediation Pumping 162
8.2.2.1 Trench 1 and Trench 2 163
8.2.2.2 Effects of Simultaneous Pumping in the Trench 1 and 1089/1104 Areas 164
8.2.2.3 1089/1104 Area 165
8.3 Aquifer Parameters 165
8.4 Water Budgets 166
8.4.1 Flow Rates Under Baseline (Nonpumping) Conditions 166
8.4.2 Remediation Pumping Impacts 167
8.5 Inflow of Contaminated Terrace Groundwater 167
9.0 Predictive Simulations 169
9.1 Elimination of Bob Lee Wash Recharge 169
9.1.1 Baseline (Nonpumping) Conditions 169
9.1.2 Remediation (Pumping) Conditions 170
9.2 Additional Pumping Locations 173
10.0 Summary and Conclusions 177
11.0 References 181

Figures

Figure 1. Shiprock Site Regional Location Map 2
Figure 2. Shiprock, New Mexico, Legacy Management Site 3
Figure 3. Historical Features at the Shiprock Site 12
Figure 4. July 1965 View Southeast of the Shiprock Mill Site 13
Figure 5. Monitoring Locations Used in This Study 19
Figure 6. Wells in the 1089/1104 Remediation Area 24
Figure 7. Trench 1 Remediation Area 27
Figure 8. Cross-Section View of the Trench 1 Remediation System 28
Figure 9. Trench 2 Remediation Area 29
Figure 10. SOARS Monitoring Locations 33
Figure 11. Aerial View of Hyporheic Flow Processes in Aquifers Adjacent to Rivers 40
Figure 12. Map View of the Groundwater Flow Conceptual Model for Baseline (nonpumping) Conditions 41
Figure 13. Cross-Section View of the Groundwater Conceptual Model for Baseline (nonpumping) Conditions 43
Figure 14. Sulfate Plume, 1999–2001 49
Figure 15. Uranium Plume, 1999–2001 50
Figure 16. Nitrate as Nitrogen Plume, 1999–2001 53
Figure 17. Map View of the Groundwater Flow Conceptual Model for Remediation (pumping) Conditions 54
Figure 18. Cross-Section View of the Groundwater Conceptual Model As Affected by Trench 1 Pumping 55
Figure 19. Focused Monitoring Locations in 2011 61
Figure 20. Pool and Riffle Sequences on the San Juan River in March 2011 65
Figure 21. Surveyed Water Surface Profiles on the San Juan River 67
Figure 22. Photographs of Riffle 4-Down in February 2011 Taken on the West Riverbank near Well 1142: View (a) Upriver, (b) Across-River, and (c) Downriver 68

Figure 23. Photograph of Pool 6 in February 2011 Taken on the West Riverbank About 300 Feet Downriver from Well 1137: View Downriver 69
Figure 24. Contoured Bedrock Surface (top of Mancos Shale) Elevations 73
Figure 25. Monitoring Wells Used To Generate Hydrographs (categorized by group number) .. 75
Figure 26. Hydrographs at Group 1, Near-River Wells, January 2011 through August 2011 76
Figure 27. Hydrographs at Group 2 Wells, West and South of the USGS Gaging Station, January 2011 through August 2011 78
Figure 28. Hydrographs at Group 3, Trench 1 Area Wells, January 2011 through August 2011 81
Figure 29. Mean River (USGS gage) and Groundwater Elevations During Semiannual Monitoring Events 83
Figure 30. Hydrographs for the USGS Gaging Station and Nearby Wells 779, 853, and 857 in 2011 85
Figure 31. Hydrographs for the USGS Gaging Station and Nearby Wells 779, 853, and 857 in 2012 86
Figure 32. Hydrographs for the USGS Gaging Station and Nearby Wells 779, 853, and 857 in 2013 87
Figure 33. Hydrographs for the USGS Gaging Station and Nearby Wells 779, 853, and 857 in 2014 88
Figure 34. Sulfate Plume in 2011 91
Figure 35. Uranium Plume in 2011 92
Figure 36. Temporal Plot of Uranium Concentrations at Well 618 94
Figure 37. Nitrate as Nitrogen Plume in 2011 97
Figure 38. Specific Conductances at Well 1111 During Four Nonpumping Periods 106
Figure 39. History of Sulfate and Uranium Concentrations and Specific Conductance at Base-of-Escarpment Wells 1111, 1112, 614, 610, and 1113 109
Figure 40. History of Sulfate and Uranium Concentrations and Specific Conductance at Base-of-Escarpment Wells 608, 1114, 1115, 1128, and 735 110
Figure 41. Boundary Conditions (in parentheses) Applied in the Numerical Modeling 113
Figure 42. Computed Groundwater Elevations (ft amsl) in the March 2011 Model of Steady-State Flow 119
Figure 43. Computed Flowpaths in the March 2011 Model of Steady-State Flow 120
Figure 44. Computed Hydraulic Head Residuals in the March 2011 Model of Steady-State Flow 121
Figure 45. Observed and Computed Groundwater Elevations in the March 2011 Model of Steady-State Flow 123
Figure 46. Three-Day Average River Elevations at the USGS Gaging Station 126
Figure 47. Observed and Computed Hydrographs at Well 779 128
Figure 48. Observed and Computed Hydrographs at Well 857 129
Figure 49. Observed and Computed Hydrographs at Well 853 130
Figure 50. Observed and Computed Hydrographs at Well 793 134
Figure 51. Observed and Computed Hydrographs at Well 1009 135
Figure 52. Observed and Computed Hydrographs at Well 1105 136
Figure 53. Observed and Computed Hydrographs at Well 1140 137
Figure 54. Observed and Computed Hydrographs at Well 1141 138
Figure 55. Computed Groundwater Elevations (ft amsl) and Flow Vectors, May 28, 2011 143
Figure 56. Computed Groundwater Elevations (ft amsl) and Flow Vectors, June 13, 2011 144
Figure 57. Computed Groundwater Elevations (ft amsl) and Flow Vectors, June 28, 2011 145

Figure 58. Computed Groundwater Elevations (ft amsl) and Flowpaths in the March 2010 Model of Steady-State Flow 146
Figure 59. Computed Hydraulic Head Residuals in the March 2010 Model of Steady-State Flow 147
Figure 60. Estimated Groundwater Elevations (ft amsl) and Flow Vectors During the Monitoring Event in September 2010 153
Figure 61. Flow Mechanisms for Distributing Contamination Northward and Northwestward from the Trench 1 Area 160
Figure 62. Computed Groundwater Elevations (ft amsl) and Flowpaths when Bob Lee Wash Recharge Is Eliminated 171
Figure 63. Computed Groundwater Elevations (ft amsl) Assuming No Bob Lee Wash Recharge and Full Remediation Pumping 172
Figure 64. Computed Groundwater Elevations (ft amsl) and Flowpaths in Response to Pumping from a New Trench 174
Figure 65. Computed Groundwater Elevations (ft amsl) and Flowpaths in Response to Pumping from Two New Wells 175

Tables

Table 1. Construction Information for Shallow Wells on the Shiprock Floodplain 21
Table 2. SOARS Monitoring Locations 32
Table 3. Estimated Water Budget for the Alluvial Aquifer in the SOWP Steady-State Flow Model 46
Table 4. Focused Monitoring Locations and Sampling Events in 2011 60
Table 5. River Surface Information for Low-Flow Conditions in March 2011 69
Table 6. Estimated Total Plume Masses in 1999–2001 and 2011 95
Table 7. Computed Water Budget in the March 2011 Model of Steady-State Flow 118
Table 8. Computed Water Budget in the March 2010 Model of Steady-State Flow 149
Table 9. Computed Water Budget in the Model That Omits Bob Lee Wash Recharge 170

Abbreviations

amsl	above mean sea level
bgs	below ground surface
cfs	cubic feet per second
DOE	U.S. Department of Energy
ESL	Environmental Sciences Laboratory
ET	evapotranspiration
ft	feet
ft^3/day	cubic feet per day
GCAP	Groundwater Compliance Action Plan
gpm	gallons per minute
in/yr	inches per year
LM	Office of Legacy Management
MCL	maximum concentration limit
mi	mile
µS/cm	microsiemens per centimeter
mg/L	milligrams per liter
mS/cm	millisiemens per centimeter
NECA	Navajo Engineering and Construction Authority
SOWP	Site Observational Work Plan
TDS	total dissolved solids
UMTRA	Uranium Mill Tailings Remedial Action (Project)
USGS	U.S. Geological Survey

Executive Summary

This report provides an updated assessment of groundwater flow processes in the floodplain alluvial aquifer (alluvial aquifer) at the Shiprock, New Mexico, Site (the site), a former uranium milling facility that is now managed by the U.S. Department of Energy (DOE) Office of Legacy Management (LM). The aquifer contains groundwater contamination that was caused by the former mill during the 1950s and 1960s. The findings presented here are based primarily on analyses of data from wells in the floodplain groundwater system and investigations by DOE and LM's Environmental Sciences Laboratory (ESL). A large portion of this study examines how groundwater flow in the alluvial aquifer is influenced by the San Juan River (river), which borders the entire length of the aquifer (7300 feet [ft]) on its east and north sides.

The updated assessment shows that the floodplain groundwater system at the Shiprock site is dynamic, with groundwater flow patterns in the alluvial aquifer changing noticeably between seasons and from year to year. The transient groundwater conditions are caused not only by variable flows in the river but also by losses of subsurface water to evapotranspiration (ET) during summer and fall months. The dynamic behavior of floodplain groundwater impacts the spatial distribution of dissolved contamination in the aquifer.

The mill, tailings piles, and raffinate ponds at the site were located on a terrace south and west of the floodplain. The floodplain is separated from the terrace by a 50 ft high escarpment consisting of Mancos Shale, the bedrock formation that underlies all alluvium at the site, including the floodplain alluvial aquifer.

A floodplain remediation system, consisting of two pumping wells near the river (wells 1089 and 1104) and two horizontal wells (Trench 1 and Trench 2) at the base of the escarpment, has induced changes in floodplain groundwater flow patterns since the mid-2000s. These changes have influenced the concentrations of mill-related contaminants such as sulfate, uranium, and nitrate. Effective groundwater remediation in the floodplain is dependent on a thorough understanding of several complex features of the groundwater system, including the interaction of river elevations and groundwater levels, the influences of evapotranspiration in warm months, inflow of contaminated groundwater from the terrace, and changing flowpaths in response to remediation pumping.

During winter and early spring months (November–April), ambient baseline groundwater flow in the south half of the floodplain is largely parallel to the escarpment separating the terrace from the floodplain. The sources of this groundwater include seepage losses from the river and potential groundwater discharges from the terrace across the escarpment. The quantity of discharge across the escarpment is uncertain and could be gradually decreasing. Though much of the surface water lost to the south half of the alluvial aquifer remains in the subsurface, inflowing river water from some sections of the river returns to the river in other sections located tens to hundreds of feet downstream. Areas of the aquifer with this type of exchange flow with the river are referred to as hyporheic zones in this report. Mixing of fresh water from the river with ambient groundwater in these zones can lead to biogeochemical reactions that affect the concentrations of site contaminants.

In winter and early spring (November–April), the north half of the alluvial aquifer is recharged by surface-water flows in Bob Lee Wash, a drainage that empties onto the floodplain from the

terrace. The surface water, which originates as artesian flow from a deep well on the upstream end of a tributary to the wash, causes groundwater to mound at the mouth of the wash and spread in a radial pattern from this part of the aquifer. Some of the recharged water diverts groundwater in the vicinity of the Trench 1 footprint toward the northeast, to a section of the river containing a flow gaging station (gaging station) operated by the U.S. Geological Survey.

In late spring and early summer (May–June) of most years, snowmelt runoff in the San Juan Mountains causes flow in the San Juan River to increase substantially, with peak river discharge typically recorded in late May or early June. Higher surface-water levels accompanying the high river runoff cause increases in groundwater elevation in the aquifer. During the period leading to peak flow, the entire length of the river adjacent to the Shiprock site floodplain appears to lose water to the aquifer in the form of bank storage, a temporary phenomenon as most of the influent fresh water eventually returns to the river after passage of peak runoff. The influent river water changes flow patterns in the aquifer from those observed in winter and early spring. Within portions of the aquifer containing high levels of contaminants, the altered subsurface flows divert groundwater in directions not seen in previous months and, in the process, help dilute the contamination. Evapotranspiration also occurs during late spring and early summer months, decreasing groundwater levels in areas with phreatophyte vegetation. The induced water-level declines increase the hydraulic gradient from the river to the aquifer on days prior to peak snowmelt runoff, thereby enhancing ongoing surface-water losses to the subsurface and causing new, temporary surface-water losses along river sections where the river normally gains in flow from groundwater discharge.

From mid-summer through fall (July–October), river discharges and elevations return to those commonly seen in winter and early spring months. As groundwater levels decrease in response to the lower river elevations, ET processes in the aquifer further decrease groundwater elevations throughout the alluvial aquifer. A portion of the ET loss is attributed to bare-ground evaporation near the mouth of Bob Lee Wash, where recharge of wash outflows creates a shallow water table. ET causes groundwater flow patterns in mid-summer, late summer, and fall to vary from those seen in winter and early spring months, particularly in the south half of the floodplain.

A variety of activities and processes at the former mill contributed contamination to terrace groundwater, which in turn flowed eastward through Mancos Shale and discharged to floodplain groundwater across the escarpment. Previous models of groundwater flow and transport at the site simulate the migration of inorganic constituents through terrace shale to the alluvial aquifer and, subsequently, through the floodplain alluvium. It is unclear whether contaminated groundwater beneath the terrace continues to discharge to the alluvial aquifer at a significant rate.

Past investigations have attributed high constituent concentrations in groundwater in some parts of the terrace to the leaching of Mancos Shale by freshwater recharge. A relatively recent study by the ESL presented evidence that Mancos Shale may be a natural source of inorganic contaminants, some of which are the same as the mill-related constituents. The potential for discharge of this "naturally contaminated" groundwater to the alluvial aquifer across the escarpment is unknown.

Despite the potential obstacles to aquifer remediation posed by the dynamic nature of the floodplain groundwater system, simulations conducted with a groundwater flow model

developed for this study indicate that combined pumping from wells 1089 and 1104 and Trenches 1 and 2 is quite effective in capturing contaminated groundwater in the alluvial aquifer. The extraction of contaminated groundwater helps prevent its discharge to the river.

Flow modeling of conditions reflective of winter and early spring months shows how simultaneous pumping from the Trench 1 area and wells 1089 and 1104 (the 1089/1104 area) creates a stagnation zone in the aquifer about 400 ft northeast of Trench 1. The stagnation zone is an important feature of the flow system because it severely reduces the mobility of local contamination, such that contaminants are less susceptible to flushing by fresh surface water that flows into the aquifer northeast of Trench 1 in response to remediation pumping. A phenomenon associated with the stagnation zone is the creation of a 300–600 ft wide swath of contaminated aquifer farther to the northeast that escapes capture by the remediation system during winter and early spring.

Contaminant concentration maps indicate that total contaminant mass in floodplain groundwater has been greatly reduced by remediation pumping that commenced in the mid-2000s. In some areas of the floodplain, contaminant levels as of 2011 had been reduced to as little as a third of the concentrations measured during 1999–2001. Of the three pumping components of the floodplain remediation system, Trench 1 appears to be most beneficial with regard to capturing and containing the transport of contaminant mass in the alluvial aquifer.

Predictive simulations were conducted with the groundwater flow model developed for this study to assess the effects of possible changes in the hydrology of the floodplain groundwater system and potential enhancements of the existing remediation system. One of the simulations showed that elimination of recharge at the mouth of Bob Lee Wash, the product of discharges from the flowing artesian well, would create a flow system in which contaminants between Trench 1 and the 1089/1104 area escape capture by existing pumping wells and trenches. On the basis of this simulation, it is recommended that flows from the artesian well be maintained.

Predictive simulations with the groundwater flow model also examined the flowpaths created by additional pumping locations in the alluvial aquifer. Modeling results suggest that groundwater remediation in the alluvial aquifer would benefit from either two new remediation wells or a new horizontal well east of Trench 1 to collect contaminated groundwater that escapes capture during certain times of the year.

This page intentionally left blank

1.0 Introduction

The Shiprock, New Mexico, Site (the site) is a former uranium- and vanadium-ore-processing mill that operated from 1954 to 1968 in the Navajo Nation near Shiprock, New Mexico. By September 1986, all tailings and structures on the former mill property were encapsulated in a disposal cell built on top of the two existing tailings piles on the Shiprock site. Local groundwater was contaminated by multiple inorganic constituents as a result of the milling operations. The U.S. Department of Energy (DOE) took over management of the site in 1978 as part of the Uranium Mill Tailings Remedial Action (UMTRA) Project. The DOE Office of Legacy Management (LM) currently manages ongoing activities at the former mill facility, including groundwater remediation.

The Shiprock site is located on the west bank of the San Juan River in the northwest corner of New Mexico (Figure 1 and Figure 2). The site is divided physiographically into two regions, terrace and floodplain, that are separated by an escarpment. Land surface elevations on the terrace are generally about 50 feet (ft) higher than comparable land surface elevations on the floodplain. Groundwater beneath the terrace flows within both weathered and competent portions of Mancos Shale bedrock and a few feet of alluvium overlying the shale. Groundwater in the floodplain area flows primarily within alluvium (floodplain alluvial aquifer or alluvial aquifer) that was deposited by the river on top of Mancos Shale. The escarpment separating the two regions is an erosion surface of the Mancos Shale that is also referred to in this report as the bedrock escarpment (Figure 2) or the Mancos Shale escarpment. The disposal cell containing tailings and other mill-site wastes sits on the terrace south and west of the escarpment.

A portion of the contamination in the alluvial aquifer was caused by surface discharge of mill effluent directly to the floodplain. Another portion of the contamination appears to have originated as infiltrated effluent on the terrace that subsequently recharged underlying saturated alluvium and Mancos Shale bedrock and eventually migrated with eastward-flowing groundwater across the escarpment to the alluvial aquifer (DOE 1998). Hydraulic and water chemistry data collected during recent years at several wells on both the terrace and the floodplain suggest that contaminated groundwater continues to flow from beneath the former mill property on the terrace to the alluvial aquifer, though the current rate of discharge to the alluvial aquifer is uncertain. The contaminants affecting groundwater in the alluvial aquifer consist solely of inorganic chemicals and include sulfate, nitrate, uranium, selenium, and ammonia.

Surface remediation at the Shiprock site, consisting of the stabilization of mill-generated tailings and the removal of contaminated shallow soils and mill structures, was completed in the mid-1980s. Remediation of groundwater contaminated by mill operations began in spring 2003. On the floodplain, the groundwater remedy made use of pumping from two vertical wells within 250 ft of the San Juan River and transmission of the pumped water through a pipeline to a lined evaporation pond south of the disposal cell (Figure 2). The dual purpose of the two pumping wells, located in a portion of the alluvial aquifer that contained some of the largest dissolved concentrations of sulfate and uranium, was to remove local contamination and prevent local contamination from discharging to the river.

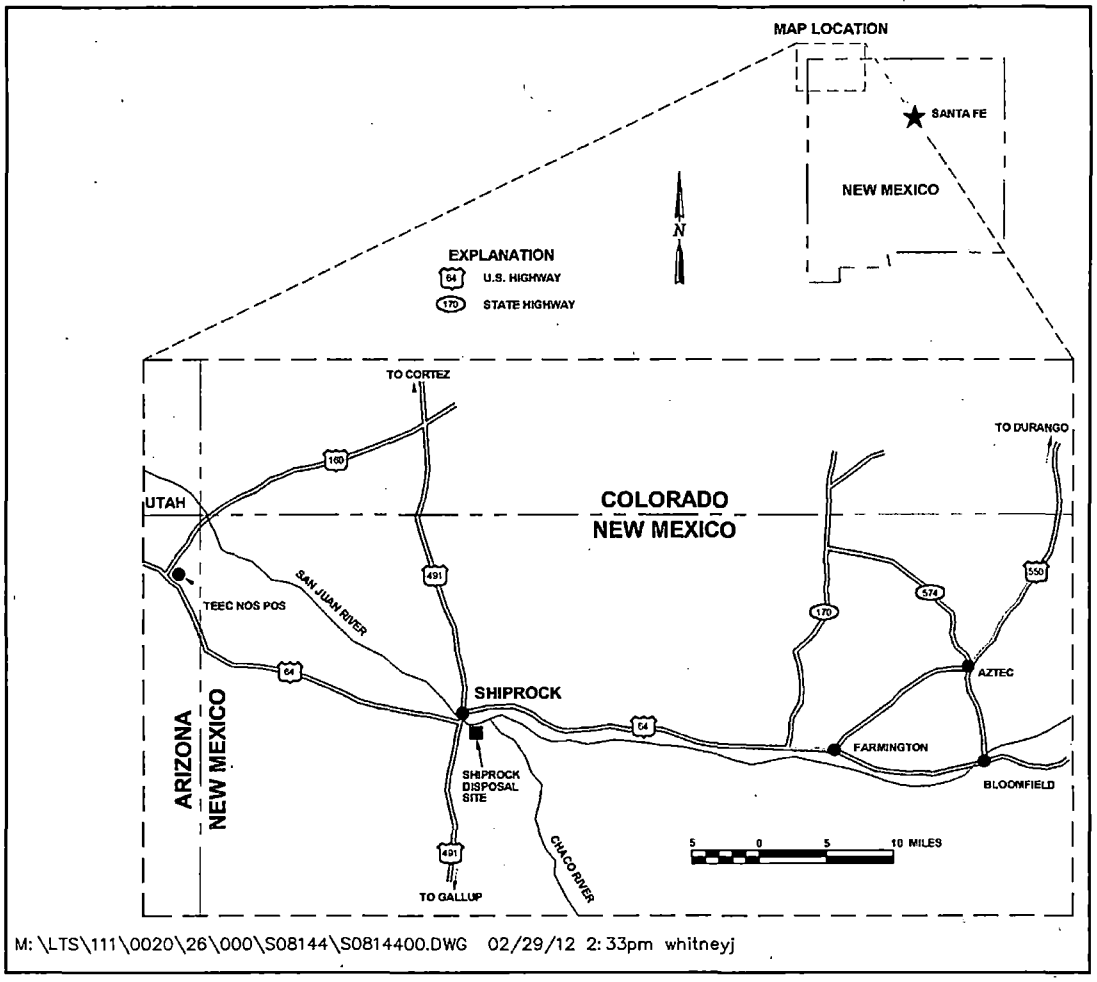

Figure 1. Shiprock Site Regional Location Map

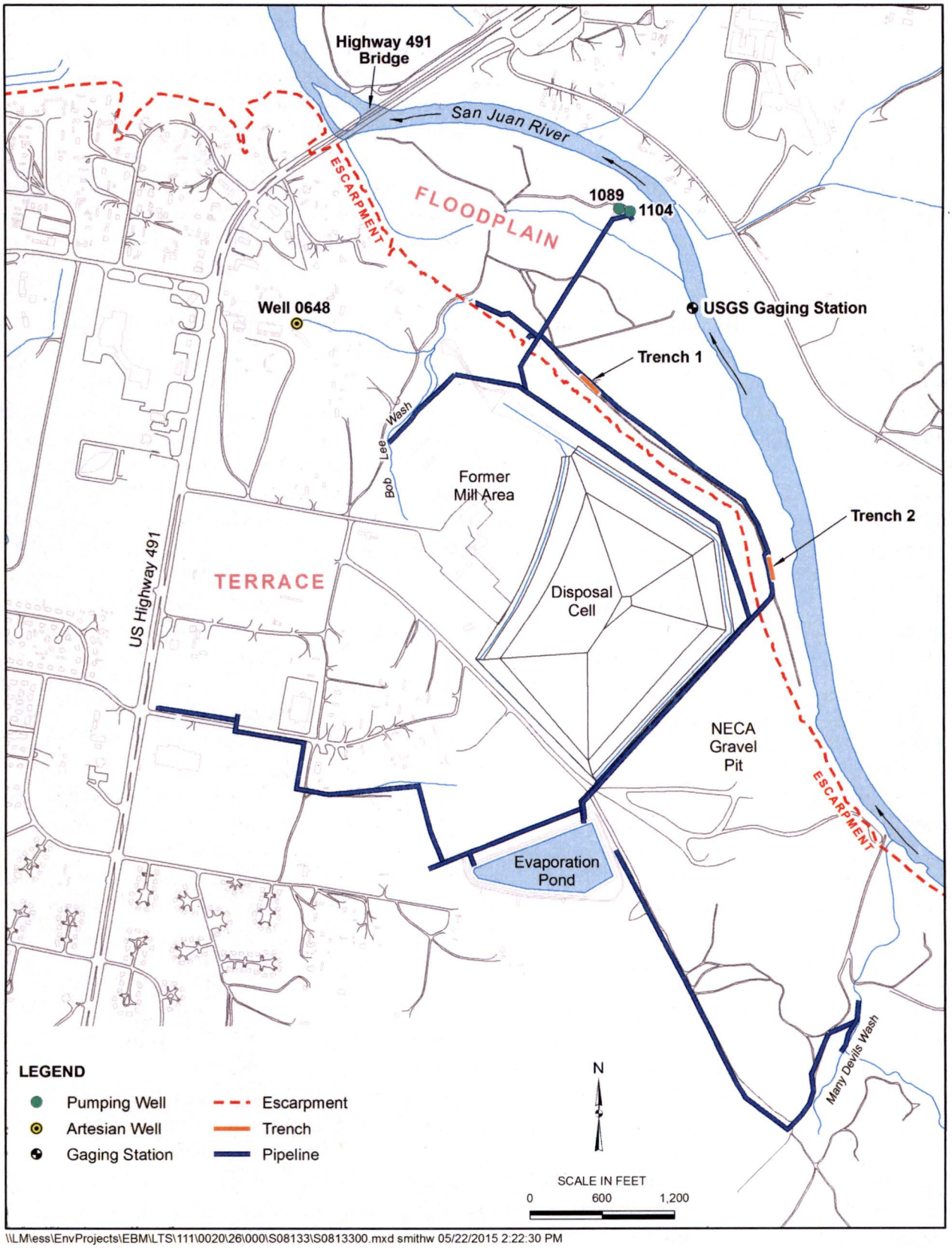

Figure 2. Shiprock, New Mexico, Legacy Management Site

Pumping rates achieved at the two wells near the river in the months immediately following the 2003 initiation of groundwater extraction were noticeably less (<3 gallons per minute [gpm]) than had been expected on the basis of an aquifer test (10–20 gpm) at an alluvial aquifer well in the late 1990s (DOE 2000). Because of the lower-than-anticipated pumping rates, one of the pumping locations was replaced within about 3 months of the start of remediation by a new pumping well (1089 in Figure 2). Groundwater extraction from the other original remediation well was also subsequently replaced in April 2005 by pumping from another new well (1104 in Figure 2). The area near the San Juan River that encompasses these two extraction wells and several nearby monitoring wells (Figure 2) is referred to in this report as the 1089/1104 remediation area, or simply the 1089/1104 area.

In spring 2006, two additional groundwater pumping systems consisting of horizontal wells in excavated trenches (Trench 1 and Trench 2) were installed in the alluvial aquifer near the base of the escarpment (Figure 2). These extraction systems were selected with the intent of both removing contaminated groundwater in the alluvial aquifer and intercepting contaminated groundwater discharging into the alluvial aquifer across the bedrock escarpment. Pumping from the trenches lessened the migration of contaminants toward the river and decreased contaminant mass between the escarpment and the river. Data collected at several monitoring wells installed in the vicinities of the trenches have been examined to evaluate the capacity of each trench system to reduce contaminant mass. The horizontal well at Trench 1 and surrounding wells are collectively referred to in this report as the Trench 1 remediation area, or the Trench 1 area. Similarly, the system consisting of the horizontal well at Trench 2 and nearby monitoring wells is called the Trench 2 remediation area, or the Trench 2 area.

Since the late 1990s, large quantities of hydraulic and water-quality data have been collected at numerous wells installed in the alluvial aquifer. These data reflect a variety of hydrologic processes occurring in the floodplain groundwater system, ranging from those representative of ambient baseline conditions (before initiation of remediation pumping) to processes in recent years reflective of full-scale, combined pumping from the 1089/1104, Trench 1, and Trench 2 areas. A common observation made with all of the collected data is that the groundwater system is dynamic, with seasonal changes in river flow, evapotranspiration (ET) associated with floodplain vegetation and a shallow saturated zone, and variable water-pumping operations causing noticeable changes in groundwater elevation and subsurface flow patterns.

With continued data collection, interest has been shown in assessing the performance of the groundwater extraction system. Although annual reports for the site (e.g., DOE 2008, 2010, 2014b) provide estimates of removed contaminant mass and depict contaminant concentration decreases in some areas of the floodplain, remediation performance is difficult to fully characterize and quantify given the dynamic nature of the groundwater system. To help meet this interest and the challenges associated with aquifer characterization, a preliminary evaluation of the Trench 1 remediation system was finalized in spring 2011 (ESL 2011b). In addition to providing a clearer understanding of various groundwater flow phenomena that impact contaminant migration, the Trench 1 study indicated that the aquifer remediation program at Shiprock would further benefit from an evaluation of groundwater flow, groundwater chemistry, and contaminant transport in all areas of the floodplain. This report presents the results of a comprehensive evaluation of the groundwater flow system. Though some aspects of local groundwater chemistry and observed contaminant distributions in the alluvial aquifer are used herein to help explain and describe flow processes in the floodplain subsurface, detailed

assessments of geochemical and contaminant transport processes in the alluvial aquifer are saved for a subsequent study.

This study uses more than 20 years of data to illustrate the dynamic nature of the groundwater system and how local contaminant transport is influenced by a variety of flow processes. The data analysis focuses on a few key topical areas. One of these is groundwater–surface water interaction, particularly the influence that the San Juan River has on seasonal groundwater flow patterns. Considerable attention is also given to the discharge of contaminated terrace groundwater to the alluvial aquifer. Prepared maps show the areas impacted by each component of the remediation system and quantitative analyses show how the system might be improved to more effectively remove contaminant mass.

A numerical model prepared for this study enhances understanding of the numerous flow processes occurring in the aquifer as well as the impacts of river–aquifer interaction on remediation activities. The numerical simulator assists in developing an updated conceptual model of the site's hydrogeology, which was last visited in 2005 (DOE 2005b). The floodplain alluvial aquifer at the Shiprock site changes greatly between the seasons in each year, as well as from year to year.

This page intentionally left blank

2.0 Study Scope

The purpose of this study is to provide an updated assessment of groundwater flow processes in the floodplain alluvial aquifer at the Shiprock site. The study is based mostly on analysis of large quantities of data that have been collected since the time of site characterization work conducted in the late 1990s. The results of that characterization effort were published in the Site Observational Work Plan (SOWP) (DOE 2000) for the former mill facility. A subsequent Groundwater Compliance Action Plan (GCAP) (DOE 2002) proposed a groundwater collection system for cleanup of groundwater across the site. In the first few years following initiation of the remediation strategy in 2003, monitoring of subsurface water on both the terrace and the floodplain revealed that groundwater behavior in response to pumping differed from projections in the SOWP (DOE 2000) and the GCAP (DOE 2002). As a consequence, DOE developed a refined conceptual model (DOE 2005b) of hydrogeologic processes at the site and recommended augmentation of the existing groundwater extraction network, including installation of the horizontal wells at Trench 1 and Trench 2. Information collected in the vicinity of the two trenches, the 1089/1104 area, and numerous monitoring wells is used in this study to develop an updated version of the floodplain conceptual model.

This study was partially motivated by findings from an evaluation of the Trench 2 system in 2006 and 2007 (DOE 2009b). In addition to revealing important information about the hydrogeology of the south end of the floodplain, the evaluation showed that the Trench 2 horizontal well was very efficient and capable of producing groundwater at a rate (20–25 gpm) that exceeded the combined pumping rate from existing floodplain pumping wells. The trench also had the capacity to intercept dissolved bedrock contamination discharging across the Mancos Shale escarpment. A flow model of the alluvial aquifer in the Trench 2 area, based on local geological, hydraulic, and water-chemistry data, assisted in developing estimates of the aquifer's local hydraulic conductivity and subsurface flow patterns under both baseline (nonpumping) and remediation (pumping) conditions. Data analysis and modeling also yielded estimates of flow rates from the Mancos Shale to the floodplain alluvium across the bedrock escarpment and the quantities of groundwater migrating through the aquifer. The study confirmed previous observations made in the SOWP (DOE 2000) regarding the significant impact that the San Juan River has on groundwater levels and highlighted the fact that the largest source of subsurface water in the Trench 2 area is seepage losses from the river.

The Trench 2 evaluation showed that groundwater originating from river seepage returns to the river over short distances within hyporheic zones. Results from the groundwater flow model for the Trench 2 study area suggested that pumping from the trench induces much greater seepage from the river into the aquifer than that which takes place under baseline conditions (about a 400 percent increase), which in turn produces a zone of fresh water, with virtually no contamination, between the trench and the river. Though contaminant concentrations on the escarpment side of the trench generally remain larger than those on the river side, continuous pumping over several months draws an increasingly larger proportion of fresh water into the horizontal well, eventually producing trench discharge concentrations that are reduced by as much as 80 percent from comparable discharge concentrations observed at the start of pumping (DOE 2009b).

The investigation of the alluvial aquifer discussed in this report is partly designed to accomplish many of the analyses that were performed for the Trench 2 area, but for the floodplain as a

whole. This updated assessment also focuses on several key topics that were not included in the scope of the Trench 2 evaluation.

2.1 Project Focus Topics

This study describes how the San Juan River interacts with the alluvial aquifer. Emphasis is placed on identifying river reaches dominated by river losses to the aquifer under baseline flow conditions and, conversely, where discharges to the river are prevalent. Similarly, a major project focus is the delineation of hyporheic zones. The study also focuses on determining the impact that seasonally high-river flows and stages have on groundwater flow patterns and advective contaminant transport. To characterize the river–aquifer interaction, river elevations have been measured along the entire length of the Shiprock site floodplain under both low-runoff and high-runoff conditions, and the resulting data have been used to develop changing water-surface profiles along the river's path for a 5-month period in 2011.

The Trench 2 evaluation made use of continuously recorded (5-minute intervals) specific conductance data collected by an automated data collection system called SOARS, an acronym for System Operation and Analysis at Remote Sites. However, the earlier study did not include analysis of equally valuable water-level data collected by SOARS at numerous wells in the vicinity of the trench. Groundwater elevations change measurably in response to pumping Trench 1, Trench 2, and the 1089/1104 area, as well as seasonal changes in the site's hydrology. These changes in turn impact contaminant migration patterns. SOARS-derived water-level histories at monitoring wells help identify such impacts and also enable improved estimates of the hydraulic properties of the alluvial aquifer. Thus a particular focus of this investigation is the utilization of SOARS data for describing the hydrogeology of the floodplain aquifer.

The SOWP (DOE 2000) and the GCAP (DOE 2002) projected that the inflow of contaminated terrace groundwater to the floodplain alluvium would decrease over several years in response to remediation pumping on the terrace and that the inflow would eventually decline to the point where remediation of the alluvial aquifer could succeed. This report examines findings from LM's Environmental Sciences Laboratory (ESL) investigations and available water-level and chemical data for the site to develop an updated understanding of the discharge of contaminated bedrock groundwater to the floodplain.

The numerical model of groundwater flow covers the entire alluvial aquifer. It is not sufficiently detailed to simulate the local effects of spatially varying aquifer properties but is designed to capture general flow directions and groundwater velocities. Emphasis is placed on calibrating the model for hydrologic conditions that tend to dominate the site during three general periods of each year, which are described as winter and early spring, the snowmelt runoff period in late spring and early summer, and late summer through fall. Capture zones created by existing components of the remediation system (i.e., wells 1089 and 1104, Trenches 1 and 2) as well as possible additional components are estimated through simulations with the model.

2.2 Project Objectives

The specific objectives of this study are:

1. Develop an updated conceptual model of groundwater flow in the floodplain alluvial aquifer under both baseline (nonpumping) and remediation (pumping) conditions.
2. Develop an understanding of how spatial and temporal variations in river levels impact groundwater flow patterns in the alluvial aquifer. Identify river reaches typically subject to river losses as well as reaches dominated by flow gains from discharging groundwater.
3. Use the river–aquifer interaction information described in study objective 2 to delineate hyporheic zones within the floodplain alluvial aquifer.
4. Describe the dynamics of the floodplain groundwater system by identifying hydrologic changes that occur during each year and between years.
5. Assess the degree to which remediation pumping prevents contaminant discharge to the San Juan River.
6. Compare current distributions of site contaminants with historical contaminant plumes in a variety of areas to assess the efficacy of the full remediation system in reducing dissolved contaminant mass.
7. Prepare an updated assessment of contaminated groundwater flow through Mancos Shale and resulting discharges of terrace groundwater to the floodplain alluvial aquifer.
8. Develop a calibrated numerical model of groundwater flow for the entire floodplain alluvial aquifer and use the model to assess how spatially variable river levels influence river–aquifer water exchange during periods of low flow on the San Juan River.
9. Use the calibrated flow model to develop approximate predictions of groundwater flow behavior in response to potential alterations of the site's hydrology and possible additions to the existing remediation system.
10. Preliminarily assess how the existing remediation system might be operated to optimize use of the existing evaporation pond or augmented to enhance contaminant mass removal.

This page intentionally left blank

3.0 Site Description

The Shiprock site lies within the northeast corner of the Navajo Nation, approximately 28 miles west of Farmington, New Mexico, and about 20 miles south of the Colorado state line (Figure 1). Today, all contaminated materials, including tailings left over from historical milling processes, are located within a 77-acre disposal cell situated on the terrace just south and west of the bedrock escarpment (Figure 2). The south end of the San Juan River floodplain associated with the site is located about 1200 ft south of Trench 2, where the river pinches out alluvium and abuts the Mancos Shale escarpment. The north end of the floodplain occurs where the river abuts the escarpment in the vicinity of the Highway 491 bridge (Figure 2). The floodplain is about 1.1 miles (mi) (5800 ft) long and 0.3 mi (1600 ft) wide at its widest point. Much of the floodplain area bordering the river is considered a riparian zone.

Two surface drainage features other than the San Juan River are capable of conveying surface-water flows at the site. Under natural conditions, Many Devils Wash, about 2000 ft south-southeast of the disposal cell (Figure 2), carries limited quantities of surface water ($\leq$3 gpm) year-round directly to the river (DOE 2000), thereby bypassing the floodplain. Under natural conditions, Bob Lee Wash, located approximately 1500 ft northwest of the disposal cell (Figure 2), is an ephemeral drainage that conveys storm runoff on the terrace toward the north end of the floodplain. However, since the late-1970s, a flowing artesian well (well 648) at the head of a small tributary to Bob Lee Wash has continuously fed surface water to the lower parts of the wash and, subsequently, to the floodplain. Prior to the wash providing an outlet for the artesian flow, beginning in 1961 when well 948 was installed, a ditch conveyed the flowing water directly north-northeastward to the floodplain (Figure 3).

3.1 Relevant Site History

The SOWP (DOE 2000) presents a large amount of background information for the Shiprock site, including a detailed history of milling operations and the development of water resources in the vicinity of the site. A complete recounting of that history is not warranted here, but several features of past activities at and near the site bear some discussion because they were influenced by or impacted groundwater flow in the alluvial aquifer. Though most of the historical summary incorporated in this section deals with processes affecting the hydrology of the site, some historical milling and site remediation activities are also discussed because they may be of equal importance as groundwater flow phenomena in helping to explain past and currently observed contaminant plume configurations.

The Shiprock mill operated from November 1954 until August 1968. Buildings used in the milling process were located just south of Bob Lee Wash, and uranium/vanadium ore was stored just north and northeast of the buildings (Figure 3). The tailings from the milling process were placed in the two large piles (north and south tailings piles) that covered most of the area currently lying within the disposal cell footprint. Tailings were delivered in slurry form to the piles (DOE 2000), indicating that much of the deposited waste consisted of water mixed with ore-processing chemicals in addition to solids. Waste liquids produced by the milling process were stored in up to 10 unlined raffinate ponds constructed along the south and southwest edge of the tailings piles (Figure 3). Figure 4 shows an oblique aerial photograph of the mill, tailings piles, raffinate ponds, and ore piles in 1965.

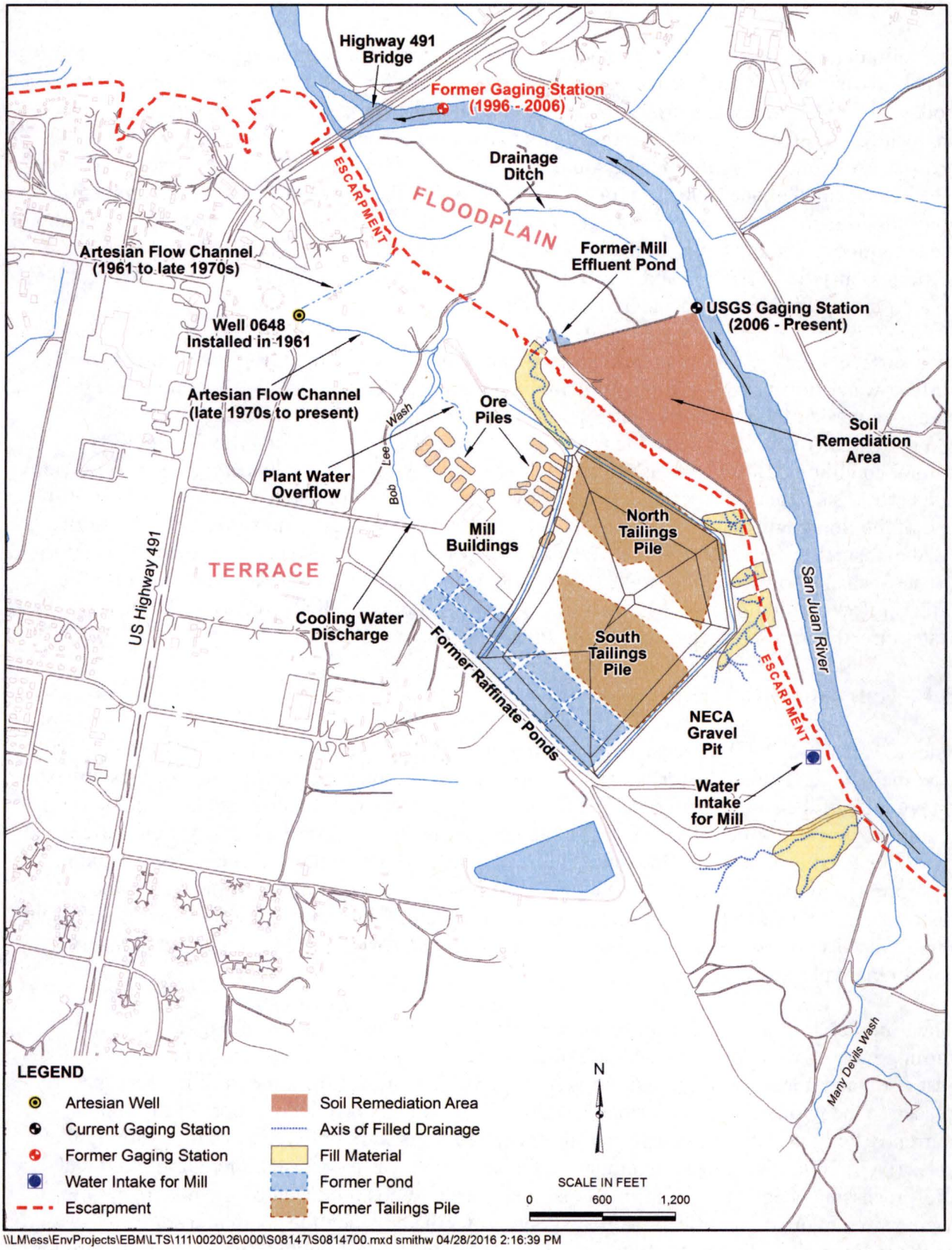

Figure 3. Historical Features at the Shiprock Site

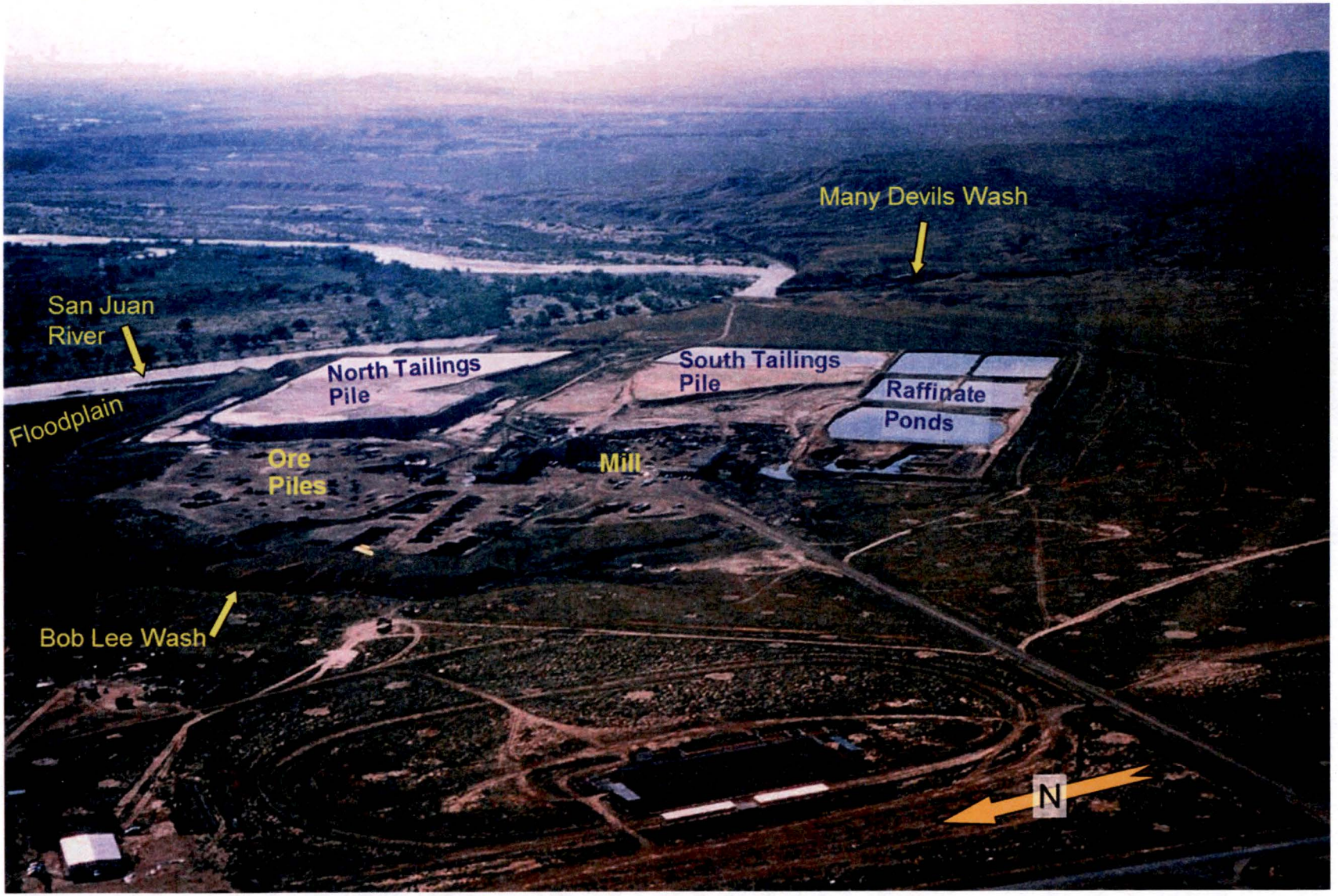

Figure 4. July 1965 View Southeast of the Shiprock Mill Site

The mill was used to process ores from two different mining areas in Arizona and Colorado, signifying that their respective mineralogical makeups, and the leachates derived from them during milling, were potentially distinguishable. The milling required a great amount of water, which was diverted from the San Juan River about 0.6 mi south-southeast of the facility (Figure 3). Methods used to extract uranium from the ores varied over the years from acid cures (sulfuric acid) to agitation leach and eventually solvent extraction. Inorganic chemicals applied in the operations included nitrate and ammonium complexes. The solvent extraction process made use of multiple organic chemicals, including di(2-ethylhexyl) phosphoric acid, tributyl phosphate, kerosene, and alcohols (DOE 1998).

In 1931, the U.S. Geological Survey (USGS) assumed responsibility for operating a gaging station on the San Juan River downstream of where the Highway 491 bridge currently spans the river. The gaging station was moved in September 1994 to a site about 500 ft upstream of the bridge (Figure 3). On June 13, 2006, the station was moved farther upstream to its current location shown in Figure 2 and Figure 3, on the Shiprock site and approximately 0.6 mile upstream of the bridge.

The predominant wind direction at the Shiprock site is from the south; stronger winds associated with frontal systems are typically from the southwest, west, and northwest (DOE 2000). In the mill operation period and for several years thereafter, occasional strong winds dislodged contaminated materials from the tailings piles and deposited the airborne dust on the floodplain. Most of the windblown contamination apparently deposited south of an east-northeast trending line that is now aligned with a dirt road extending from the USGS gaging station to the base of the escarpment about 300 ft northwest of Trench 1 (Figure 2). Shallow soil excavation on the floodplain during surface remediation activities in later years (soil remediation area in Figure 3) removed the windblown contamination to levels below the cleanup requirements.

In the milling era, the Shiprock area south of the San Juan River and west of the mill gained population, and agricultural use increased. These changes required additional sources of water. In 1956, the Bureau of Indian Affairs completed the construction of an irrigation project in the terrace area south of the San Juan River (DOE 2000) and west of the current location of Highway 491 (Figure 3). By 1960, irrigated farming was well established in the project area. The availability of water changed the character of the terrace area and the floodplain area along the San Juan River.

In 1961, a deep well (1850 ft deep) was installed on the terrace at the head of what is now a tributary to Bob Lee Wash. Drilled for oil-and-gas exploration purposes, the well tapped groundwater in the Morrison Formation, which lies below the Mancos Shale and maintains pressures sufficient to drive formation water to the land surface. Known in the UMTRA Project as well 648 (Figure 2 and Figure 3), or the flowing artesian well, it was allowed to feed subsurface water to the land surface at an estimated rate of 64 gpm (DOE 2000). For several years after the well was drilled, artesian water appeared to flow directly east-northeastward to the floodplain (Figure 3). At some time during the late-1970s, the flow was diverted into the southeast-oriented tributary that now connects the artesian well to Bob Lee Wash. The surface flow into Bob Lee Wash continues to this day, and that portion of the flow that is not lost to evaporation and transpiration in the wash channel, or recharge of underlying groundwater in the Mancos Shale, migrates to the floodplain, where much of it recharges the alluvial aquifer and creates a groundwater mound. The floodplain area at the mouth of Bob Lee Wash receiving the

artesian flow has historically been referred to as a wetland, particularly since much of the groundwater in the mounding area is very shallow (less than 3 ft deep) or contains surface water that was rejected from the subsurface. Water elevations observed in the groundwater mounding area during some months of high evaporation and transpiration (midsummer through early fall) appear to be 1–2 ft lower than water levels measured during winter and early spring.

Vegetation increased dramatically on the floodplain north and east of the mill site during the milling period due to increased availability of water, for both milling and sundry other uses. As early as the summer of 1955, drainage of mill effluent northward onto the floodplain was evident by the presence of an effluent pond near the mouth of a small drainage, or arroyo, incising the terrace directly north of the mill buildings area (Figure 3) (DOE 2000). Additional, smaller ponds were also apparently on the floodplain in the vicinity of the main effluent pond (USPHS 1962, DOE 2000). Aerial photographs of the site during milling years included in various documents (e.g., DOE 1994, 2000) suggest that surface water was also occasionally present at the time in a drainage ditch that traversed the floodplain, extending west-northwest from the river just north of the current USGS gage location to the escarpment about 800 ft northwest of Bob Lee Wash (Figure 3). This small waterway appeared to sustain local floodplain vegetation and merged with another surface-water ditch at the escarpment that hugged the base of the escarpment from the mouth of Bob Lee Wash to the San Juan River at the Highway 491 bridge (USPHS 1962). Between 1961 and the late 1970s, prior to the diversion of flowing artesian well discharge toward Bob Lee Wash, surface water from that well apparently emptied into the ditch at the base of the escarpment (Figure 3) and about 800 ft northwest of the Bob Lee Wash outlet. The relatively abundant vegetation on the floodplain at the Shiprock site from the early 1950s through much of the 1970s, sustained by water used for milling and other uses, contrasted with a sparseness of vegetation at the same time in the floodplain south of the San Juan River about 1 mile upstream from the mill site (DOE 2000). The stark contrast between the two areas reflected the impact that anthropogenic water sources had on the local region near the town of Shiprock.

In 1963 the Navajo Dam was completed on the San Juan River about 75 miles upstream and east of Shiprock. Before the dam, river flow fluctuated greatly through the year, ranging from extreme low flows in the fall and winter to sometimes extreme high flows in the spring and early summer, in response to snowmelt conditions in the river's headwaters in the San Juan Mountains. In most years, the snowmelt runoff was high enough to cover the floodplain for periods of several days to weeks. These periodic high flows scoured much of the vegetation off the floodplain and created numerous drainage and distributary channels. Fluctuations in river stage became less extreme after 1963 with the control on river flows made possible by construction of the dam. This control of the river has nearly eliminated scouring during flood events and has allowed vegetation to become established on much of the site's floodplain area as well as on floodplains upstream and downstream of the site.

Stabilization of tailings at the site and preliminary cleanup of contaminated features on the land surface began in the early 1970s. Radiation survey data collected in 1974 made it possible to identify the extent of windblown and water-transported tailings to the floodplain, and surface decontamination work began in earnest in early 1975. Much of the surface remediation work in the mid- to late-1970s was performed by personnel of the Navajo Engineering and Construction Authority (NECA). In addition to excavating contaminated surface soils and backfilling with clean materials in the south half of the floodplain, the surface work included the filling of

multiple small drainages emptying out on the floodplain in the vicinity of the escarpment (Figure 3) between Bob Lee Wash and Many Devils Wash. Surface materials from the former ore storage area north of the mill buildings (Figure 3 and Figure 4) were used to fill in the small drainage that had been used during milling to convey and discharge mill waste to the effluent pond just north of the bedrock escarpment (DOE 2000). Surface remediation work continued through 1978, when DOE began managing site operations under the Uranium Mill Tailings Radiation Control Act. By May 1980, the small pond(s) on the floodplain that had been used to store mill effluent just north of the escarpment had been filled in with soil, and the NECA gravel pit (Figure 3) had begun operating. By September 1986, all tailings and associated materials (including contaminated materials from offsite vicinity properties) were encapsulated in the disposal cell built on top of the existing tailings piles.

Limited groundwater characterization work was performed in the 1980s as part of the UMTRA Project, and comprehensive characterization of the subsurface at the site hit full stride in the mid- to late-1990s. Groundwater remediation in the form of pumping from multiple vertical wells and water collection trenches was initiated over the full site in March 2003.

3.2 Sources of Groundwater Contamination in the Floodplain

Much of the contamination currently observed in floodplain groundwater resulted from the infiltration of contaminated liquids on the terrace in the vicinity of former mill operations and subsequent transport toward the floodplain via the terrace groundwater system. Though some subsurface aqueous-phase contamination migrating toward the floodplain is detected in seeps on the escarpment wall, most of the contamination appears to have discharged directly to the alluvial aquifer from the Mancos Shale. Infiltration of contaminated liquid likely occurred over the 30-plus-year period between mill startup in 1954 and completion of surface remediation in 1986. During the milling era, contaminants entered the subsurface via leakage from unlined raffinate ponds and the leaching by rainfall of materials piled in the ore storage area. Contaminants in tailings were leached by both mill water and precipitation until the disposal cell was completed.

Other historical sources of contamination in the floodplain alluvial aquifer include mill-related liquids deposited on the floodplain surface either through accidental or intended means. For example, in August 1960, a large volume of acidic waste effluent spilled from the northwest end of the raffinate ponds and flowed down Bob Lee Wash to the north half of the floodplain (USPHS 1963, DOE 2000). Bob Lee Wash also received plant-water overflows from the mill via a small tributary located directly north of the ore piles and discharge of cooling water farther up the wash drainage and near the northwest end of the raffinate ponds (Figure 3) (USPHS 1962). As previously mentioned, plant effluent also flowed into the small drainage extending from the northwest end of the tailings area to the floodplain. Accordingly, seepage from the effluent pond(s) constructed as early as 1955 on the floodplain at the base of the bedrock escarpment to receive that mill effluent also provided a potential contaminant source. Some of the infiltrated waste water from milling and subsurface water leached from tailings surfaced in the additional small drainages that emptied onto the floodplain across the escarpment farther to the south of the effluent arroyo and directly east of the north tailings pile (Figure 3). Measured uranium concentrations in these latter small drainages in November 1960 ranged from about 3.8 milligrams per liter (mg/L) to 4.8 mg/L (USPHS 1962).

Leaching of contamination left in solid form in floodplain soils and deeper alluvium is a source of contaminants in floodplain groundwater, both historically and currently. For example, the dissolution of windblown tailings that deposited on the floodplain surface and subsequently escaped remedial excavation can contribute to groundwater contamination. Additional solid-phase constituents subject to leaching are attributed to contaminated surface water and groundwater that migrated to the alluvial aquifer but subsequently partitioned into the solid phase from an aqueous phase. Because they are potentially subject to slow dissolution by subsurface water (e.g., rising groundwater during periods of high-river flow, downward seepage of infiltrated surface water through the unsaturated zone), the solid-phase constituents represent secondary sources of contamination that can slow the rate at which the aquifer is remediated. Examples of such secondary sources include constituents that adsorbed to hydrous ferric oxide, covering sediment grains or minerals that precipitated from solution due to the presence of chemically reducing conditions.

The SOWP (2000) discusses two separate campaigns for sampling and analyzing soils and sediments, one in late 1998 and early 1999, and the other in October and December 1999, that demonstrated the presence of solid-phase subsurface contamination in several different parts of the floodplain. Soil and sediment uranium concentrations on the floodplain measured during the campaigns ranged from 0.23 to 35.6 milligrams per kilogram (mg/kg). An earlier sediment sampling event conducted in support of the Baseline Risk Assessment for the Shiprock site (DOE 1994) revealed an elevated solid-phase concentration for uranium of 44 mg/kg near the former effluent pond at the outlet of the small drainage extending northwestward from the northwest corner of the tailings area (Figure 3).

Examination of the various mechanisms by which contaminants have migrated to the alluvial aquifer reveals uncertainties regarding source terms for contaminant plumes and their eventual disposition. For example, it is difficult to discern from available information if the floodplain plumes are currently fed by terrace contamination via subsurface water discharge across the Mancos Shale escarpment. Similarly, the potential for residual moisture in disposal cell tailings to seep downward into the terrace groundwater system and then migrate toward the alluvial aquifer is unknown. Unfortunately, no reliable methods have been identified for measuring either contaminant release from the disposal cell or contaminant discharge across the escarpment. Because of the uncertainties regarding such processes, it is not feasible to predict the duration of contaminant sources beneath the terrace and, as a consequence, the long-term fate of contaminants in floodplain groundwater.

It should be noted that water from the flowing artesian well on the terrace (well 648) that recharges the aquifer at the mouth of Bob Lee Wash is not considered a source of groundwater contamination. The total dissolved solids (TDS) concentration of the well discharge is about 3000 mg/L (DOE 2000), which according to salinity categories established by McCutcheon et al. (1992) classifies this water as slightly saline. Reported uranium concentrations in well 648 flows are less than 0.005 mg/L, and the nitrate (as nitrate) concentrations are less than 1 mg/L. Most of the salinity in the flowing artesian water is attributed to sulfate, with concentrations of about 2000 mg/L.

3.3 Historical Water Monitoring

Wells were drilled in the floodplain alluvial aquifer as early as 1984 for site characterization purposes, and DOE began collecting data from them the same year. Additional wells, well points, and test pits were installed in following years. Well installation activity increased significantly during two periods in the 1990s to support a comprehensive groundwater characterization investigation conducted in support of the SOWP. A concerted effort was made during the SOWP investigation to gather groundwater-chemistry data from about 20 temporary test pits with the intent of using the single-event data to supplement water-quality information at the wells. Since publication of the final SOWP (DOE 2000), even more wells have been installed in the alluvial aquifer; most of these have been monitored for the purpose of assessing the progress of groundwater remediation that began in 2003. Both hydraulic (water level) and water-quality (sample) data are collected at wells that compose the floodplain monitoring network.

Since monitoring began, many of the wells installed in the alluvial aquifer in earlier years have been abandoned. Excluding wells that were drilled into deeper portions of the Mancos Shale underlying the alluvial aquifer, the current groundwater monitoring system on the floodplain consists of 79 monitoring wells and two pumping wells (1089 and 1104). Figure 5 is an aerial photograph showing the locations of shallow wells composing the current monitoring network, and Table 1 presents an itemized summary of the location coordinates and construction information for each well.

In recent years, samples have been collected semiannually from floodplain wells. The number of locations sampled has varied between monitoring events, partly to minimize potentially redundant groundwater-quality information from densely packed monitoring wells surrounding each of the three remediation areas. Consequently, it is common to encounter data sets from some sampling events that are larger than those from others.

Because the San Juan River is known to both strongly influence the chemistry of floodplain groundwater as well as receive groundwater discharge, DOE has consistently sampled surface water at multiple locations on the river adjacent to the site. In addition, water has occasionally been sampled at a few onsite locations that periodically receive surface-water flow, often in response to increased river levels that push groundwater elevations above the local land surface. Surface-water sampling sites shown in Figure 5 identify locations from which water-quality data have been examined in this report to assess potential interactions between groundwater and surface water.

Figure 5 also shows the locations of three water-collection sumps on the floodplain that are sampled during semiannual monitoring events. Each sump consists of a pipe, or casing, from which water is pumped and delivered to the pipeline feeding the evaporation pond on the terrace (Figure 2). The sump identified as 1109 on the north end of Trench 2 collects water drawn into the trench pipe, and sump 1110 serves the equivalent purpose at Trench 1. Sump 1118 (Figure 5) collects water through a pipeline from two seeps—425 and 426—that, prior to the sump's installation, were sites of groundwater discharge from the exposed Mancos Shale escarpment.

Figure 5. Monitoring Locations Used in This Study

This page intentionally left blank

Table 1. Construction Information for Shallow Wells on the Shiprock Floodplain

Well	Easting (ft)	Northing (ft)	Model *x*-Coordinate (ft)	Model *y*-Coordinate (ft)	Date Established	Surface Elevation (ft amsl)	Depth to Bedrock (ft)	Bedrock Elevation (ft amsl)	Casing Depth (ft)	Casing Bottom Elevation (ft amsl)	Borehole Depth (ft)	Borehole Bottom Elevation (ft amsl)	Zone of Completion	Well Type	SOARS Location	Date Instrumented
608	251712.58	2101434.86	4,574.43	888.84	8/29/85	4,891.67	10	4,881.67	17	4,874.67	19	4,872.67	Km	Monitor	No	
609	251704.91	2101450.02	4,558.30	894.17	8/30/85	4,890.97	8	4,882.97	10.8	4,880.17	14	4,876.97	Al	Monitor	No	
610	251334.83	2101686.65	4,129.09	800.73	9/3/85	4,892.24	13	4,879.24	11	4,881.24	15	4,877.24	Al	Monitor	No	
611	251324.05	2101693.09	4,116.91	797.68	9/3/85	4,892.35	13	4,879.35	16.25	4,876.1	22	4,870.35	Al-Km	Monitor	No	
612	251560.91	2101985.43	4,078.48	1,171.97	9/4/85	4,891.91	14.5	4,877.41	12	4,879.91	15	4,876.91	Al	Monitor	No	
613	250943.68	2101991.72	3,636.66	740.92	9/4/85	4,889.92	14	4,875.92	12	4,877.92	15	4,874.92	Al	Monitor	No	
614	250953.07	2101985.26	3,647.87	742.96	9/4/85	4,890.3	14	4,876.3	17	4,873.3	19	4,871.3	Al-Km	Monitor	No	
615	250564.45	2102542.15	2,979.55	863.38	9/6/85	4,890.83	13	4,877.83	11.5	4,879.33	14	4,876.83	Al	Monitor	No	
617	250761.09	2102937.07	2,840.25	1,281.98	9/5/85	4,890.05	19.8	4,870.25	12	4,878.05	20	4,870.05	Al	Monitor	No	
618	250748.52	2102934.43	2,833.20	1,271.24	9/5/85	4,889.87	20	4,869.87	18	4,871.87	21	4,868.87	Al	Monitor	No	
619	250401.87	2103321.9	2,314.16	1,301.22	9/6/85	4,890.42	18	4,872.42	15	4,875.42	20	4,870.42	Al	Monitor	No	
620	250243.13	2102960.74	2,456.51	933.29	8/27/85	4,888.18	17	4,871.18	20	4,868.18	23	4,865.18	Al-Km	Monitor	No	
621	250252.85	2102960.06	2,463.87	939.66	8/28/85	4,888.33	16.5	4,871.83	17	4,871.33	19	4,869.33	Al	Monitor	No	
622	250263.63	2102958.94	2,472.30	946.48	8/28/85	4,888.51	NA	NA	12	4,876.51	16	4,872.51	Al	Monitor	No	
623	250256.67	2103409.01	2,149.81	1,260.49	9/7/85	4,889.27	17	4,872.27	17	4,872.27	23	4,866.27	Al	Monitor	No	
624	250252.71	2103396.91	2,155.54	1,249.13	9/7/85	4,889.29	18	4,871.29	22	4,867.29	24	4,865.29	Al-Km	Monitor	No	
625	250249.62	2103384.86	2,161.85	1,238.41	9/7/85	4,889.28	NA	NA	11.5	4,877.78	17	4,872.28	Al	Monitor	No	
626	249941.38	2103324.5	1,986.02	978.14	9/8/85	4,888.48	19	4,869.48	16.5	4,871.98	20	4,868.48	Al	Monitor	No	
627	249650.71	2103526.75	1,637.34	916.37	9/8/85	4,887.48	17	4,870.48	15	4,872.48	20	4,867.48	Al	Monitor	No	
628	249660.32	2103517.40	1,650.74	916.53	9/9/85	4,887.84	NA	NA	12	4,875.84	15	4,872.84	Al	Monitor	No	
629	249378.67	2103359.79	1,562.37	606.11	9/9/85	4,887.29	13	4,874.29	17	4,870.29	20	4,867.29	Al-Km	Monitor	No	
630	249382.75	2103349.44	1,572.56	601.65	9/9/85	4,887.65	13	4,874.65	12	4,875.65	15	4,872.65	Al	Monitor	No	
734	248608.49	2104505.13	208.46	874.30	3/25/93	4,886	NA	NA	7	4,879	7	4,879	Al	Monitor	No	
735	252193.67	2099904.08	5,995.45	143.54	3/26/93	4,894.53	NA	NA	9	4,885.53	9	4,885.53	Al	Monitor	Yes	Mar-11
736	249808.04	2104420.64	1,118.11	1,660.81	3/24/93	4,887.2	NA	NA	7	4,880.2	7	4,880.2	Al	Monitor	No	
766	250686.97	2103964.44	2,062.82	1,957.70	10/28/99	4,888.68	NA	NA	9	4,879.68	9	4,879.68	Al	Monitor	Yes	Aug-09
768	250340.45	2103147.09	2,393.98	1,134.01	10/28/99	4,889.28	NA	NA	7.33	4,881.95	7.33	4,881.95	Al	Monitor	No	
773	251394.19	2101742.40	4,131.82	882.12	10/28/99	4,891.5	NA	NA	6.75	4,884.75	6.75	4,884.75	Al	Monitor	No	
775	250663.37	2103476.13	2,390.65	1,595.02	10/28/99	4,888.92	NA	NA	7	4,881.92	7	4,881.92	Al	Monitor	No	
779	251034.71	2103162.67	2,874.96	1,634.91	10/28/99	4,890.93	NA	NA	9.75	4,881.18	9.75	4,881.18	Al	Monitor	Yes	Mar-11
792	250522.04	2102957.99	2,656.09	1,128.13	3/1/01	4,888.79	NA	NA	8.3	4,880.49	8.3	4,880.49	Al	Monitor	No	
793	250757.62	2102721.00	2,990.24	1,126.42	3/1/01	4,888.38	NA	NA	7.5	4,880.88	7.5	4,880.88	Al	Monitor	Yes	Aug-09
794	250922.60	2102525.73	3,244.93	1,104.45	3/1/01	4,890.34	NA	NA	8.4	4,881.94	8.4	4,881.94	Al	Monitor	No	
795	251027.98	2102519.13	3,324.26	1,174.13	3/1/01	4,890.03	NA	NA	9	4,881.03	9	4,881.03	Al	Monitor	No	
798	250654.34	2103237.75	2,552.45	1,419.73	3/1/01	4,888.83	NA	NA	9.5	4,879.33	9.5	4,879.33	Al	Monitor	No	
853	251196.38	2102501.58	3,455.98	1,280.52	10/11/98	4,888.81	16	4,872.81	15.3	4,873.51	16.5	4,872.31	Al	Monitor	Yes	Mar-11
854	250820.81	2103849.23	2,238.96	1,970.49	10/25/98	4,888.3	NA	NA	11.75	4,876.55	12.95	4,875.35	Al	Monitor	Yes	Oct-09
855	249057.21	2103849.57	988.99	726.36	10/24/98	4,885.59	17.6	4,867.99	15.1	4,870.49	17.8	4,867.79	Al	Monitor	No	
856	249110.63	2104395.65	641.54	1,151.02	10/12/98	4,884.83	24	4,860.83	24.1	4,860.73	24.5	4,860.33	Al	Monitor	No	
857	251160.35	2103029.83	3,057.72	1,629.42	10/11/98	4,891.61	19	4,872.61	18.5	4,873.11	19.2	4,872.41	Al	Monitor	Yes	Mar-11
858	251540.03	2101963.3	4,079.30	1,141.55	9/25/98	4,891.38	21	4,870.38	20.6	4,870.78	25.3	4,866.08	Al	Monitor	No	
859	251528.87	2101971.57	4,065.56	1,139.54	9/26/98	4,891.37	21	4,870.37	19.9	4,871.47	24.5	4,866.87	Al	Monitor	No	
1008	250769.64	2103812.23	2,228.80	1,908.17	4/13/00	4,888.72	15.5	4,873.22	17.2	4,871.52	17.2	4,871.52	Al	Monitor	Yes	Oct-09
1009	250818.64	2102533.18	3,166.01	1,036.38	4/12/00	4,890.29	17	4,873.29	17.7	4,872.59	17.7	4,872.59	Al	Monitor	Yes	Aug-09
1010	251082.8	2103015.92	3,012.58	1,564.85	4/12/00	4,890.41	18.5	4,871.909	19	4,871.25	19	4,871.41	Al	Monitor	No	
1013	251128.54	2102516.7	3,397.24	1,243.36	4/11/00	4,889.27	16	4,873.267	22.3	4,866.7	22.3	4,866.97	Al-Km	Monitor	No	

Table 1 (continued). Construction Information for Shallow Wells on the Shiprock Floodplain

Well	Easting (ft)	Northing (ft)	Model *x*-Coordinate (ft)	Model *y*-Coordinate (ft)	Date Established	Surface Elevation (ft amsl)	Depth to Bedrock (ft)	Bedrock Elevation (ft amsl)	Casing Depth (ft)	Casing Bottom Elevation (ft amsl)	Borehole Depth (ft)	Borehole Bottom Elevation (ft amsl)	Zone of Completion	Well Type	SOARS Location	Date Instrumented
1075	250665.87	2103843.51	2,133.20	1,857.12	8/26/02	4,887.9	15.5	4,872.4	18.5	4,869.4	18.5	4,869.4	Al	Monitor	Yes	Aug-09
1077	250818.86	2103795.24	2,275.67	1,930.86	8/27/02	4,888.7	15	4,873.7	17.5	4,871.2	17.5	4,871.2	Al	Monitor	Yes	Oct-09
1089	250701.57	2103894.19	2,122.74	1,918.22	6/25/03	4,890.61	14.5	4,876.11	15.2	4,875.41	15.2	4,875.41	Al	Pumping	Yes	Dec-05
1104	250793.46	2103871.34	2,203.98	1,966.86	2005	4,889.42	14.49	4,874.925	15	4,874.42	15	4,874.42	Al	Pumping	Yes	Nov-05
1105	250570.78	2102531.4	2,991.62	860.23	3/3/05	4,889.67	14	4,875.666	19.5	4,870.17	20	4,869.67	Al	Monitor	Yes	Oct-09
1109-A	251942.90	2100949.10	5,080.39	707.13	Apr-06	4,892.41	NA	NA	~8	~4,884.5	~8	~4,884.5	Al	Monitor	Yes	Mar-07
1109-C	251963.40	2100849.30	5,165.34	650.87	Apr-06	4,894.67	NA	NA	~10	~4,884.5	~10	~4,884.5	Al	Monitor	Yes	Mar-07
1110-A	250413.52	2102480.21	2,916.31	713.00	Apr-06	4,887.46	NA	NA	~9	~4,878.5	~9	~4,878.5	Al	Monitor	Yes	Oct-09
1110-C	250468.85	2102427.63	2,992.61	714.78	Apr-06	4,888.35	NA	NA	~10	~4,878.5	~10	~4,878.5	Al	Monitor	Yes	Oct-09
1111	250385.69	2102461.69	2,909.65	680.24	6/7/06	4,887.9	NA	NA	12	4,875.9	12	4,875.9	Al	Monitor	Yes	Oct-09
1112	250501.75	2102343.41	3,075.35	678.31	6/7/06	4,893.86	NA	NA	12	4,881.86	12	4,881.86	Al	Monitor	Yes	Oct-09
1113	251518.51	2101586.06	4,330.23	859.05	6/7/06	4,896.08	12	4,884.08	12	4,884.08	12	4,884.08	Al	Monitor	No	
1114	251814.76	2101265	4,766.69	840.57	6/6/06	4,890.92	12	4,878.92	12	4,878.92	12	4,878.92	Al	Monitor	No	
1115	251890.03	2100964.85	5,031.81	680.98	6/6/06	4,893.4	12	4,881.4	12	4,881.4	12	4,881.4	Al	Monitor	Yes	Mar-07
1116	251905.87	2100804.96	5,155.85	578.86	6/6/06	4,896.39	12	4,884.39	12	4,884.39	12	4,884.39	Al	Monitor	No	
1117	252003.66	2100839.64	5,200.68	672.43	6/6/06	4,894.37	12	4,882.37	12	4,882.37	12	4,882.37	Al	Monitor	Yes	Mar-07
1125	252031.01	2100974.88	5,124.64	787.57	2/6/07	4,893.75	11.57	4,882.18	11.57	4,882.18	11.57	4,882.18	Al	Monitor	Yes	Mar-07
1126	251913.87	2101062.4	4,979.88	766.93	2/6/07	4,893.33	12.81	4,880.52	12.81	4,880.52	12.81	4,880.52	Al	Monitor	Yes	Mar-07
1127	251990.57	2100759.41	5,248.01	606.34	2/6/07	4,894.81	14.41	4,880.4	14.41	4,880.4	14.41	4,880.4	Al	Monitor	Yes	Aug-06
1128	251919.39	2100812.07	5,160.42	593.44	2/6/07	4,895.64	12.11	4,883.53	12.11	4,883.53	12.11	4,883.53	Al	Monitor	Yes	Mar-07
1129	252060.48	2100824.23	5,251.82	701.60	2/6/07	4,893.56	10.58	4,882.98	10.58	4,882.98	10.58	4,882.98	Al	Monitor	Yes	Mar-07
1130	252111.29	2100823.65	5,288.23	737.04	2/6/07	4,893.29	9.73	4,883.56	9.73	4,883.56	9.73	4,883.56	Al	Monitor	Yes	Mar-07
1131	252033.32	2100903.05	5,176.96	738.29	2/7/07	4,892.63	10.55	4,882.08	10.55	4,882.08	10.55	4,882.08	Al	Monitor	Yes	Mar-07
1132	251977.86	2100903.53	5,137.32	699.50	2/7/07	4,892.22	11.37	4,880.85	11.37	4,880.85	11.37	4,880.85	Al	Monitor	Yes	Mar-07
1133	251909.38	2100891.9	5,097.00	642.94	2/6/07	4,894.42	11.54	4,882.88	11.54	4,882.88	11.54	4,882.88	Al	Monitor	Yes	Mar-07
1134	251968.2	2100980.43	5,076.21	747.18	2/7/07	4,893.74	13.46	4,880.28	13.46	4,879.87	13.46	4,879.87	Al	Monitor	Yes	Mar-07
1135	250325.89	2104285.56	1,580.38	1,930.48	1/26/10	4,887.88	11.6	4,876.281	11.6	4,876.28	11.6	4,876.28	Al	Monitor	Yes	Mar-11
1136	251156.56	2103434.57	2,769.46	1,913.56	1/27/10	4,889.14	11.5	4,877.639	11.5	4,877.64	11.5	4,877.64	Al	Monitor	Yes	Mar-11
1137	250867.09	2104014.35	2,155.25	2,120.16	1/26/10	4,888.63	15	4,873.632	14.61	4,873.46	15	4,873.63	Al	Monitor	Yes	Mar-10
1138	250841.08	2103984.38	2,157.96	2,080.57	1/26/10	4,888.84	13.3	4,875.545	13.3	4,875.04	13.3	4,875.54	Al	Monitor	No	
1139	250803.52	2103944.22	2,159.68	2,025.61	1/26/10	4,887.48	11.4	4,876.076	11.4	4,875.73	11.4	4,876.08	Al	Monitor	No	
1140	250453.12	2102498.35	2,931.57	753.79	5/15/09	4,888.59	NA	NA	12.8	4,875.79	12.9	4,875.69	Al	Monitor	Yes	Oct-09
1141	250556.36	2102408.55	3,068.09	763.00	5/15/09	4,889.85	NA	NA	10.8	4,879.05	10.9	4,878.95	Al	Monitor	Yes	Oct-09
1142	251593.08	2102435.96	3,783.39	1,513.92	1/27/10	4,891.64	14.21	4,877.433	14.21	4,877.43	14.21	4,877.43	Al	Monitor	No	
1143	249461.11	2104392.09	892.41	1,395.79	1/25/10	4,885.28	13.3	4,871.979	13.3	4,871.98	13.3	4,871.98	Al	Monitor	No	

Abbreviations:
amsl = above mean sea level; Al = alluvium; Km = Mancos Shale; NA = not applicable

Chemical analyses of samples collected from the trench sumps represent mixtures of groundwater collected along the full length of each system's horizontal well. Water pumped from sump 1118 is a composite of the two seeps and groundwater seeping through small openings to the sump casing. As shown in Figure 5, the outlet for the small drainage that was used to deliver mill effluent to the pond just north of the escarpment (Figure 3) during milling years and was subsequently filled with soils from the ore storage area (Section 3.1) is near seep 425 and sump 1118.

Results from the water monitoring activities described above along with other useful information, such as geologic and construction logs for shallow floodplain wells, are documented in an LM database called GEMS (Geospatial Environmental Mapping System).

3.4 Floodplain Remediation System

The GCAP (DOE 2002) established a compliance strategy for the floodplain alluvial aquifer that consisted of natural flushing supplemented by groundwater extraction via pumping wells. The groundwater pumping was initially planned for an area near the San Juan River in which concentrations of contaminants were identified as being some of the highest at the Shiprock site (the 1089/1104 area). The original design of the remediation system called for the construction of two pumping wells, identified as wells 1075 and 1077 (Figure 5). The pumping was considered a best management practice that would eliminate groundwater discharge to the river in the area of the high concentrations (DOE 2003a) and reduce contaminant levels such that natural flushing would eventually become the dominant remediation mechanism.

Since 2003, the year that pumping from wells 1075 and 1077 began, the remediation system on the floodplain has expanded. The following sections describe the various components of the remediation system in more detail.

3.4.1 Extraction Wells Remediation System

The 1089/1104 area is located near the river (Figure 2), about 1000 ft northwest of the USGS gaging station, and 1500 ft north of Trench 1. Well 1089 is about 220 ft from the river, and well 1104 is approximately 180 ft from the river. Several monitoring wells in the vicinity of the two pumping wells (Figure 6) assist in assessing the impacts of groundwater extraction in the area.

Previous investigations of the Shiprock site have indicated that the purpose of groundwater pumping in the 1089/1104 area is to decrease discharge to the river of contaminated groundwater in this portion of the aquifer (e.g., DOE 2005b, p. 6-4; DOE 2002, p. B-8). This is because monitoring of the river just north of the area has suggested that such discharge could pose a potential risk to aquatic life (DOE 2002, p. 3-6). Accordingly, pumping the aquifer at this location such that surface water is pulled from the river toward wells 1089 and 1104 is considered a best management practice (DOE 2005b, p. 5-4; DOE 2002, p. 3-6).

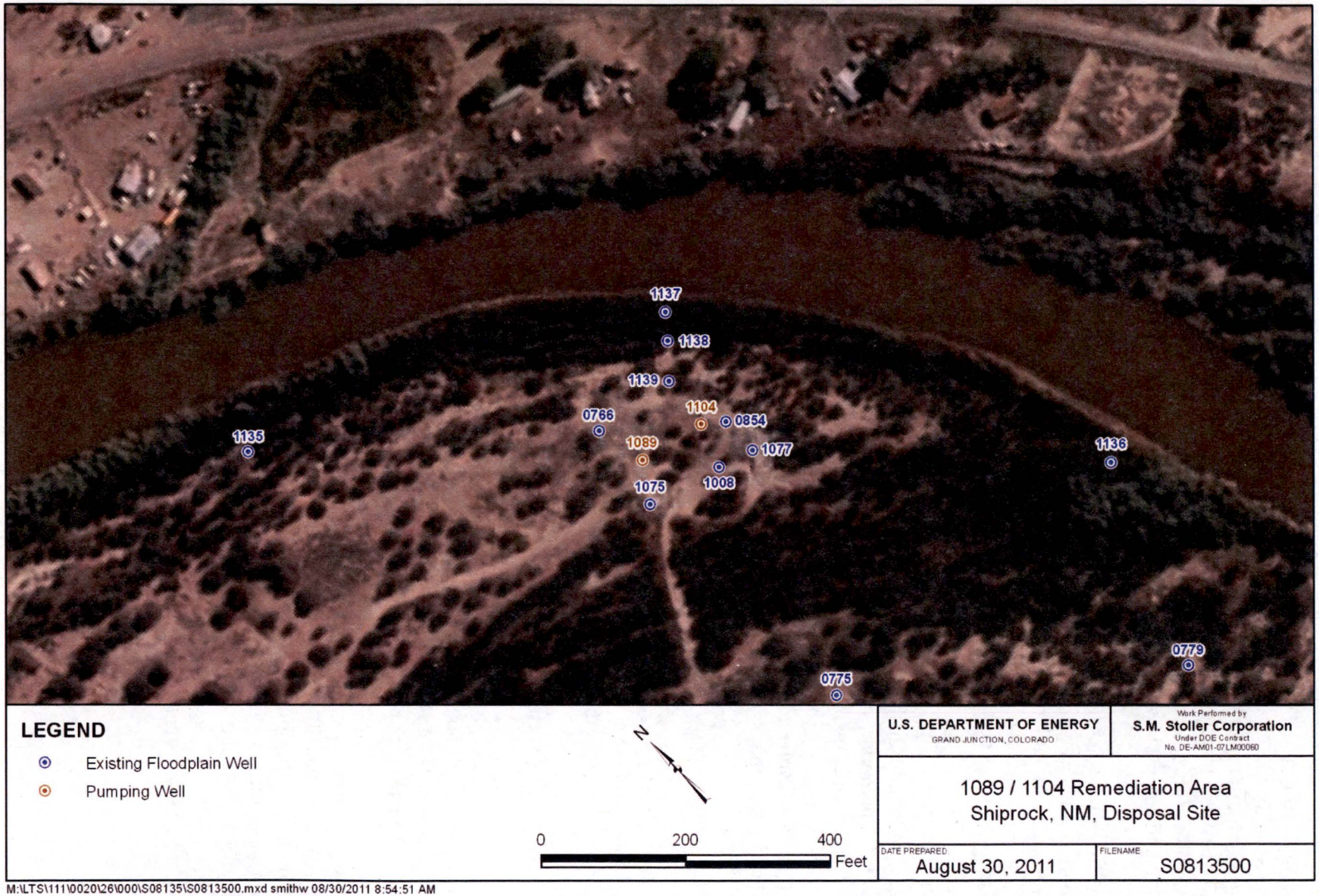

Figure 6. Wells in the 1089/1104 Remediation Area

Wells 1075 and 1077 were installed in August 2003 to a depth of about 18 ft below ground surface (bgs). Mancos Shale bedrock was encountered at a depth of about 15 ft bgs in both wells. Under conditions typically seen between midsummer and early spring, during which flows on the river are not heavily impacted by snowmelt in the mountains, the saturated alluvial thickness in these 6-inch-diameter wells when not being pumped was approximately 7 ft. Both wells used 10 ft of mill-slotted casing in their borehole segments within alluvium. Pumping began at wells 1075 and 1077 in March 2003 with the objective of extracting 10–20 gpm per well. After nearly 4 months of pumping, neither well was producing more than 3 gpm (DOE 2003b). Local water-elevation data collected at the time indicated that both pumping wells were very inefficient, meaning that water levels in each well during pumping appeared much lower than levels just outside the well casing. The low hydraulic efficiency (Driscoll 1989) was attributed to particle clogging of slots in the well casings and the gravel packs emplaced around the casings, which impeded groundwater outside of the pumping wells from flowing freely into the well casings. Despite attempts to increase their efficiency using well redevelopment techniques, the extraction rates achieved at the wells did not noticeably improve.

With the intent of replacing well 1075 as a groundwater extraction location, well 1089 was installed in June 2003 using techniques that differed from those used to install the two original pumping wells. Specifically, well 1089 was constructed using 24-inch-diameter (24-inch) steel culvert pipe in a trench excavated to bedrock, which was encountered at a depth of 14.5 ft bgs. The bottom 5 feet of the culvert pipe was torch-slotted to allow the entry of groundwater in response to pumping.

Pumping of well-1089 water into the remediation system commenced in late June 2003 (DOE 2003b), and pumping rates approaching 6 to 7 gpm were achieved at this location during the first year of the well's operation (DOE 2004, 2005a). The technical explanation for well 1089 achieving greater water production than well 1075 was never formally investigated. However, it is possible that the 24-inch pipe used for casing at well 1089 contributed to the greater pumping rate, as the large surface area of the pipe helped limit inflow velocities through the torch-cut slots in the pipe. With lower inflow velocities, the potential for clogging of the slots by entrained aquifer sediment particles was reduced. This hypothesis suggests that the hydraulic efficiency of the 24-inch culvert pipe at well 1089 was greater than the efficiency provided by the 6-inch mill-slotted casing at well 1075.

Well 1077 remained part of the floodplain remediation system through most of 2005. Pumping rates at the well typically ranged between 0.2 and 1.0 gpm and averaged about 0.5 to 0.6 gpm (DOE 2003b, DOE 2005a, DOE 2006). Using construction techniques similar to those employed for the installation of well 1089 (i.e., 24-inch, torch-slotted steel culvert used for well casing), DOE installed well 1104 in April 2005. As a replacement pumping well for well 1077, well 1104 was added to the remediation system in December 2005. Similar to the other pumping wells in the area, bedrock was observed at a depth of 14.5 ft bgs at this location. During its first 1.5 years of operation, pumping rates at well 1104 tended to range between 1 and 3 gpm. Though these rates were higher than those previously achieved at well 1077, they remained less than the pumping rates at well 1089. This indicated that factors other than well construction were likely limiting groundwater extraction from the well.

In recent years, pumping rates at well 1089 have typically ranged between 5 and 12 gpm and averaged about 6 gpm. The comparable range of rates at well 1104 has been 1 to 4 gpm, and the

average rate at this location has been about 2 gpm. Wells 1075 and 1077 continue to be used as monitoring wells that assist in evaluating remediation progress in the 1089/1104 area.

3.4.2 Trench 1 Remediation System

Trench 1 is a horizontal well constructed in the alluvial aquifer directly northwest of the former mill area, near the base of the bedrock escarpment, and about 1000 ft west-southwest of the San Juan River at the gaging station (Figure 2). As mentioned in Section 1, it recovers contaminated groundwater in the alluvial aquifer and also intercepts contaminated groundwater migrating across the Mancos Shale escarpment. The large collection area provided by the trench results in groundwater production than that achieved at either well 1089 or well 1104. The trench is approximately 200 ft in length, 2 ft wide, and 15 ft deep. The collection pipe that constitutes the horizontal well is a 4-inch-diameter, perforated, high-density polyethylene (HDPE) pipe connected to a 12-inch-diameter vertical sump pipe (sump 1110 in Figure 5). Half-inch diameter circular perforations in the pipe (two perforations on each side at 5-inch centers) allow the entry of groundwater.

Several monitoring wells located in the Trench 1 area (Figure 7) provide data that assist in evaluating remediation progress from pumping of the trench. Two of the wells, 1110-A and 1110-C, facilitate monitoring of water levels and specific conductance in groundwater occurring within gravel that was used as trench backfill surrounding the horizontal well. Figure 8, which presents a cross-section view of the Trench 1 system, refers to these two wells as ports A and C, respectively. As indicated in Figure 8, ports B and D are also screened in the trench backfill; however, no monitoring data are collected from these wells.

Water deliveries from Trench 1 into the Shiprock site remediation system began in April 2006. Except for sporadic shutdowns in pumping for maintenance and other purposes, groundwater production from the trench has been relatively constant. In recent years, periods of nonpumping have been more prolonged than in earlier years because of occasional breaks in the groundwater remediation pipeline and concerns regarding high water levels in the evaporation pond. The rate of groundwater extraction at the trench typically ranges between 5 and 12 gpm. Occasionally, pumping rates there approach 20 to 25 gpm.

Prior to the preliminary Trench 1 study (ESL 2011b) and this study of the floodplain as a whole, no attempt had been made to formally assess the extent of groundwater capture created by pumping at Trench 1. Nonetheless, general observations made regarding groundwater levels and flow patterns in areas surrounding the trench indicated that the capture zone was quite large, extending as much as 1300 ft northwest, 300–400 ft northeast, and 1800 ft southeast from the trench.

Figure 7. Trench 1 Remediation Area

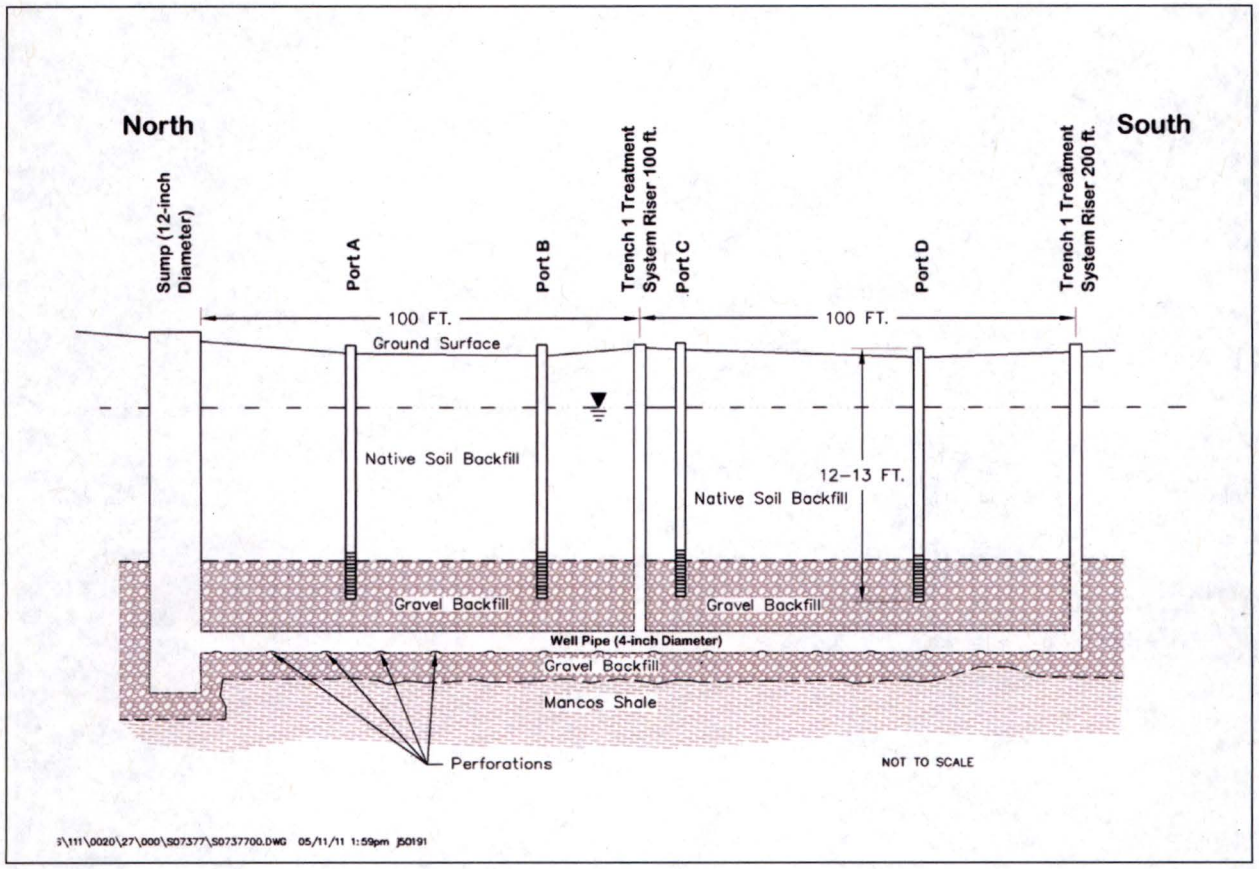

Figure 8. Cross-Section View of the Trench 1 Remediation System

3.4.3 Trench 2 Remediation System

As shown in Figure 2 and Figure 5, Trench 2 is located approximately 1900 ft southeast of Trench 1, about 1200 ft north of where the floodplain pinches out on its south end, and 160 ft west of the river. Excavated in alluvium at the base of the bedrock escarpment, Trench 2 was constructed in much the same manner as Trench 1. The horizontal well at this location is 200 ft long and lies about 15 ft bgs. The cross-section depiction of the Trench 1 system in Figure 8 generally applies to Trench 2 as well, with the exception that ports A, B, C, and D are located at different points along the excavation than occurs at Trench 1. The vertical water collection pipe on the north end of the horizontal well is referred to as sump 1109 (Figure 5), and ports A and C, screened in the trench backfill, correspond to monitoring wells 1109-A and 1109-C, respectively (Figure 5). As with Trench 1, the two monitoring wells known as Port B and Port D at Trench 2 are not used to collect water-level and water-chemistry data.

Numerous wells were installed in the area surrounding Trench 2 (Figure 9) during 2006 and 2007. Water-level and water-chemistry data collected at these monitoring locations were useful for evaluating the efficacy of this part of the remediation system during the Trench 2 evaluation (DOE 2009b), and the data also revealed key aspects of river–aquifer interaction in this part of the floodplain.

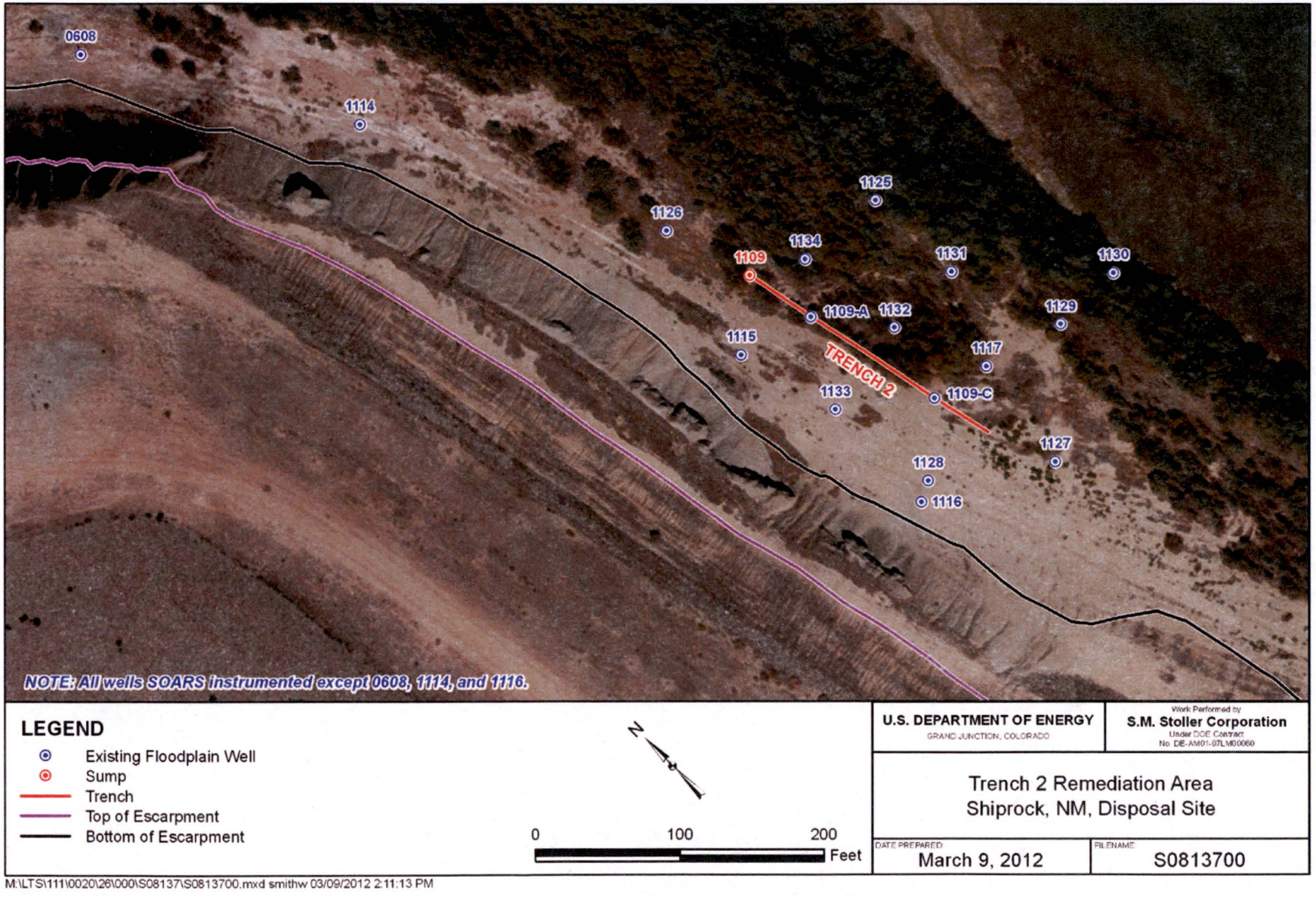

Figure 9. Trench 2 Remediation Area

Test pumping of groundwater at Trench 2 was conducted with the system during two separate multiday periods in April 2006, and continuous pumping of the system began during the first week of May 2006. In the initial 3 years following system startup, pumping rates from Trench 2 typically ranged between 15 and 20 gpm, which were higher than rates achieved at Trench 1 (typically 5–12 gpm). Though the causes of the higher pumping rates from Trench 2 versus those from Trench 1 were unclear, possible reasons include greater hydraulic conductivities for the alluvium surrounding the horizontal well at Trench 2, closer proximity of the trench to the river, and a larger area of high-permeability alluvium between the trench and the low-permeability bedrock.

Given the trench's location in the thin section of alluvium comprising the south third of the floodplain (80 ft from the base of the escarpment and 160 ft from the river), the impacts of pumping were limited to a narrow portion of the alluvial aquifer. Groundwater modeling conducted as part of the Trench 2 study indicated that the capture zone for the horizontal well extended about 400 ft to the north-northeast from the trench footprint, about midway between wells 608 and 1114 (Figure 5 and Figure 9). The pinching out of the aquifer against the bedrock escarpment on the south end of the floodplain limited groundwater capture south of the trench to a distance of about 1200 ft. Comparison of these capture extents with those estimated for Trench 1 (Section 3.4.2) indicates that the groundwater capture zone for Trench 2 is much smaller.

In recent years, groundwater extraction from the trench has been somewhat sporadic, and rates have varied from as low as 5 gpm on some occasions to as much as 20 gpm during others. The sporadic pumping is attributed to occasional pipeline breaks and concerns regarding high water levels in the evaporation pond.

3.4.4 Seep Collection Sump

During the first few years of groundwater remediation on the floodplain, subsurface water discharging from the bedrock escarpment wall at seeps 425 and 426 (Figure 5) was excluded from the remediation system. In August 2006, DOE began to capture the water in both seeps and pipe it to sump 1118, a vertical pipe installed in floodplain alluvium approximately 60 ft east of seep 425.

Prior to their inclusion in the remediation system, measured flow rates at seeps 425 and 426 were variable. Flow rates at seep 425 ranged from 0.05 to 0.8 gpm, and the rates at seep 426 varied between 0 and 2.2 gpm. The magnitudes of these flow rates provided some indication of the rates of subsurface discharge that might be expected from the terrace area to floodplain alluvium across the bedrock escarpment. The large variability in seep flows suggested that discharge rates directly to the alluvium from the terrace could also change with time. The only currently available measure of flow rates at seeps 425 and 426 is the pumping rate from sump 1118, which combines the respective discharges from these two locations. Since early August 2006, monitored daily average pumping rates from sump 1118 for delivery to the evaporation pond have ranged from 0 to 5.6 gpm and have averaged about 0.5 gpm. These pumping rates are not reflective of seep flow alone, as some groundwater seeps through openings to the sump 1118 casing.

3.5 SOARS Monitoring

The SOARS system at the Shiprock site gathers data at 5-minute intervals using sensors installed in monitoring wells, pumping wells, trench sumps, and the seep collection sump (1118). Data loggers store the monitored information, and a telemetering system transmits the stored data via telephone back to LM offices in Grand Junction, Colorado. SOARS has provided pumping rate data from wells 1089 and 1104 since late 2005, and pumping rates from the sumps at Trench 1 (location 1110) and Trench 2 (location 1109) since April 2006. At some SOARS locations affected by either pumping or changing river levels, water temperature and specific-conductance data are also collected and transmitted to the Grand Junction office.

Water-level data are automatically collected at all monitoring wells included in the SOARS network. In August 2006, well 1127 in the Trench 2 area was the first monitoring well added to the SOARS network. Since that time more than 30 additional monitoring wells have been added to the system. Several monitoring wells are monitored for specific-conductance data in addition to water levels. Sixteen monitoring wells and 4 pumping locations are also monitored for water temperature.

Figure 10 presents an aerial photograph showing all SOARS locations in the floodplain at the Shiprock site. Table 2 lists the floodplain SOARS locations, the dates they were added to SOARS, and the data automatically collected at them. The SOARS data are stored in a separate database maintained by LM. An assessment of the accuracy of data provided by many of the SOARS locations in the floodplain was presented in the preliminary evaluation of the Trench 1 system (ESL 2011b).

3.6 River Gaging Station

The USGS gaging station located on the west bank of the San Juan River at the site (Figure 2 and Figure 5) provides surface-water-level data that are collected at 15-minute intervals from a sensor installed at the station. The data consist of gage-height (stage) measurements above a reference datum, which are translated into estimated river flows. The flow estimates are developed from rating-curve (Kennedy 1984) information, which is periodically updated using actual field-based measurements of river flow. USGS transmits the 15-minute stage data to a central location using a telemetering system.

USGS publishes stage and flow data for its surface-water gaging stations through Internet sites that it maintains. The universal resource locator for the station at the Shiprock site is http://waterdata.usgs.gov/nwis/inventory?agency_code=USGS&site_no=09368000. Data collected on 15-minute intervals can be downloaded from the Internet by the public for the most recent 120-day period of time. Daily average river flows are available from the Internet site for times preceding the 120-day time span; estimated flows from as early as October 1934 are available.

Table 2. SOARS Monitoring Locations

Location	Location Type/ Description	Date Instrumented	Location on Floodplain	Data Collected			
				Water Level	Specific Conductance	Temperature	Pumping Rate
735	Monitoring Well[a]	Mar-11	South end of floodplain	x		x	
766	Monitoring Well	Aug-09	1089/1104 Area	x	x	x	
779	Monitoring Well[a]	Mar-11	Near USGS Gage	x		x	
793	Monitoring Well	Aug-09	~400 ft east-northeast of Trench 1	x	x	x	
853	Monitoring Well[a]	Mar-11	~700 ft east of Trench 1	x		x	
854	Monitoring Well	Oct-09	1089/1104 Area	x	x	x	
857	Monitoring Well[a]	Mar-11	Near USGS Gage	x		x	
1008	Monitoring Well	Oct-09	1089/1104 Area	x	x	x	
1009	Monitoring Well	Aug-09	~350 ft east of Trench 1	x	x	x	
1075	Monitoring Well	Aug-09	1089/1104 Area	x	x	x	
1077	Monitoring Well	Oct-09	1089/1104 Area	x	x	x	
1089	Pumping Well	Dec-05	1089/1104 Area	x	x	x	x
1104	Pumping Well	Nov-05	1089/1104 Area	x	x	x	x
1105	Monitoring Well	Oct-09	Trench 1 Area	x	x	x	
1109	Trench 2 Sump	Apr-06	Trench 2 Area	x	x	x	x
1109-A	Trench 2 Port A	Mar-07	Trench 2 Area	x			
1109-C	Trench 2 Port C	Mar-07	Trench 2 Area	x			
1110	Trench 1 Sump	Apr-06	Trench 1 Area	x	x	x	x
1110-A	Trench 1 Port A	Oct-09	Trench 1 Area	x	x	x	
1110-C	Trench 1 Port C	Oct-09	Trench 1 Area	x	x	x	
1111	Monitoring Well	Oct-09	Trench 1 Area	x	x	x	
1112	Monitoring Well	Oct-09	Trench 1 Area	x	x	x	
1115	Monitoring Well	Mar-07	Trench 2 Area	x	x		
1117	Monitoring Well	Mar-07	Trench 2 Area	x	x	x	
1118	Collection Sump for Seeps 425 and 426	Aug-06	Between Trench 1 and mouth of Bob Lee Wash	x			x
1125	Monitoring Well	Mar-07	Trench 2 Area	x			
1126	Monitoring Well	Mar-07	Trench 2 Area	x			
1127	Monitoring Well	Aug-06	Trench 2 Area	x			
1128	Monitoring Well	Mar-07	Trench 2 Area	x			
1129	Monitoring Well	Mar-07	Trench 2 Area	x			
1130	Monitoring Well	Mar-07	Trench 2 Area	x			
1131	Monitoring Well	Mar-07	Trench 2 Area	x			
1132	Monitoring Well	Mar-07	Trench 2 Area	x	x	x	
1133	Monitoring Well	Mar-07	Trench 2 Area	x			
1134	Monitoring Well	Mar-07	Trench 2 Area	x			
1135	Monitoring Well[a]	Mar-11	~500 ft north-northwest of well 1089	x		x	
1136	Monitoring Well[a]	Mar-11	~750 ft south-southeast of well 1089	x		x	
1137	Monitoring Well	Mar-10	1089/1104 Area	x	x	x	
1140	Monitoring Well	Oct-09	Trench 1 Area	x	x	x	
1141	Monitoring Well	Oct-09	Trench 1 Area	x	x	x	

Note:
[a] Instrumented in 2011 for this study.

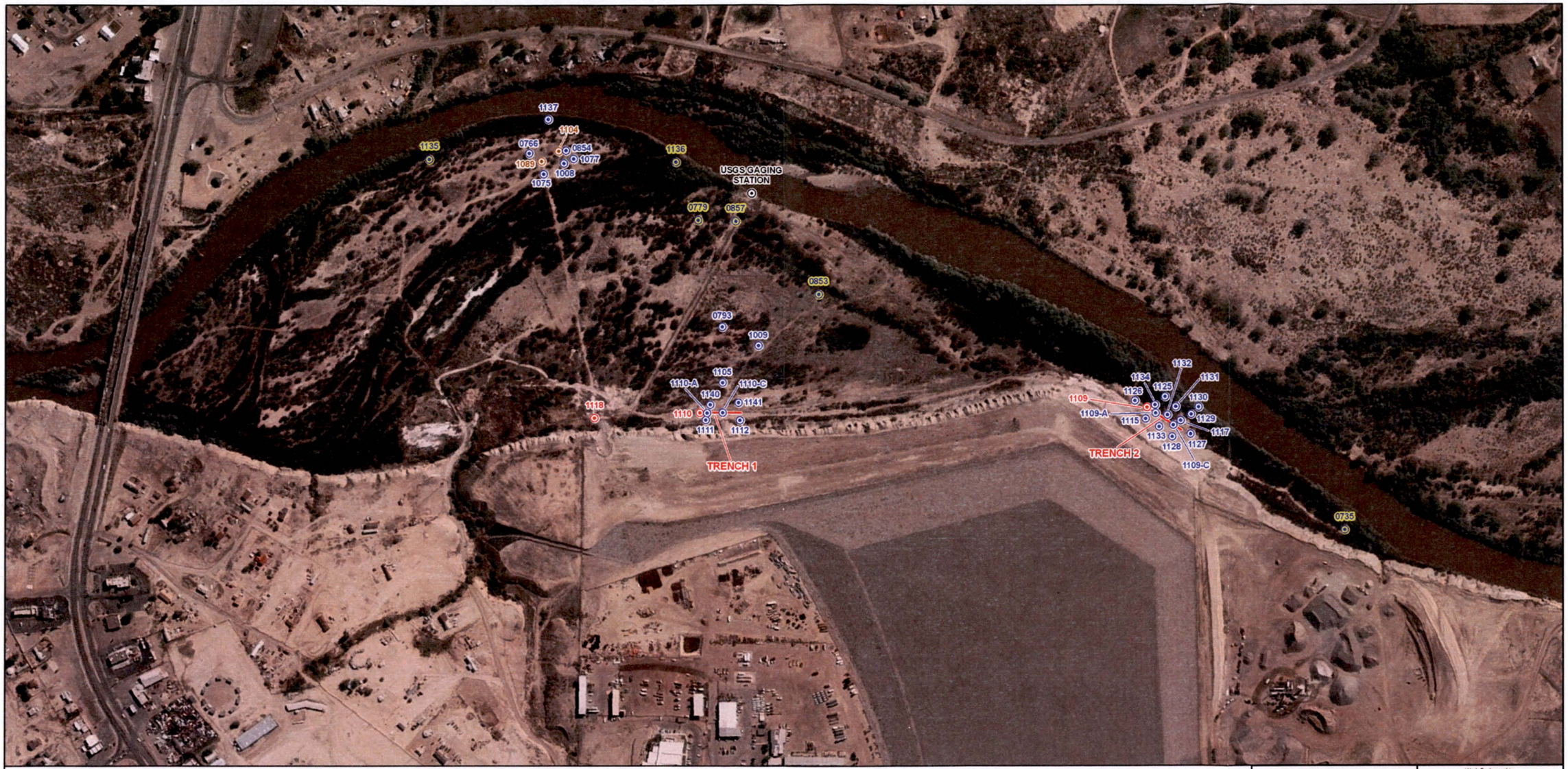

Figure 10. SOARS Monitoring Locations

This page intentionally left blank

As mentioned in Section 3.1, the USGS gaging station was located about 500 ft upstream of the Highway 491 bridge between September 1994 and early summer 2006 (Figure 3). When moved to its current location on the Shiprock site (0.6 mile upstream of the bridge, Figure 2 and Figure 5) on June 13, 2006, USGS constructed the station such that gage-height readings would be identical to those measured at the previous location. This step meant that, if needed for this or a future study, surface-water elevations at the current gage location could be reconstructed for several consecutive years beginning in October 1995. Such an extended record of surface-water elevations adjacent to the floodplain could be useful for determining how and to what degree the river impacts groundwater flow in the alluvial aquifer each year.

This page intentionally left blank

4.0 Existing Conceptual Model

Prior to conducting this latest study of floodplain groundwater, DOE had viewed annual remediation performance results at the site mostly from the perspective of a hydrogeologic conceptual model presented in the SOWP (DOE 2000). When pumping was first proposed in what is now the 1089/1104 area, DOE used the SOWP conceptual model to roughly envision how groundwater extraction in this particular locale (close to the river and distant from the escarpment) might impact baseline groundwater flow patterns and associated contaminant plume configurations delineated in the late 1990s and early 2000s. Using information presented regarding hydraulic inefficiencies at pumping wells 1075 and 1077 (Section 3.4.1), as reported in a revised conceptual model of the Shiprock site (DOE 2005b), rough predictions of the influence of Trenches 1 and 2 on groundwater flow and transport beneath the floodplain were similarly made prior to their installation in spring 2006. The hydraulic and water-chemistry data collected and analyzed during the subsequent evaluation of the Trench 2 remediation system (DOE 2009b) further enhanced DOE's understanding of groundwater flow processes in the alluvial aquifer and helped complete the existing conceptual model of the floodplain's hydrogeology, which was used to plan this study.

This section summarizes the existing conceptual model of groundwater flow processes in the floodplain alluvial aquifer and examines how the flow potentially contributed to observed historical contaminant distributions in the aquifer. The following sections discuss physical characteristics of the alluvial aquifer, hypotheses regarding water exchange between the aquifer and the San Juan River, groundwater flow patterns and aquifer water budgets under baseline (nonpumping) conditions, historical contaminant plume configurations in the alluvial aquifer, and expected flow patterns under remediation (pumping) conditions. The existing model is based on a compendium of findings from pre-2011 investigations, dating back to as early as site characterization work in the mid-1980s and extending through the initial and final versions of the SOWP (DOE 1995b, 2000), the refined conceptual model (DOE 2005b), and the Trench 2 evaluation (DOE 2009b). Using more recent information and data analyses conducted from 2011 to 2015, including simulations of groundwater flow with the floodplain wide numerical model, the conceptual model is subsequently updated in Section 8.0.

4.1 General Hydrogeology

Floodplain groundwater occurs primarily within Quaternary alluvium that overlies Mancos Shale of Cretaceous age. The alluvial aquifer is considered unconfined over most of the floodplain and consists largely of unconsolidated sand, gravel, and cobbles (basal gravels) that were deposited by the San Juan River on Mancos Shale bedrock. In most areas on the floodplain, finer-grained alluvial sediments consisting of fine- to coarse-grained sand, silt, and some clay overlie the basal gravels. The thickness of the shallow, finer-grained alluvium ranges from about 2 to 6 ft in the south third of the floodplain to approximately 8 to 12 ft in the north half. The combined thickness of basal gravels and fine-grained surficial materials varies considerably across the floodplain but can be as much as 25 ft on the floodplain's north end. The uppermost few feet of Mancos Shale below the alluvium is typically soft and weathered.

The surface of the Mancos Shale bedrock beneath the floodplain is irregular. To a large degree, this irregularity was caused by prehistoric flows of the river that incised the bedrock surface, creating paleochannels that were subsequently filled with coarse-grained sediments. The

presence of such channels is expected given the preponderance of the basal gravels, which are typically the bed load deposits associated with high-energy environments of rapidly flowing streams and rivers. Previous investigations of the floodplain hydrology at the site (DOE 1995b, Tsosie 1997, DOE 2000) have suggested specific locations for the suspected paleochannels, but the surmised bedrock surfaces vary greatly between the studies, suggesting that bedrock topography beneath the floodplain remains uncertain. In general, bedrock elevations decrease from south to north, ranging from about 4885 ft above mean sea level (amsl) near the southern tip of the floodplain to slightly above 4860 ft amsl on the north end of the floodplain. In comparison, the land surface elevation is relatively flat, ranging from about 4896 to 4887 ft amsl, with no visually apparent trends in surface elevation from south to north.

The saturated thickness of the floodplain alluvial aquifer under baseline flow conditions varies both spatially and with time. Temporal variations in saturated thickness at any given location, which may be as large as 3 to 4 ft, are primarily caused by seasonal changes in river stage, with the highest stages occurring most often in May or June. During low-flow periods on the river, the aquifer's saturated thickness varies from about 4 to 5 ft on the floodplain's south end to 15 to 20 ft on the north end. Depth to groundwater when not affected by high river stage generally ranges from 3 to 7 ft in most parts of the floodplain. The shallowest groundwater in the floodplain is observed in the wetland area near the mouth of Bob Lee Wash.

The hydraulic conductivity of the floodplain alluvium has the potential to vary by more than an order of magnitude (e.g., 5–300 ft/day), with the coarse basal materials generally having the largest conductivities. Given the relatively thin saturated thickness of the alluvial aquifer ($\leq$20 ft), groundwater flow has typically been described as two-dimensional and horizontal. Accordingly, the limited saturated thickness makes it difficult to characterize any vertical groundwater movement between the shallowest and deepest alluvial sediments. The hydraulic conductivities used to represent the aquifer are intended to represent the combined, effective permeability of both the deeper and shallow alluvium.

Though some of the earliest modeling investigations of the alluvial aquifer (DOE 1995, Henry 1995) used a hydraulic conductivity of 35 ft/day to simulate flow in the floodplain subsurface, more recent investigations suggest that larger values are more representative of the aquifer as a whole. An analysis of data collected during an 18-hour aquifer pumping test conducted at well 858 (DOE 2000) indicated that hydraulic conductivity of the aquifer could be as great as 110 ft/day, and the calibrated model developed for the SOWP used a representative value of 100 ft/day. Calibration of the model developed for the Trench 2 evaluation (DOE 2009b) indicated that 85 ft/day was a value reflective of the south third of the floodplain. These latter values suggest that effective hydraulic conductivities in most areas of the aquifer range between 50 and 130 ft/day and are mostly representative of the deeper basal gravels.

Groundwater flow in the south half of the alluvial aquifer is generally from south to north, whereas flow directions ranging from northwest to northeast are observed in the northern half due to groundwater mounding at the mouth of Bob Lee Wash. Horizontal hydraulic gradients in the aquifer under baseline flow conditions vary between dimensionless values of 0.001 and 0.003, and the largest gradients are often observed in the vicinity of the groundwater mounding.

Though it is well known that seasonal changes in river flow often lead to temporary changes in groundwater level of a foot or more in the alluvial aquifer, the groundwater domain has been

treated as a steady-state flow system in previous investigations that incorporate numerical modeling (DOE 1995a, 2000, 2009b; Knight Piesold 2002). This conceptualization effectively assumes that flow directions and groundwater velocities remain relatively constant despite the fact that water elevations are susceptible to change. In comparison, simulations of contaminant transport at the site to evaluate remediation approaches have, by necessity, been transient in nature. However, other than the changing groundwater conditions induced by groundwater pumping, the boundary conditions (e.g., river elevations) and other processes invoked in the flow portions of the transient simulations have been treated as steady-state phenomena.

Because groundwater flow has traditionally been viewed as a steady-state process in numerical models of the site, limited effort has been made to quantify aquifer storage properties that determine how, for instance, the rate at which groundwater levels increase in response to increases in river stage. The sole aquifer pumping test performed in the alluvial aquifer (at well 858) produced estimates of both aquifer storativity (0.0006–0.0008) and specific yield (0.05–0.12) (DOE 2000). Short-term (<1 day) responses of groundwater level to hydraulic stresses such as pumping tend to be governed by storativity, whereas specific yield is expected to determine the longer-term response. If the floodplain system truly behaves like an unconfined aquifer, the use of a specific yield value in flow models of the aquifer should result in more accurate predictions of water-level change. Ideally, specific yield estimates stemming from aquifer tests should be close in value to aquifer porosity, which is expected to be somewhere between 0.2 and 0.35 (20 to 35 percent). The flow and transport modeling performed for the SOWP (DOE 2000) used a porosity of 0.3 to represent the alluvial aquifer.

The observed 3-fold increase in saturated thickness from south to north in the alluvial aquifer implies that groundwater flow increases along the floodplain's 5800 ft length. This gradual increase in flow is caused by various water sources that add to the groundwater system with flow distance to the north. The following report sections describe groundwater flow patterns typically seen in the alluvial aquifer and the nature of water sources contributing to the flow.

4.2 River–Aquifer Exchange

Under low- to average-flow conditions on the San Juan River, surface water is expected to seep laterally from the river into the aquifer at river pools located upstream of distinct riffles, with much of this water returning to the river below the downstream end of the riffles. This sequence of river loss followed by return flow, as dictated by basic principles of water hydraulics, leads to the hyporheic zones that can impact groundwater chemistry (Winter et al. 1998). In addition to surface water seeping laterally into the aquifer, the river loses water to riverbed sediments near the upstream ends of riffles, creating hyporheic zones beneath the river as well (Harvey and Wagner 2000). The extent of water incursion into riverbed and aquifer sediments is affected by the rate of decrease in river elevation along each riffle, with steeper riffles causing larger incursions.

Seepage losses from multiple, sequential pool-and-riffle sequences can create a nested subsurface flow network (e.g., Bencala et al. 2011), in which two or more shorter hyporheic flowpaths are "nested" between the starting (river loss) and ending (river gain) parts of larger hyporheic flowpaths. The illustration in Figure 11 shows an aerial view of a hypothetical nested system containing three separate hyporheic flowpaths associated with two river riffles separating three pools. The concept of nested hyporheic flow can be expanded to envision how some longer

subsurface flowpaths have the capacity to span several smaller hyporheic zones. Nested flowpaths of this type appear to occur at the Shiprock site, such that the river becomes an important source of much of the groundwater migrating from south to north through the southern two-thirds of the alluvial aquifer.

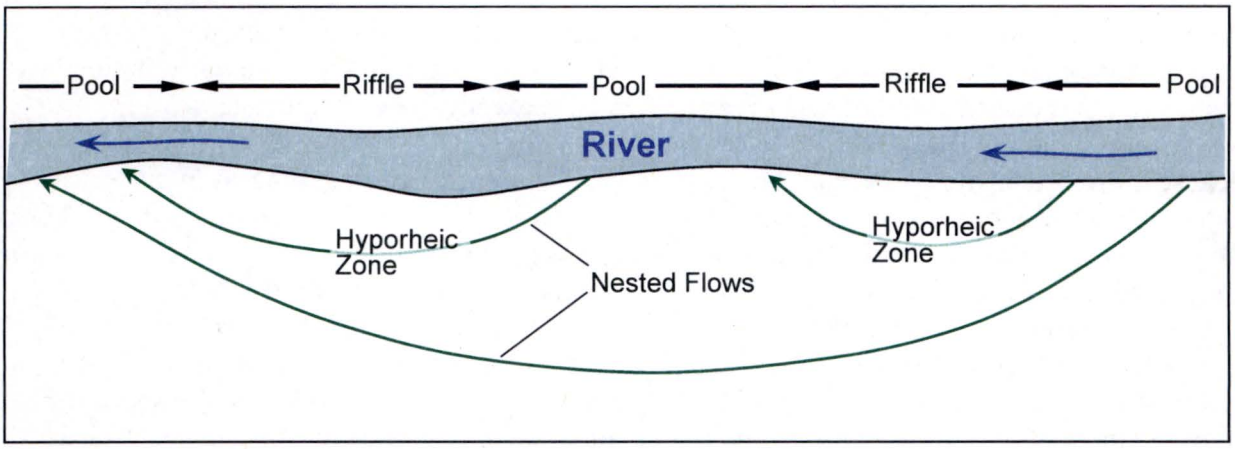

Figure 11. Aerial View of Hyporheic Flow Processes in Aquifers Adjacent to Rivers

The expressions "hyporheic zone" and "hyporheic flow" are used liberally in this report. Recent scientific papers on groundwater/surface-water interactions (e.g., Bencala 2011) have tended to ascribe these descriptors to flowpaths that are on the order of tens of feet long and in which the residence time of the infiltrated surface water within the subsurface is limited to hours to several days. This contrasts with identified flowpaths that are hundreds or thousands of feet long and residence times that encompass months or years. As discussed in subsequent sections, hyporheic flowpaths in this study can vary in length from a few hundred feet to more than 1000 ft. As long as the river water lost to the alluvial aquifer returns to the river prior to reaching the north end of the floodplain, the aquifer area affected by this flow is considered a hyporheic zone.

Though alluvial aquifer flow is commonly assumed to be a steady-state process, the increased river stages that occur each May and June due to snowmelt runoff probably cause the river to lose additional water to the aquifer. This is a temporary phenomenon called bank storage (Winter et al. 1998), as the lost water typically returns to the river with passage of the high-river flow. Nonetheless, the seasonal incursion of river water into aquifer sediments has the potential to affect flow patterns close to the river as well as influence local groundwater chemistry. Generally, bank storage impacts on floodplain groundwater persist longer if the aquifer behaves like an unconfined flow system.

4.3 Baseline Flow Conditions

Taking into consideration the numerous phenomena affecting groundwater in the floodplain, Figure 12 presents a map view of groundwater flow patterns expected in the alluvial aquifer under baseline (nonpumping) conditions. This illustration depicts the flow system as existing in a steady state, with four water sources (recharge from Bob Lee Wash, river losses, recharge from precipitation, bedrock discharge) contributing to aquifer inflow, and two processes (evapotranspiration, river gains) contributing to aquifer outflow. Figure 13 shows a cross-section view of the conceptualized groundwater domain. This latter graphic is not to scale and is

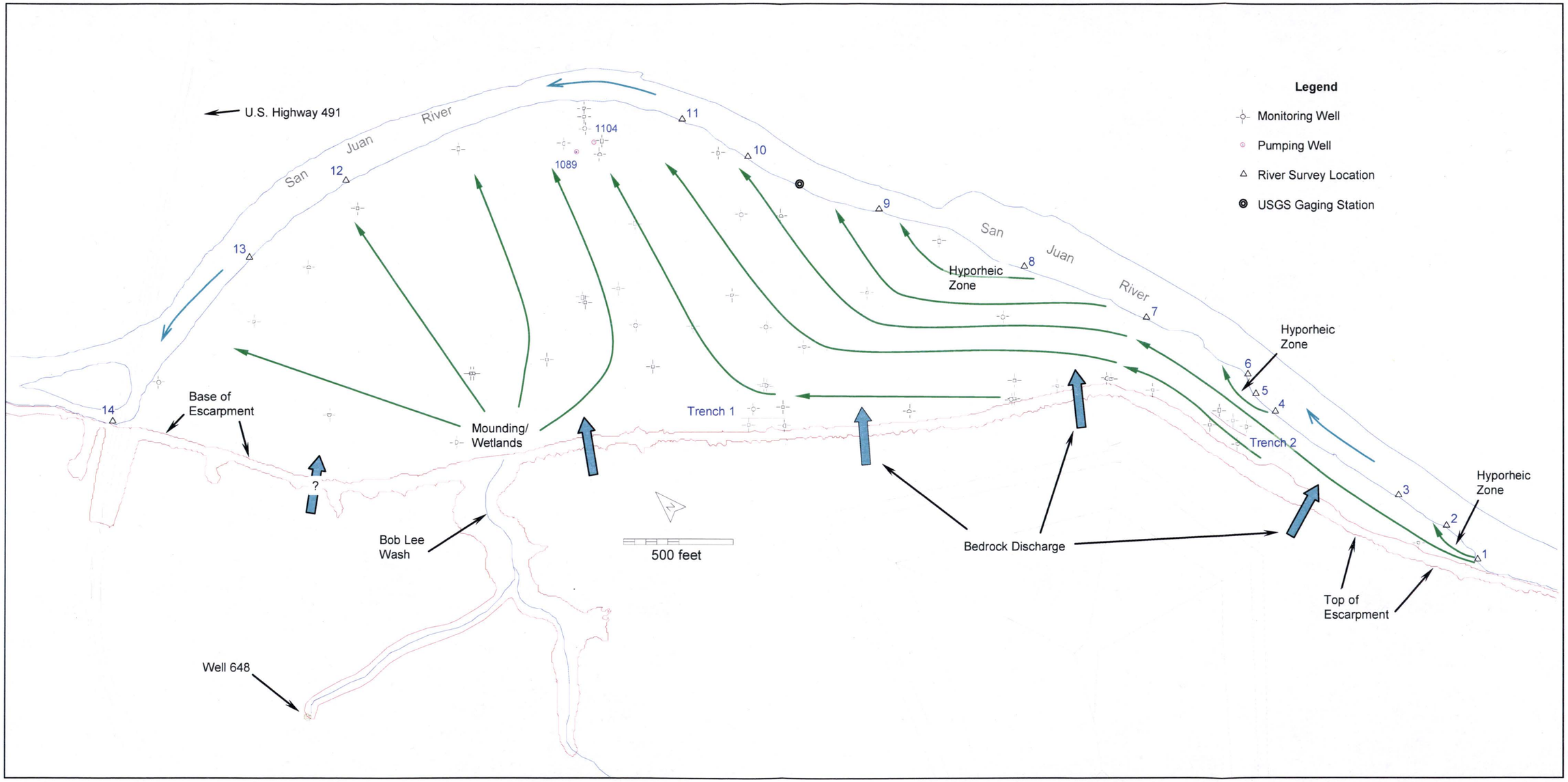

Figure 12. Map View of the Groundwater Flow Conceptual Model for Baseline (nonpumping) Conditions

This page intentionally left blank

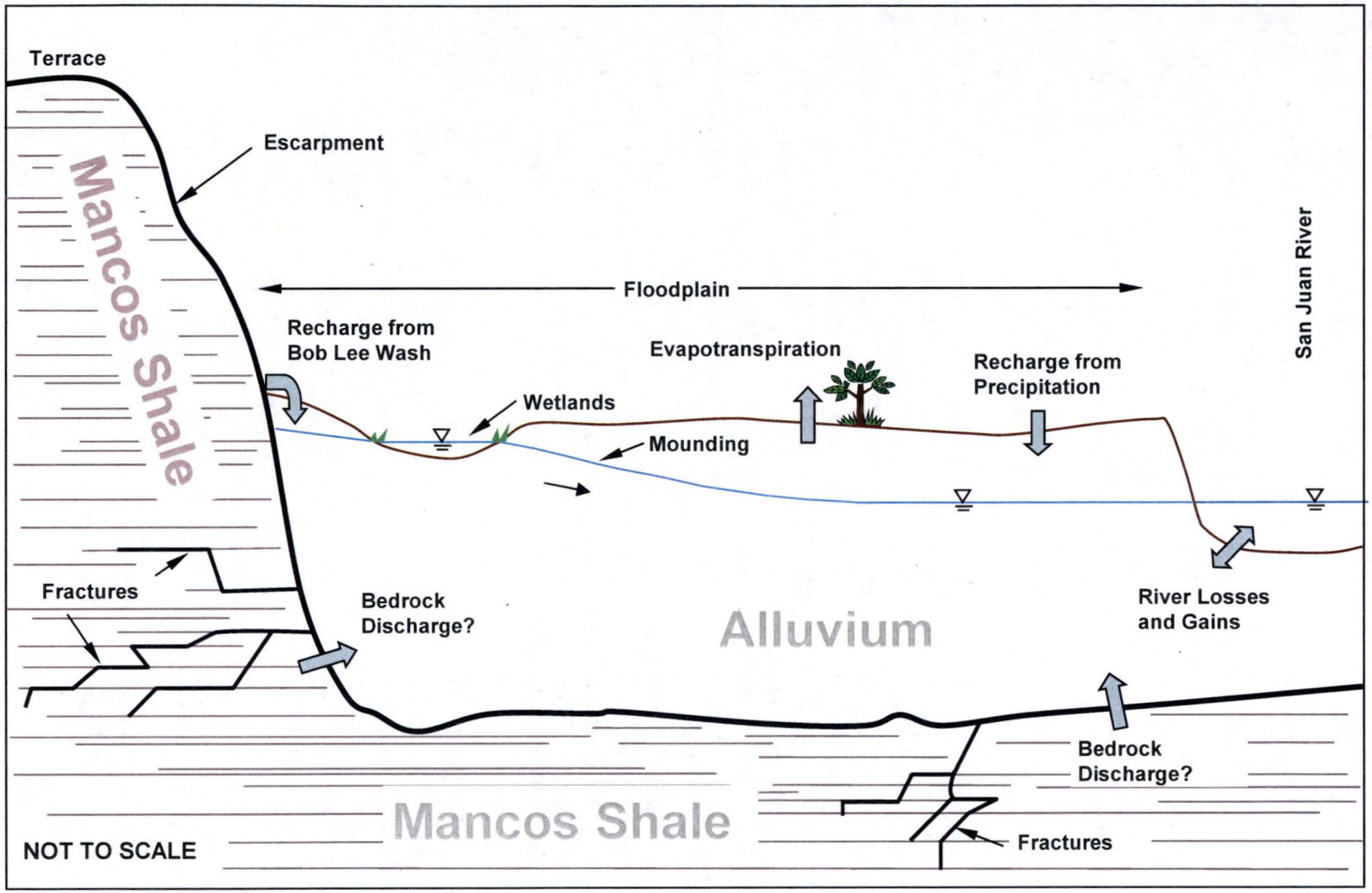

Figure 13. Cross-Section View of the Groundwater Conceptual Model for Baseline (nonpumping) Conditions

intended only to show the hydrologic processes that influence flow in the alluvial aquifer; i.e., it does not represent an actual section through the aquifer. As a consequence, some features shown in the graphic, such as the sloping water table, may appear distorted.

Figure 12 is similar to a map of generalized flow components adopted in the SOWP (DOE 2000, Figures 4–13), in which flow in the south half of the floodplain mostly parallels the river. Most of this water is assumed to originate as river losses that occur at pools on the upstream ends of three assumed hyporheic zones. The three assumed hyporheic flowpaths in Figure 12 coincide with riffles that are identified visually using simple descriptive criteria, as discussed later in Section 5. Groundwater in the north half of the floodplain exhibits considerably different patterns, with mounding at the mouth of Bob Lee Wash dominating local flow and causing water to spread radially from the wash outlet and eventually discharge to the river. The mounding, which can lead to periodic surface-water ponding (Figure 13), helps divert groundwater in the Trench 1 area northward to the 1089/1104 area where it subsequently discharges to the river.

Figure 12 shows bedrock discharge from the terrace area occurring along the entire length of the escarpment between the south end of the floodplain and the Bob Lee Wash outlet. As discussed in site reports, most of the discharge is assumed to occur through bedding plane fractures or less hydraulically resistant layers in the shale (Figure 13). The SOWP conceptual model indicated that the bedrock discharge was, in some form or another, a legacy of the former mill (e.g., raffinate water, leached tailings water, transient drainage from the disposal cell). This observation was premised on high salinity and relatively large concentrations of sulfate, nitrate, and uranium in alluvial groundwater at the base of the escarpment from the south end of the floodplain to Bob Lee Wash. A numerical model of groundwater flow and contaminant transport presented in the SOWP (DOE 2000) assumed that the source for the contamination was spatially limited to the disposal cell footprint, and an updated version of that model prepared by Knight Piesold (2002) was based on the same assumption. Thus, the assumed bedrock discharge of contaminants at high concentrations to the floodplain between its south end and Bob Lee Wash implies that contamination originating in the footprint historically migrated in terrace groundwater at least 1000 ft to the southeast from the cell area and 1400 ft to the northwest from the cell area.

Prior to the start of remediation pumping from Trenches 1 and 2 in 2006, confirmation of high-salinity bedrock discharge between the south end of the floodplain and Trench 1 was provided by high constituent concentrations observed over several years in numerous wells at the base of this portion of the escarpment (e.g., wells 735, 1133, 608, 611, 614, 1111, 1112, Figure 5). Since 2006, the elevated concentrations at these near-escarpment locations have fluctuated, but generally decreased. Much of the general concentration decrease can be attributed to induced inflows of river water by pumping from the trenches. Discharge of bedrock groundwater across the escarpment between Trench 1 and Bob Lee Wash has been inferred from historically high constituent concentrations measured in samples from seeps 425 and 426 and, during recent years, at sump 1118 (Figure 5).

It is unknown whether terrace groundwater discharges to the alluvial aquifer between Bob Lee Wash and the north end of the floodplain, given that no monitoring wells are located directly at the base of the escarpment in this area. Thus, the arrow in Figure 12 signifying bedrock discharge northwest of the wash is flagged with a question mark. It is possible that flowing artesian water from well 648 may percolate into Mancos Shale bedrock along the tributary

connecting the well and Bob Lee Wash (Figure 12), thereby providing groundwater that could eventually discharge to the alluvial aquifer in areas north of the wash.

The cross-sectional depiction of the existing conceptual model (Figure 13) allows for possible bedrock discharge to the alluvial aquifer at significant distances from the escarpment via fracture flow in the underlying Mancos Shale. Such an inflow source was mentioned as a possibility in the Trench 2 evaluation (DOE 2009b), but no evidence could be found during the evaluation for bedrock discharge far from the escarpment. There was, however, indirect evidence of bedrock discharge, in the form of persistently high specific conductances during trench pumping at well 1126 (Figure 5 and Figure 9), northwest of Trench 2 and approximately 65 ft from the escarpment. To date, no other studies have been conducted to evaluate whether bedrock discharge occurs at greater distances from the escarpment. The preliminary evaluation of Trench 1 (DOE 2011) suggested that discharge of bedrock groundwater near the river could be a source of high contaminant concentrations in the 1089/1104 area.

ET of groundwater, representing a combination of bare-ground evaporation from a shallow water table, water transpiration from shallow-rooted plants, and water transpiration by phreatophyte vegetation rooted in saturated alluvium, is a component of groundwater outflow. However, ET was not explicitly evaluated in the conceptual and numerical models presented in the SOWP (DOE 2000); rather it was implicitly taken into account when developing estimates of areal recharge (i.e., net recharge) from precipitation. Moreover, because groundwater flow beneath the floodplain is assumed to be at steady state, the existing conceptual model does not account for the potentially significant effects of ET from extensive floodplain vegetation between the growing months of mid-April through late-October.

Though it is likely that areal recharge from precipitation occurs across the floodplain (Figure 13), the average rate of recharge remains uncertain. In the steady-state model developed for an earlier version of the SOWP (DOE 1995b), DOE (1995a) estimated that areal recharge was substantial, amounting to about a quarter of total inflow to the alluvial aquifer. In comparison, a separate calibrated model developed by Henry (1995) used a low average recharge rate of 0.2 inch per year (in/yr), which represented 2 percent of the total simulated inflow. In the model developed for the final SOWP (DOE 2000), the assumed recharge rate was 2.1 in/yr, and areal recharge from precipitation was about 12 percent of total aquifer inflow. Such a wide range of estimated recharge values is not surprising given that recharge rates are difficult to measure in field studies, rates can vary substantially with location, and recharge is a component of a flow model that can be arbitrarily increased or decreased in proportion to the assumed hydraulic conductivity for an aquifer.

4.4 Water Budget

The final design of the groundwater remedy at the Shiprock site, as presented in the GCAP (DOE 2002), was not based on the numerical model prepared for the SOWP (DOE 2000), but rather a revised version of that model prepared by Knight Piesold (2002). Components of the estimated water budget used to assist in developing the earlier model were presented in tabular form in the SOWP, but a comparable table for the Knight Piesold model was not formally published. This section describes the SOWP flow model (DOE 2000) and summarizes how inputs to that model were revised to develop the Knight Piesold (2002) model.

The SOWP model (DOE 2000) consisted of four layers, with top-to-bottom layers for the terrace representing terrace alluvium (layer 1), weathered Mancos Shale (layer 2), and the upper and lower layers of unweathered (competent) Mancos Shale (layers 3 and 4). In the floodplain, all four model layers were used to represent the alluvial aquifer. Though seasonal changes on the San Juan River were known to affect groundwater elevations and, potentially, groundwater flow directions in the alluvial aquifer, the model assumed that groundwater flow could be treated as a steady-state process. The flow system simulated in the model was considered representative of hydrogeologic conditions in 2001. This approach effectively assumed that flow directions did not change materially as groundwater elevations increased and decreased due to seasonal variations in river elevation or changes in other hydrologic stresses such as aerial recharge from precipitation or evapotranspiration.

The final, calibrated version of the flow model in the SOWP (DOE 2000) was developed using a uniform hydraulic conductivity of 100 ft/day for all four layers representing the floodplain alluvium. Hydraulic conductivities of 10, 0.2, and 0.1 ft/day were assigned uniformly to terrace alluvium (Layer 1), terrace weathered Mancos Shale (Layer 2), and terrace unweathered shale (Layers 3 and 4), respectively. The magnitudes of some components of the resulting computed water budget for the alluvial-aquifer portion of the calibrated steady-state model were specifically listed in the SOWP (DOE 2000). To arrive at a complete model budget for the purposes of this report, the remaining components were estimated using additional calculations presented in the SOWP. Table 3 presents the resulting water budget.

Table 3. Estimated Water Budget for the Alluvial Aquifer in the SOWP Steady-State Flow Model

Flow Component	(ft^3/day)	(gpm)	(%)
Inflow			
Seepage losses from the river	3,600	18.7	16
Infiltration of precipitation	2,600	13.5	12
Recharge from Bob Lee Wash	12,320	64.0	56
Bedrock discharge across the escarpment	3,600	18.7	16
Outflow			
Discharge to the river	22,120	114.9	100

The sum of the individual inflow components in Table 3 indicates that the total inflow to the alluvial aquifer in the SOWP model (DOE 2000) was 22,120 cubic feet per day (ft^3/day) (114.9 gpm). The largest source of inflow was attributed to the recharge of flows from Bob Lee Wash, which amounted to 12,320 ft^3/day, or 56 percent of the total inflow (Table 3). The next largest inflow components consisted of equal quantities of river loss to the aquifer and bedrock discharge across the escarpment, with each being 3600 ft^3/day (18.7 gpm). Though the bedrock inflow component represented a relatively small portion (16 percent) of the total estimated water inflow, high concentrations of contaminants in the inflowing Mancos Shale groundwater showed large impacts on alluvial aquifer chemistry (DOE 2000). The estimated discharge to the river of 22,120 ft^3/day (114.9 gpm), all of which occurred along the north half of the floodplain, was assumed to be the only outflow component of the water budget for the alluvial aquifer (Table 3).

Knight Piesold (2002) used the flow model from the SOWP (DOE 2000) to develop revised estimates of groundwater flow components in both the terrace and floodplain portions of the

groundwater system. Though the assumed recharge from infiltration of Bob Lee Wash flow in the revised model was set equal to the wash inflow adopted in the previous model (12,320 ft^3/day or 64 gpm) and the hydraulic conductivity assigned to the alluvial aquifer was identical to the value used in the SOWP (100 ft/day), some model inputs were treated as uncertain and variable. In particular, the hydraulic conductivities for the terrace alluvium and the weathered and unweathered Mancos shale were allowed to vary (Knight Piesold 2002), as was the rate of recharge from precipitation on the alluvial aquifer. With this approach, multiple stochastic (probabilistic) simulations were conducted with the model using random combinations of the variable parameters. Upon completing the simulations, an optimal combination of model inputs was identified, such that the resulting model comported well with the results from aquifer testing in both the terrace and alluvial-aquifer groundwater systems. The optimal Knight Piesold (2002) model used hydraulic conductivities of 11, 0.0012, and 0.02 ft/day, respectively, for the terrace alluvium, unweathered Mancos Shale bedrock, and weathered Mancos Shale bedrock, which were 110, 1.2 and 10 percent of their SOWP counterparts. In addition, the final rate of recharge from precipitation was set at 0.18 in/yr, whereas the rate in the SOWP model (DOE 2000) was 2.1 in/yr.

Because the hydraulic conductivities for the Mancos Shale in the revised model were considerably lower than those used earlier, the volumetric rate of groundwater discharge across the bedrock escarpment in the Knight Piesold (2002) model was expected to be lower than that computed in the final SOWP model (DOE 2000). However, the model-computed inflow to the alluvial aquifer from the Mancos Shale is unknown because the revised water budget for the alluvial aquifer was not reported in either the Knight Piesold (2002) report or the GCAP (DOE 2002). Similarly, river losses to the aquifer and aquifer discharges to the river in the revised model remain unknown. The combination of the above-mentioned aerial recharge rate of 0.18 in/yr and a total floodplain area of 124 acres suggests that the volumetric recharge rate from precipitation on the floodplain in the revised model was about 220 ft^3/day, or 1.1 gpm. This value is only about 8 percent of the recharge rate applied in the calibrated SOWP model (DOE 2000).

Using the revised, optimal model, Knight Piesold (2002) performed transient simulations of uranium transport to assess a groundwater remediation approach that called for the installation of a 4000 ft long slurry wall and associated interceptor drain at the base of the Mancos Shale escarpment. The proposed barrier extended from near the south end of the floodplain to about 500 ft southeast of the mouth of Bob Lee Wash. Information presented subsequently in the GCAP (DOE 2002) indicated that the Knight Piesold (2002) model predicted the interceptor drain would capture about 3–5 gpm of flow from the terrace via discharge from the Mancos Shale across the escarpment. This range of discharge values, which provided some indication of the rate of groundwater inflow from the terrace to the alluvium between the south end of the floodplain and Bob Lee Wash, suggested that the flow across the escarpment in the final Knight Piesold (2002) model was somewhere between a sixth and a third of the bedrock inflow used in the SOWP (DOE 2000) model (18.7 gpm).

4.5 Historical Contaminant Plumes

Groundwater flow patterns shown in Figure 12 have traditionally been considered responsible for contaminant plume configurations observed in the alluvial aquifer prior to the start of remediation pumping in spring 2003. The plumes have been depicted in a variety of documents, including the SOWP (DOE 2000), the GCAP (DOE 2002), and the refined conceptual model

(DOE 2005b), using either concentration contours (isopleths) or color floods. Interpretation of the spatial distribution of contaminants presented in these plots has been instrumental in developing the existing conceptual model of groundwater flow.

4.5.1 Sulfate and Uranium

Figure 14 and Figure 15 present color-flood portrayals of the sulfate and uranium plumes, respectively, in the floodplain during the years 1999–2001. These historical plume configurations are insightful because they generally comport with the flow patterns assumed in the existing conceptual model. Specifically, both plots show a continuous plume extending directly north from the Trench 1 area to the 1089/1104 area, in alignment with the assumed flowpath between the respective areas (Figure 12). In addition, both color floods show a crescent-shaped area of relatively low concentration between the river and the escarpment and extending south-southeastward (upstream) along the river for about 1200 ft from the USGS gaging station. This latter feature, common to both plots, is reflective of inflowing fresh water from the river in association with the largest hyporheic zone assumed to exist at the site (approximately 900 ft upriver from the USGS gaging station, Figure 12). The color-flood plots for sulfate and uranium during 1999–2001 suggest that the inflow of river water to the aquifer some 1000–1500 ft southeast of the USGS gaging station was preventing contamination in the vicinity of wells 608, 610, and 614 at the base of the escarpment from migrating more than a few hundred feet from the escarpment and in the direction of the river.

Close inspection of the uranium plot in Figure 15 reveals a subtle plume feature indicative of variations from the flowpaths illustrated in Figure 12. In particular, the core of the plume lobe extending from the Trench 1 area to the 1089/1104 area during 1999–2001 and exhibiting concentrations of 1 mg/L and higher is quite wide, spanning distances ranging from 500 to 1000 ft. Conventional reasoning regarding contaminant transport would suggest that these widths could be attributed solely to transverse dispersion caused by aquifer heterogeneity (Domenico and Schwartz 1998). However, they could also imply that groundwater flow directions in this part of the floodplain have historically diverged at times from the assumed flowpaths illustrated in Figure 12, with the result being a plume that appears much wider than that observed in a steady-state flow field (Goode and Konikow 2000, Cirpka and Attinger 2003). This feature of the uranium plume during 1999–2001 is also observed in the sulfate plume for that period (Figure 14).

An additional feature of the historical uranium plume in Figure 15 worthy of mention is the occurrence of relatively high contaminant concentrations on the east flank of the plume lobe connecting the Trench 1 and 1089/1104 areas. Uranium concentrations during 1999–2001 in this area, at wells 779, 616, 794, and 795, ranged from about 0.4 to more than 0.9 mg/L, clearly exceeding the UMTRA groundwater standard for uranium of 0.044 mg/L. It is difficult to attribute these latter uranium occurrences simply to the effects of transverse dispersion, especially since the affected wells lie well east (600 ft) of the flowpath assumed responsible for delivering contamination to the 1089/1104 area (Figure 12). This again suggests that changing flow patterns in past years likely played a role in distributing uranium contamination to areas far from the observed plume core during the 1999–2001 time period.

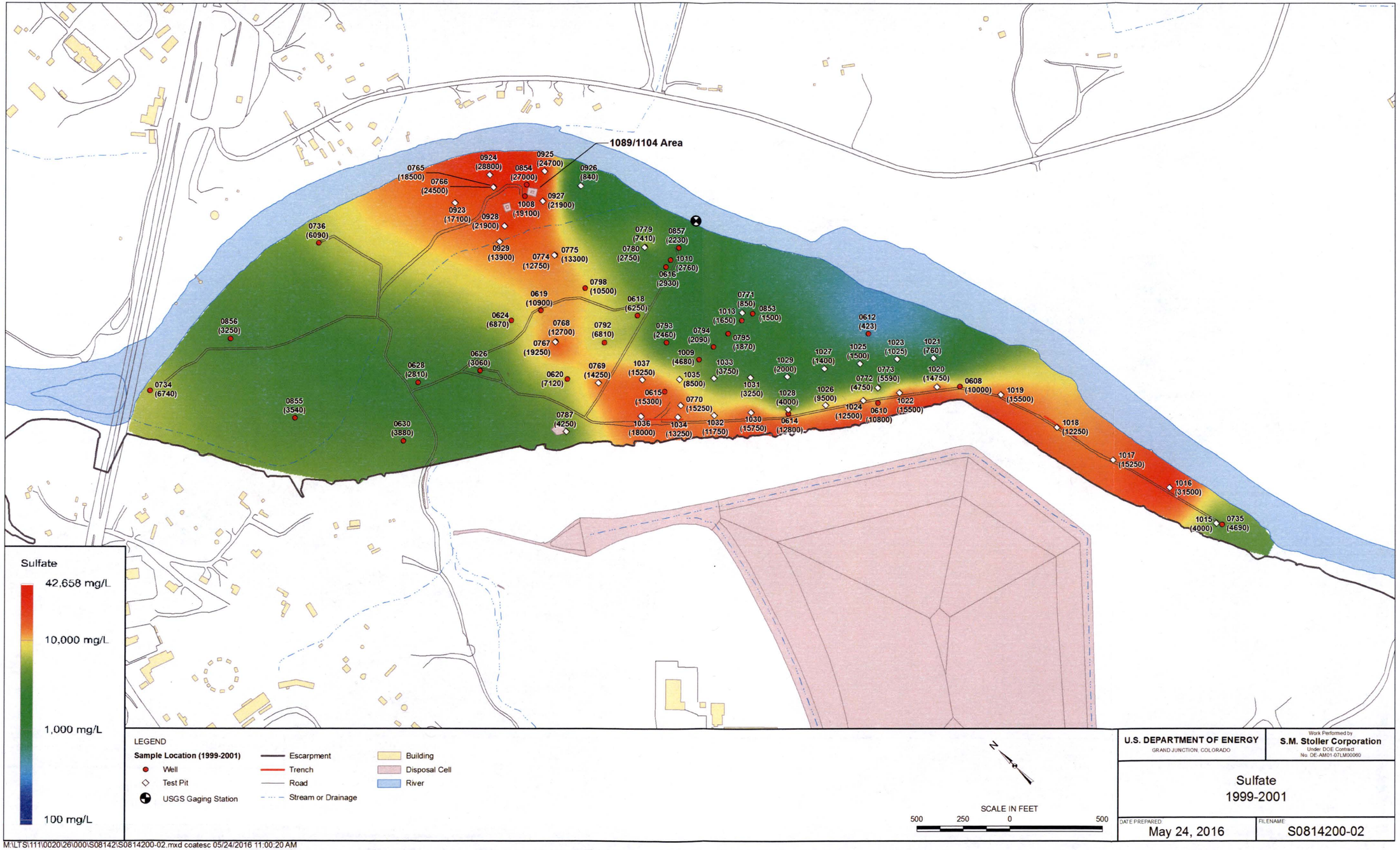

Figure 14. Sulfate Plume, 1999–2001

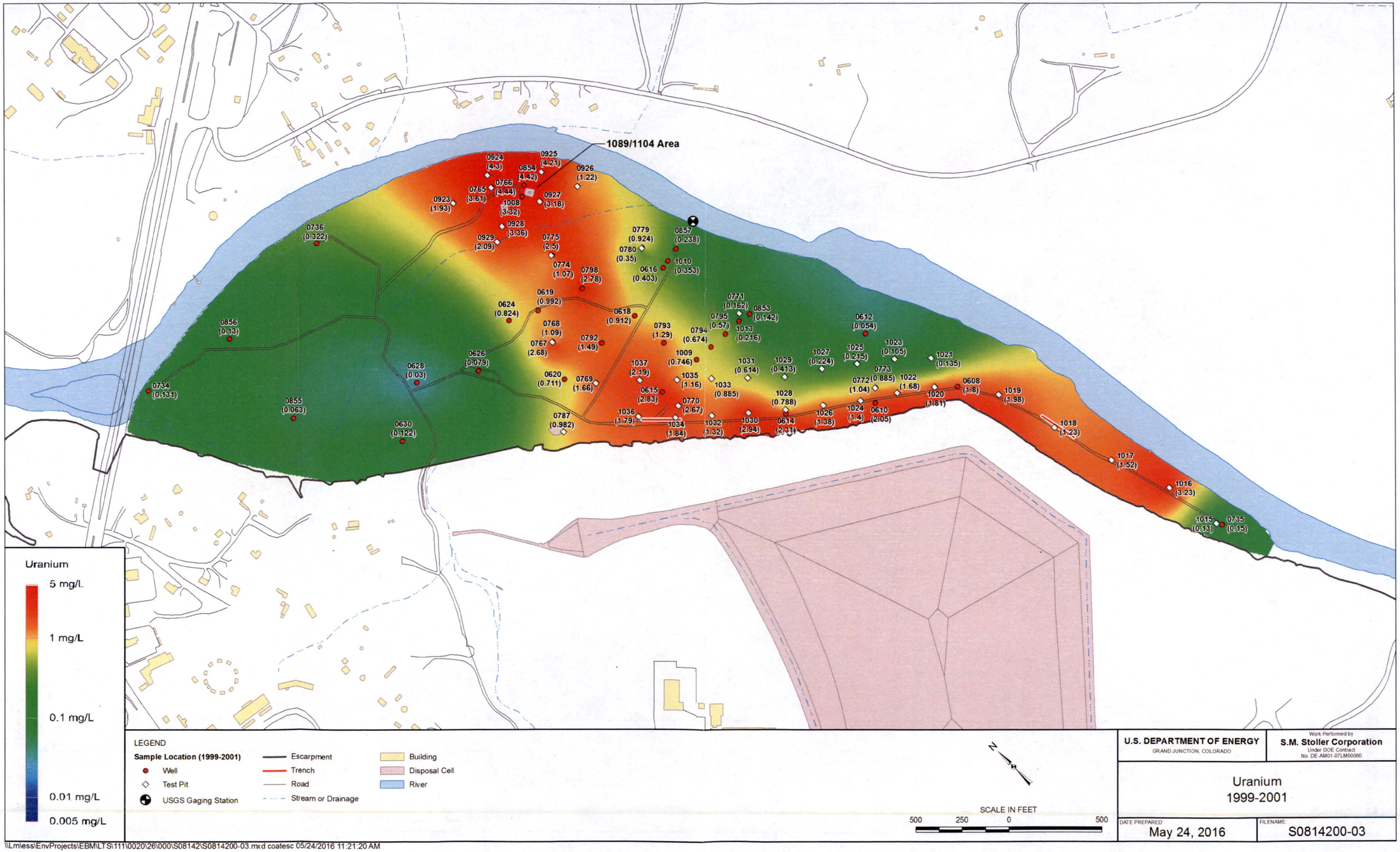

Figure 15. Uranium Plume, 1999–2001

The color-flood interpretation of sulfate and uranium concentrations (Figure 14 and Figure 15) in the southern tip of the floodplain, between the current Trench 2 location and well 735, is not necessarily representative of contaminant levels close to the river during the 1999–2001 period. The limited number of test pits that were sampled in this area at the time did not reflect local, limited inflow of fresh water from the river in the vicinity of the two smallest hyporheic zones delineated in Figure 12.

4.5.2 Groundwater Salinity and Density

Historical sulfate concentrations exceeding 12,000 mg/L (Figure 14) at the base of the escarpment and in the plume lobe extending from the Trench 1 area to the 1089/1104 area indicated that groundwater was highly saline in these locales during 1999–2001, and TDS levels measured at several wells at the time supported this observation. For example, TDS concentrations in 1999 and 2000 at wells 608 and 614, at the base of the escarpment, were in the range of 20,000–25,000 mg/L (DOE 2000). At well 615, 150 ft north of the current Trench 1 footprint, TDS levels at the time were on the order of 25,000 mg/L. Even higher TDS concentrations would have been measured in the 1089/1104 area given that some of the largest sulfate concentrations (20,000–29,000 mg/L) were observed here in the late 1990s (Figure 14).

Specific conductance measurements taken at many floodplain wells and test pits during 1999–2001 also indicated that the contaminated groundwater was highly saline. During those years, specific conductances at sampling locations between the Trench 1 and 1089/1104 areas commonly ranged from 5600 to 30,000 microsiemens per centimeter (μS/cm); these values roughly corresponded to TDS concentrations that varied from 5000 to 30,000 mg/L in this portion of the plume.

As mentioned in Section 4.3, groundwater mounding at the mouth of Bob Lee Wash, due to recharge of mildly saline water from artesian well 648, helped divert groundwater flow and contaminant plumes toward the 1089/1104 area from the Trench 1 area (Figure 12). However, the plume orientation in this part of the aquifer was also likely affected by groundwater salinity, as water densities tied to TDS concentrations of 10,000 mg/L or more are sufficiently large to impact groundwater flow in freshwater aquifers (e.g., Huff 2004). In particular, it is likely that density-driven advection (e.g., Zhang and Schwartz 1995) on both sides of the plumes caused them to spread laterally, more so than would occur in a low-salinity plume. This would help contribute to the wide plume widths observed for uranium and sulfate in the 1999–2001 time frame (Section 4.5.1).

It is also likely that some of the higher-density water in the floodplain subsurface sank into depressions in the bedrock surface along plume flowpaths, rendering much of it immobile (DOE 1995a). These pockets of highly saline groundwater would have subsequently become long-term sources of contamination for fresher (less saline) water migrating through shallower horizons in the saturated zone.

4.5.3 Nitrate

The spatial distribution of nitrate in the alluvial aquifer in the 1999–2001 time frame (Figure 16) was distinctive in that it differed greatly from sulfate and uranium distributions. Rather than exhibiting a continuous plume core between the Trench 1 and 1089/1104 areas, the nitrate plume

was broken and disjointed. Relatively large nitrate concentrations were observed in the 1089/1104 area (200–500 mg/L nitrate as N) at the time, but the spotty plume configuration in hydraulically upgradient areas (Figure 16) suggested that ambient microbially mediated chemical reactions affecting nitrate concentrations were pervasive. Reactions associated with nitrification were likely taking place, since this biologically driven process was capable of generating nitrate by oxidizing ammonium applied in the milling process. Degradation of nitrate via microbially mediated denitrification was also probably occurring, thereby helping to limit nitrate discharge to the river in preremediation years. With multiple chemical processes affecting nitrate concentrations, it was difficult to envision how flow patterns shown in Figure 12 were responsible for creating the 1999–2001 nitrate plume.

4.6 Remediation Flow Patterns

Figure 17 shows flow patterns associated with the existing conceptual model of groundwater flow under remediation (pumping) conditions, with groundwater extraction taking place at all three components of the remediation system. As illustrated, some of the largest changes in baseline flow direction occur in response to operations at Trench 2, where pumping induces flow from portions of the river lying directly to the east. Trench 2 is also assumed to pull in surface water from the southernmost tip of the alluvial aquifer and to capture groundwater discharging from bedrock as far as 500 ft north of the trench. Most of these flow-system features were observed in the Trench 2 evaluation (DOE 2009b).

As in the case of Trench 2, the existing conceptual model assumes that Trench 1 pumping induces flows from the San Juan River. However, rather than pulling in water from a part of the river located directly northeast of the trench, the induced river seepage occurs about 1600 ft to the southeast of the trench (Figure 17). The trench is also conceptualized as collecting bedrock discharge from about 2800 ft of escarpment area and from groundwater originating as recharge from Bob Lee Wash outflow, about 1000 ft to the northwest.

Figure 18 provides a cross-section depiction of the conceptual model for groundwater flow in response to remediation pumping, including induced river seepage and capture of water in the groundwater mounding area. As in the case of the cross-section conceptualization of flow under baseline conditions (Figure 13), Figure 18 does not represent an actual section through the alluvial aquifer, is not to scale, and is intended only to show the processes that influence groundwater movement in the alluvial aquifer. Accordingly, features shown in the cross-section graphic may appear distorted.

The capture zones created by pumping at Trench 1 are assumed to extend mostly to the southeast and northwest because groundwater naturally converges on the trench area from these directions (Figure 12). This effect is similar to the flow patterns observed in situations where a pumping well is located within a regional flow field (Domenico and Schwartz 1998, Section 19.3). An advantage of the resultant flow field is that it induces an influx of relatively uncontaminated groundwater from two areas (the river and Bob Lee Wash), which mixes with more-contaminated groundwater from north of the trench and the escarpment. The inflowing fresh water is expected to eventually flush contaminants out of zones that have historically exhibited some of the greatest contaminant concentrations.

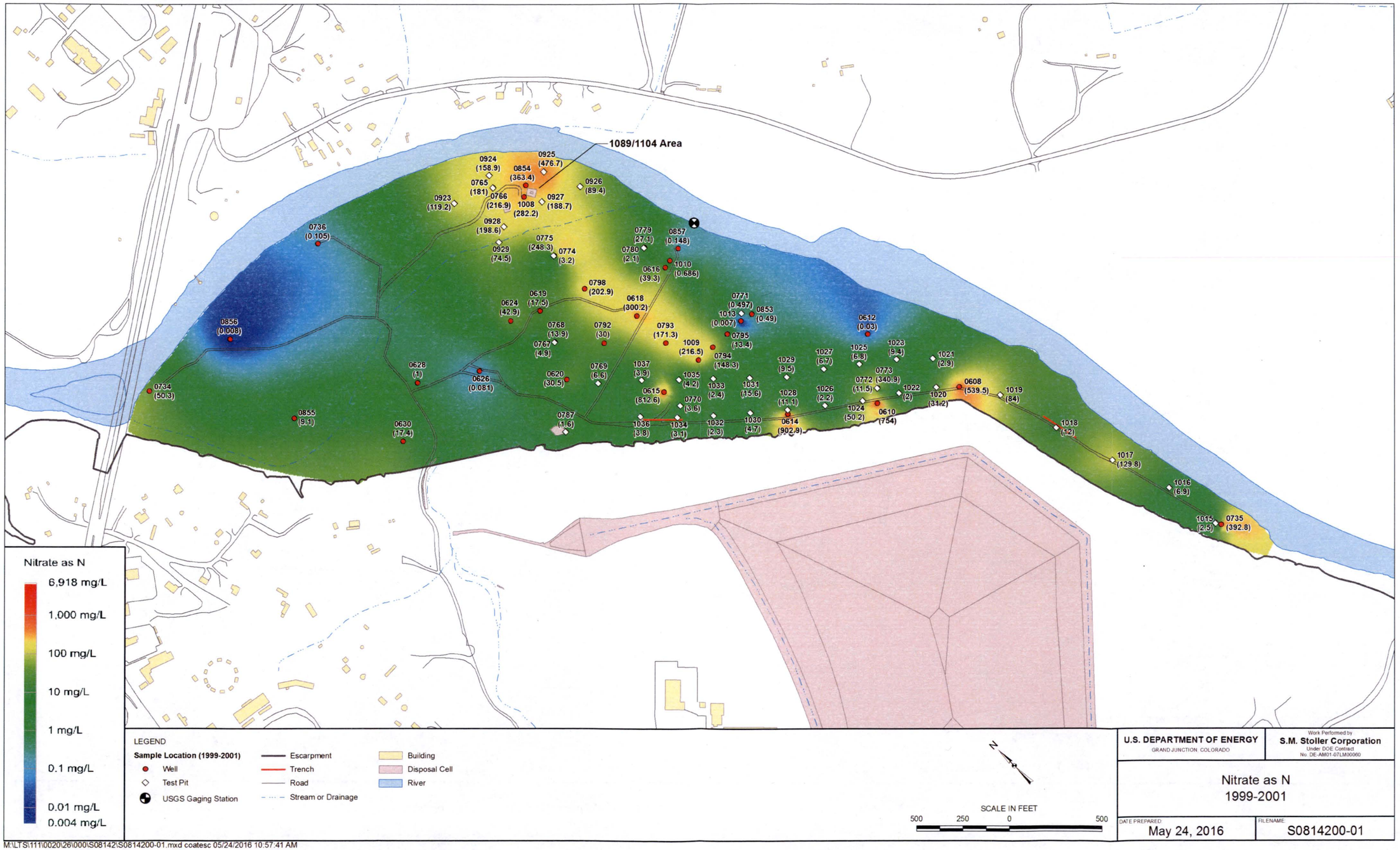

Figure 16. Nitrate as Nitrogen Plume, 1999–2001

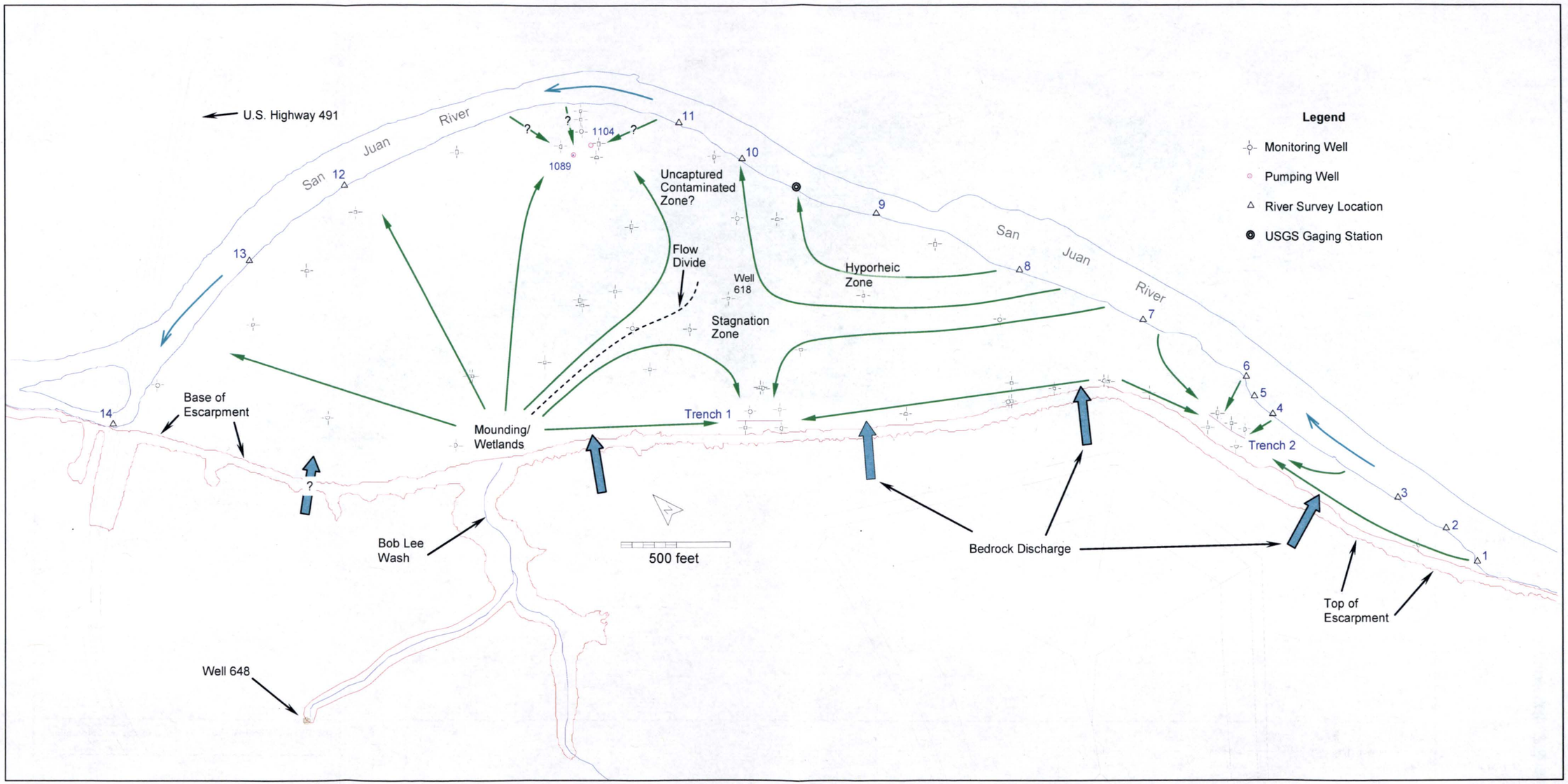

Figure 17. Map View of the Groundwater Flow Conceptual Model for Remediation (pumping) Conditions

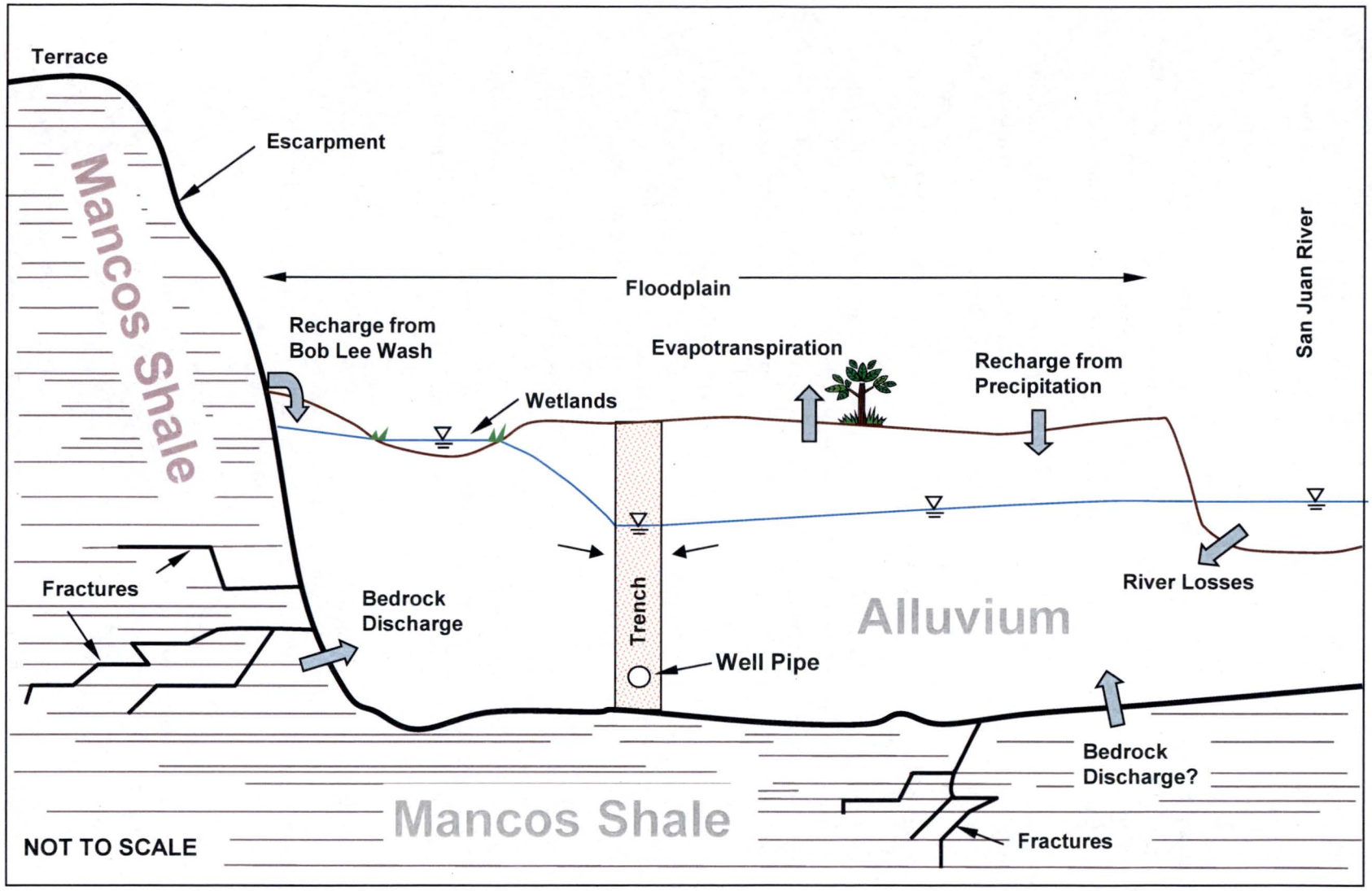

Figure 18. Cross-Section View of the Groundwater Conceptual Model As Affected by Trench 1 Pumping

The capture zone for pumping wells 1089 and 1104 is assumed to lie mostly to the south and southwest of the two wells, as these are the directions from which groundwater apparently flows toward the area under baseline conditions (Figure 12). As shown in Figure 17, the existing conceptual model assumes that pumping from the two wells also has the potential to induce seepage and inflow from the river. However, the arrows signifying this type of flow are flagged with question marks because it is unclear in the existing conceptual model whether the effects of pumping extend as far as the river. As shown in hydraulic studies of a pumping well near a river (e.g., Newsom and Wilson 1988, Wilson and Linderfelt 1991), the well must achieve a critical pumping rate before drawdowns created by the pumping reach the river. It is unknown whether the combined pumping from wells 1089 and 1104 attains such a critical rate, which depends on distance to the river and angle and rate of ambient flow toward the river, among other factors.

The preceding discussion regarding capture of river water by pumping at the 1089/1104 area is germane to this study because of, as mentioned in Section 3.4.1, potential risks to aquatic life (DOE 2002, p. 3-6) posed by the discharge of contaminated groundwater to surface water in this area. Accordingly, decreases in discharge to the river have been identified as the purpose of groundwater pumping in the 1089/1104 area (DOE 2005b, p. 5-4, p. 6-4; DOE 2002, p. B-8).

An additional, subtle change in aquifer flow patterns is expected in response to simultaneous pumping from Trench 1 and wells 1089 and 1104. Specifically, the location for return flow to the river within the largest hyporheic zone (near the USGS gaging station) is extended farther downstream (Figure 17) than that which occurs under baseline flow conditions (Figure 12).

The combined pumping from Trench 1 and wells in the 1089/1104 area leads to the creation of a flow divide between the two areas (Figure 17). Because the location of the divide can vary depending on respective pumping rates at the two locations and changing river elevations, the existing conceptual model treats this possibility as a system uncertainty. The combination of groundwater extraction from both pumping centers and the incursion of river water in the large hyporheic zone also has the potential to produce a stagnation zone (Domenico and Schwartz 1998, pp. 264–265) in which groundwater velocities are extremely low and contaminant migration is limited. The flow patterns drawn in Figure 17 to represent the existing conceptual model indicate that the stagnation zone is expected about 500–1000 ft northeast of Trench 1. Less contaminant removal is expected in the area of low groundwater velocities than in areas subject to active groundwater flow.

The flow patterns in Figure 17 suggest that contaminated portions of the aquifer northeast of the stagnation zone might escape capture by either pumping center. If this is the case, the uncaptured contaminated groundwater is expected to migrate farther to the northeast and discharge to the river somewhere between the USGS gaging station and the 1089/1104 area.

Under the existing conceptual model, some general trends regarding contaminant distributions are expected as remediation pumping continues. The influx of fresh water from the river will produce concentrations in near-river areas that are much lower than those observed farther inland. Assuming that Trench 1 successfully intercepts all contaminated bedrock discharge entering the capture zone, the 1089/1104 area should eventually become dominated by fresh water, unless it is affected by another, unknown contaminant source far from the escarpment (e.g., upward flow from underlying Mancos Shale). Uncontaminated water should also eventually dominate groundwater on the river side of the two trenches. In contrast, relatively

large contaminant concentrations may persist on the escarpment side of the trenches if contaminated terrace groundwater continues to flow into floodplain alluvium across the escarpment.

This page intentionally left blank

5.0 Field Activities in 2011

In addition to traditional semiannual sampling events and year-round SOARS monitoring, data collection activities were expanded in 2011 to address the project focus topics discussed in Section 2.1 (river influences on the alluvial aquifer, groundwater-level changes measured in SOARS, potential for continued discharge of bedrock groundwater across the escarpment, floodplain-wide groundwater modeling). This section summarizes those activities.

Because one of the project objectives called for a better understanding of groundwater flow processes under baseline, or nonpumping, conditions, pumping was shut down at all three components of the remediation system (1089/1104 area, Trench 1, Trench 2) between February 20 and April 24, 2011. Monitoring wells in the floodplain were sampled three different times during that period.

5.1 Monitoring Wells

Water samples were collected from a select group of shallow wells across the floodplain during five project-specific monitoring events in 2011, one each during January, February, April, May, and July. The combination of analytical results from these events and results from a scheduled semiannual sampling event during March 23–26 made it possible examine groundwater chemistry every 1 to 2 months during winter, spring, and early summer. The sampling results from 2011 are not analyzed in this report because the study's principal purpose is to assess groundwater flow processes (Section 2.0) in the alluvial aquifer. However, it is anticipated that the groundwater-chemistry data collected between January and June of 2011 will be helpful in future evaluations of geochemical and transport phenomena in floodplain groundwater. Among the products stemming from such a future investigation is an improved understanding of how changing groundwater flow patterns brought on by seasonal changes in river elevations could in turn lead to temporally variable water chemistry in some parts of the floodplain.

The focused monitoring in 2011 took place at 31 wells and one surface-water location on the river (Figure 19) near the USGS gaging station. Table 4 lists the dates for the five monitoring events and the sampling locations that were included in each event. A variety of factors were considered in selecting the 31 well locations. First, it was important to include locations that were considered representative of the different general types of water chemistry occurring in floodplain groundwater. Wells located relatively close to the river were selected for the focused monitoring network because of their potential for reflecting changing groundwater chemistry induced by changing river elevations. Finally, an attempt was made to monitor wells that are not regularly included in the semiannual sampling events.

5.2 New SOARS Wells

Six monitoring wells within 300 ft of the river were added to the SOARS network in spring 2011 specifically for the purpose of aiding this study (Figure 10). These locations were chosen for the additional insight they could provide regarding the river's influence on floodplain groundwater. As indicated in Table 2, each well was instrumented to measure temporal variations in groundwater level and water temperature. As with other SOARS locations on the floodplain, the data were collected at 5-minute intervals. Temperatures were included in the data collection because they potentially help identify incursions of river water into alluvial aquifers (e.g., Stonestrom and Constantz 2003).

Table 4. Focused Monitoring Locations and Sampling Events in 2011

Well	Sampling Event				
	Jan 25–27, 2011	Feb 23–24, 2011	Apr 18–20, 2011	May 17–18, 2011	Jul 18–20, 2011
Groundwater Locations					
609	x	x	x	x	x
614	x	x	x	x	x
615	x	x	x	x	x
618	x	x	x	x	x
619	x	x	x	x	x
623	x	x	x	x	x
626	x	x	x	x	x
630	x	x	x	x	x
735	x	x	x	x	x
768	x	x	x	x	x
773	x	x	x	x	x
775	x	x	x	x	x
779	x	x	x	x	x
792	x	x	x	x	x
853	x	x	x	x	x
855	x	x	x	x	x
856	x	x	x	x	x
858	x	x	x	x	x
1009	x	x	x	x	x
1010	x	x	x	x	x
1075	x	x	x	x	x
1077	x	x	x	x	x
1112	x	x	x	x	x
1115	x	x	x	x	x
1117	x	x	x	x	x
1125	x	x	x	x	x
1135	x	x	x	x	x
1136	x	x	x	x	x
1139	x	x	x	x	x
1142	x	x	x	x	x
1143	x	x	x	x	x
Surface-Water Locations					
899			x	x	x

Figure 19. Focused Monitoring Locations in 2011

This page intentionally left blank

5.3 River Elevation Surveys

Comprehensive understanding of river–aquifer interactions during 2011 required the determination of river elevation profiles (river profiles) at two key times along the entire length of river bordering the floodplain. One river profile was sought for the low-flow conditions that are typically observed in winter and early spring at the site, before river discharge begins to increase due to snowmelt runoff from the San Juan Mountains. The other profile was sought for high-flow conditions occurring during the peak snowmelt months of May and June, and preferably at the time of maximum river flow for the year.

An engineering firm was hired to collect the survey data used to construct the river profiles. River-elevation data collected in March 2011, during which time river flows remained less than 950 cubic feet per second (cfs), supplied the data for the low-flow profile. The high-runoff survey was conducted on June 10, 2011, which fortuitously was one of the highest flow days of the year (>8000 cfs).

5.3.1 Low-Flow Survey

In February 2011, the entire length of the river along the floodplain was visually inspected for possible riffle locations. The physical characteristics used to identify riffle sections included shallow water depth, exposed gravels or boulders in the riverbed, a rippled (wavy) water surface, and rapid water velocity in comparison to the velocity in upstream and downstream sections. On the basis of these criteria, four different sections were selected as being likely riffle locations. Of these, three were identical to the riffles identified in the existing conceptual model (Figure 12) adjacent to the south half of the floodplain, and the fourth was located about 400 ft downriver from the USGS gaging station.

Additional field activity in February resulted in the flagging of 20 points along the river at which surface-water elevations were sought during the planned engineering survey. Eight of these were located at the upstream and downstream ends of the previously identified riffles, and the remaining 12 were spread equally among other river sections. Many of the flagged sites were placed near the middle of river sections that appeared to comprise pools with uniformly sloped water surfaces.

Unfortunately, no arrangements were made with the engineering contractor to collect all 20 river water elevations in a single day. As a consequence, 19 water elevations were measured over 3 days during March 2011 (March 4, 8, and 9), and the final water elevation, on the downstream edge of the Highway 491 bridge, was collected on March 20. The water elevations were determined using DOE survey benchmarks tied to the Shiprock site. Though daily average flows in the river varied somewhat among the survey days (835–931 cfs), inspection of the resulting elevation data suggested that a profile representative of low-flow conditions on the river could be achieved without using all 20 surveyed elevations. Specifically, it was confirmed that many of the survey points were located in the middle of pools with constant surface slopes, rendering them unnecessary for defining water slopes that control hyporheic flow zones. Ultimately, 14 surveyed elevations were used to define the low-flow river profile.

The March 2011 profile divided the entire river reach adjacent to the site into seven pools and six riffles, as labeled in Figure 20. The resulting low-flow profile (Figure 21) showed a total

decrease in water elevation between the upstream and downstream ends of the floodplain of approximately 10.3 ft. The largest drop in water elevation linked to any single riffle occurred at Riffle 4, which was assigned upstream (4-Up) and downstream (4-Down) components. With a total water elevation decrease of 3.27 ft over a river distance of about 700 ft, Riffle 4-Down was identified as the same drop in river level associated with the largest hyporheic zone in the existing conceptual model (Figure 12). Similarly, Riffles 1 and 3 were correlated with the remaining two hyporheic zones assumed present in the existing conceptual model.

Figure 22 contains three photographs of Riffle 4-Down in February 2011. The pictures were taken at a single location on the west bank of the river near well 1142 (Figure 5) and comprise upriver (Figure 22a), across-river (Figure 22b), and downriver (Figure 22c) views of the riffle. Trees assigned labels on the far side of the river help to visually connect the photographs, providing a panoramic perspective of the riffle's features (shallow water depth, exposed boulders, rippled surface), all of which make it easily identifiable in the field. Because these pictures were taken in late winter, much of the slow-moving surface water along the riverbank was frozen.

To illustrate how river pools are generally distinguishable from riffles, Figure 23 contains a photograph of Pool 6 that was taken in February 2011, on the west bank of the river about 300 ft downriver of Well 1137 (Figure 5). The most noticeable feature of the river surface here is its placid (nonrippled) surface, which results from greater water depths and lower water velocities than those associated with the visually apparent riffles. As in the case of Riffle 4-Down (Figure 22), the slow-moving water along the riverbank was mostly frozen. Of some interest is the additional ice, in the form of flocs, seen floating on the water surface in Pool 6 (Figure 23) during visual inspection of the river in February. Though this latter feature was commonly observed in the river reach between Riffle 5 and the Highway 491 bridge, it was not considered a distinguishing characteristic of pools on the river during winter months.

5.3.1.1 River Gage Elevation

The elevations at river-survey locations 9 and 10, both of which were surveyed on March 8, were used in conjunction with USGS benchmark information for the gaging station to develop a method for converting reported gage heights at the station into local river levels based on DOE survey benchmarks. The analysis indicated that the river elevation at the station (gage elevation) could be computed by adding the gage height to a datum elevation of 4876.0 ft amsl. This relationship became useful later in the study for the purpose of estimating water-surface profiles at other times.

From the various gage heights recorded at the gaging station during the engineering survey in March 2011, a gage height of 7.89 ft, or a gage elevation of 4883.89 ft amsl, was selected as being representative of the low-flow profile illustrated in Figure 21. The corresponding river flow associated with the low-flow survey was 874 cfs.

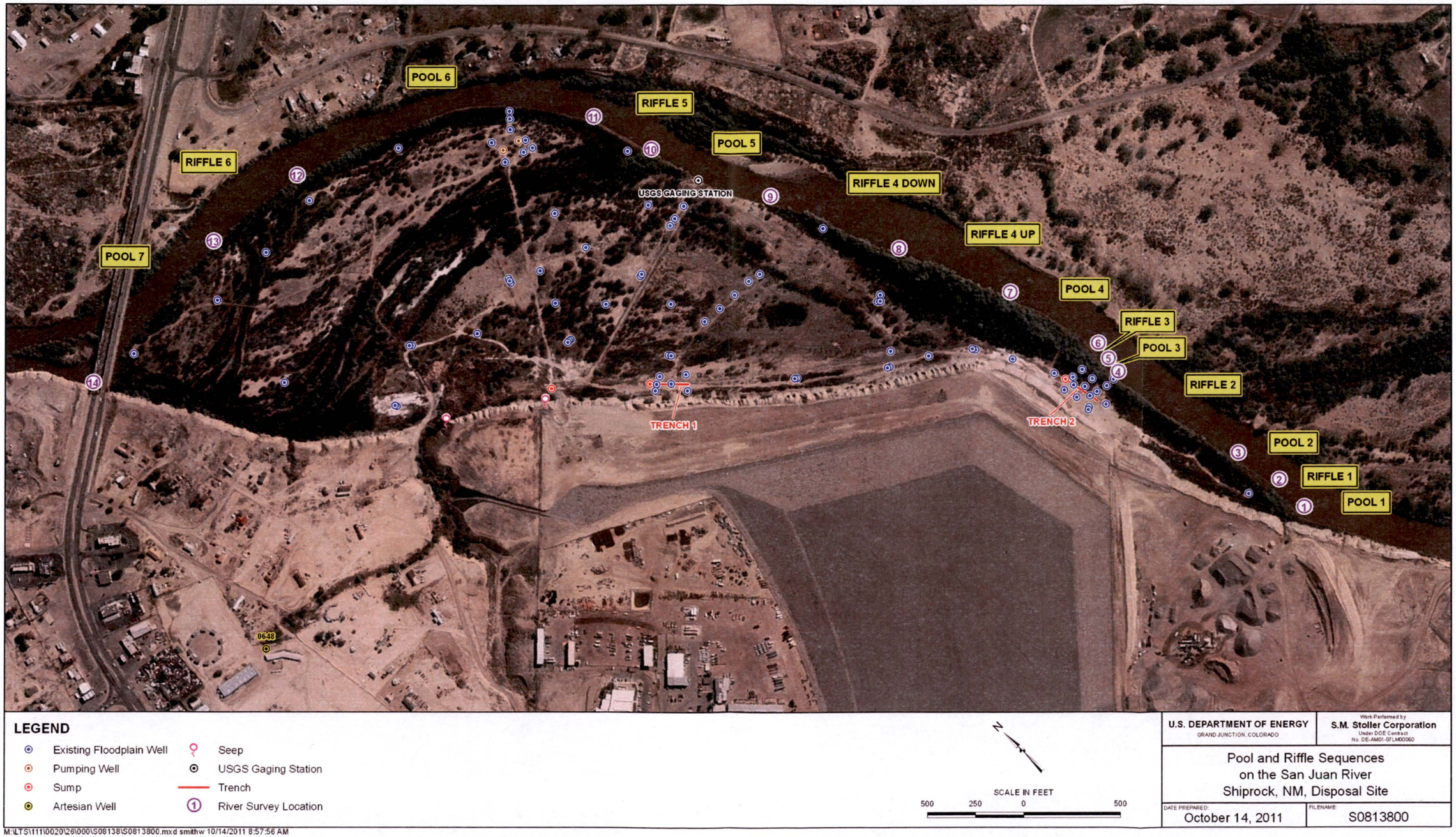

Figure 20. Pool and Riffle Sequences on the San Juan River in March 2011

This page intentionally left blank

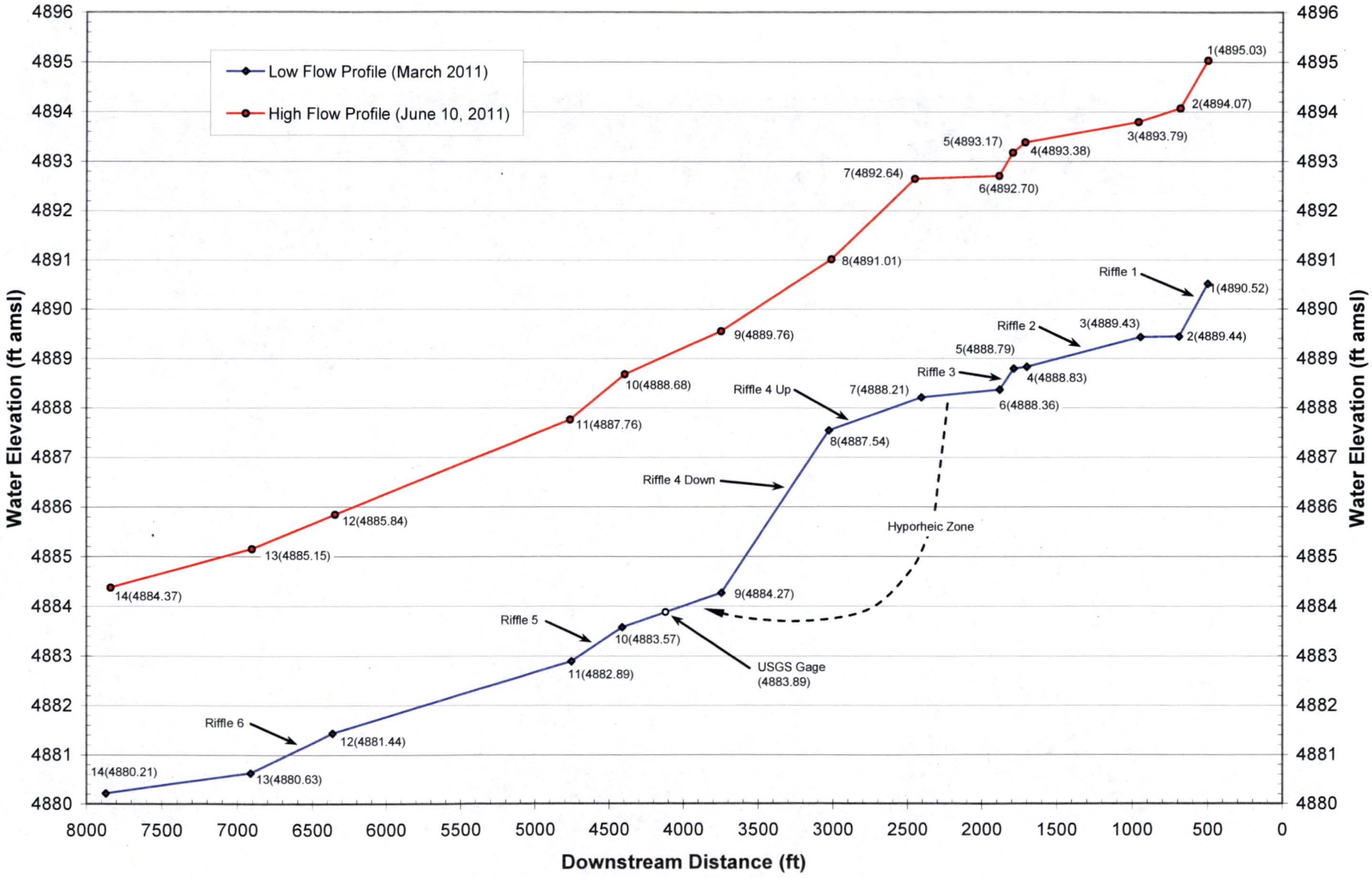

Figure 21. Surveyed Water Surface Profiles on the San Juan River

Figure 22. Photographs of Riffle 4-Down in February 2011 Taken on the West Riverbank near Well 1142: View (a) Upriver, (b) Across-River, and (c) Downriver (note shallow water depths, exposed boulders, rippled water surface, and ice near the riverbank)

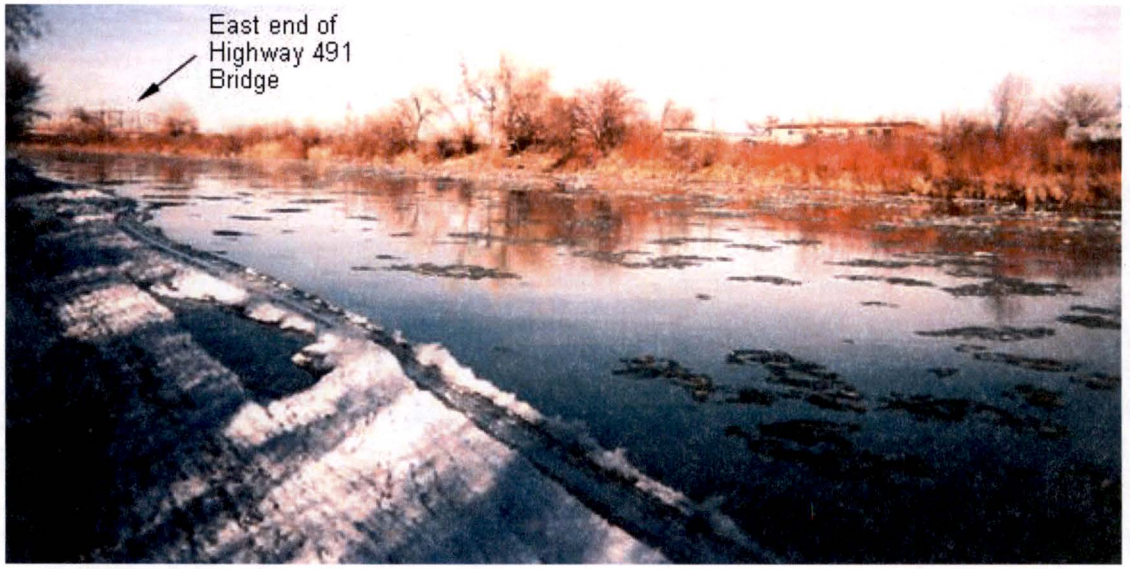

Figure 23. Photograph of Pool 6 in February 2011 Taken on the West Riverbank About 300 Feet Downriver from Well 1137: View Downriver (note placid water surface and floating ice flocs)

5.3.1.2 Pool and Riffle Slopes

Data used to construct the low-flow river profile are listed in Table 5 along with calculated slopes for the water surface in each pond and riffle reach. As this tabulation indicates, pool slopes ranged from 0.005 to 0.104 percent, and the mean pool slope was 0.052 percent; riffle slopes varied from 0.08 to 0.561 percent, and averaged 0.286 percent.

Table 5. River Surface Information for Low-Flow Conditions in March 2011

River Survey Location	Profile Cumulative Distance (ft)	Water Elevation (ft amsl)	Pool/Riffle Designation	Water Slope (%)
NA	0	NA	NA	NA
1	500.0	4,890.52	Pool 1	NA
2	691.6	4,889.44	Riffle 1	0.561
3	944.6	4,889.43	Pool 2	0.005
4	1,699.0	4,888.83	Riffle 2	0.080
5	1,786.2	4,888.79	Pool 3	0.039
6	1,881.4	4,888.36	Riffle 3	0.451
7	2,407.1	4,888.21	Pool 4	0.029
8	3,025.3	4,887.54	Riffle 4-Up	0.108
9	3,743.3	4,884.27	Riffle 4-Down	0.456
10	4,411.7	4,883.57	Pool 5	0.104
11	4,755.3	4,882.89	Riffle 5	0.199
12	6,363.1	4,881.44	Pool 6	0.090
13	6,914.1	4,880.63	Riffle 6	0.147
14	7,870.3	4,880.21	Pool 7	0.043

Notes:
Average pool slope = 0.052%; average riffle slope = 0.286%.

Abbreviation:
NA = not applicable

The water slopes listed in Table 5 help explain why Riffles 1, 3, and 4-Down were readily identifiable in previous studies and were, therefore, incorporated in the existing conceptual model (Figure 12). The higher water velocities associated with these river sections in comparison to those of pools were easy to discern during low-flow conditions on the river, as the slopes for all three exceeded 0.45 percent. In contrast, the less-steep slopes of the remaining riffle sections (Riffles 2, 4-Up, 5, and 6), ranging from 0.08 to 0.199 percent, were less apparent. Identification of the milder-sloped riffles and the hyporheic flows tied to them is dependent on the collection of accurate elevation-survey data. Given that the water-elevation data were collected on four different days with different river flows (Section 5.1), the water slopes listed in Table 5 for the less apparent riffles should be considered rough estimates.

5.3.2 High-Flow Survey

The survey of river elevations under high river-flow conditions was conducted on June 10, 2011. Flows in the river fluctuated significantly during daylight hours on this date, ranging from 7830 to 8770 cfs and averaging approximately 8270 cfs. The flow profile generated from the survey, shown in Figure 21, indicates that river elevations during this period of peak flow were generally about 4 ft higher than they were in March of this year. Similar to the low-flow survey results, the total river surface drop between the upstream and downstream ends of the floodplain was about 10.7 ft. Unlike the low-flow profile, however, some of the previously identified riffle sections were obscured during high flow and replaced with a gradually varied profile that erased the effects of river-channel controls (Mosley and McKerchar 1992).

A notable feature of the high-flow profile was the complete removal of an explicit river-surface drop in the Riffle 4 area. Instead of showing a distinct local decrease in water elevation, the Riffle 4 area appeared to be located on the upstream end of a relatively smooth, concave-shaped profile that extended about 5500 ft upriver from the Highway 491 bridge to river survey location 7 (Figure 21). The nearly curvilinear shape of this profile suggested that it formed an M1 backwater profile (Chow 1959, p. 228) behind a partial channel obstruction, which in this case was the highway bridge. Upstream of river survey location 7, the relatively steep surface-water slopes associated with Riffles 1 and 3 appeared to remain intact.

The high-flow river profile suggests that river–aquifer exchange processes during buildup to peak flow in the river change greatly from those occurring under low-flow conditions. These changes in turn alter flow patterns and plume migration in the aquifer. Similarly, interactions between the river and aquifer during flow recession following peak river discharge are likely affected. Sections 7 and 8 discuss how high-runoff conditions on the river appear to influence flow and transport in the alluvial aquifer.

6.0 Updated Assessment of the Alluvial Aquifer

Information that became available during this study made it possible to refine DOE's understanding of groundwater flow in the alluvial aquifer and to assess remediation progress for the entire floodplain. Included in the list of items that were developed using the new data was a revised contour map of bedrock surface (top of Mancos Shale) elevations.

6.1 Bedrock Elevations

The new map of contoured bedrock elevations was based mostly on identified Mancos Shale elevations at floodplain wells deep enough to contact the shale, as listed in Table 1. These data were augmented with bedrock elevation information from the well logs for several monitoring wells screened within deeper portions of Mancos Shale. Posting of the available data suggested that the bedrock surface is quite irregular, with surface elevations in some cases varying by 1 to 4 ft over distances of less than 100 ft. Such observations could be attributed to measurement error, but given that prehistoric incision of the bedrock surface by the river was largely responsible for bedrock topography, relatively large changes in elevation over short distances were considered plausible. Variable bedrock elevations at multiple, closely spaced wells in some parts of the floodplain meant that some subjectivity was involved in drawing the bedrock-surface contours.

Figure 24 presents the resulting bedrock-surface map and the data used to construct it. In accordance with earlier descriptions of the surface, contoured bedrock elevations range from about 4885 ft amsl on the south end of the floodplain to 4865 ft amsl on the north end, signifying an elevation drop of about 20 ft. An apparent feature in the plotted surface is the presence of a long (2500–3000 ft), northwest-oriented paleochannel in the northern two-thirds of the floodplain. The bedrock surface gradually rises as much as 5 ft on either side of the paleochannel, with bedrock elevations close to the west bank of the river higher than those in the floodplain interior. Also worthy of mention is the interpreted presence of a northeast-oriented, tributary paleochannel in the 1089/1104 area. This feature could provide enhanced hydraulic connection between the river and the channel in comparison to areas about 500 ft upstream and downstream. Note that the contoured elevations in Figure 24 bear some resemblance to the bedrock surface map included in the SOWP (DOE 2000, Figure 4-7). The new bedrock surface map was used to generate data representing the base of the alluvial aquifer in the modeling performed for this study.

6.2 Well Hydrographs

Water-level data at a variety of monitoring wells included in SOARS were examined to better understand how the alluvial aquifer responds to (1) seasonal increases in river runoff during May and June of each year and (2) variable pumping rates at Trench 1. Ultimately, 11 well locations were used in this evaluation (Figure 25), and the monitoring period examined extended from January 1, 2011, to September 1, 2011. As described in Section 7, "Groundwater Flow Modeling," the resulting groundwater hydrographs proved useful for identifying representative values of the aquifer's hydraulic conductivity and specific yield.

The hydrographs were analyzed by categorizing the wells into three groups (Figure 25) that reflected their relative distance from the San Juan River. Group 1 (wells 1135, 1136, and 1137)

was considered representative of near-river locations (30–80 ft from the river). Group 2, referred to as wells west and south of the USGS gaging station, consisted of wells 779, 853, and 857, located about 230, 350, and 160 ft, respectively, from the river. Water elevations at Group 2 wells change in response to variable river flows, but appear unaffected by remediation pumping. Group 3 wells consisted of wells in the Trench 1 area (wells 793, 1009, 1105, 1140, and 1141), which lie anywhere from 650 to 1050 ft from the river. Water elevations in this latter category were expected to show the least response to changes in river level and relatively clear responses to pumping from Trench 1.

6.2.1 Group 1—Wells Close to the San Juan River

Figure 26 shows the hydrographs for the Group 1, near-river wells along with the measured water elevation at the USGS gaging station (gage elevation) during the 8-month monitoring period. Pumping rates from well 1089 are also included to ascertain whether the pumping showed signs of influencing the monitoring wells, located 150–650 ft from the remediation well. Large variations in river level and the remediation pumping rate during the monitoring period provided sufficient data to identify which hydraulic stress (river or pumping), if any, influenced responses in the hydrographs.

As indicated in Figure 26, gage elevations (1) remained relatively stable during the initial 3 months (January–March) of monitoring; (2) fluctuated significantly during the following 4 months (April–July), including the period of peak river flow in early June; and (3) stabilized again during the last month (August). Well 1137, the only near-river well with continuously recorded water levels for the entire monitoring period, quickly tracked the smallest changes in river level (gage elevation) during these time spans. Wells 1135 and 1136, added to SOARS in mid-April, also quickly tracked gage elevations, but many of the smaller changes in river level were not seen in the hydrographs for these wells. Collectively, these observations suggested that the hydraulic connection between river and aquifer was strong and that the hydraulic conductivities of riverbed and riverbank deposits as well as aquifer alluvium close to the river were relatively high. Well 1137, closest to the river (30 ft), showed the greatest change in water elevation with each change in river level.

Inspection of the well-1137 hydrograph and simultaneous pumping rates at well 1089 (Figure 26) shows no apparent connection between the two. This observation suggests that remediation pumping in the 1089/1104 area does not attain the critical pumping rate required to induce flow from the river (see Section 4.6), which in turn suggests that the pumping is unable to prevent local discharge of contamination to the river.

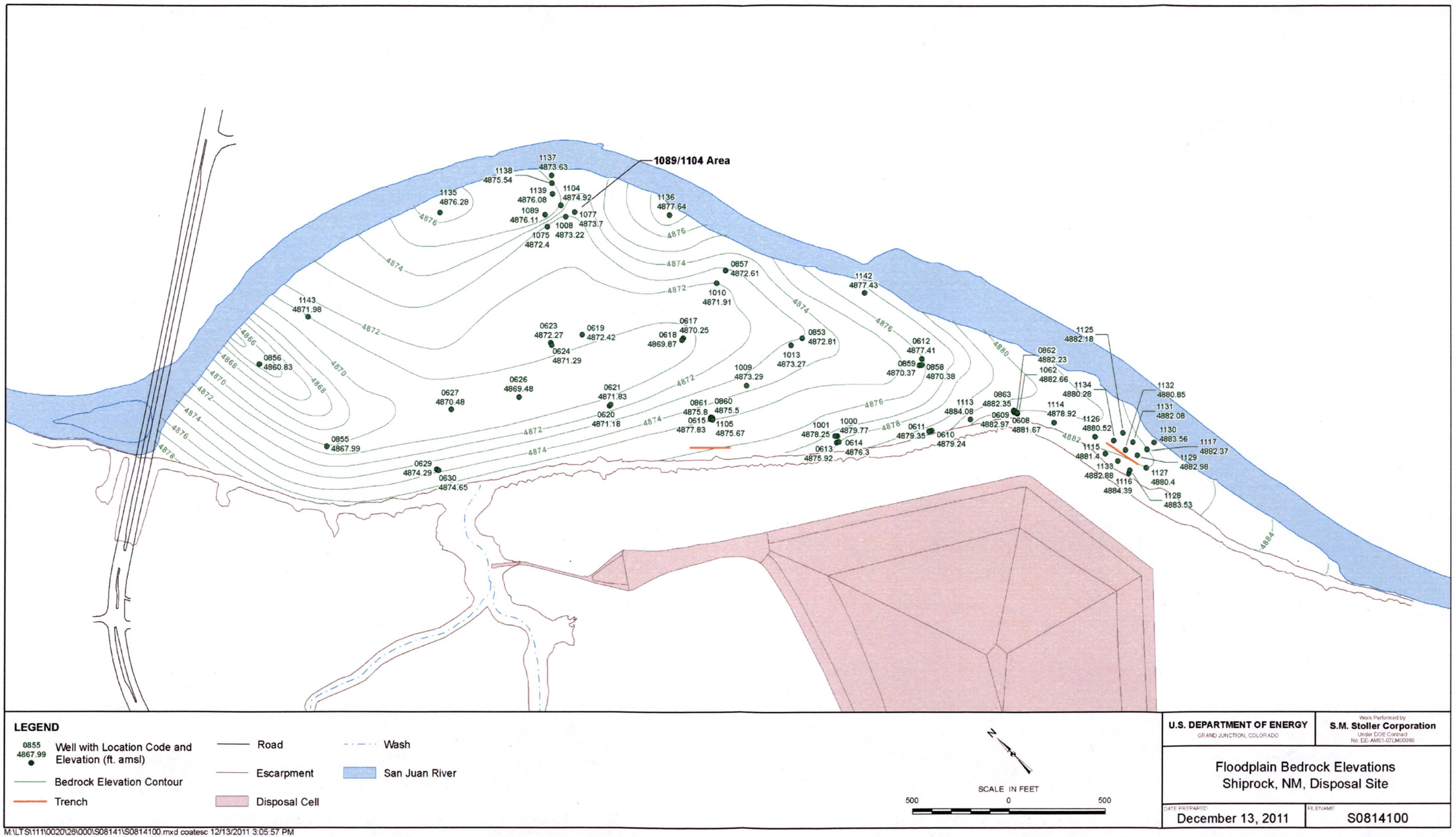

Figure 24. Contoured Bedrock Surface (top of Mancos Shale) Elevations
(contours were generated using average elevations in areas containing multiple postings; posted elevations considered anomalously low or high were not precisely honored)

This page intentionally left blank

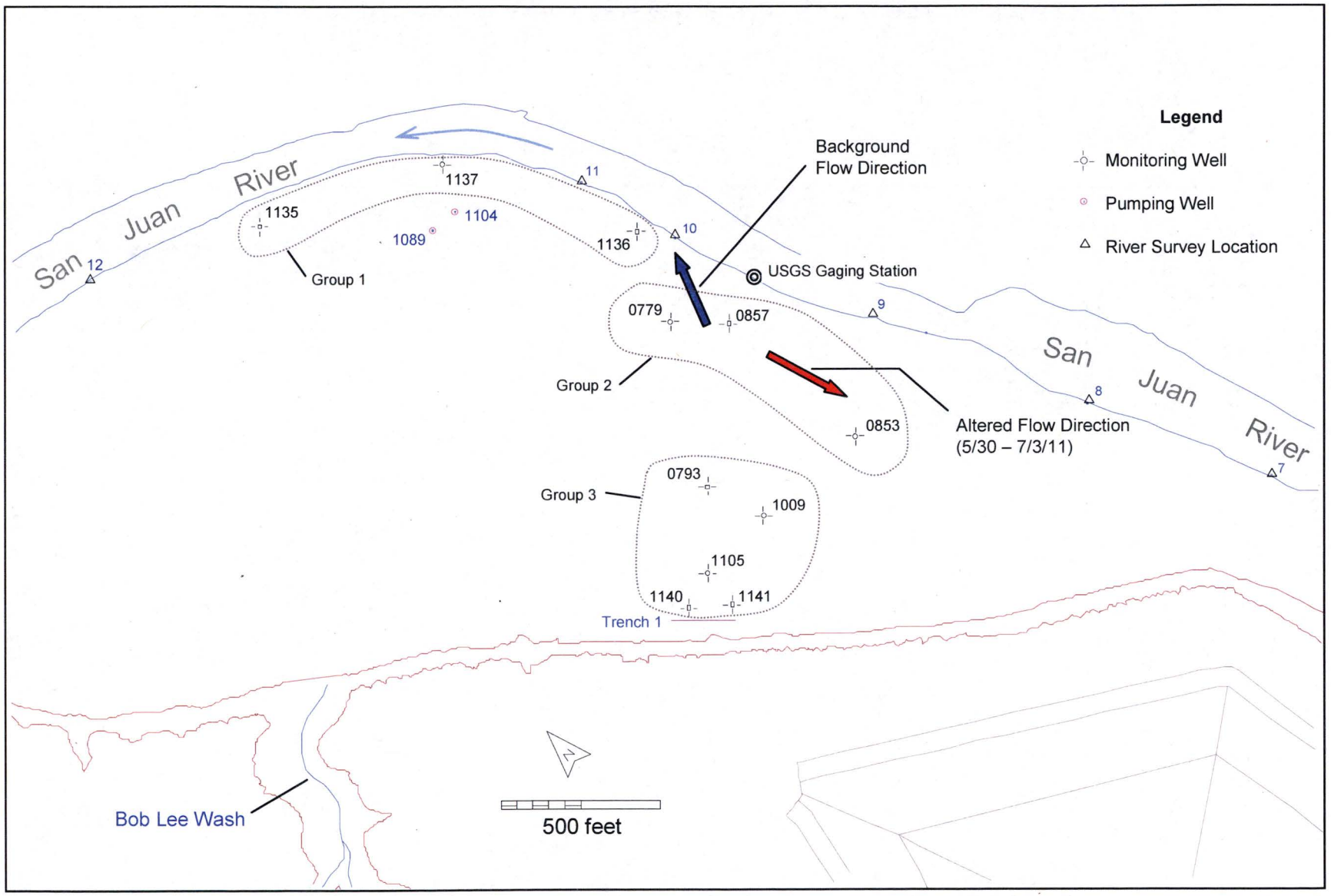

Figure 25. Monitoring Wells Used To Generate Hydrographs (categorized by group number)

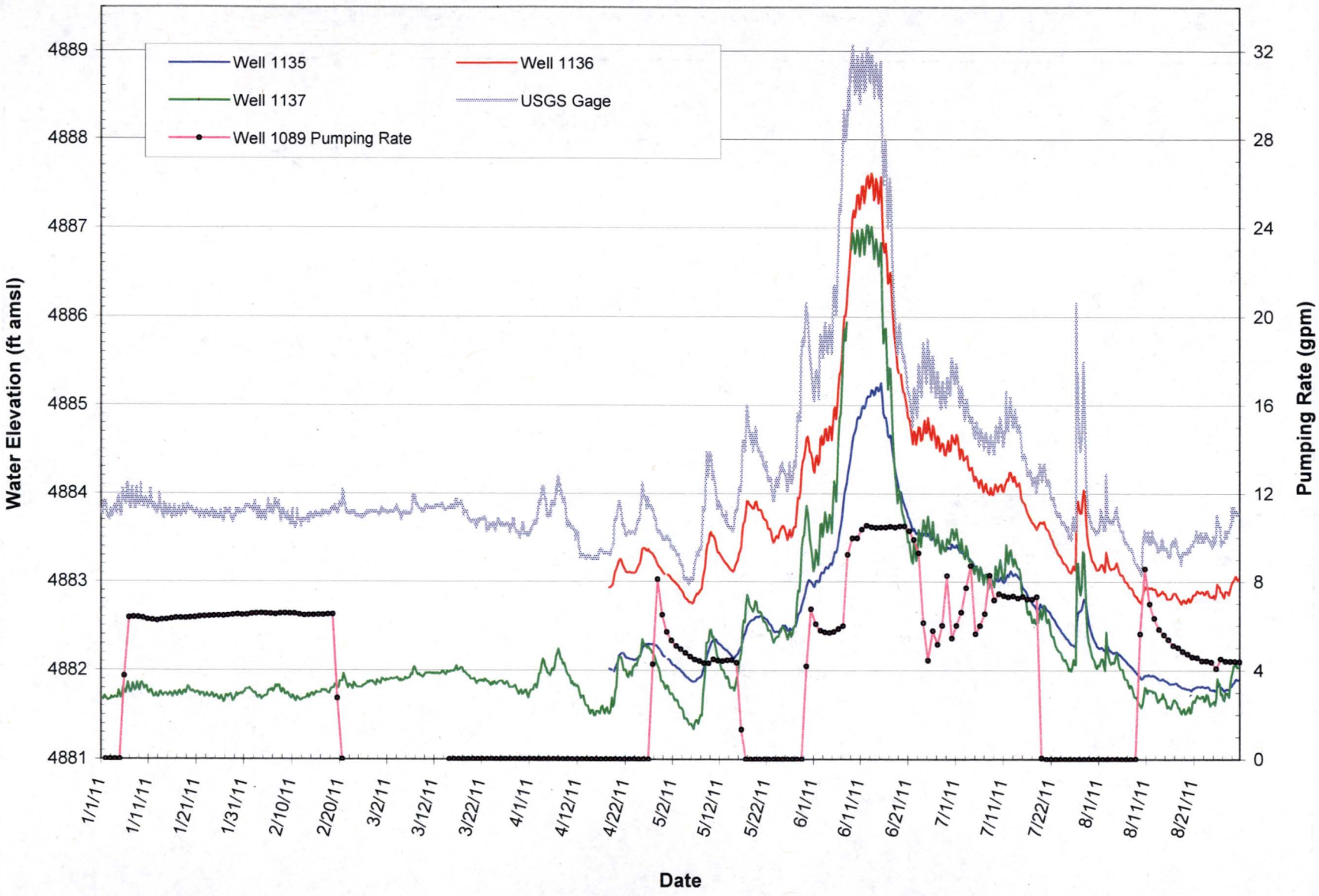

Figure 26. Hydrographs at Group 1, Near-River Wells, January 2011 through August 2011

To better discern whether pumping in the 1089/1104 area induces inflow from the river, water elevations collected during each semiannual sampling event at monitoring wells 1137, 1138, and 1139 (see Figure 6 for locations) were examined. Since these three wells lie about 40–50 ft from each other along a line extending from the river toward the pumping wells (well 1137 is closest to the river), their respective water levels, if collected on the same day and during a pumping period that lasted the entire monitoring event, would be expected to show decreases with distance away from the river if the pumping was drawing water from the river. Inspection of water-level data in GEMS through September 2014 revealed that eight semiannual sampling events (March 2010, September 2010, September 2011, March 2012, March 2013, September 2013, March 2014, September 2014) met the required criteria and that measured water elevations during six of those events (March 2010, September 2010, September 2011, March 2012, September 2013, September 2014) were decreasing with distance from the river. Measured water levels at well 1137 during the six events that showed water-level decreases away from the river were 0.05–0.25 ft higher than corresponding elevations at well 1138, and water levels in well 1138 were 0.05–0.5 ft higher than corresponding levels at well 1139. During the remaining two events meeting the criteria (March 2013, March 2014), measured water elevations at the three wells were all within a narrow range that spanned no more than 0.1 ft. This suggested that, though water levels in these instances increased with distance from the river, the measured water elevations were essentially equal to each other. All in all, the results from the eight events meeting the criteria (water levels at all three wells measured the same day, remediation pumping taking place) indicated that the hydraulic gradient created by the pumping was mild in the vicinity of the river, but groundwater extraction from wells 1089 and 1104 generally prevents local contamination from discharging to the river.

Note that the monitoring events in September of the respective years took place when groundwater levels were expected to be at their lowest each year due to groundwater discharge via evapotranspiration. Accordingly, it is possible that ET was inducing river losses to the aquifer during those events. In contrast, the apparent river losses to the aquifer during the monitoring events in March 2010 and March 2012, when ET was likely insignificant, indicates that remediation pumping in the local area is strong enough to intercept northward-flowing groundwater without the assistance of increased ET on the floodplain (i.e., the conceptual model shown in Figure 17 for the 1089/1104 area is valid).

6.2.2 Group 2—Wells West and South of the River Gaging Station

Figure 27 illustrates the hydrographs at wells 779, 853, and 857 (Group 2 wells) from early March 2011, when the wells were first connected to SOARS, through August 2011. The pumping rate at well 1104, the closest pumping site to the USGS gaging station (Figure 5), is also plotted for the purpose of detecting water-level responses in the monitoring wells, if any, to the pumping. Though all three hydrographs show clear responses to changing river levels, pumping at well 1104 has no discernible effect on water levels in the monitoring wells (Figure 27), which are located at least 700 ft away.

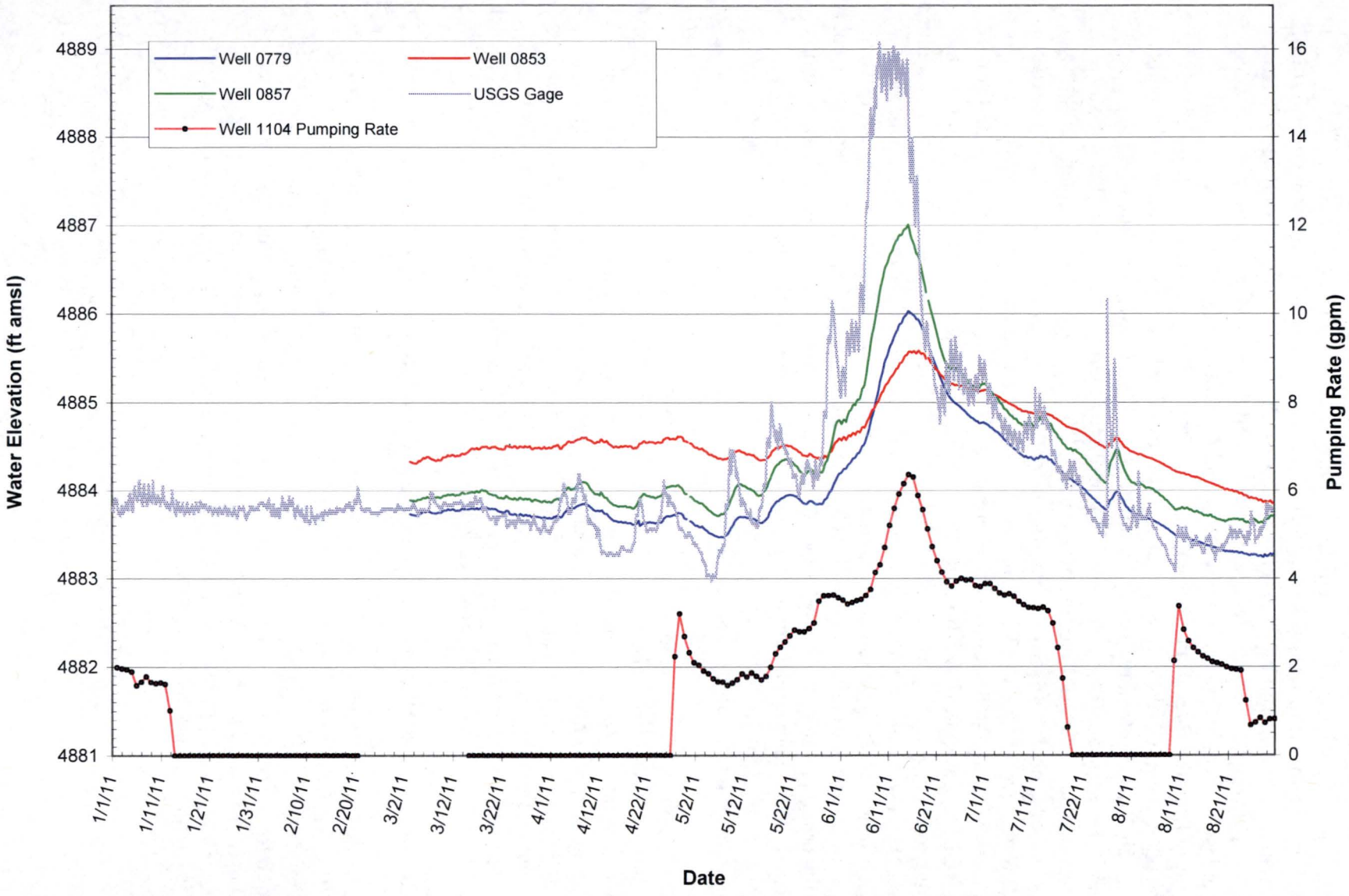

Figure 27. Hydrographs at Group 2 Wells, West and South of the USGS Gaging Station, January 2011 through August 2011

A notable feature of the hydrographs in Figure 27 is an apparent flow reversal between well 857 and the river at the gaging station during the buildup to peak river flow from snowmelt during May and June 2011. The flow reversal was observed during each of two periods in mid-May lasting about 2 to 4 days, and subsequently for about a month between late May and late June. Seepage losses from rivers to nearby groundwater induced by such reversals in hydraulic gradient, leading to temporary bank storage (Section 4.2), are common in river–aquifer systems affected by seasonal runoff due to snowmelt (e.g., Huntington and Niswonger 2012, Winter et al. 1998). Bank storage in the floodplain alluvial aquifer during May and June 2011 is discussed in more detail in Section 7.3.2.6, which describes simulated groundwater flow patterns with a transient version of the groundwater flow model developed for this study.

In general, hydrographs at the three wells west and south of the USGS gaging station reflected aquifer behavior that was expected. In particular, changes in measured water levels at these wells were muted in comparison to the changes in gage elevation, and the peak water level in each well (in June) was delayed (about 6 to 7 days) beyond the initial peak flow in the river (Figure 27). Moreover, prior to the onset of high snowmelt runoff in late May, water levels in the Group 2 wells comported with the prevailing north to northeast flow direction in this area, with well 853 exhibiting the largest water elevations, well 779 the lowest, and well 857 showing intermediate elevations. However, unexpected behavior began to appear on May 30 when water levels in well 857 began exceeding those in well 853, reversing the ambient north-northeastward flow between the wells (Figure 12) to southward flow (Figure 25). The flow reversal continued through July 11, after the peak river flow had passed (Figure 27). Though this anomalous behavior was potentially attributable to erroneous water-level measurements at well 853, that possibility appeared unlikely given that water elevations in the three wells returned to their usual order through the remainder of July and into August.

The temporary reversal in flow direction between wells 853 and 857 is notable for the length of time it lasted, which exceeded a month. It suggests that contamination in the vicinity of well 857 might be spread more to the southeast each year, expanding the breadth of plumes in the area. This type of spreading falls under the category of temporally variable flowpaths discussed in Section 4.5.1 regarding the existing conceptual model.

Note that water elevations at well 779 also temporarily exceeded those at well 853, beginning on June 11 and extending through June 23 (Figure 27). However, for reasons given in the following paragraph, this change in relative water levels did not appear to cause temporary flow from well 779 to well 853.

Throughout the time span in which water elevations at well 857 exceeded those at well 853 (May 30–July 3), water levels at well 779 remained less than the elevations at well 857. This observation suggested that some groundwater in the well-857 area during this period was capable of flowing toward the well-779 area while also flowing southeastward toward well 853. Correspondingly, it meant that a localized area of high groundwater elevation, such as a groundwater ridge, or mound, was temporarily present in the well-857 area, and that water was potentially splaying from the ridge in all directions (divergent flow) except toward the river. The likely source of the ridge water was enhanced, concentrated river losses to the aquifer in the vicinity of the USGS gaging station (Figure 25) that, at least temporarily (late May to late June), exceeded rates of river loss upstream and downstream of the station.

The exact cause of a temporary groundwater ridge near the river during a high flow period cannot be discerned using water elevations alone. Nonetheless, its occurrence suggests that the degree of hydraulic connection between the river and the aquifer varies with location, making it possible for some parts of the aquifer to respond more quickly than others to major changes in river stage. This explanation in turn implies that sediments affecting river–aquifer interaction are heterogeneous, such that aquifer hydraulic conductivity in some locales is significantly larger than in others. Geologic heterogeneity, whether in the sediments comprising riverbeds and riverbanks or aquifer materials in near-river zones, has been shown to strongly influence groundwater/surface-water exchange in research studies of river–aquifer interaction (e.g., Cardenas et al. 2004, Fleckenstein et al. 2006).

The 6- to 7-day delay between initial peak flows in the river and peak water levels in the three Group 2 wells (Figure 27) indicates that the alluvial aquifer behaves like an unconfined aquifer, with responses to hydrologic stresses governed by aquifer specific yield rather than storativity. If aquifer storativity determined the response, the time delay between the river and the wells would be smaller than that illustrated in Figure 27.

6.2.3 Group 3—Wells in the Trench 1 Area

Well hydrographs from the Group 3 area (Trench 1 area) during the initial 4 months of 2011 (Figure 28) showed no sign of being affected by variable river levels but were influenced by pumping at Trench 1. The most subtle influences of pumping were observed at wells 793 and 1009, about 410 and 330 ft, respectively, from the trench. Induced drawdowns at these two wells in response to remediation pumping in February 2011 were limited to about 0.3 ft. In contrast, larger drawdowns at the two wells of about 0.5 ft in May and 1 ft between late June and late August (Figure 28) appeared to be caused by a combination of Trench 1 pumping and ET in the local area. A time delay of about 2–4 days was observed between initiation of trench pumping and corresponding reduction in water elevation at wells 793 and 1009, which is representative of an unconfined aquifer.

At wells located closer to the trench (1105, 1140, 1141), water-level drawdowns in response to the pumping appeared to be instantaneous (Figure 28). The least amount of drawdown among the three wells was observed at well 1105, which is the farthest from Trench 1 (more than 100 ft northeast of the trench). Of some interest were the much larger drawdowns observed at well 1140 in comparison to those at well 1141, especially since both wells lie about 40–45 ft northeast of the trench. A difference of about 1 ft in the wells' respective water levels during pumping suggested that local aquifer materials are quite heterogeneous and that the hydraulic conductivity of alluvium surrounding well 1140 is substantially lower than the conductivity of sediments near well 1141. Such heterogeneity implies variable rates of contaminant capture along the 200 ft long trench when it is pumped.

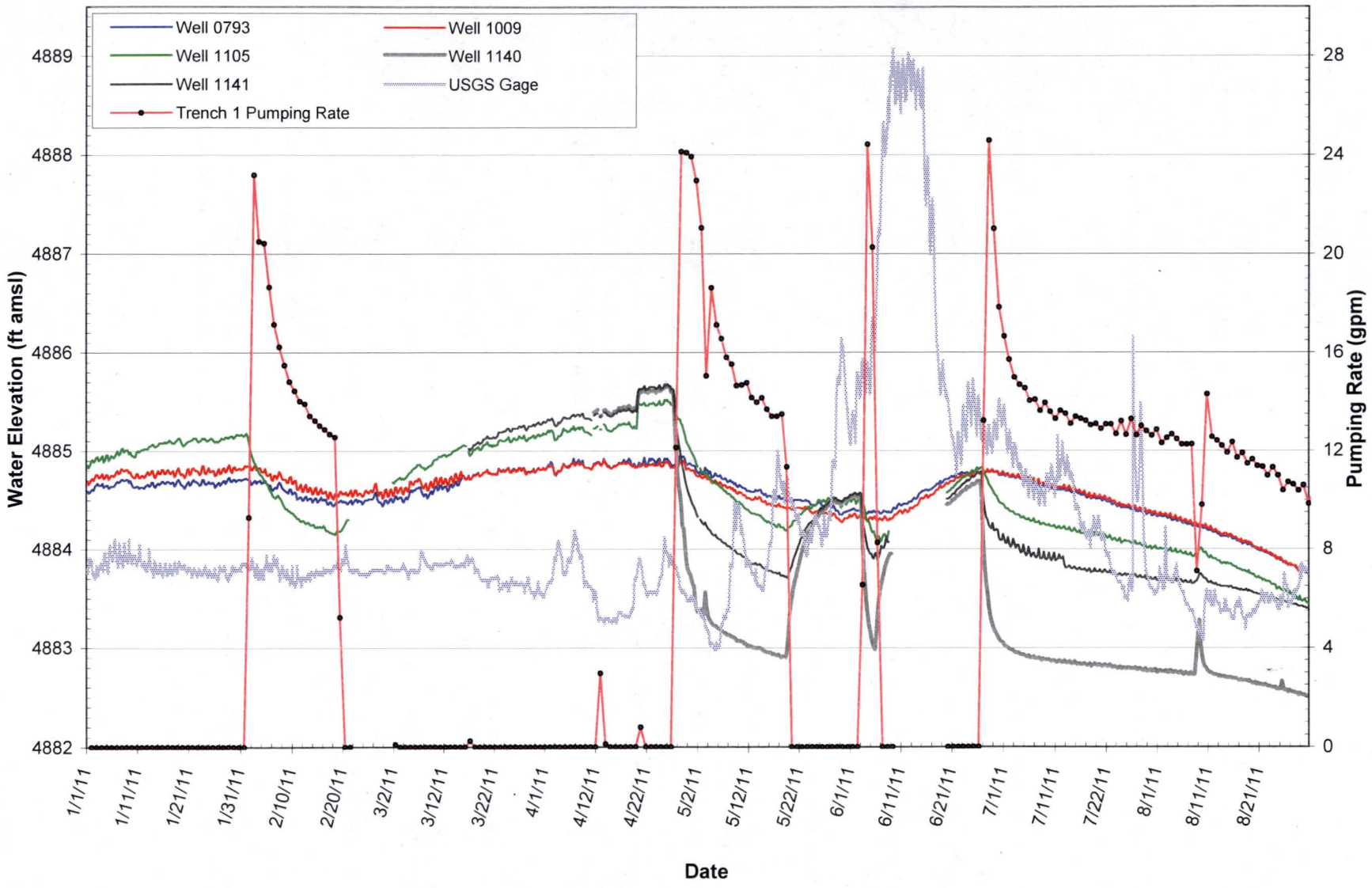

Figure 28. Hydrographs at Group 3, Trench 1 Area Wells, January 2011 through August 2011

6.3 Seasonal Changes in Groundwater Elevation

Preliminary assessment of groundwater-elevation data collected during fall monitoring events at the site indicated that water levels at wells in the vicinity of the USGS gage are often distinctly lower than the comparable river elevations measured at the gage, suggesting that the river potentially loses water to the aquifer in late-summer and early-fall months. Though river losses to the aquifer were known to occur during the buildup to peak river runoff from spring snowmelt (see discussion in Section 6.2.2), they were not anticipated during periods of much lower river flow in late summer and early fall. Because contributions of river water to the aquifer later each year potentially impact contaminant concentrations in near-river areas, seasonal relationships between river and groundwater levels were investigated further.

A review of previous studies of the Shiprock site also revealed that low groundwater elevations in late summer in comparison to equivalent river levels were noticed as early as the late 1980s as part of an investigation of the hydrochemistry of the floodplain alluvial aquifer (DOE 1987). The hydrochemistry report used this observation to argue that the river acts a line source of groundwater for the aquifer during summer and fall seasons. However, no explanation was given in the report (DOE 1987) for the comparatively low groundwater levels at this time of year.

6.3.1 Assessment of Semiannual Monitoring Data

To determine whether reversals in river–aquifer exchange are relatively common during early-fall monitoring events in comparison to events in early spring, the means of measured water elevations at all wells across the floodplain during each semiannual monitoring event between 2006 and 2011 were compared with equivalent river elevations at the USGS gage. Since each monitoring event typically consumed 3–4 days of time, the computed means of groundwater levels were actually the means of elevations measured over each event's duration, both at the USGS gaging station and at individual wells included in the groundwater calculations.

The results, illustrated in a bar graph in Figure 29, reveal a pattern that is repeated 5 of the 6 years included in the analysis. With the exception of 2008, mean river gage levels during each year's fall and spring events are typically within 0.4 ft of each other, but mean floodplain wide groundwater elevations in the fall tend to be 1 to 2 ft lower than mean elevations in the spring. Anomalously high flows in the river in spring 2008 (March 5–6), averaging more than 3400 cfs, made it impossible to discern such a pattern for that year. Though this simple analysis made use of water elevations at some wells affected by remediation pumping, the impact of the pumping-influenced water elevations on the overall observed pattern appeared to be minor. The observation of consistently lower groundwater levels in the fall was significant because it meant that groundwater flow patterns in the floodplain could vary noticeably between the spring and fall seasons, thereby altering contaminant movement with the onset of each new season.

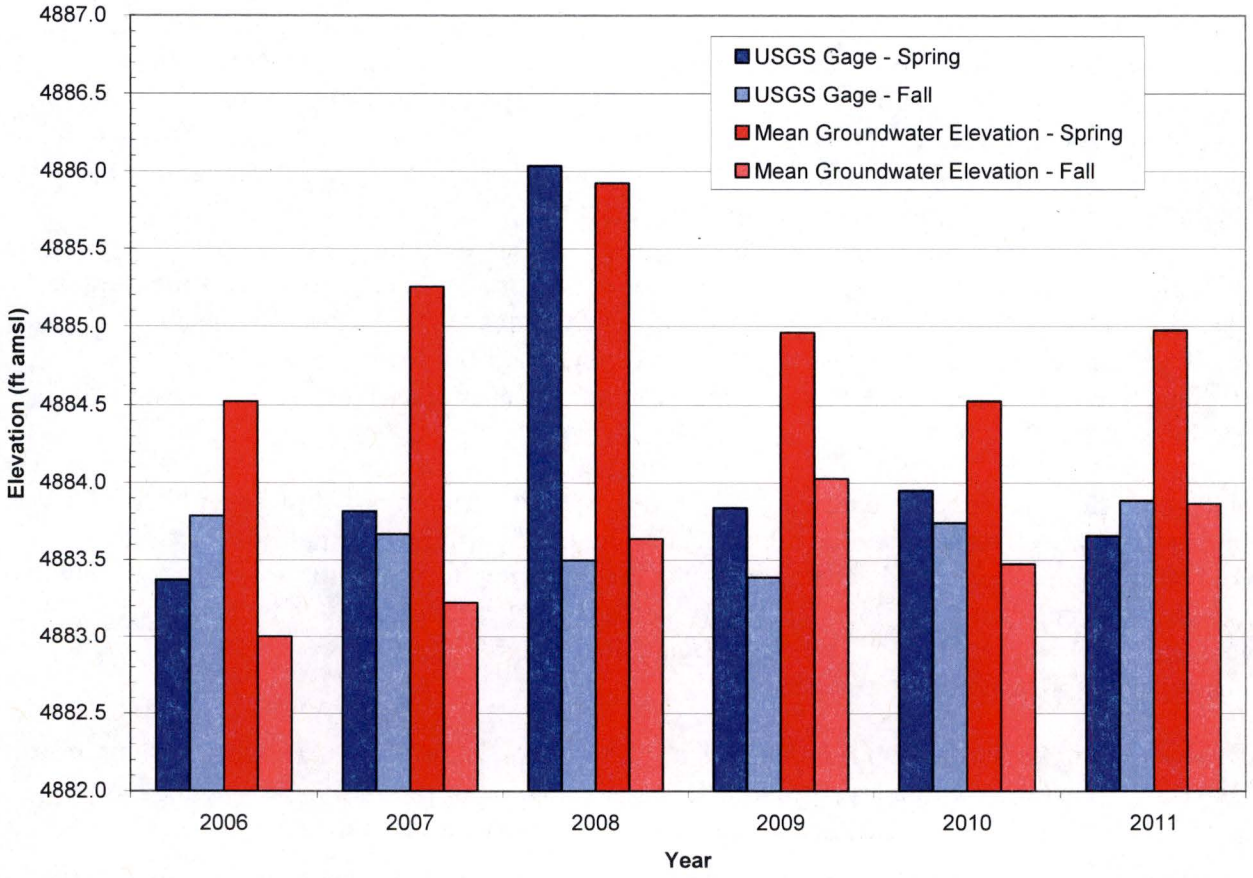

Figure 29. Mean River (USGS gage) and Groundwater Elevations During Semiannual Monitoring Events

Comparison of mean water levels from spring and fall monitoring events, by itself, does not reveal an explanation for the apparently lower groundwater elevations in the fall, but increased groundwater outflow via ET during midsummer, late summer, and early fall months is a plausible cause (see Huntington and Niswonger 2012). Most, if not all, vegetation on the floodplain is not expected to transpire water during colder periods (mid-October through mid-April) in the Shiprock area, but transpiration rates during the remaining time, with relatively warm weather, should be high. This is particularly true for local phreatophytes (e.g., tamarisk, cottonwoods), whose roots directly tap the water table. It is also likely that bare-ground evaporation of very shallow groundwater and some surface water takes place in the mounding area near the outlet of Bob Lee Wash during warm months. In addition to reducing the magnitude of the mounding near the wash outlet, the direct evaporation limits the net recharge of flowing artesian water from terrace-well 648.

6.3.2 Hydrographs for Wells West and South of the USGS Gaging Station

Hydrographs for individual floodplain wells were examined in search of further evidence that ET reduces groundwater levels in the alluvial aquifer during warm months in comparison to groundwater levels during preceding winter and early-spring months. The locations used for this purpose were the three wells previously identified as Group 2 wells (wells 779, 853, and 857), which are located west and south of the USGS gage (Figure 25) and are unaffected by remediation pumping (Section 6.2.2). Continuously monitored groundwater elevations at each of these wells were plotted for calendar years 2011, 2012, 2013, and 2014, as shown, respectively,

in Figure 30 through Figure 33. In addition, measured surface-water elevations at the river gage were plotted during two different seasons each year. The first season was meant to reflect relatively stable water elevations seen in the winter and early-spring season, when ET of alluvial groundwater is considered insignificant, and prior to the onset of rising river levels associated with snowmelt runoff from the San Juan Mountains. Measured water levels for the river and groundwater during this season are considered representative of conditions during the spring semiannual sampling event at the site, which typically occurs in March of each year (DOE 2014b). The second season was selected to reflect summer and fall months, following the high snowmelt runoff period that typically occurs each May and June. Observations made at this time of year, referred to in this report as the late-summer and fall period, are considered representative of the semi-annual monitoring event that usually takes place in either August or September (DOE 2014b).

Selection of the time periods representative of the respective winter/early-spring and late-summer/fall seasons was somewhat arbitrary. For the most part, the time periods were chosen to avoid large changes in groundwater elevation at the three monitoring wells caused by substantial, long-lasting changes in river flow. Relatively stable river flows, as indicated by graphs of average daily flow at the gaging station in Figure 30 through Figure 33, were also preferred for selecting the representative time periods.

As shown in Figure 30 through Figure 33, daily water-level data were occasionally missing from the hydrographs for individual wells. Nonetheless, evaluation of the well hydrographs that contained continuous daily data each season led to the following general findings:

- Water levels in the three Group 2 wells are lower in the late-summer/fall season than in the winter/early-spring season even though the river discharge and gage elevation are generally similar in value between the two seasons. This is particularly true for wells 779 and 853, which are located farther from the river than well 857 and are, therefore, less affected than well 857 by short-term changes in river elevation.
- The river loses water to the alluvial aquifer frequently during the late-summer/fall season, whereas groundwater in the vicinity of wells 857 and 853 mostly discharges to the river during the winter/early-spring season.
- Minor differences in measured groundwater elevations between the respective seasons were observed in 2013, which appeared to be partly due to a much higher average river flow during the late-summer/early-fall season (749 cfs) than during the winter/early-spring period (567 cfs). Nevertheless, the 2013 hydrographs indicated that the river frequently lost water to the aquifer in the late-summer/fall period, whereas groundwater discharge to the river dominated the preceding winter/early-spring season.

The hydrographs shown in Figure 30 through Figure 33 suggest that groundwater flow directions in the vicinity of the USGS gage are changing quickly, not only during the period of high snowmelt runoff but also frequently during the late-summer/fall period. This observation further suggests that advective transport of contaminants in the alluvial aquifer is also frequently changing direction. Short of any evidence for alternative causes of decreased groundwater elevations during mid-summer, late-summer, and fall months, ET of alluvial groundwater provides the most likely explanation for the river losses and changing transport directions. Winter et al. (1998) discuss how seasonal transpiration of groundwater by phreatophytes on floodplains adjoining rivers in the western United States induces seepage loss of surface water.

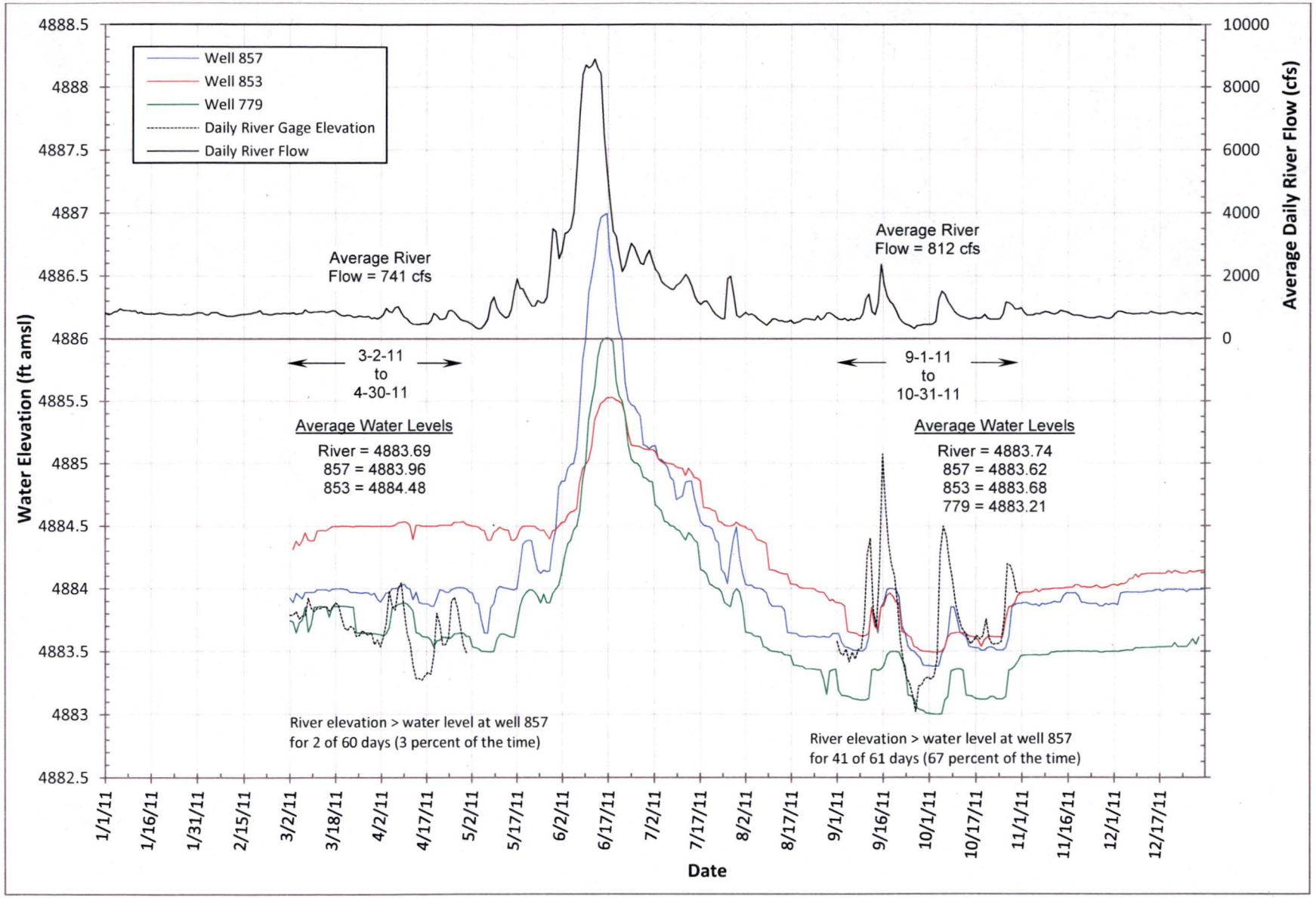

Figure 30. Hydrographs for the USGS Gaging Station and Nearby Wells 779, 853, and 857 in 2011

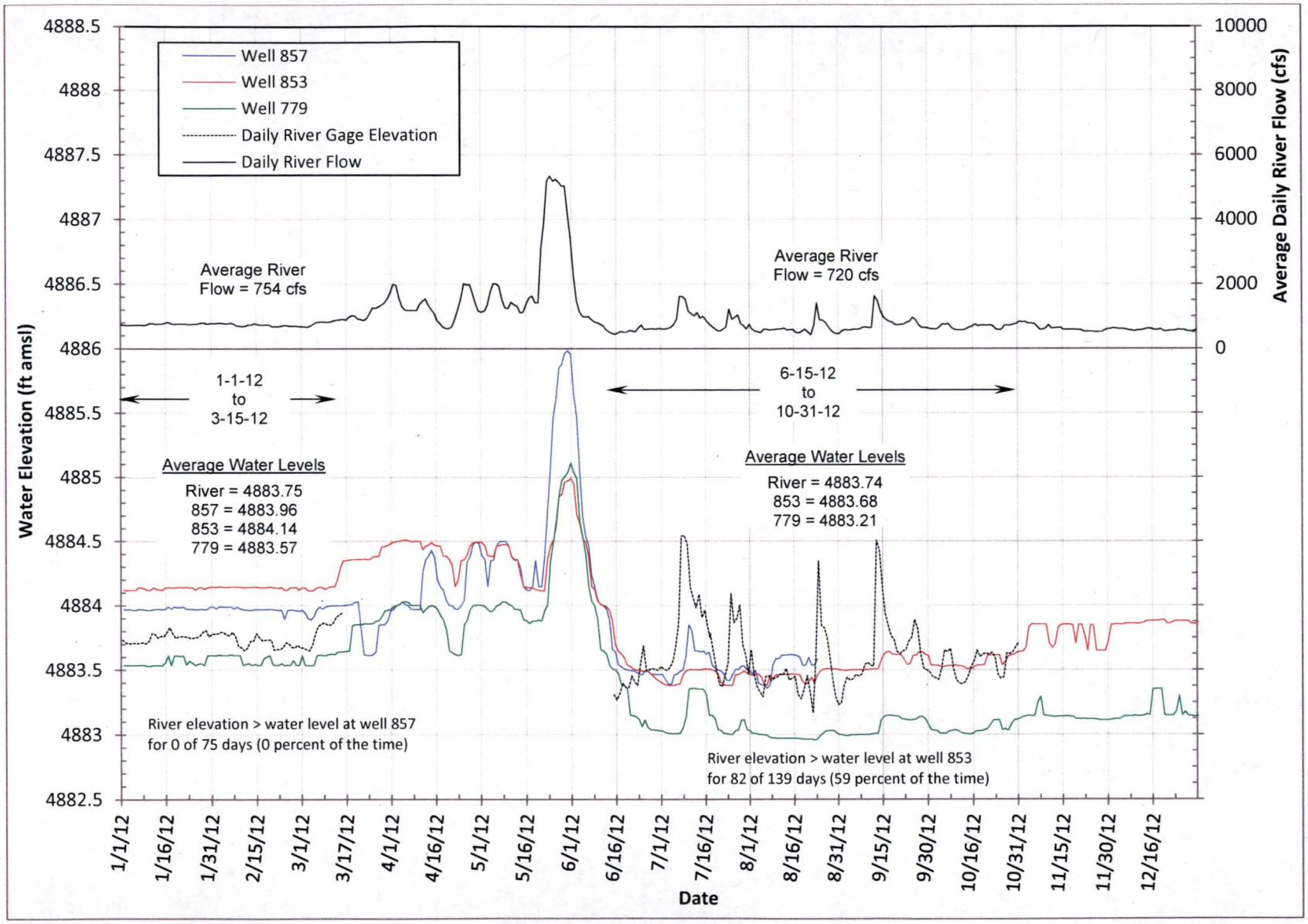

Figure 31. Hydrographs for the USGS Gaging Station and Nearby Wells 779, 853, and 857 in 2012

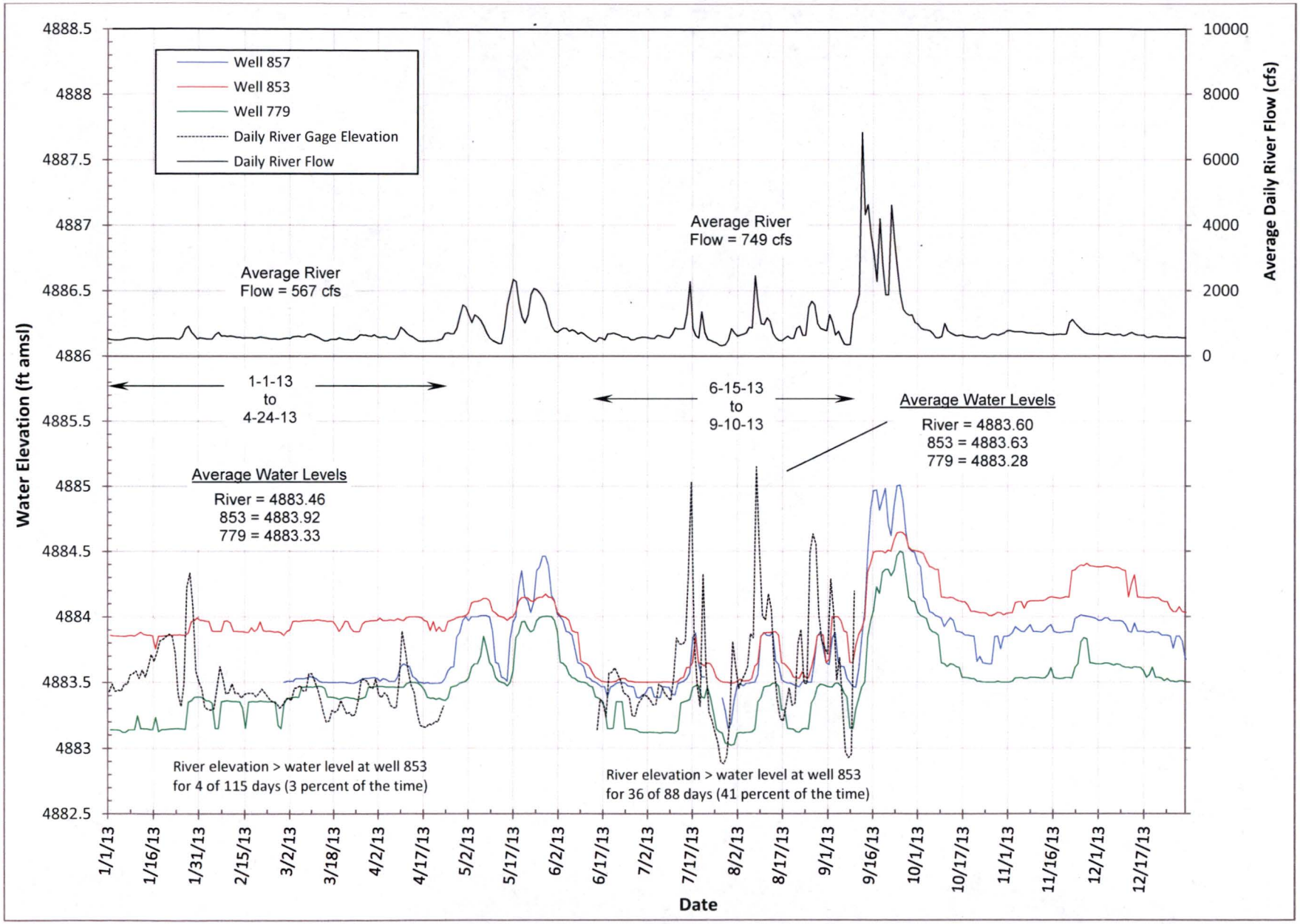

Figure 32. Hydrographs for the USGS Gaging Station and Nearby Wells 779, 853, and 857 in 2013

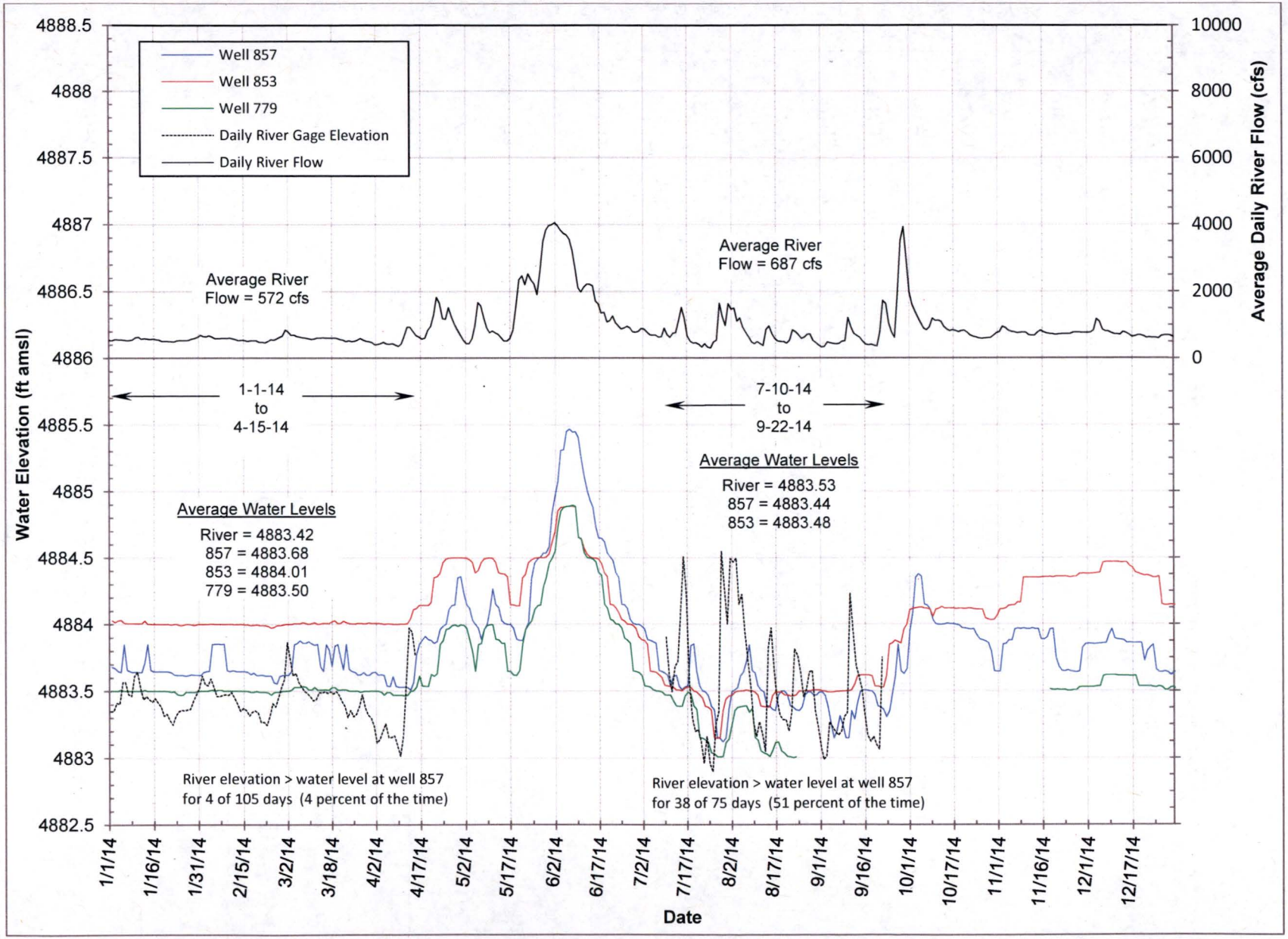

Figure 33. Hydrographs for the USGS Gaging Station and Nearby Wells 779, 853, and 857 in 2014

6.3.3 Significance of Evapotranspiration Losses

Transpiration of water from the alluvial aquifer in late summer and fall is important partly because it signifies that water uptake by vegetation could be an alternative form of remediation pumping, and partly because the apparent river losses to the aquifer during this time of year could impact groundwater chemistry, e.g., contaminant concentrations, in the vicinity of the river. In addition, changes in flow direction associated with spatially variable ET might help explain the apparent lateral spreading of the uranium and sulfate plumes on the northward-trending plume lobes between Trench 1 and the 1089/1104 area (Section 4.5.1).

Detailed analysis of measured groundwater levels at the numerous alluvial monitoring wells on the floodplain (Figure 5) would be required to confirm seasonal variations in flow direction. One approach would be to contour measured water elevations during the respective early spring and fall monitoring events over multiple years. However, such contouring can be quite subjective and is susceptible to interpretation error. Alternatively, a more rigorous determination of temporally variable flow directions could be achieved with three-point estimators of local magnitude and orientation of the hydraulic gradient (e.g., McKenna and Wahi 2006). This latter approach would be most effective if key monitoring wells were fitted with transducers and logging equipment for recording water elevation over relatively short intervals (e.g., 15 minutes) and the collected data were included in SOARS. Computed three-point estimations of gradient based on "continuous" water-level data in both surface water and groundwater would enable identification of not only gradually changing flow directions between seasons but also rapid changes in response to episodic hydrologic events, and the mechanisms responsible for those changes.

Additional lines of evidence supporting the hypothesis that the river recharges the alluvial aquifer during late summer and early fall are presented in Section 7, which describes simulations made with the groundwater flow model produced for this study. For example, it is shown how transient model runs fall short of capturing lower groundwater levels in late summer if losses to ET are not taken into account. In addition, simulation of the alluvial-aquifer flow field in September 2010 suggests that ET causes groundwater levels to be noticeably less than nearby river elevations along most sections of the river adjoining the floodplain.

6.4 Contaminant Plumes in 2011

Map views of contaminant plumes included in recent annual performance reports for the entire Shiprock site (e.g., DOE 2009a, 2010, 2012, 2013, 2014b) have provided indications that remediation pumping has led to significant reduction of contaminant mass in the floodplain. In addition, temporal plots of constituent concentrations at several wells in the preliminary Trench 1 evaluation (ESL 2011b) have confirmed remediation progress in the Trench 1 and 1089/1104 areas. Color-flood plots of contaminant concentration presented in this section augment those reports by focusing solely on recent configurations of the sulfate, uranium, and nitrate plumes in floodplain groundwater in 2011. Most of the data used to construct the plots were based on sample results from the semiannual monitoring event in March 2011, but several of the concentrations were derived from samples collected during the preceding (September 2010) monitoring event. The large-scale plume maps (scale of 1 inch = 500 ft) shown in following sections help clarify the extent to which the existing remediation system has been successful in reducing plume sizes and limiting contaminant discharges to the river.

6.4.1 Sulfate and Uranium

Figure 34 and Figure 35 show plots of mapped sulfate and uranium concentrations, respectively, in the alluvial aquifer during 2011. Comparison of both figures with the 1999–2001 distributions (Figure 14 and Figure 15) demonstrate that the total dissolved mass and the concentrations associated with each of the contaminants at most wells were greatly reduced between the two times. For sulfate, some of the most noticeable decreases took place at the base of the escarpment between the two trenches and in the 1089/1104 area. Whereas the peak observed sulfate concentration in the 1089/1104 area during 1999–2001 was 28,800 mg/L, the greatest concentration in this area in 2011 was 11,300 mg/L. As documented in previous assessments of the southern third of the floodplain (e.g., DOE 2009b, DOE 2011), pumping at Trench 2 continues to pull in fresh water from nearby portions of the river, thereby creating a zone virtually free of sulfate contamination between the trench and the river (Figure 34).

Many of the largest reductions in uranium concentration took place within the former, north-oriented plume lobe that connected the Trench 1 and 1089/1104 areas. Here, uranium levels that approached 3 mg/L in 1999-2001 were reduced to concentrations in 2011 that were mostly less than 1 mg/L (Figure 35). Uranium in the 1089/1104 area in 2011 tended to range from about 0.2 to 1.4 mg/L, whereas the concentration range for this constituent in the same locale in the 1999–2001 time frame was 1.2 to 4.4 mg/L (Figure 15). Though somewhat high levels of uranium persisted in 2011 at the base of the escarpment between Trench 1 and Trench 2 (0.7–2 mg/L, Figure 35), the reductions in concentration here in comparison to 1999–2001 were also apparent.

Wells within 200 ft of Trench 1 (e.g., wells 615, 1105, 1111, 1112, 1140, 1141) continued to exhibit relatively high concentrations of both sulfate and uranium in 2011, though the levels of these contaminants in the vicinity of the trench appeared to have decreased (Figure 34 and Figure 35) in comparison to concentrations observed during 1999–2001 (Figure 14 and Figure 15). On the east side of the trench, the apparent contaminant persistence could be attributed to the long curvilinear flowpaths (Figure 17) that dissolved sulfate and uranium migrate along. In 2011, concentrations of sulfate and uranium had the potential to remain at wells on the southwest side of Trench 1 (wells 1111 and 1112) if contaminated terrace groundwater near the trench location at the time continued to discharge to the alluvial aquifer across the escarpment.

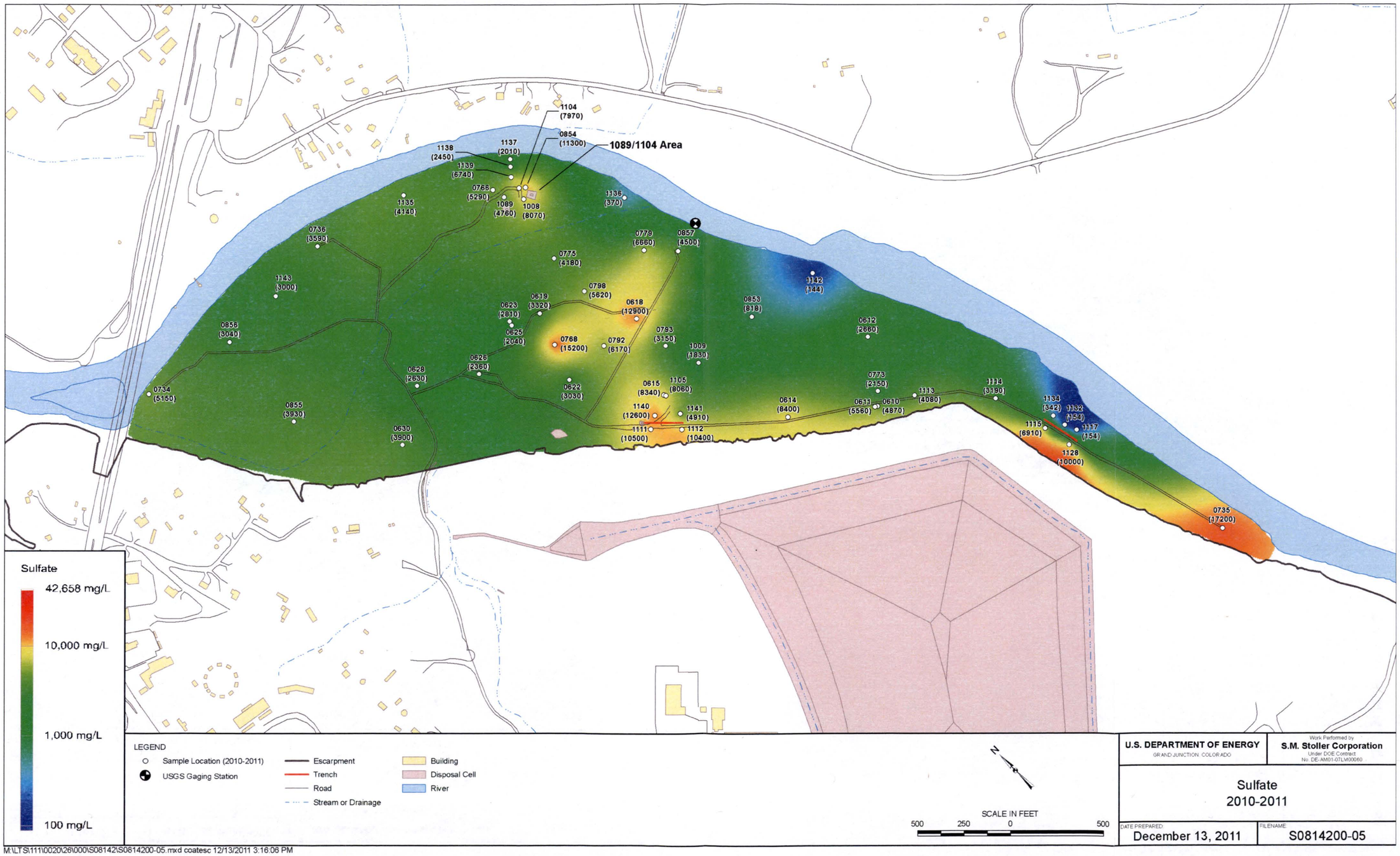

Figure 34. Sulfate Plume in 2011

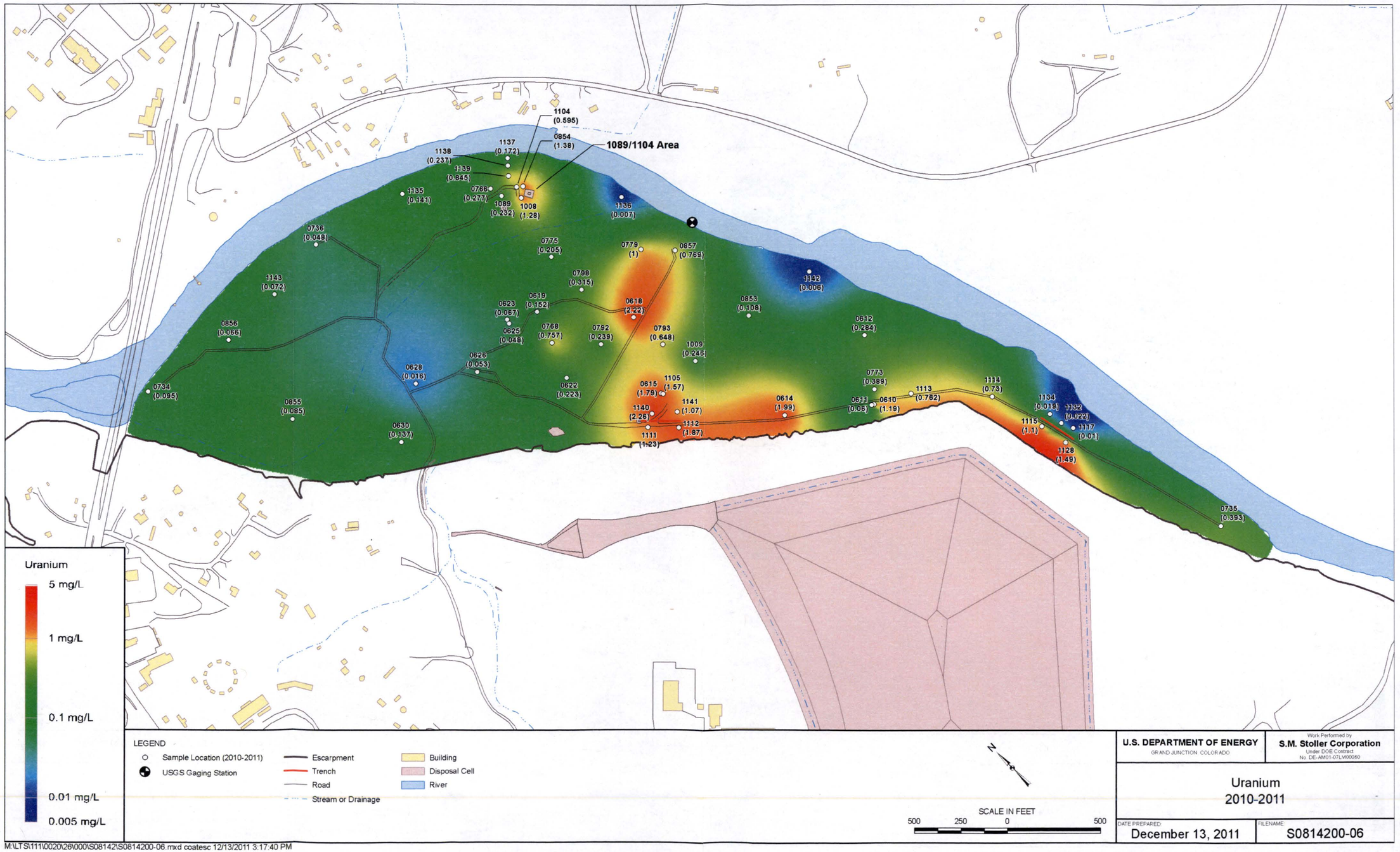

Figure 35. Uranium Plume in 2011

An isolated area of relatively high sulfate and uranium concentrations persisted in 2011 in the vicinity of well 618, about 600 ft northeast of Trench 1. Of some interest is the fact that measured sulfate and uranium levels at this well at the time (Figure 34 and Figure 35) were greater than concentrations measured during the 1999–2001 period (Figure 14 and Figure 15). The reason for the higher contaminant levels in 2011 is unclear. Possible explanations might be found in the flowpaths, which were assumed in the existing model to result from simultaneous remediation pumping in the Trench 1 and 1089/1104 areas (Figure 17) and the stagnation zone a short distance southwest of well 618. If the elevated concentrations in the well 618 area were the result of groundwater flow phenomena, whether due to baseline processes or flow patterns associated with remediation pumping, the low groundwater velocities in the area associated with the stagnation zone were expected to slow aquifer flushing with fresh water, thereby allowing the high concentrations to persist for multiple years.

It is also possible that the high concentrations observed at and near well 618 in 2011 were caused by something other than groundwater flow processes. Another alternative examined was a change in water sampling procedure during the early 2000s. Though "high-flow" methods aimed at purging three casing volumes of water from the well were traditionally implemented at the Shiprock site, a conversion to "low-flow" techniques began in March 2002, and these same methods were applied in following years through 2011. A graph of uranium levels at well 618 through 2011 (Figure 36) indicates that an increase in concentrations of this constituent coincided with the change in sampling method and that subsequent concentrations remained higher than those resulting from earlier high-flow methods.

In recent years, an investigation by the ESL (DOE 2014a, 2015b) has shown that salinity in multiple alluvial-aquifer wells at the Shiprock site increases significantly with depth in the well casings, including at well 618. In some cases, the recorded specific conductances near the bottom of wells have approached values as great as 18,000 µS/cm, providing additional evidence that density-dependent flow occurs in the alluvial aquifer. Uranium concentrations measured at 0.5-foot intervals in well 618 have also shown significant increases with depth, from values of about 0.5 mg/L near the top of the well screen to as large as 1.9 mg/L near the bottom of the well. This finding, in conjunction with the apparently different concentrations stemming from changes in sampling method (Figure 36), suggests that low-flow sampling at well 618 collects water from deeper parts of the well (see Section 4.5.3), whereas purge sampling at the well represents a composite of waters from multiple well depths.

Examples of increasing constituent concentrations with depth in the alluvial aquifer similar to those observed for specific conductance and uranium at well 618 were also found in earlier descriptions presented in the GCAP (DOE 2002) of nitrate contamination in floodplain groundwater. In particular, nitrate concentration data from samples collected from several test pits, well points, and alluvial wells near the base of the escarpment east of the disposal cell revealed that nitrate concentrations varied with sampling depth. The samples collected from the test pits and well points, which were considered representative of shallow groundwater, had lower nitrate concentration than samples collected from the wells, which were screened mainly in lower parts of the alluvial aquifer (DOE 2002).

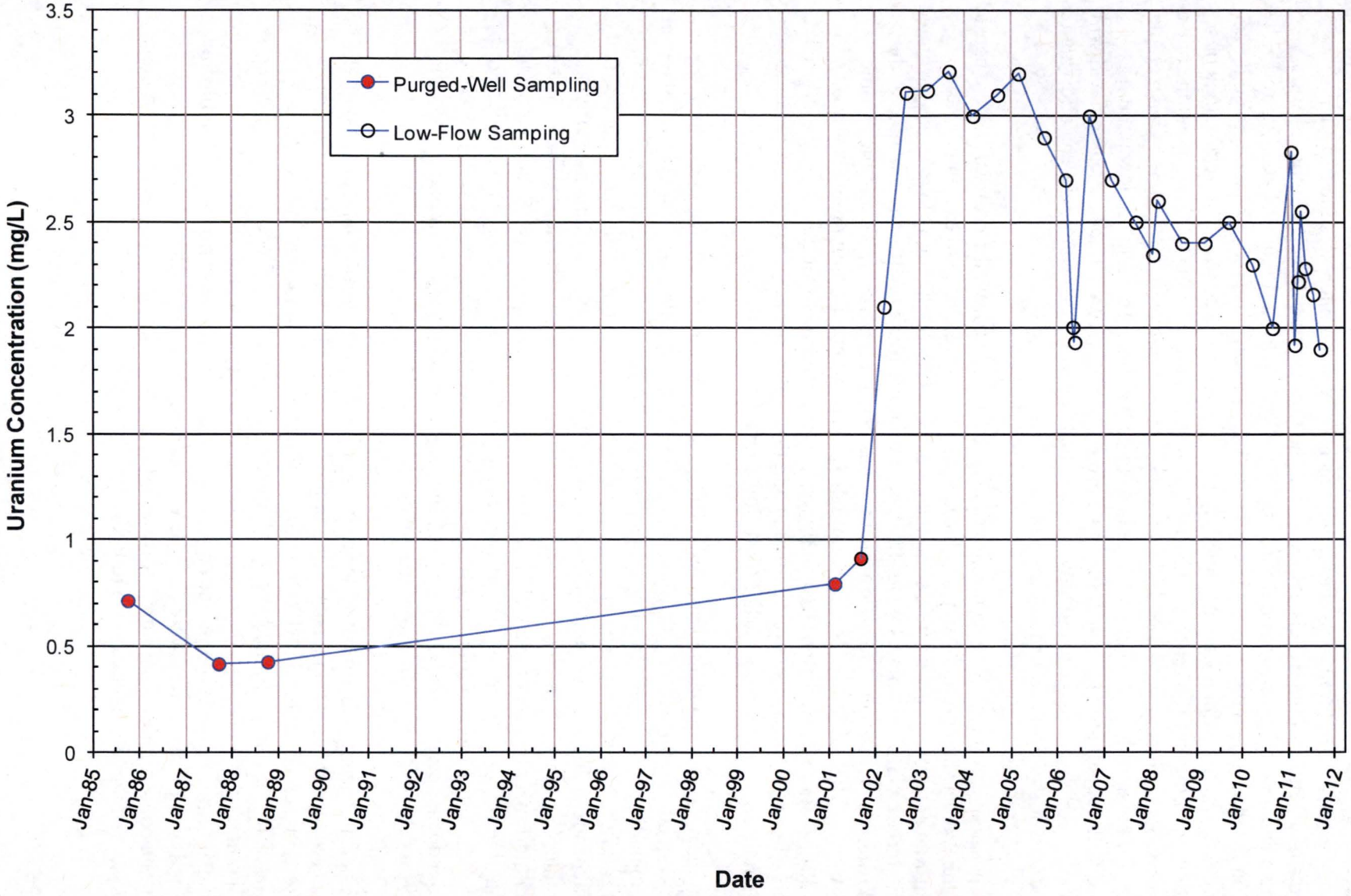

Figure 36. Temporal Plot of Uranium Concentrations at Well 618

The plumes shown in Figure 34 and Figure 35 demonstrate that pumping at Trench 1 since spring 2006 has successfully intercepted contamination converging on the trench area from the northwest and southeast, thereby preventing further contaminant migration toward the 1089/1104 area. This observation suggests that Trench 1 pumping is an effective component of the compliance strategy for the floodplain aquifer.

6.4.2 Nitrate

The spatial distribution of nitrate (as nitrogen [N]) concentrations in 2011 (Figure 37) indicates that remediation pumping has also contributed to the mass reduction of this contaminant. Though nitrate as N levels in wells at the base of the escarpment in 2011 tended to remain above the applicable drinking water standard (10 mg/L), most monitoring locations away from the escarpment that previously had high nitrate levels were showing concentrations below the standard in 2011. Naturally occurring denitrification in these areas was expected to decrease nitrate concentrations even further after 2011.

6.4.3 Reductions in Plume Mass

The degree to which the sulfate, uranium, and nitrate contamination was reduced during the first 8 years since groundwater remediation began in 2003 was estimated using the concentration–contour plots for the plumes in 1999–2001 (Figure 14 through Figure 16) and 2011 (Figure 34, Figure 35, and Figure 37). The plume for each contaminant was digitized to produce a local concentration tied to the spatial coordinates of each cell in the numerical model produced for this study (see Section 7), and contaminant mass associated with that location was computed by multiplying the concentration by the aquifer's saturated volume within the cell. Subsequent summation of the individual cell masses resulted in the total plume mass. Because the volume of groundwater in the alluvial aquifer changes with variations in river flow and, apparently, in response to ET discharges during summer and early fall months, a single, baseline configuration of the aquifer flow was chosen for the saturated volume calculations. The configuration selected for this purpose was the calibrated model of assumed steady-state flow conditions in March of 2011, as described in Section 7.3.1.

Table 6 lists the resulting plume masses for each contaminant at the two different times. The table also lists the mass reduction and percent removal estimates that are attributed to 8 years of remediation pumping. As shown, the reduced mass fractions ranged from 40 (sulfate) to 72 (nitrate as N) percent.

Table 6. Estimated Total Plume Masses in 1999–2001 and 2011

Contaminant	Plume Mass in 1999–2001		Plume Mass in 2011		Mass Reduction From 8 Years of Remediation		Percent Reduction
	(kg)	(lb)	(kg)	(lb)	(kg)	(lb)	
Sulfate	2,927,990	6,441,580	1,766,280	3,885,810	1,161,710	2,555,770	40
Uranium	335	735	120	270	215	465	64
Nitrate (as N)	13,640	30,000	3,880	8,530	9,760	21,470	72

Abbreviations:
kg = kilograms, lb = pounds

6.5 Contaminant Sources in Terrace Groundwater

As part of an assessment of contamination in terrace groundwater, the SOWP (DOE 2000) reported that inorganic contamination beneath some areas of the terrace was sourced solely by natural leaching of the underlying Mancos Shale. This was mostly considered true for sulfate, uranium, and selenium in terrace groundwater in irrigated areas west of what is now Highway 491. In contrast, the ratio of activity concentrations for the radionuclides uranium-234 (U-234) and uranium-238 (U-238) in Mancos Shale wells near the mill indicated that bedrock groundwater contamination close to the escarpment was mostly, if not entirely, caused by mill-related processes (DOE 2000). The uranium isotope data further suggested that flow of bedrock groundwater near the mill site to the floodplain was the source of contamination in the alluvial aquifer. The SOWP (DOE 2000) did not allow for the possibility that physical and chemical processes in Mancos Shale beneath the terrace affected contaminant transport to the floodplain.

A separate investigation conducted by the ESL on behalf of LM (ESL 2011a) examined the potential for Mancos Shale in Colorado, New Mexico, and Utah to be a natural source of several inorganic constituents in regional groundwater systems. Findings made in the Mancos Shale study (natural contamination report) provided multiple lines of evidence that high salinity levels and high concentrations of sulfate, uranium, nitrate, and selenium resulted from natural leaching of the shale by subsurface water. The natural contamination report was based on samples collected from 51 sites containing outcrops of Mancos Shale. Five of the sampling sites were near Shiprock, and one of these was a seep discharging from shale in Many Devils Wash, about 2000 ft east-southeast of the disposal cell at the Shiprock site. All samples collected at the sampling sites in the Shiprock area indicated that relatively high levels of sulfate, uranium, nitrate, and salinity (specific conductance) were produced by the leaching of local Mancos Shale. High salinity at the Many Devils Wash location was indicated by a specific conductance that exceeded 37,000 µS/cm. Similarly, sulfate, uranium, and nitrate (as nitrate) concentrations at the wash seep were about 22,000, 0.17, and 3100 mg/L, respectively. The natural contamination report (ESL 2011a) also showed that groundwater flowing through Mancos Shale dissolved natural organic matter in the shale, producing relatively high concentrations of dissolved organic carbon, a natural source of electron donors that facilitate microbially mediated chemical reactions affecting the dissolved concentrations of inorganic constituents.

The above-mentioned findings in the SOWP (DOE 2000) and the natural contamination report (ESL 2011a) are germane to this study because of the local presence of Mancos Shale (below the terrace, in the escarpment, and in bedrock underlying the floodplain aquifer) and the fact that several of the aqueous constituents attributed to leaching of shale are also considered mill-generated contaminants in the alluvial aquifer. Though numerous reports on the Shiprock site attribute the greater bulk of contamination in both terrace and floodplain groundwater in the vicinity of the former mill to mill processes, leaching of the Mancos Shale has potentially contributed to some of the high concentrations observed in the floodplain alluvial aquifer. With such a conceptual model, it is reasonable to assume that contamination in floodplain groundwater since the mid-1980s could have resulted from one of the following processes in Mancos Shale: (1) conservative (nonreactive) transport of mill-related constituents from the terrace to the floodplain; (2) discharge of naturally occurring contamination from the terrace to floodplain groundwater; and (3) reactive transport of mill-related constituents whose concentrations are modified while in the shale. Under the last process, it is assumed that constituent concentrations could be affected by leaching of the shale or additional transport processes, such as sorption, biologically mediated reactions, and fracture–matrix interactions.

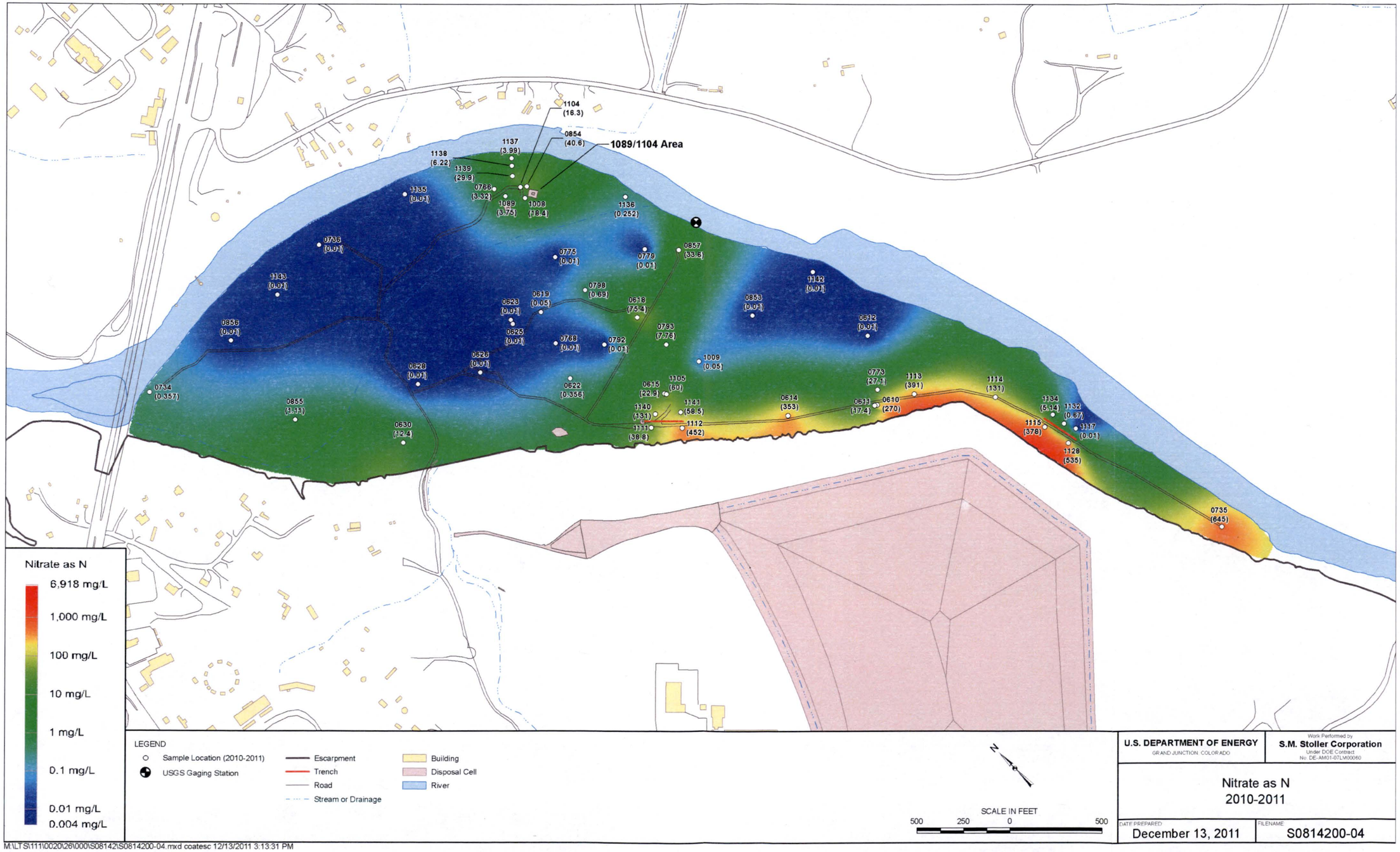

Figure 37. Nitrate as Nitrogen Plume in 2011

This page intentionally left blank

If bedrock discharge of "naturally contaminated" water is present at the Shiprock site, it probably occurs along portions of the escarpment located farthest from mill features (i.e., mill buildings, ore piles, raffinate ponds, tailings piles). Accordingly, parts of the escarpment located between the Bob Lee Wash outlet and the river near Highway 491 might be considered candidate sites for natural contaminant discharge from the terrace to the floodplain. As mentioned in Section 4.3, percolation of water into Mancos Shale bedrock along the tributary connecting the well and Bob Lee Wash (Figure 2) could be a source of terrace groundwater that eventually discharges to the alluvial aquifer in areas north of the wash outlet. On the other hand, mill-related contaminant discharges to the floodplain in areas northwest of the wash outlet are unlikely because terrace groundwater that migrated northwestward from the former mill area was expected to discharge to Bob Lee Wash, which incises the terrace multiple tens of feet.

6.5.1 Discharge to the Alluvial Aquifer

Virtually all studies of the Shiprock site that have examined the combined hydrogeology of the terrace and floodplain areas have identified discharge of terrace groundwater across the escarpment as the primary source of contamination in the floodplain alluvial aquifer. Though one of the earliest groundwater flow models developed for the site (DOE 1995a) did not directly simulate this discharge, the initial SOWP (DOE 1995b) indicated that contamination would be delivered to the floodplain by this process. Much of the bedrock discharge was attributed to eastward and northeastward flows off of a groundwater mound beneath the terrace caused by recharge of water used for milling operations (DOE 1995b). The model developed for the final SOWP (DOE 2000) explicitly accounted for recharge that became bedrock discharge to the floodplain, as did the Knight Piesold (2002) model that was used to develop the GCAP (DOE 2002).

More recent studies have also concluded that discharge of bedrock groundwater to the floodplain alluvium plays a crucial role in the creation and eventual disposition of groundwater contamination in the alluvial aquifer. The refined conceptual model (DOE 2005b) contained evidence that flow through Mancos Shale occurs mostly within less-resistant shale layers and bedding-plane fractures, on the top of thin bentonite beds and a prominent calcareous siltstone bed, and within occasional vertical fractures in the shale. Because much of the flow takes place in secondary-permeability features (i.e., fractures) that can react strongly to spatially and temporally variable recharge processes, discharge of contaminated terrace groundwater across the escarpment is also expected to be highly variable. The groundwater flow and transport model developed for the Trench 2 study (DOE 2009b) would not have been able to capture generally observed features of contaminant transport in the south third of the alluvial aquifer had it not accounted for discharge of bedrock groundwater across the escarpment. A more recent evaluation of the internal water balance for the disposal cell at the Shiprock site (DOE 2012) indicated that contaminated tailings fluids percolated into native subsurface materials on the terrace for approximately 15 years when ponded fluids were present over the materials. As a consequence, contaminated fluids are expected to remain in and adsorb to the subsurface sediments, including the Mancos Shale, and slowly and continually flush to groundwater by recharge (DOE 2012).

Though nearly all versions of the conceptual model for the floodplain alluvial aquifer at the Shiprock site explicitly include inflow of contaminated terrace groundwater, primarily across the

escarpment, the numerical models developed for the SOWP (DOE 2000) and Knight Piesold (DOE 2002) are the only quantitative tools used to assess how bedrock discharge across the escarpment might change in future years and how such changes will impact floodplain groundwater. Both of these models were based on assumed pumping rates from remediation wells installed at several locations on the terrace and concomitant declines in terrace groundwater elevations, such that the rate of bedrock discharge would decrease to the point where cleanup of the floodplain alluvial aquifer was feasible (DOE 2000, 2002). Periodic evaluations of remediation progress at the Shiprock site since remediation pumping began in 2003 (DOE 2003a, 2003b, 2004, 2005a, 2006, 2007, 2008, 2009a, 2010, 2012, 2013, 2014b) indicate that reductions (drawdowns) in terrace groundwater levels have not been as large as originally predicted through modeling. It is difficult to ascertain how actual groundwater drawdowns beneath the terrace have affected flows across the escarpment to the alluvial aquifer. Accordingly, contaminant discharge to the floodplain remains uncertain, as does the time it will take for bedrock discharge to decline sufficiently for aquifer remediation to be successful.

It should be noted that the flow model developed for this study would not have been able to successfully match observed groundwater levels in March 2011 and March 2010 (see model calibration discussions in Section 7) if discharge of bedrock groundwater across the escarpment had not been included as a component of the model. This finding suggests that flows across the escarpment, such as those derived from the modeling (Section 7.3.1.3), were present in the Shiprock groundwater system as recently as 5 years ago.

6.5.2 Quantifying Mancos Shale Flows

Given the uncertainties associated with the discharge of contaminated terrace groundwater to the floodplain alluvial aquifer, better methods for characterizing bedrock discharge rates are needed. Unfortunately, other than using improved flow and transport models to match observed water levels and concentrations in floodplain alluvium, readily available technologies do not appear to meet this need. This is because subsurface flow from the terrace to the floodplain mostly takes place in preferential flow zones in shale, such as in secondary-permeability features that are difficult to pinpoint, let alone to quantify the flow rates within them. Flow from the terrace to the floodplain through fractured shale can be described as an equivalent porous medium process that is both spatially and temporally variable. It is not feasible to determine accurate values of the equivalent hydraulic conductivities that govern the secondary-permeability flows through Mancos Shale in areas hydraulically upgradient of the escarpment.

The most definitive evidence of persistent bedrock groundwater discharge to floodplain alluvium is the continued presence of contamination in the alluvial aquifer, particularly at the base of the Mancos Shale escarpment. Reasonable estimates of bedrock contaminant discharges were derived from the models developed for the SOWP (DOE 2000) and the Trench 2 study (DOE 2009b), primarily by adjusting the flows and contaminant levels within them to achieve relatively good fits to observed constituent concentrations in the alluvial aquifer. However, the uncertainties involved are such that model-derived discharges to the aquifer could easily differ from actual inflows by as much as an order of magnitude. Unfortunately, current monitoring requirements at the Shiprock site do not call for explicit steps to track inflows to the alluvial aquifer from the terrace.

6.6 Evidence of Bedrock Inflow

This study examined available water-level and water-chemistry data collected at the Shiprock site for evidence that contaminated terrace groundwater has been discharging to the floodplain alluvial aquifer during the past few years. The data analysis focused partly on elevated salinity and contaminant concentrations in the alluvial aquifer near the foot of the escarpment and whether contaminant indicators in these areas are decreasing to low values reflective of successful aquifer remediation. Persistence of relatively high concentrations near the escarpment, if any, might be attributed to continued discharge of Mancos Shale groundwater to floodplain alluvium. The data analysis also evaluated water-elevation and water-chemistry data at terrace wells near the escarpment.

6.6.1 Groundwater Levels at Wells Near the Escarpment

Groundwater levels and contaminant concentrations at multiple wells installed near the escarpment were examined in the SOWP (DOE 2000) for evidence that bedrock groundwater beneath the terrace was discharging to the floodplain in 2000 and causing the relatively high contaminant concentrations observed at the time at the base of the escarpment (Figure 14, Figure 15, and Figure 16). The resulting water-elevation data, posted at well locations along three cross sections traversing the escarpment near the northeast border of the disposal cell (Figures 4-31, 4-32, and 4-33 in the SOWP [DOE 2000]), did little to support the hypothesis that terrace groundwater levels were higher than groundwater elevations in the floodplain alluvium and that bedrock groundwater was flowing from the terrace to the floodplain. At two of the cross sections, wells completed on the terrace and near the top of the escarpment in Mancos Shale were either dry or showed water levels that were substantially less than the groundwater levels in corresponding wells completed in the floodplain alluvial aquifer. At the third section, the water levels in 2000 at one terrace well completed in shale above the floodplain and two other terrace wells completed well below the base of the alluvial aquifer were all higher than comparable water elevations in floodplain alluvial wells (DOE 2000). Since that time, however, data collected at all three terrace wells in the third section indicate that they have essentially gone dry.

The SOWP (DOE 2000) evaluation of near-escarpment water levels indicated that the terrace wells along the above-mentioned cross sections were not intercepting portions of the Mancos Shale that are hydraulically connected to floodplain groundwater. The evaluation also showed that water levels at several floodplain wells completed in Mancos Shale were distinctly lower than corresponding water elevations in wells completed in overlying alluvium. The combination of this latter observation with either dry conditions or very low groundwater levels at corresponding terrace wells suggested that much of the water found in competent (unweathered) Mancos Shale at the Shiprock site occurs in zones that are largely, if not completely, separated from a shallower groundwater system in bedrock that is hydraulically connected to floodplain alluvium. This hypothesis was supported by sulfate and uranium concentrations at Mancos Shale wells along the cross sections, which are much lower than corresponding concentrations for these constituents in floodplain alluvial wells (DOE 2000, Section 4.4.2.1).

Two additional sets of bedrock and alluvial aquifer wells at the escarpment near the northeast border of the disposal cell were examined in this study in search of terrace wells that have water levels representative of bedrock groundwater flowing to the floodplain. One of these sets,

consisting of terrace bedrock well MW1 near the top of the escarpment and floodplain alluvial wells 610 and 611 (see Figure 5 for well locations), showed the terrace water elevations consistently 15–20 ft higher than floodplain levels, implying that local Mancos Shale groundwater continuously discharges to the floodplain. However, inspection of the water chemistries at these wells revealed that sulfate and uranium concentrations in the bedrock well are always much lower than corresponding concentrations in the alluvial aquifer wells, as also observed at the three cross sections mentioned above. Thus, data from this specific set of wells do not support the idea of direct flow of contaminated water from the terrace to floodplain groundwater in the vicinity of floodplain wells 610 and 611.

Flow of bedrock groundwater to the floodplain alluvial aquifer does appear possible, however, in the vicinity of terrace well 600 (see Figure 5 for location), which is completed in Mancos Shale at the top of the escarpment in the general vicinity of floodplain wells 613 and 614. From the late 1980s through 2014, hydraulic heads at this terrace well have consistently been about 30–35 ft higher than equivalent water levels in the nearby floodplain wells. In addition, sulfate and uranium concentrations at well 600 prior to remediation pumping at the trenches (in spring 2006) have been of the same general magnitude as, though typically slightly lower than, those observed at the two floodplain wells.

The discussions above regarding comparative water elevations in near-escarpment wells highlight the challenges of using groundwater-level data to first identify hydraulic connection between parts of the Mancos Shale and nearby floodplain groundwater and to subsequently estimate groundwater discharges across the escarpment using Darcy's Law. Values for the parameters used to derive the flows (i.e., the hydraulic gradient between terrace groundwater and the alluvial aquifer, and the representative hydraulic conductivity and cross-sectional area for the equivalent porous medium represented by less-resistant shale layers and bedding-plane fractures) are necessarily rough estimates.

Unlike the near-escarpment wells, it is easier to establish that groundwater elevations in terrace groundwater at greater distances from the top of the escarpment (e.g., greater than 500 ft) are consistently higher than comparable floodplain water levels. Nonetheless, quantification of groundwater flows between terrace bedrock and the floodplain alluvial aquifer remains a challenge due to the uncertainties regarding effective hydraulic conductivities, effective cross-sectional areas, and hydraulic gradients between the two media. Moreover, the distance west of the escarpment at which terrace groundwater is more likely to flow westward as opposed to eastward toward the floodplain is unknown.

6.6.2 Multivariate Statistics Study

Evidence for a common source of contaminants in terrace groundwater near the mill site and floodplain alluvial groundwater near the base of the escarpment was reported in a DOE study of water chemistry at multiple sites in the Shiprock area (ESL 2012). In addition to using graphical methods to portray the major ion chemistry of water samples collected at various locations near Shiprock, the ESL investigation used multivariate statistical approaches to distinguish groundwater derived from leaching of Mancos Shale from other sources, such as groundwater contaminated by mill-related processes at the Shiprock site. The "multivariate statistics study" presented evidence that so-called tailings groundwater in the vicinity of the former mill site had virtually the same chemical signature as multiple floodplain wells at the base of the escarpment

and that the tailings-water signature was distinctly different from the chemistry of groundwater resulting solely from leaching of the Mancos Shale.

As part of the multivariate statistics study (ESL 2012), Stiff diagrams were constructed from water samples collected in March 2012 at four terrace wells near the disposal cell (two wells near the easternmost cell corner and two wells north of the cell), and in September 2011 at seven alluvial-aquifer locations at the base of the escarpment between Trench 2 and the outlet of Bob Lee Wash (wells 610, 614, 1111, 1112, 1113, and 1115, and sump 1118). All of these Stiff diagrams had a characteristic shape referred to as an Erlenmeyer flask, or simply a flask shape, and the source of the groundwater in each case was considered to be tailings-related (i.e., mill-related). In contrast, all remaining water samples in the study had a shape referred to as a tilted hourglass, which was considered representative of groundwater stemming mostly, if not entirely, from the leaching of Mancos Shale. The tailings and escarpment water samples had sodium-plus-potassium concentrations that were distinctly lower than those reflective of the Mancos Shale (ESL 2012).

The analyses of major ion data in the multivariate statistics report (ESL 2012) can be used to make the argument that alluvial-aquifer groundwater at the base of the escarpment was mostly, and perhaps entirely, derived from terrace groundwater that was contaminated by mill-related processes (e.g., leaching of tailings) and subsequently migrated through Mancos Shale to the floodplain. The information presented in the report does not address whether transport processes in the Mancos Shale (e.g., adsorption, fracture-matrix exchange, leaching of shale) are capable of affecting concentrations of contaminants originating in near-surface sediments on the terrace from milling activity.

6.6.3 Rebound of Specific Conductance near Trench 1

Recent temporal histories of specific conductances at near-escarpment floodplain wells were also examined for evidence of discharge of terrace groundwater to the floodplain. Specifically, the data were searched to identify rebound of specific conductance each time pumping at the remediation trenches was shut down. This analysis required the continuous records of specific conductance in SOARS, which meant that the data were only available for wells located near Trench 1 and Trench 2. Further inspection revealed that the continuous data useful for the analysis were only available for the Trench 1 area, as specific conductance records for the only near-escarpment well collecting these data in the Trench 2 area (well 1115) have been discontinuous.

Examination of daily pumping rates at the Trench 1 sump (well 1110) from November 2009 through November 2014 indicates that pumping was shut off during all or large parts of five different periods that lasted anywhere from 10 days to several months. The hydrograph at this location during the same time span showed groundwater levels recovering as much as 3 to 4 ft each time pumping was stopped, typically within a day of the pump shutoff. These quick and sizeable drawdown recoveries suggested that quick inflow of high-salinity groundwater from the nearby escarpment was at least possible.

The capacity of salinity to rebound in the near-escarpment area during the above-mentioned periods of limited pumping and nonpumping was assessed by inspecting continuous specific conductance data from SOARS monitoring wells 1110-A, 1110-C, 1111, and 1112 (see Figure 7

for locations). The first two of these wells are located directly above Trench 1 and about 50 ft from the base of the escarpment. The latter two locations are on the escarpment side of Trench 1, 15–20 ft from the base of the escarpment and about 170 ft from each other.

The specific-conductance histories at the four Trench 1 area SOARS wells showed mixed results regarding the capacity for salinity rebound. Some of the general findings from examination of the histories are:

- Rebound in response to shutoff of the well 1110 sump was almost instantaneous in some cases, whereas in others the response lagged by as much as week or more. Both types of response were often seen in the same well.
- The magnitude of rebound in specific conductance varied greatly between the various periods of nonpumping that were investigated; this held true for each of the four monitoring wells.
- Observed recoveries in specific conductance in response to cessation of pumping ranged from 0 to 10,000 mS/cm.
- There was some evidence that the magnitude of specific-conductance rebound decreased with each successive period of nonpumping.
- Recovery of specific conductance did not vary noticeably with distance from the escarpment. Overall, the magnitude of salinity rebound in wells 1110-A and 1110-C, directly above the horizontal well in Trench 1, was similar to that observed at wells 1111 and 1112, closer to the escarpment.

In lieu of presenting specific conductance histories for all four of the SOARS wells, an analysis of the graphs of salinity rebound at just one of the wells is adequate for illustrating the types of responses that occur in the vicinity of Trench 1. Accordingly, Figure 38 shows temporal plots of specific conductance at well 1111 for four of the five nonpumping periods occurring between November 2009 and November 2014. The length of the nonpumping periods varies from as little as a month to as much as 9 months.

As shown in Figure 38, salinity rebound at Well 1111 during the first period of nonpumping was muted for about 2 months after the pump was shut off in October 2010, and an eventual recovery in specific conductance from about 11,000 to 21,000 mS/cm was delayed until January 2011. Subsequently, specific conductance fluctuated between about 15,000 and 21,000 mS/cm until the initial nonpumping period ended in late June 2011. In contrast, rebound was relatively rapid after the following cessation of pumping that began in June 2012, requiring about a week for specific conductance to increase from 12,000 to 21,500 mS/cm. Moreover, salinity values generally remained high for most of the second nonpumping period, appearing to decrease noticeably only just prior the end of the period in August 2012.

The salinity response at Well 1111 during the third nonpumping period (Figure 38) was very mild, as specific conductance increased only about 1000 mS/cm after nonpumping from the Well 1110 sump was initiated in late March 2014. The reason for such limited rebound was unclear, as the preceding concentration histories at this location and the three other SOARS wells examined gave no indication of a major reduction in contamination levels in the Trench 1 area. Note that the salinity response during the fourth and final nonpumping period between mid-August 2014 and late November 2014 was also mild, as specific conductance initially

increased from about 13,000 to 18,000 mS/cm and remained relatively stable over the following 1.5 months. Subsequently, specific conductance levels at Well 1111 showed signs of decreasing to about 13,000 mS/cm, the salinity level that was present just prior to turning off the pumping at Trench 1.

In general, the examination of specific conductance histories at wells in the Trench 1 area indicates that they are of limited use for identifying local inflows of contaminated bedrock groundwater across the escarpment. Moreover, given that the only near-escarpment SOARS wells with continuous conductance records are in the vicinity of Trench 1, the available data are incapable of identifying inflows of terrace groundwater farther to the south near the escarpment, in areas that have historically shown high salinity. This suggests that more informative data might be collected if additional wells at the base of the escarpment were instrumented with specific-conductance sensors. In addition, longer testing might be required before salinity rebound might be considered a reliable indicator of contaminant inflow from terrace sources. As an example, continuous steady pumping from Trench 1 for a year followed by nonpumping for as much as 2 or more years would be more likely to reveal possible inflow locations along the escarpment. These durations would allow for at least some flushing of contaminated water away from near-escarpment locations in response to remediation pumping and sufficient time for contaminated terrace water, if any, to reenter the flushed areas.

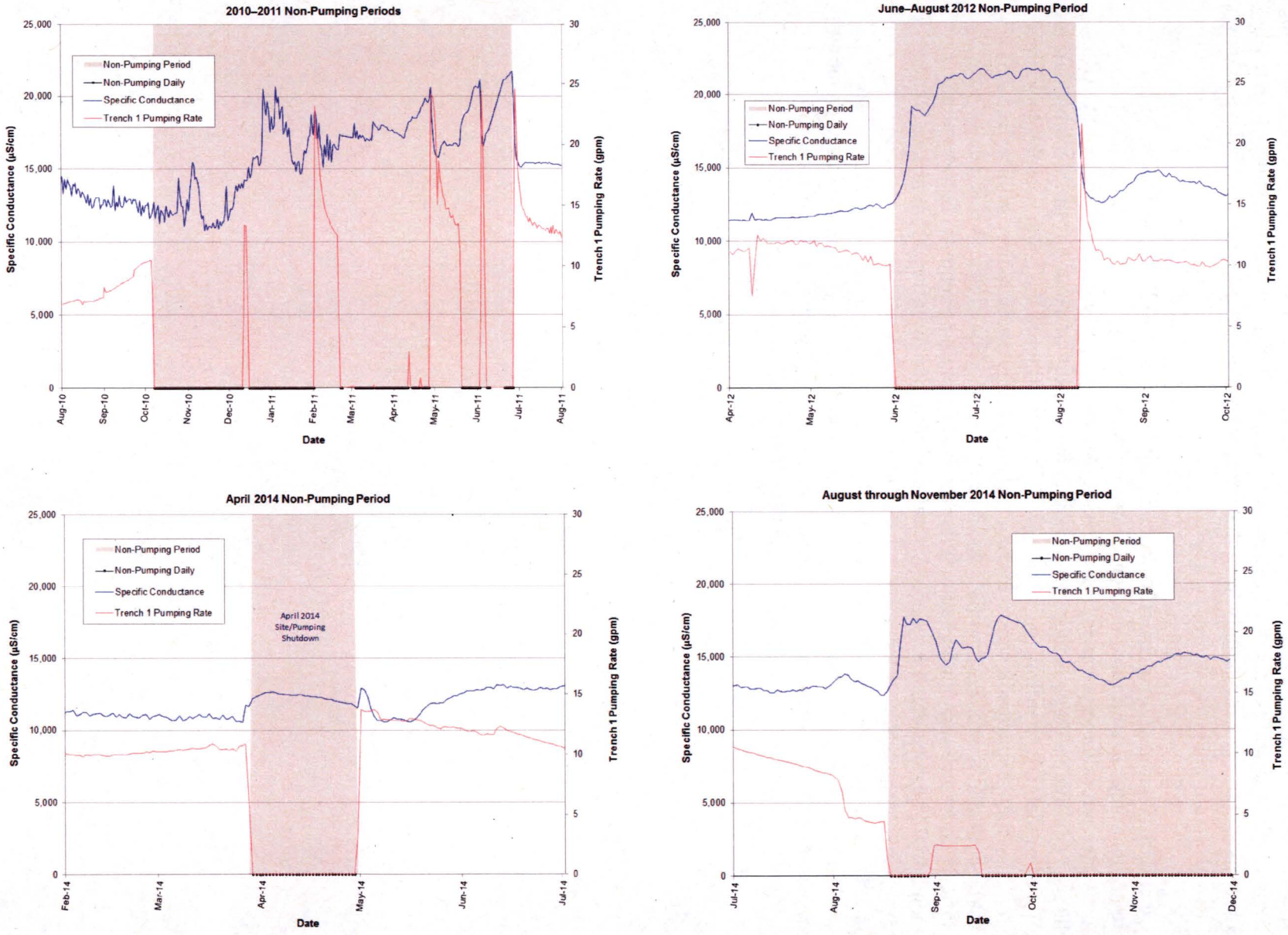

Figure 38. Specific Conductances at Well 1111 During Four Nonpumping Periods

6.6.4 Concentration Histories in Wells at the Base of the Escarpment

The potential for contaminated terrace groundwater to discharge to the floodplain alluvial aquifer was further evaluated with temporal plots of contaminant indicators at near-escarpment wells from 2000 through 2014. Two sets of the temporal histories were used for this purpose, with one set consisting of wells extending from near Trench 1 to about 1300 ft southeast of the trench (wells 1111, 1112, 614, 610, and 1113), and the second consisting of wells extending from about 600 ft north-northwest of Trench 2 to 1000 ft south-southeast of the trench (wells 608, 1114, 1115, 1128, and 735).

Figure 39 shows the temporal history of sulfate concentration, uranium concentration, and specific conductance at the first set of near-escarpment wells. In general, each of these contaminant indicators shows consistent decreases since remediation pumping at Trench 1 was initiated in spring 2006. However, sulfate and uranium concentrations appear to have stabilized somewhat between 2011 and 2014 at wells 1111, 610, and 1113. The reason for this potential leveling out of concentration is unknown, but continued inflow of contaminated terrace groundwater to the aquifer is a possible cause. Regardless of the processes affecting near-escarpment concentrations in alluvium near and southeast of Trench 1, uranium concentrations in 2014 at the wells remain in a range of 0.5 to 1 mg/L, well above the UMTRA standard of 0.044 mg/L. Despite the fact that pumping from Trench 1 had removed more than 95,000 kilograms (kg) of sulfate and about 8.2 kg of uranium from the alluvial aquifer as of March 2014 (DOE 2014b), the temporal histories of contaminant indicators at near-escarpment wells (Figure 39) indicate that full aquifer remediation at the foot of the escarpment is several years away.

The temporal plots for the second set of wells (Figure 40) also indicate that full remediation has not been achieved in near-escarpment portions of the alluvial aquifer affected by pumping from Trench 2. Rather, the sulfate and uranium concentrations at these wells suggest that contaminant levels have either stabilized or increased between 2008 and 2014. This observation in turn suggests that progress toward full remediation near Trench 2 and in the southern third of the aquifer is less than that achieved in areas closer to Trench 1. This result may reflect the fact that Trench 2 tends to remove less contamination from the aquifer than Trench 1, as groundwater withdrawals from the trench had removed only about 18,700 kg of sulfate and 2.7 kg of uranium as of March 2014 (DOE 2014b). Alternatively, it is possible that contaminant rebound is greater in the south third of the aquifer. Nevertheless, the data presented in Figure 40 are insufficient to attribute persistent sulfate and uranium concentrations in near-escarpment areas to the inflow of contaminated terrace groundwater.

6.7 Further Evaluation of Contaminant Discharge to the Floodplain

Further data analysis relevant to flow and transport processes in the vicinity of the escarpment will be needed for future evaluations of the groundwater remedy at the Shiprock site (DOE 2015a). The results of surface geophysical surveys conducted on the terrace (e.g., DOE 1996) could be helpful for this purpose. In addition, field inspection of 24 northeast-striking vertical joints identified at gullies in the escarpment wall during site characterization in support of the SOWP (DOE 2000) might shed light on hydraulic pathways connecting the terrace to the floodplain. Tsosie (1997) noted the presence of northeast-oriented fracturing in Mancos

Shale at the escarpment and indicated that most of the gullies cutting the escarpment wall were fracture-induced.

Visual observation and collection of discharge of terrace groundwater across the escarpment wall would provide the most direct evidence of continuing contaminant sources beneath the terrace. Though monitoring of Seeps 425 and 426 for several years (e.g., DOE 1991, GEMS database) demonstrated persistent contaminant discharge from the terrace at elevations above the floodplain surface, no effort has been made to expose possible discharges across the escarpment at elevations beneath the floodplain surface. Attempts to directly reveal subsurface seepage across the wall would likely require the installation of hydraulic barriers surrounding an area of some length abutting the escarpment, followed by the removal of groundwater from the area via pumping and subsequent excavation of floodplain alluvium within the isolated area. An investigation of this type would involve considerable effort and funding, but it might cost less than a field campaign requiring the installation of Mancos Shale wells on the terrace. As discussed in Section 6.6.1, the installation of a trio of wells completed at various depths in the Mancos Shale at three separate locations on the terrace in near-escarpment areas was generally unsuccessful in identifying preferential pathways connecting the terrace to the floodplain.

As an alternative to conducting expensive field investigations, consideration might be given to the simple injection of a nonreactive tracer into a terrace well that is completed in Mancos Shale and appears to intercept groundwater that has the potential to migrate to the floodplain. Subsequent detection of the tracer in an alluvial-aquifer well near the base of the escarpment would at least indicate that flows from the terrace to the floodplain are taking place. Tracer injection and monitoring is relatively inexpensive, and would be easy to repeat over the lifespan of monitoring events at the Shiprock site. Terrace well 600, installed in 1982, provides an existing location near the escarpment (see Figure 5) where tracer injection could be conducted.

The most efficient and thorough approach to assessing potential discharge of contaminated groundwater from the terrace to the floodplain involves continued monitoring of alluvial wells at the base of the escarpment. The logic is that continued influx is likely if relatively large contaminant concentrations persist at these wells in future years. Conversely, concentrations would be expected to gradually decline if discharge of terrace groundwater has either ceased or is steadily decreasing. However, findings presented in this section regarding contaminant plume evolution and assessments of groundwater flow in the vicinity of the escarpment suggest that the results of near-escarpment monitoring would be clearer if unaffected by Trench 1 and Trench 2. This would require cessation of pumping from both trench sumps for a lengthy period, perhaps for multiple years. This approach to evaluating groundwater inflows would also benefit from the installation of additional monitoring wells at the foot of the escarpment, particularly given that trans-escarpment discharges are likely to be both spatially variable and temporally variable.

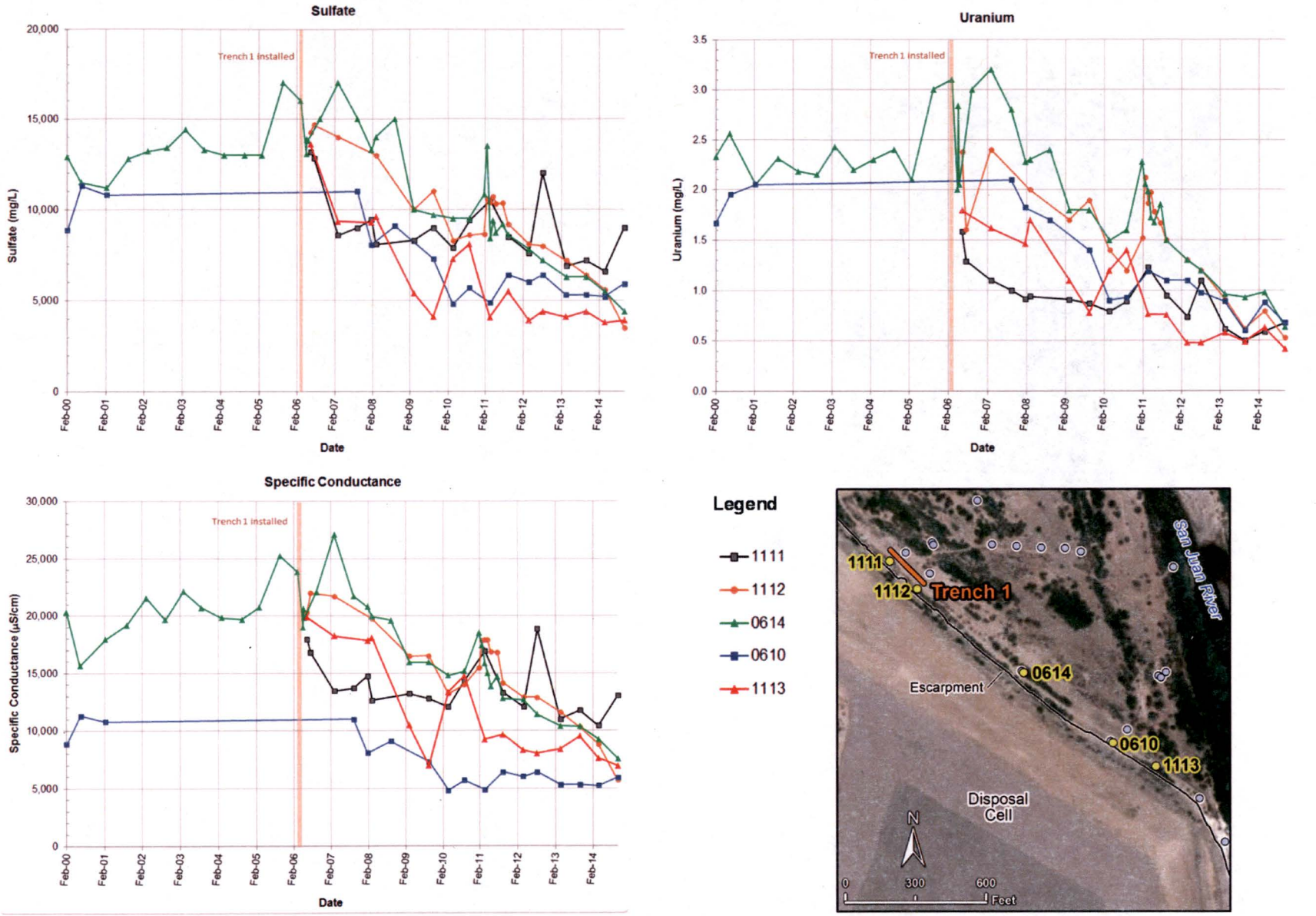

Figure 39. History of Sulfate and Uranium Concentrations and Specific Conductance at Base-of-Escarpment Wells 1111, 1112, 614, 610, and 1113

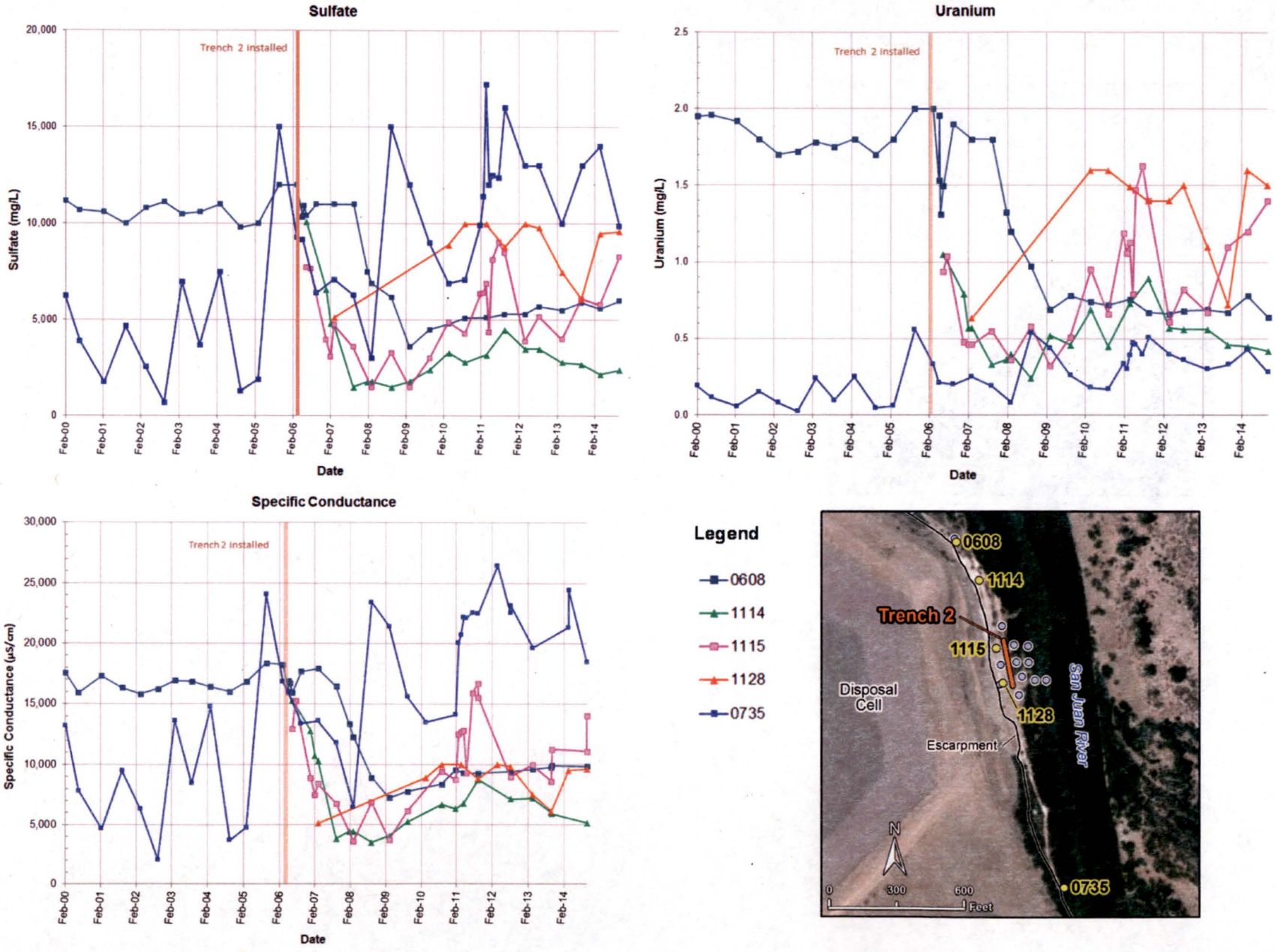

Figure 40. History of Sulfate and Uranium Concentrations and Specific Conductance at Base-of-Escarpment Wells 608, 1114, 1115, 1128, and 735

7.0 Groundwater Flow Modeling

The groundwater flow model developed for this study was designed for approximating flow processes in the alluvial aquifer and was not intended to be a detailed predictor of aquifer response to remedial actions. Rather than accounting for aquifer heterogeneity, calibration of the model largely focused on the determination of a single, representative value of aquifer hydraulic conductivity and a similar representative value of storativity (or specific yield), both of which could be applied uniformly over the entire floodplain while maintaining an ability to capture general aquifer behavior. Despite the likelihood that density-dependent flow driven by high water salinity affected flow direction in past years (Section 4.5.2), the model was constructed to simulate two-dimensional, horizontal flow of low-salinity groundwater in a single aquifer layer. This approach was taken because of the limited saturated thickness of the alluvial groundwater system (5–20 ft) and the fact that data reflective of variations of salinity with depth in the aquifer were available for just a limited number of locations. No attempt was made to simulate flow beneath the San Juan River; rather, the west edge of the river was assigned boundary conditions that permitted flow to occur both to and from the river.

The computer code used to model groundwater flow was MODFLOW (Harbaugh and McDonald 1996), a finite-difference simulator developed and maintained by USGS. The particle tracking module MODPATH (Pollock 1989) was employed to delineate flowpaths in the groundwater system. Combined use of these codes was managed within version 4 of the graphical user interface referred to as Groundwater Vistas (ESI 2001).

7.1 Model Construction

The upgradient and downgradient ends of the model were selected to coincide with the south and north ends of the floodplain, respectively. Finite-difference rows were aligned with the Trench 1 footprint (44.88 degrees west of north). Consequently, model columns tended to be oriented orthogonal to the escarpment and the river. The model consisted of 238 rows and 630 columns. Row spacing varied between 2 and 10 ft, with the thinnest rows being assigned to the area encompassing the Trench 1 footprint. Column widths were assigned a uniform value of 10 ft. Because finite-difference blocks outside the floodplain footprint were treated as inactive, the total number of active blocks in the model was 56,189. The lower left corner of the finite-difference grid was located at Shiprock site coordinates of 247843.87 ft east and 2104032.6 ft north.

The bedrock-surface elevations illustrated in Figure 24 were digitized and incorporated in the model as base elevations for the floodplain aquifer. No attempt was made to account for any water exchanges that might occur between the alluvial aquifer and underlying Mancos Shale bedrock. This assumed that the shale formed an impermeable boundary at the base of aquifer. In lieu of simulating groundwater flow in Mancos Shale beneath the terrace, the model treated the escarpment as a prescribed flow boundary, where inflows represent discharges of terrace groundwater from Mancos Shale into the alluvial aquifer.

Unlike the models developed for the SOWP (DOE 2000), the GCAP (DOE 2002), the Knight Piesold (2002) investigation, and the Trench 2 evaluation (DOE 2009b), it was assumed in this flow model that aerial recharge from precipitation was insignificant in comparison to other water sources and, therefore, could be ignored. This assumption was partly based on the low recharge

rate of 1.1 gpm applied in the Knight Piesold (2002) model (Section 4.4), which in turn was used to develop the GCAP (DOE 2002).

Calibration of the flow model in this study was achieved using recharge of Bob Lee Wash flows, river losses, and bedrock discharges across the Mancos Shale escarpment as the sources of subsurface water, and discharge to the river as the sole outflow process. Despite evidence that ET potentially comprises a substantial portion of aquifer outflow (e.g., Section 6.3), especially in summer and fall, no attempt was made to directly account for this water budget component in the modeling. This latter decision stemmed primarily from a lack of information indicative of where, when, and at what rates ET removes groundwater from the aquifer.

7.2 Boundary Conditions

As shown in Figure 41, multiple types of boundary conditions were employed in the model. In conformance with methods employed in models focused on simulation of groundwater/surface-water interactions (e.g., Packman and Bencala 2000), prescribed hydraulic heads corresponding to measured and estimated surface-water elevations were assigned to model blocks along the west side of the river. Though it is known that groundwater/surface-water exchanges are influenced by riverbed topography (i.e., bed forms) as well as river-surface elevation (e.g., Cardenas et al. 2004), this approach to accounting for river losses and gains assumed that riverbed effects were effectively represented by the prescribed surface-water elevations.

Groundwater extraction from each of the three remediation pumping systems was handled with prescribed flow boundary conditions. Total water discharges from Trench 1 (prescribed flow) due to pumping were divided equally among 20 contiguous model blocks. Total pumping rates at Trench 2 were divided among 34 different blocks traversed by the footprint of the horizontal well in the trench. A tool available in Groundwater Vistas (ESI 2001) made it possible to allocate the total trench flow in proportion to the length of well footprint within each affected block.

Recharge from Bob Lee Wash discharge was assumed to occur at a uniform rate within the greater share of a circular area centered about 250 ft from the base of the bedrock escarpment (Figure 41). The center of the circle was placed at Shiprock site coordinates 249680.14 ft east and 2103339.15 ft north, and the radius of the circle was 300 ft.

Prescribed flow boundary conditions were also used along the base of the escarpment to represent the inflow of contaminated water across the Mancos Shale escarpment. The uniform value of bedrock inflow per foot of escarpment length included in the flow model developed for the Trench 2 evaluation (0.07 ft^3/day) (DOE 2009b) was initially assigned to the southernmost 3600 ft of escarpment, between the floodplain's south end and the Bob Lee Wash outlet. Though it is possible that surface water in the channel connecting well 648 and Bob Lee Wash percolates into terrace groundwater that eventually discharges to the alluvial aquifer north of the wash outlet (Section 4.3), it was assumed in the model that bedrock discharge does not occur between the wash outlet and the north edge of the floodplain. During model calibration, the rate of bedrock inflow was adjusted along various portions of the escarpment south of Bob Lee Wash until suitable fits to measured water levels were achieved.

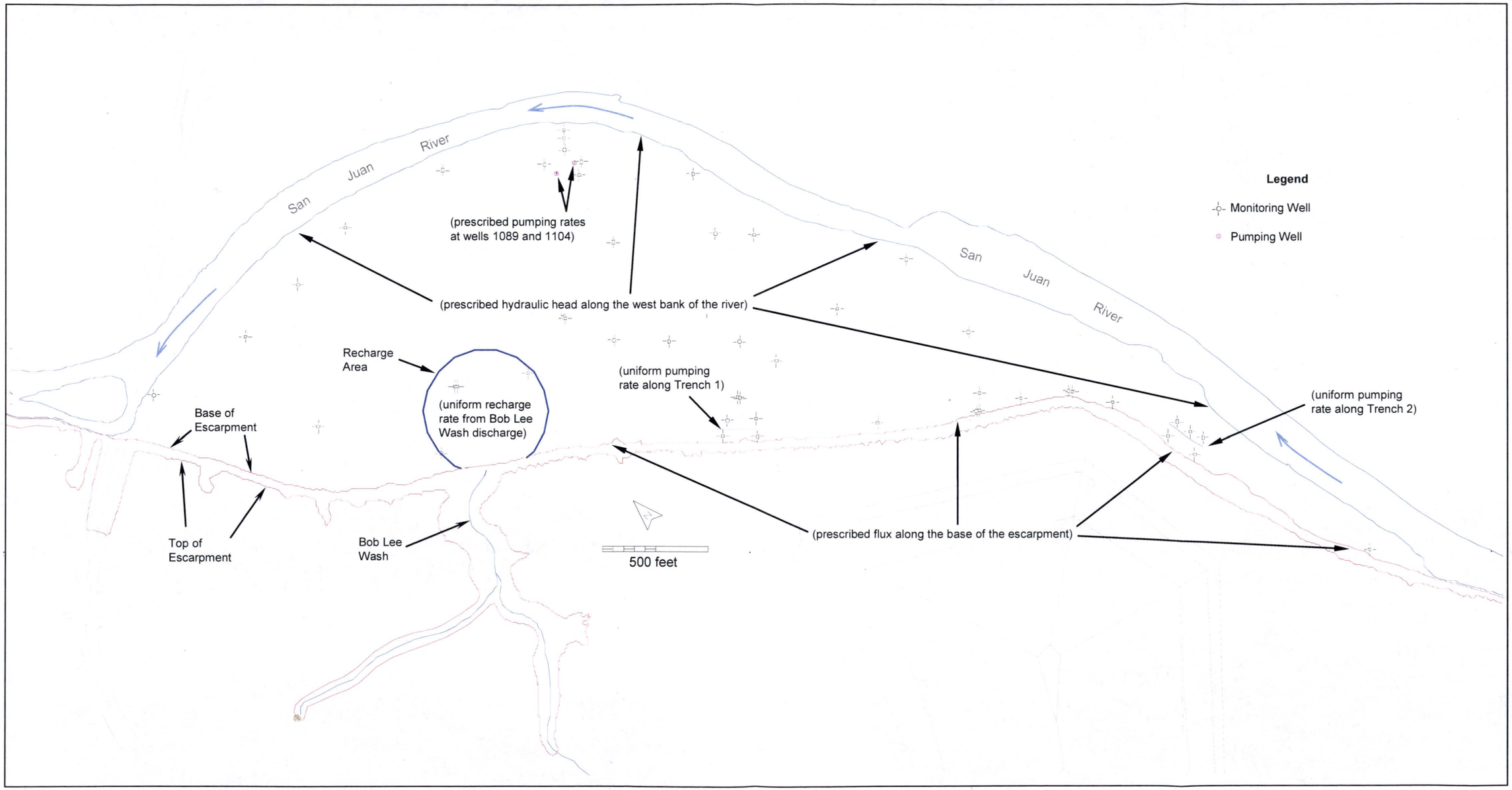

Figure 41. Boundary Conditions (in parentheses) Applied in the Numerical Modeling

This page intentionally left blank

7.3 Model Calibration

Model calibration was achieved by matching observed groundwater conditions associated with two different flow states within the groundwater system. The first flow state consisted of relatively steady groundwater conditions observed during the semiannual monitoring event of March 22–25, 2011. The remediation system was not operating at that time, as pumping had been terminated 1 to 2 months earlier at wells 1089 and 1104 and at the trenches. River levels remained relatively steady during this period as they had during the preceding 2 months (see well hydrographs in Section 6.2); as a result, groundwater levels measured during the monitoring event were considered representative of a steady-state flow system.

The second flow state represented a transient groundwater system in 2011 centered on changes in groundwater elevation during the snowmelt runoff months of May and June. The objective in this case was to adjust input parameters within feasible ranges such that model output in two key areas of the floodplain produced reasonable matches to several of the well hydrographs discussed in Section 6.2. The transient flow model was constructed to simulate groundwater levels from March 24, 2011, in the middle of the semiannual monitoring event, through August 2011, the last month included in the analysis of well hydrographs. The calibration achieved with transient simulations was considered a valuable addition to the foregoing steady-state modeling because it facilitated the determination of parameters representative of aquifer storage processes as well as parameters reflective of aquifer permeability.

Attempts were made to identify additional calibration objectives, such as the matching of any measured flows of surface water or groundwater within the floodplain area. In particular, the site was inspected on multiple occasions for springs or seeps that could be monitored for flows that might be used as calibration targets. However, no expressions of groundwater discharge were found on the floodplain or near the river.

No attempt was made to use calculated groundwater flows or fluxes (using Darcy's Law) as calibration targets, primarily because the calculated values would require assumed values of hydraulic conductivity, which is actually a key parameter that is adjusted during model calibration to achieve reasonable fits between measured and model-computed hydraulic heads. Such an approach produces indefensible results because it is based on circular logic, wherein the modeler begins with what he or she is trying to end up with via calibration. This does not mean that the modeler cannot assess whether local values of hydraulic conductivity and hydraulic gradient resulting from calibration produce a calculated local flow that is realistic. Such calculations can easily be performed postcalibration to ascertain whether the resulting flow seems reasonable and within a range that would be expected based on available site data (i.e., groundwater elevations, results from aquifer tests).

7.3.1 Nonpumping Conditions in March 2011

Because the model of groundwater conditions in March 2011 simulated steady-state flow, all model inputs were treated as constant with time. River-surface elevations were represented by prescribed hydraulic heads that were fixed in the calibration simulations. Prescribed model outflows at the extraction wells and the two trenches were not needed because remediation pumping had been shut off. Model parameters adjusted during calibration included aquifer

hydraulic conductivity, bedrock discharge rates across the Mancos Shale escarpment, and the uniform recharge rate applied to the circular area at the mouth of Bob Lee Wash.

The mean river gage elevation during the March 22–25 monitoring event was 4883.65 ft amsl, or 0.24 ft below the gage elevation linked with the low-flow river survey (4883.89 ft amsl). The following algorithm was applied to develop steady-state river elevations along the entire length of the floodplain that were used as prescribed hydraulic heads at 679 model blocks assigned to the river:

$$H_{riv} = H_{low} - (G_{low} - G_{riv}) \quad (1)$$

where H_{riv} = prescribed river elevation (ft amsl),
H_{low} = river elevation linked to the low-flow survey (ft amsl),
G_{low} = river gage elevation linked to the low-flow survey (4883.89 ft amsl), and
G_{riv} = measured river gage elevation (4883.65 ft amsl).

This method produced a river profile that duplicated the elevation drops seen at each pool and riffle in the low-flow profile displayed in Figure 20 while capturing the lower elevations expected at the river during the March 22–25 event.

The objective of calibrating the steady-state model was to find a combination of model inputs that resulted in a reasonable match between groundwater levels computed by the model and observed water elevations at 48 monitoring wells in March 2011. In modeling parlance, the 48 wells were referred to as target wells, and the water elevations recorded at the wells were called calibration targets, or target elevations.

Various quantitative measures of the calibration effort were used to gauge its success. All measures made use of the hydraulic head residual, or head residual, at each target well, which was calculated by subtracting the model-computed water elevation for that location from the target elevation. The goal of calibration was to minimize the mean of all 48 residuals while meeting additional modeling criteria. Numerous combinations of uniform hydraulic conductivity, Bob Lee Wash recharge rate, and bedrock discharge rates were tested before reasonable matches with the target elevations were achieved. Promising parameter sets were subsequently employed in transient model simulations to determine whether they adequately reproduced the well hydrographs selected for transient model calibration (see Section 6.3.2). This resulted in an iterative process between the March 2011 steady-state model and the calibrated transient model and culminated in a final parameter set that performed well in both types of simulation.

The final calibrated model of steady-state flow used a hydraulic conductivity of 80 ft/day, a uniform recharge rate of 0.032 ft/day (140 inches per year) in the Bob Lee Wash recharge area, and three different sets of bedrock discharge rates. Between the south end of the floodplain and a portion of the escarpment near well 608 (Figure 5), the adopted bedrock discharge rate was 0.08 ft^3/day (4.15×10^{-4} gpm) per foot of escarpment length. Between well 1113 and 120 ft northwest of the north end of Trench 1, the prescribed bedrock discharge rate was 0.2 ft^3/day (1.04×10^{-3} gpm) per foot of escarpment length. The final escarpment section assigned subsurface inflow from the terrace extended from Bob Lee Wash to 120 ft north of Trench 1, where the prescribed discharge rate was set at 0.6 ft^3/day (3.11×10^{-3} gpm) per foot of escarpment length. These rates resulted in volumetric inflow rates of 162.2 ft^3/day (0.84 gpm),

355.2 ft^3/day (1.84 gpm), and 552 ft^3/day (2.86 gpm) in the respective escarpment sections (see Figure 42).

Figure 42 presents a contour map of groundwater elevations produced by the steady-state model of flow in March 2011. A notable feature of this potentiometric surface is its resemblance to groundwater flow components depicted in Figure 4–13 in the SOWP (DOE 2000). The plotted water elevations in the northern half of the floodplain for March 2011 are also similar to a contour map of groundwater levels for February 2000 included in the preliminary Trench 1 evaluation (ESL 2011b).

7.3.1.1 Flow Patterns

Flowpaths associated with the potentiometric surface in Figure 42 were delineated using the MODPATH (Pollock 1989) particle tracking module in Groundwater Vistas. The resulting particle tracks for the March 2011 steady-state model, shown in Figure 43, are generally similar to the flowpaths previously adopted in the existing conceptual model of baseline flow conditions (Figure 12). However, there are also significant differences between the two flow configurations, especially between Trench 1 and the river. In particular, rather than producing a north-oriented flowpath directly connecting the Trench 1 and 1089/1104 areas, the steady-state model indicates that groundwater leaving the Trench 1 area migrates more to the northeast, in the direction of monitoring wells 779 and 857 (Figure 43). This flowpath fails to explain how contamination emanating from the escarpment in the Trench 1 area was able to migrate to the 1089/1104 area and, in the process, create a contaminant plume lobe that historically linked the Trench 1 and 1089/1104 areas (Figure 14 and Figure 15).

7.3.1.2 Calibration Measures

Several measures of model calibration indicate that the steady-state flow model performs well in matching measured groundwater levels in March 2011. A map view of computed head residuals (Figure 44) suggests that the number of positive residuals (underpredicted hydraulic heads) is about equal to the number of negative residuals (overpredicted hydraulic head) and absolute values of the residuals are all relatively small (<0.5 ft). These general observations are borne out by a plot of model-computed groundwater elevations versus target (observed) water elevations (Figure 45), with all 48 data values remaining relatively close to a straight line (1:1 correlation) representative of a perfect calibrated model. The mean of the absolute values of all head residuals is limited to 0.17 ft, providing further evidence of calibration success. The minimum residual is –0.34 ft and the maximum is 0.46 ft, suggesting a reasonable balance between underpredicted and overpredicted hydraulic heads. The standard deviation of the residuals is limited to 0.21 ft. Division of this value by the variation in observed water elevations (9.04 ft) results in a dimensionless value of 0.023, a measure that is also indicative of a well-calibrated model.

As shown in Figure 44, the largest underpredictions of groundwater elevation in the calibrated model tended to be concentrated in an area directly north of Trench 1, between the Trench 1 and 1089/1104 areas. This observation suggests that aquifer heterogeneity has a significant impact on local groundwater movement and that more accurate simulations of groundwater flow could be achieved by allowing hydraulic conductivity to vary spatially across the floodplain. It might also

indicate that a better match with measured water elevations between Trench 1 and the 1089/1104 area could be achieved by accounting for potential density-dependent flow (see Section 4.5.2).

7.3.1.3 Water Budget

The water budget produced by the steady-state flow model of baseline groundwater conditions in March 2011 (Table 7) indicates that the largest source of water inflow to the alluvial aquifer is recharge from Bob Lee Wash, composing more than 73 percent of the total inflow. The second largest water source consists of river losses (~18 percent), and bedrock discharge comprises about 9 percent of the total inflow. The calibrated model suggests that, during periods when the remediation system is not operating, flows in the river are relatively low, ET does not contribute to groundwater outflow, and 62 gpm is circulating through the floodplain groundwater system. All of this water is discharged to the San Juan River, primarily in the north half of the floodplain.

Table 7. Computed Water Budget in the March 2011 Model of Steady-State Flow

Flow Component	(ft^3/day)	(gpm)	(%)
Inflow			
Seepage losses from the river	2,120	11.0	17.8
Recharge from Bob Lee Wash	8,720	45.3	73.2
Bedrock discharge	1,070	5.6	9.0
Outflow			
Discharge to the river	11,910	61.9	100.0

The computed recharge rate for the assumed area of infiltration at the mouth of Bob Lee Wash is approximately 45 gpm, a value that is about 70 percent of the reported rate of artesian discharge from terrace well 648 (64 gpm, see Section 3.1) in the SOWP (DOE 2000). This result implies that about a third of the surface water normally flowing down the wash during winter and spring months does not recharge the alluvial aquifer. Because ET processes were not likely prominent during March 2011, the water budget for the calibrated steady-state flow model suggests that a high percentage of the surface water emptying onto the floodplain from Bob Lee Wash at the time does not become recharge and instead flows northwestward as surface water and discharges to the river. Evidence for such discharge of surface water to the river at the north end of the floodplain has been looked for in recent years but has not been observed.

An alternative explanation for the disparity between the Bob Lee Wash recharge rate derived from the flow model and discharge rate from well 648 as reported in the SOWP (DOE 2000) might be found by examining surface-water flows in and losses from the channels connecting well 648 and the Bob Lee Wash outlet. As discussed in Section 4.3, the potential exists for seepage losses from the channel conveying artesian water from well 648 to the Bob Lee Wash channel to recharge underlying groundwater beneath the terrace that eventually discharges to the floodplain alluvial aquifer north of the wash outlet. Such losses could substantially reduce the surface-water discharge that is available for recharge near the wash outlet. Alternatively, it is possible that the 64-gpm flow rate from well 648 when the SOWP (DOE 2000) was developed is an overestimate of the actual flow at the time, or that the flow rate in 2000 was greater than the artesian flow rate occurring in 2011.

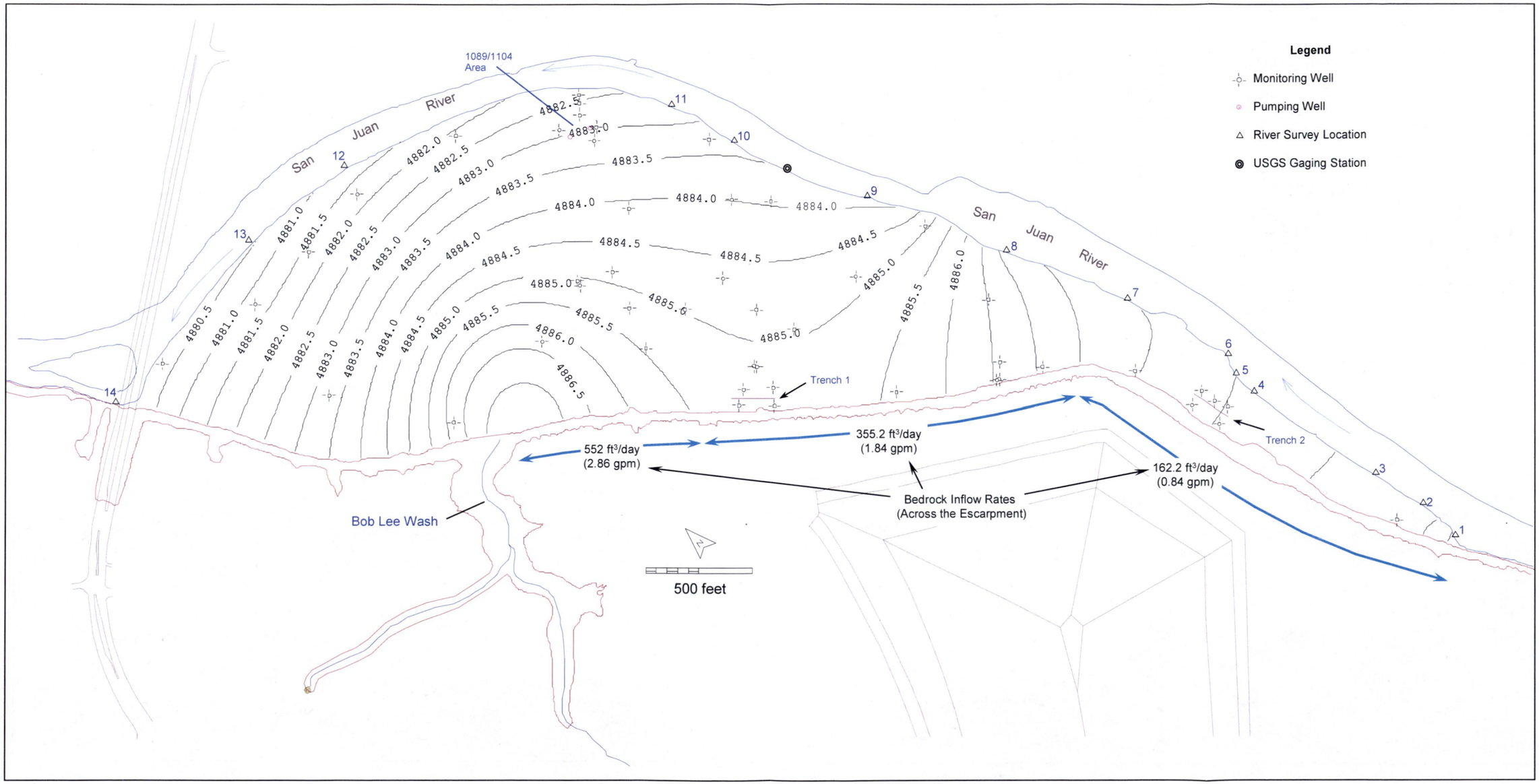

Figure 42. Computed Groundwater Elevations (ft amsl) in the March 2011 Model of Steady-State Flow

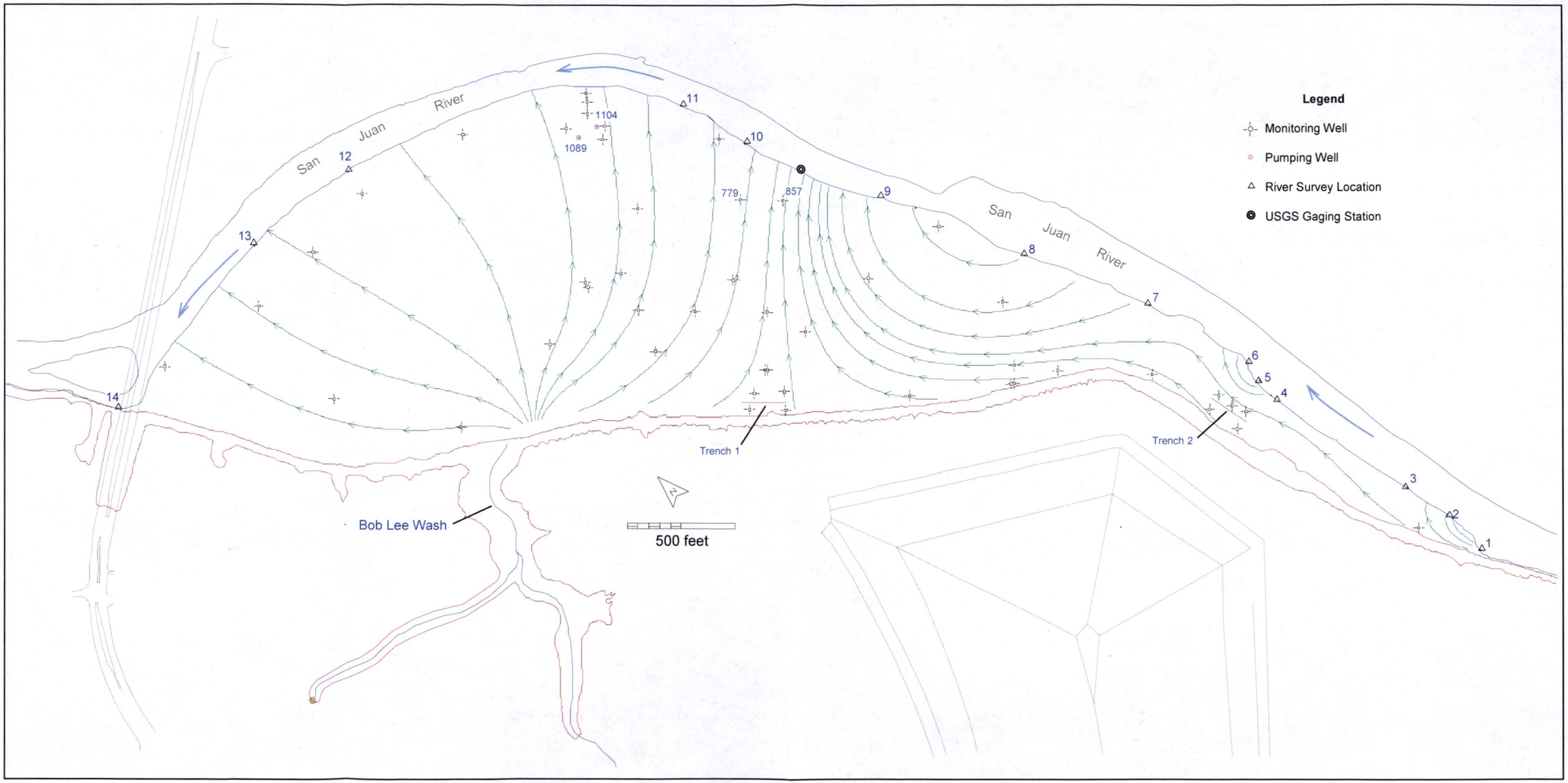

Figure 43. Computed Flowpaths in the March 2011 Model of Steady-State Flow

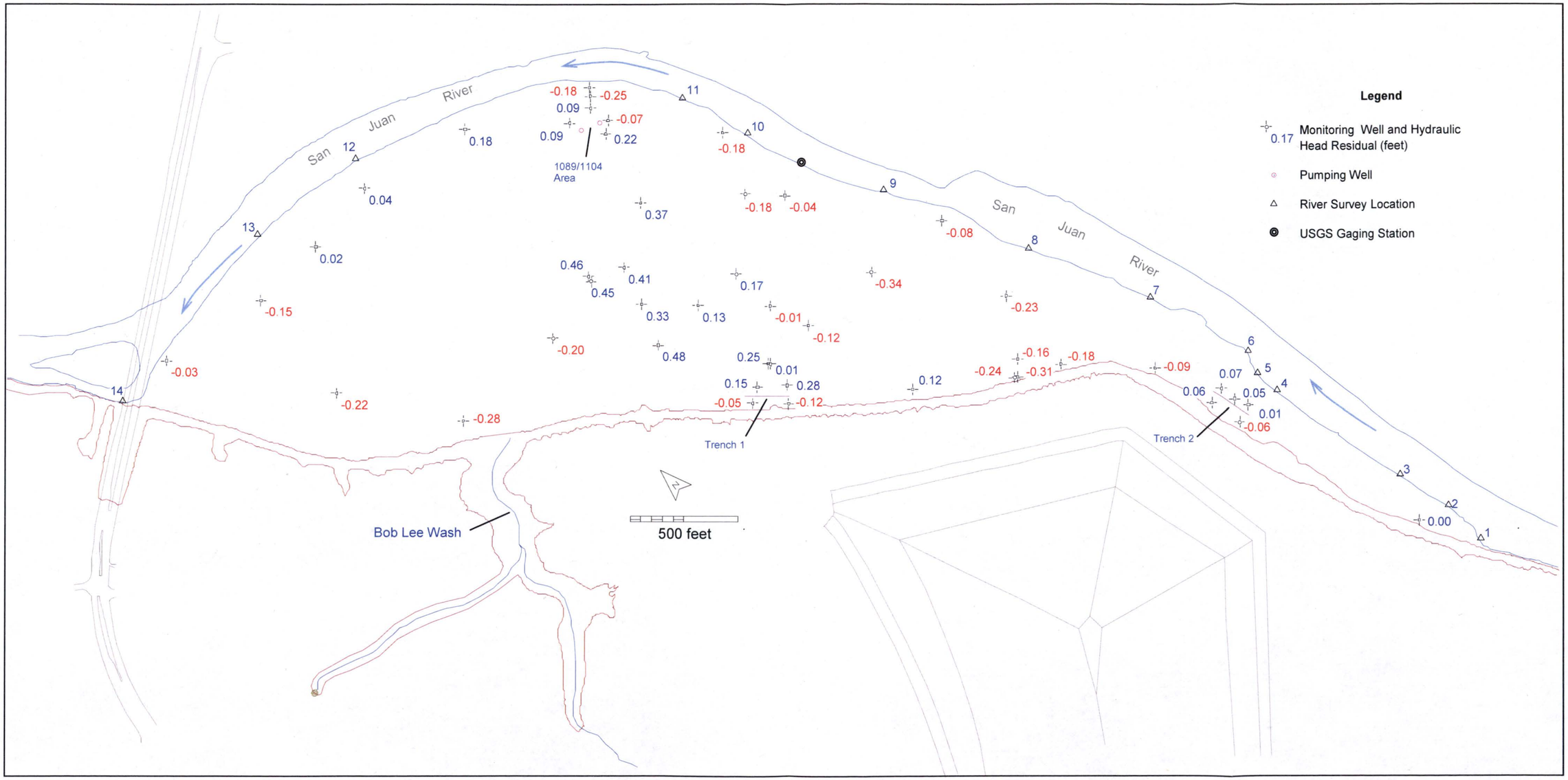

Figure 44. Computed Hydraulic Head Residuals in the March 2011 Model of Steady-State Flow

This page intentionally left blank

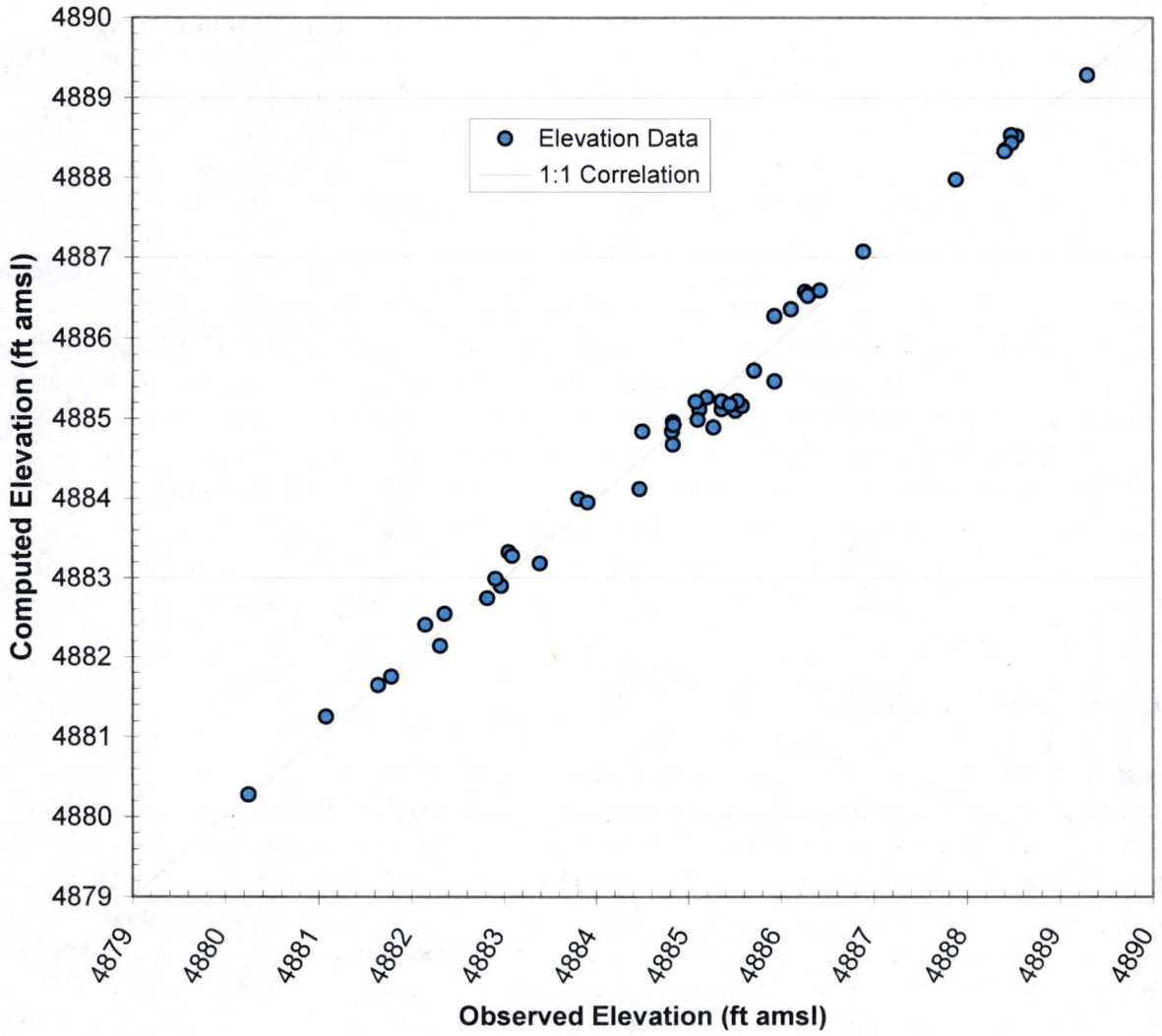

Figure 45. Observed and Computed Groundwater Elevations in the March 2011 Model of Steady-State Flow

The flow in Bob Lee Wash and the recharge rate from its outflow to the floodplain remains an uncertain component of the water budget for the alluvial aquifer. The project would benefit from new measurements of flow in the wash, both at the flowing artesian well and at the mouth of the wash. Flow at the wash outlet is important for improving estimates of recharge from well 648 discharge, the largest water source for the floodplain aquifer (e.g., Table 7). The utility of the flow measurements would be greatly enhanced if they were effectively continuous (i.e., measured at intervals of several minutes as opposed to days) and stored for further evaluation using data recorders. Ensuring the accuracy of continuously monitored wash flows using semipermanently installed flow monitoring devices, such as weirs or Parshall flumes, would comport with challenges outlined for the Shiprock site in coming years (DOE 2015a).

The total flow rate through the entire floodplain groundwater system (~60 gpm) is of interest because it comprises about 54 percent of the total system flow adopted in a water budget developed for the floodplain in the SOWP (DOE 2000). The large discrepancy between the two models is attributed mostly to the fact that the SOWP model assumed that all 64 gpm discharging from artesian well 648 on the terrace recharges the alluvial aquifer. In addition, the larger

uniform hydraulic conductivity applied uniformly in the SOWP model (100 ft/day) in comparison to 80 ft/day adopted in this study signifies that more groundwater flow is needed in the SOWP (DOE 2000) analysis to match potentiometric surfaces commonly observed in the alluvial aquifer during the month of March. The total rate of bedrock discharge computed by the model of steady-state flow in March 2011 (5.6 gpm, Table 7) is also noteworthy because it represents less than a third of the bedrock inflow that was derived from the calibrated model developed for the SOWP (18.7 gpm, see Section 4.4).

The lack of a published water budget for the model used in the GCAP (DOE 2002) prevents a thorough comparison of budget components in the March 2011 model (Table 7) with equivalent components in the Knight Piesold (2002) evaluation, which was used develop the groundwater remedy for the Shiprock site. However, it should be noted that the 5.6 gpm value in Table 7 for bedrock discharge across the escarpment compares favorably with the estimated range of bedrock discharges derived from application of the Knight Piesold model (3–5 gpm, see Section 4.4) in the GCAP (DOE 2002). A distinct difference between the two assessments is seen in the treatment of recharge from precipitation. The Knight Piesold model assumed the rate of recharge on the floodplain was 1.1 gpm, whereas recharge from precipitation was assumed negligible in this study.

7.3.1.4 Groundwater Velocities

A computational tool in Groundwater Vistas was used to calculate average linear velocities (Freeze and Cherry 1979) in groundwater associated with the steady-state flow model of flow conditions in March 2011. The tool made use of computed groundwater elevations, the calibrated value of hydraulic conductivity (80 ft/day), and an assumed aquifer porosity of 0.25 (25 percent). Resulting velocities varied widely, ranging from a low of 0.2 ft/day in some locations to as much as 2 ft/day in a small area northwest of the zone of groundwater mounding. The largest average linear velocity calculated for areas identified as contaminated during the years 1999–2001 (contaminant plumes are shown in Figure 14 through Figure 16) was about 1.6 ft/day. As a rough indicator of the mobility of a contaminant when it is not being captured by pumping, this value suggested that a contaminant could migrate close to 100 ft away from a remediation pumping center during a 60-day period. For Trenches 1 and 2, this distance was considered short enough such that the resumption of groundwater extraction after 60 days of no pumping would lead to recapture of contaminants leaving either trench footprint. In contrast, some contaminated groundwater in the 1089/1104 area might discharge to the river if pumping was stopped for 60 days at wells 1089 or 1104.

7.3.2 Transient Flow Model

Simulation of transient flow from March 24, 2011, through the following August meant that the model would have to account for changing water elevations on the river and variable pumping rates at wells 1089 and 1104 and the two trenches. To simplify the model, bedrock discharge rates were assumed to remain constant throughout the simulation period and equal to the rates adopted in the calibrated steady-state flow model for March 2011. In addition, the constant recharge rate assigned to the Bob Lee Wash outlet area in the steady-state model (45.3 gpm total) was also applied to the transient model. Starting hydraulic heads in the transient model were derived using data interpolation tools built into Groundwater Vistas and the 48 target elevations employed in the steady-state model.

During initial planning for the transient model, consideration was given to the possibility of accounting for daily changes in river elevation as well as daily pumping rates in all components of the remediation system. However, this approach was abandoned because the computational effort involved in the simulation of daily hydraulic stresses was more demanding than could be justified for this study. Consequently, an alternative approach was adopted wherein average river elevations and remediation pumping over 3-day periods would be used as model input. It was believed that this model simplification would still make it possible to account for the larger variations in the hydrograph water elevations presented in Section 6.2.

7.3.2.1 Changing River Profiles

Calculation of 3-day averages for well and trench pumping rates for model input was easily accomplished using SOARS data. The determination of prescribed hydraulic heads along the river was also relatively simple for 3-day periods wherein the river-stage elevation was less than the elevation linked to the March 2011 survey (4883.89 ft amsl), as these were calculated using Equation (1). However, the development of prescribed river levels corresponding to higher river flows was more problematic because of the very different profiles previously linked to low and high flows (Figure 21) as a result of the engineering surveys (Section 5.3.1).

Different algorithms were tested to identify a method for calculating representative water-surface profiles intermediate between the low- and high-flow profiles produced from the engineering surveys. The algorithm ultimately chosen to compute such intermediate elevations at each of the 679 model blocks used to represent the river was

$$H_{riv} = H_{low} + [(G_{riv} - G_{low})/(G_{high} - G_{low})](H_{high} - H_{low}) \quad (2)$$

where H_{riv} = prescribed river elevation (ft amsl),
H_{low} = river elevation linked to the low-flow survey (ft amsl),
G_{riv} = measured river gage elevation (ft amsl),
G_{low} = river gage elevation linked to the low-flow survey (4883.89 ft amsl),
G_{high} = river gage elevation linked to the high-flow survey (4889.03 ft amsl), and
H_{high} = river elevation linked to the high-flow survey (ft amsl).

During the period leading up to peak flow in the river (May 10–June 10, 2011), this approach resulted in a sequence of profiles that, in addition to assigning successively higher elevations to the prescribed-head model blocks, were intermediate in shape between the two survey profiles and ultimately approximated the shape of the high-flow profile derived from the engineering survey on June 10, 2011 (Figure 21).

The values used for G_{riv} in Equations (1) and (2) for calculation of transient model input represented 3-day averages. To develop some perspective on how the 3-day average river gage elevations represented actual gage elevations (15-minute data) for the simulation period, the two sets of data between early March and early September were compared (Figure 46). As this graph shows, the 3-day averages removed many of the short-duration elevation spikes that occurred during the simulation period. However, long-duration elevation decreases and increases, including the 2- to 3-week elevation increase leading up to the peak yearly flow in early June, were captured. At a minimum, the 3-day average river profiles generated using Equations (1) and (2) were expected to result in a transient model run that adequately simulated the peak groundwater elevations observed in well hydrographs.

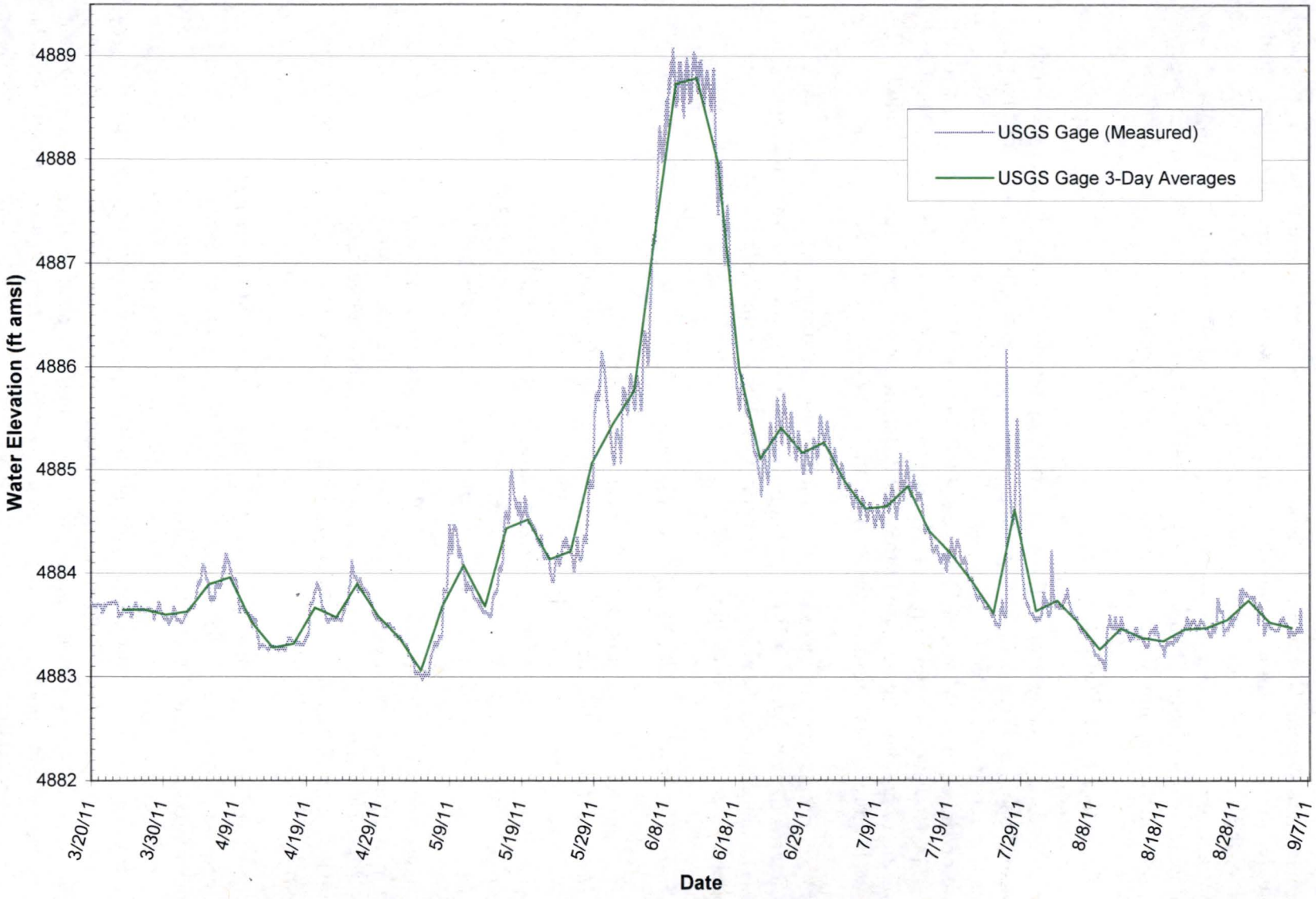

Figure 46. Three-Day Average River Elevations at the USGS Gaging Station

7.3.2.2 Aquifer Specific Yield

Several different values of aquifer storativity were employed in calibration runs with the transient model to identify a value that resulted in reasonable matches with the hydrographs for SOARS wells located (1) west and south of the USGS gaging station (Group 2 wells, Figure 25) and (2) in the Trench 1 area (Group 3 wells, Figure 25). This exercise indicated that the relatively low values representative of a confined aquifer produced poor matches to the hydrographs, particularly when combined with the values of hydraulic conductivity used for the alluvial aquifer in the SOWP (DOE 2000) model (100 ft/day), the Knight Piesold (2002) model (100 ft/day), the Trench 2 evaluation (DOE 2009b) model (85 ft/day), and the model for this study (80 ft/day). Ultimately, a value of 0.25 was combined with the previously mentioned hydraulic conductivity of 80 ft/day to produce reasonable fits with most of the hydrograph elevations included in the transient model calibration effort. This large number was considered representative of the aquifer's specific yield and indicated that the floodplain groundwater system responds to hydrologic stresses as if it were unconfined. The specific yield value can also be considered an estimate of the aquifer's effective porosity.

7.3.2.3 Simulated Hydrographs at Group 2 Wells (West and South of the USGS Gaging Station)

Figure 47, Figure 48, and Figure 49 illustrate the hydrographs produced by the calibrated transient model for wells 779, 857, and 853 respectively. Of these plots, the model-generated hydrograph for well 857 provides the best match to corresponding measured groundwater elevations, which appeared to be solely influenced by changing river elevations during the simulation period (Section 6.2.2). As expected, the use of 3-day average river elevations for prescribed heads in the model diminishes the model's ability to capture short-term elevation spikes in the hydrograph, but the general magnitudes of the observed water elevations are adequately simulated, particularly during the rising-limb portion of the hydrograph prior to its peak near the beginning of the third week in June.

The tendency of model-computed water levels for well 857 to exceed corresponding measured levels that compose much of the recession limb of the hydrograph (Figure 48), as well as in following summer months, appears to be related to the model's exclusion of ET losses from groundwater during summer. Had the model possessed the capability to account for seasonal transpiration of water from phreatophyte vegetation in areas surrounding the well, it is likely that it would have provided a better match to the observed water elevations at well 857 from late June through August 2011. Similarly, a reduction in the modeled Bob Lee Wash recharge rate would probably have also improved the model's ability to match the summer portion of the well-857 hydrograph.

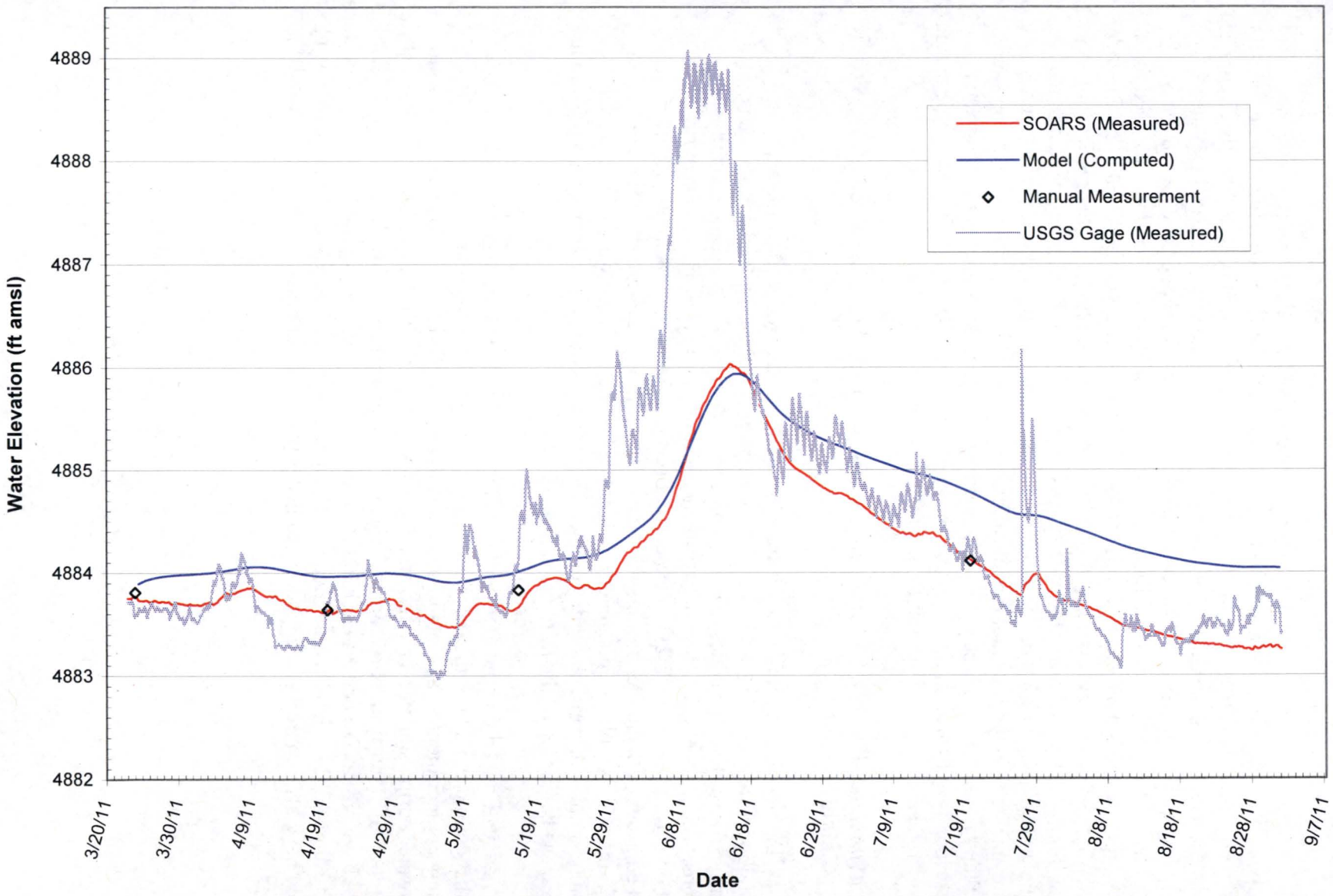

Figure 47. Observed and Computed Hydrographs at Well 779

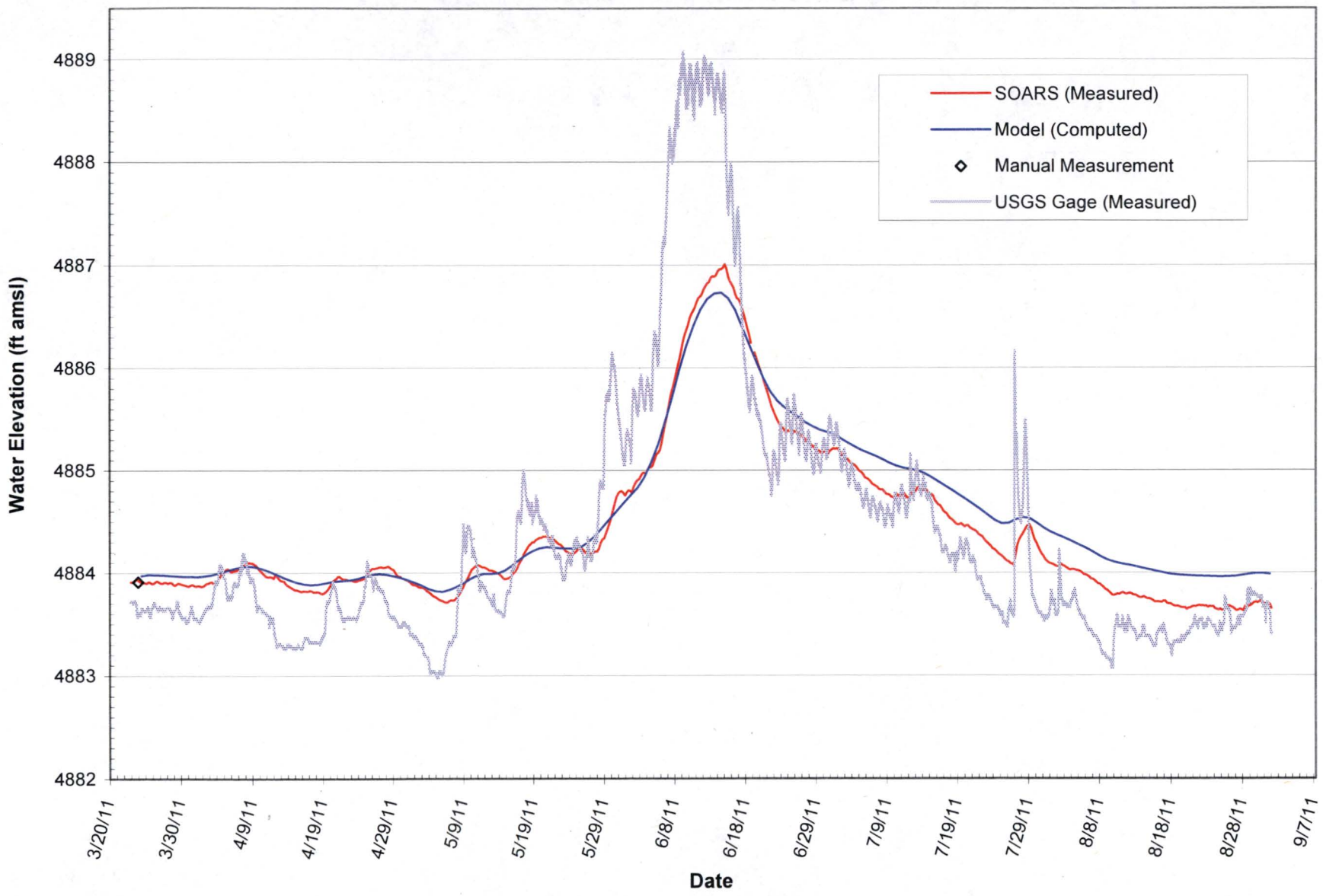

Figure 48. Observed and Computed Hydrographs at Well 857

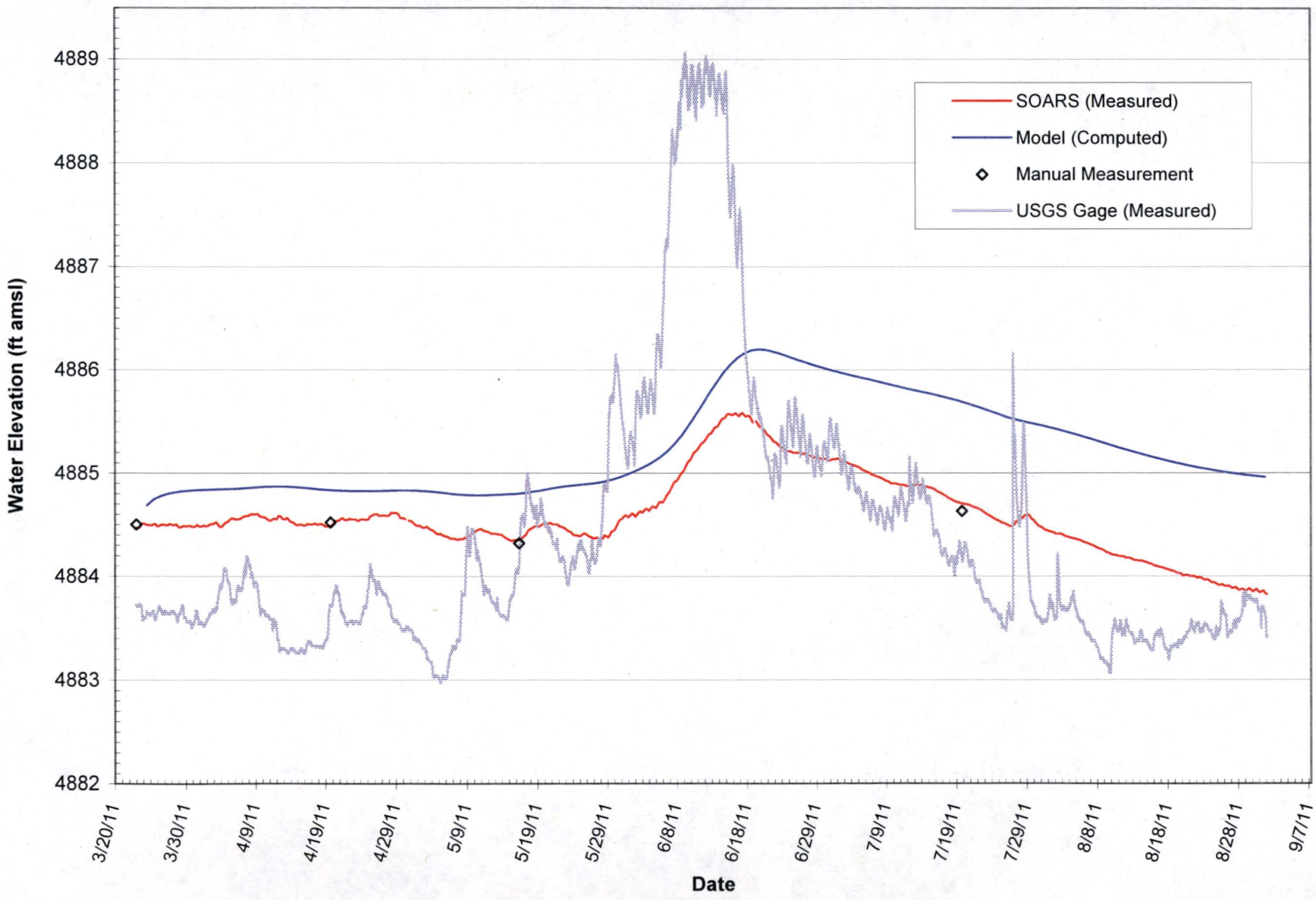

Figure 49. Observed and Computed Hydrographs at Well 853

The model appeared to perform well in matching the observed peak groundwater elevation at well 779 in mid-June 2011 (Figure 47) but tended to overpredict hydraulic heads at this well at all other times. During the first two months of simulation, overpredictions of head were generally limited to about 0.2 to 0.4 ft, but the discrepancy between observed and computed water elevations was even greater between late June and August of the year, sometimes approaching 0.8 ft. During the calibration effort, some consideration was given to the possibility that the combined hydraulic conductivity/specific yield parameter set adopted in the model (80 ft/day and 0.25) was not optimal for the floodplain as a whole. Though this is probably the case, it is just as likely that the model could have achieved a better fit to the observed hydrograph at well 779 by accounting for aquifer heterogeneity and ET effects, with the latter being applied during summer months.

Of the three wells included in this category of hydrograph comparisons, the worst fit between observed and computed groundwater levels occurred at well 853 (Figure 49). Though the transient model consistently overpredicted hydraulic heads at this well, such a result was at least partially expected since the calibrated steady-state model discussed in Section 7.3.1 had overpredicted the groundwater elevation here by more than 0.3 ft. Similarly, given the anomalous temporal behavior of water levels in well 853 during the high river-runoff period in June 2011 (Section 6.2.2), the possibility that spatial and temporal variations in the hydraulic connection between river and aquifer may contribute to local hydrograph discrepancies cannot be ruled out. Again, these observations suggest that modeling of groundwater flow in areas west and south of the river gaging station could be improved by accounting for aquifer heterogeneity and ET processes.

7.3.2.4 Accounting for Evapotranspiration Effects

The apparent overprediction of hydraulic heads at wells 779, 857, and 853 during mid- and late-summer months (Figure 47, Figure 48, and Figure 49, respectively), largely because the model did not account for ET during summer 2011, suggested that the transient model would benefit from the inclusion of ET losses in warmer months. However, this approach was not taken because the steps required to produce a defensible model that incorporates ET were beyond the scope of this study.

The capacity for ET to remove groundwater from the alluvial aquifer is expected to vary greatly across the floodplain because the occurrence of phreatophytes on the floodplain is variable, with some parts of the site containing thick phreatophyte stands and others virtually devoid of plant growth. Thus, defensible estimates of transpiration losses from various parts of the floodplain could only be developed through field studies specifically designed to measure such losses. Moreover, much of the ET expected each summer is bare-ground evaporation in the shallow water-table area receiving recharge from Bob Lee Wash outflows. Though information is available in the scientific literature regarding evaporation rates from surface water in this part of New Mexico, simulation of evaporation loss of groundwater in bare-ground zones requires study of how the losses vary with depth to the water table in the uppermost sediments comprising the aquifer.

Additional challenges to quantifying ET at the Shiprock site stem from the fact that ET rates vary over time, between months and from year to year, depending on changing weather conditions. Well-planned studies, involving techniques and equipment specifically designed to quantify ET

rates and volumes, will be required to ascertain how vegetation and meteorology at the site influence the spatial and temporal variability of ET.

Modeling based on a single assumed ET rate applied uniformly across the floodplain and from year to year would not result in a reliable simulator of groundwater flow and aquifer cleanup at the Shiprock site. Just as it is important to utilize monitored pumping rates from the wells and trenches in the alluvial aquifer to ascertain their effects on aquifer remediation, it is equally important to account for spatially and temporally variable ET rates. This is particularly true given that transpiration processes each summer are potentially functioning as a separate system for removing floodplain groundwater and its entrained contaminants.

7.3.2.5 Simulated Hydrographs at Wells in the Group 3 (Trench 1) Area

Calibration efforts aimed at matching the hydrographs at wells in the Trench 1 area were particularly informative because they revealed how the aquifer tends to respond to remediation pumping in a part of the floodplain that appeared to be unaffected by increased river levels during the high-river-flow weeks from late May through mid-June 2011 (see Section 6.2.3). With the exception of well 1140, the simulated hydrographs at all wells included in this category were reasonable approximations of those generated from measurements.

Figure 50 and Figure 51 present model-computed hydrographs for well 793 and 1009, respectively, the SOARS wells located farthest from Trench 1. Both temporal plots suggest that the transient model performed well in approximating observed groundwater elevations from the simulation starting time in late March 2011 to mid-May, including the period of continuous pumping from Trench 1 between late April and May 20. After mid-May, however, the observed and computed hydrographs begin diverging from each other, apparently because of the model's inability to simulate ET losses. Overpredictions of hydraulic head at these two wells become very apparent in midsummer, after passage of the snowmelt runoff peak in the river, and eventually approach values of 0.8–1 ft in late August of the year. This latter observation, free of any influences provided by changing river levels, suggests that a model capable of accurately simulating the gross effects of ET from late spring through early fall would produce a reliable predictor of groundwater flow. This seems particularly true given that the differences in average groundwater elevation at monitoring wells across the floodplain between spring and fall monitoring events tend to fall in the range of 1–2 ft (Section 6.3 and Section 6.4).

Observed and model-computed hydrographs at well 1105 (Figure 52), 130 ft northeast of Trench 1, further attest to the model's ability to reasonably approximate hydraulic heads during the spring season. As with the hydrographs for wells 793 and 1009, water elevations predicted by the transient model begin to noticeably diverge from corresponding observed levels in early June, and the model overpredictions tend to increase progressively through summer months.

As shown in Figure 53, the transient model tends to underpredict drawdowns at well 1140 created by Trench 1 pumping in early May 2011. This observation suggests that the uniform hydraulic conductivity adopted in the model (80 ft/day) is greater than the conductivity of aquifer materials in the vicinity of the well. Though drawdown is also underpredicted at well 1140 in response to a short-duration (4 days) pumping event at the trench in early June, it is likely that some of the difference between observed and computed water levels at this time is caused by the use of 3-day average pumping rates in the transient simulation as well as the effects of ET.

As with all other SOARS wells included in the transient model calibration effort, the model's inability to simulate the influences of ET at well 1140 during summer months is apparent (Figure 53). The model's overprediction of groundwater levels at this well by as much as 1 ft during Trench 1 pumping in July and August can be partially attributed to the relatively high hydraulic conductivity used in the model, but is also probably due to the fact that groundwater losses to ET are not simulated.

Unlike at well 1140, the transient flow model produces computed hydraulic heads at well 1141 (Figure 54) that reasonably track corresponding observed water elevations through early June. Thus, it appears that a hydraulic conductivity of 80 ft/day is representative of alluvium in this particular near-trench area. The appropriateness of parameters adopted in the transient model for simulating groundwater flow in the vicinity of well 1141 is also manifested in acceptable discrepancies between observed and computed water levels during late summer months, which remain well short of 1 ft despite the model's inability to account for ET losses.

The apparent influences of ET on groundwater flow in the vicinity of Trench 1, in addition to the impacts on flow in areas closer to the river (Section 7.3.2.3), highlight the importance of developing a better understanding of how ET processes vary both spatially and temporally at the Shiprock site. As discussed in Section 7.3.2.4, reliable and defensible simulation of these processes requires techniques that are more sophisticated than the assumption of a single ET rate applied uniformly across the floodplain in the alluvial aquifer model.

7.3.2.6 Transient Flow Patterns in the High-Runoff Period

The degree to which increased river levels in late May and June 2011 impacted groundwater flow patterns in the alluvial aquifer is examined with maps of model-computed hydraulic heads and associated flow vectors at three different times. The first map captures simulated groundwater flow conditions on May 28 (Figure 55), during a period of fluctuating river levels reflective of the initial stages of snowmelt runoff. In general, flow patterns at this time are similar to those expected when all three components of the remediation system were pumping (Figure 17). However, as indicated by flow vectors near the river, the rising river is causing surface water to seep into the aquifer along the entire length of the floodplain, including the area near river survey location 14 under the Highway 491 bridge. General flow patterns are also starting to diverge from those displayed in Figure 17, with one of the most notable effects being flowpaths a few hundred feet from the river's edge that also parallel the river for hundreds to thousands of feet (Figure 55).

Computed hydraulic heads and flow vectors for June 13, 2011 (Figure 56), during peak runoff in the river, suggest that the high river levels are now impacting flow patterns as much as 1000 ft from the river's edge. One of the impacts appears as northwestward flow in the area lying directly between the Trench 1 and 1089/1104 areas, indicating that the radial flow associated with groundwater mounding at the mouth of Bob Lee Wash no longer dominates flow between the two areas, as previously indicated by flow patterns produced by the calibrated steady-state model (Figure 432) of groundwater flow under baseline (nonpumping) conditions. In addition, a relatively wide swath of flow vectors pointing northwestward from the 1089/1104 area toward the Highway 491 bridge suggests that contaminated water from this area is migrating parallel to the river rather than directly toward it.

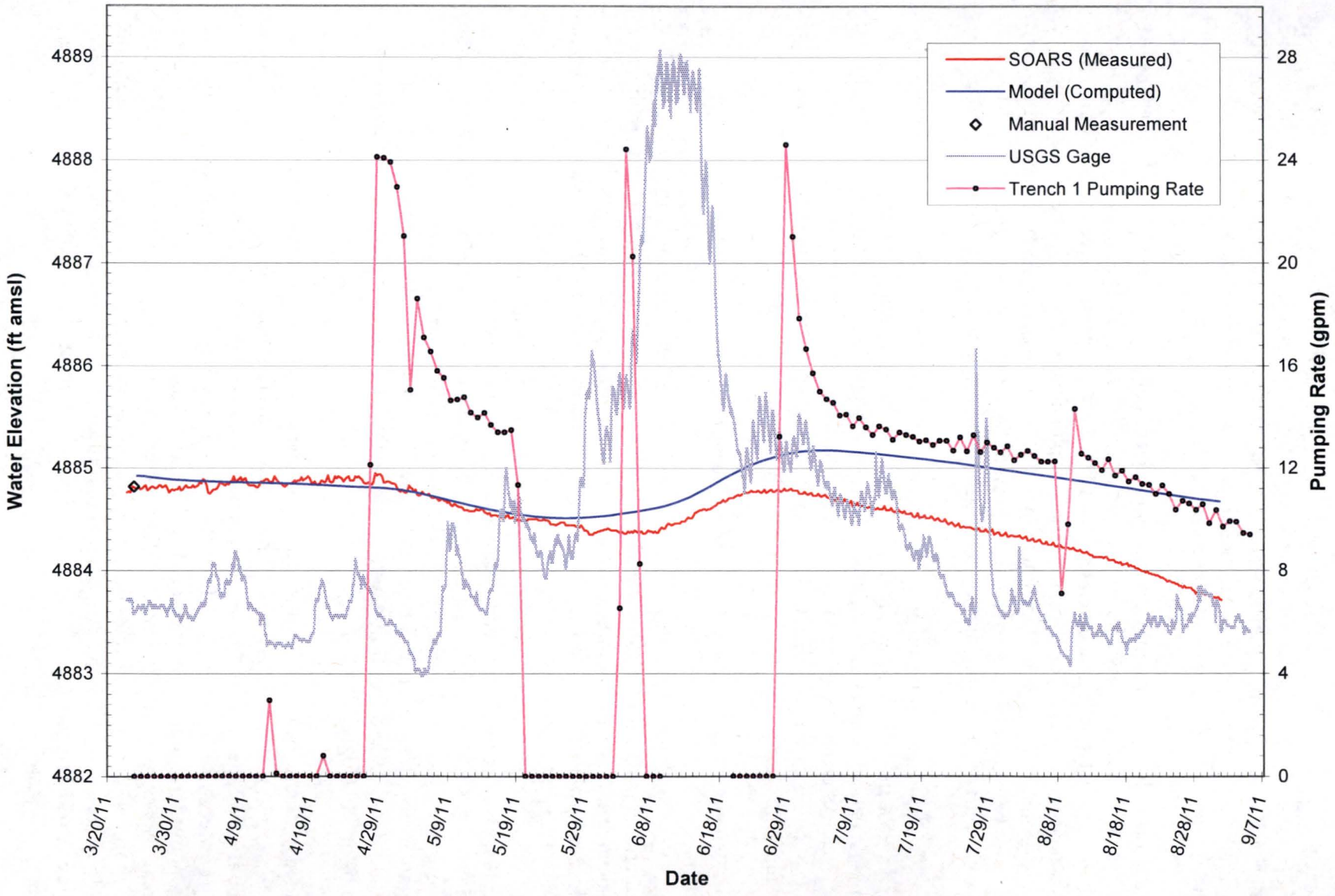

Figure 50. Observed and Computed Hydrographs at Well 793

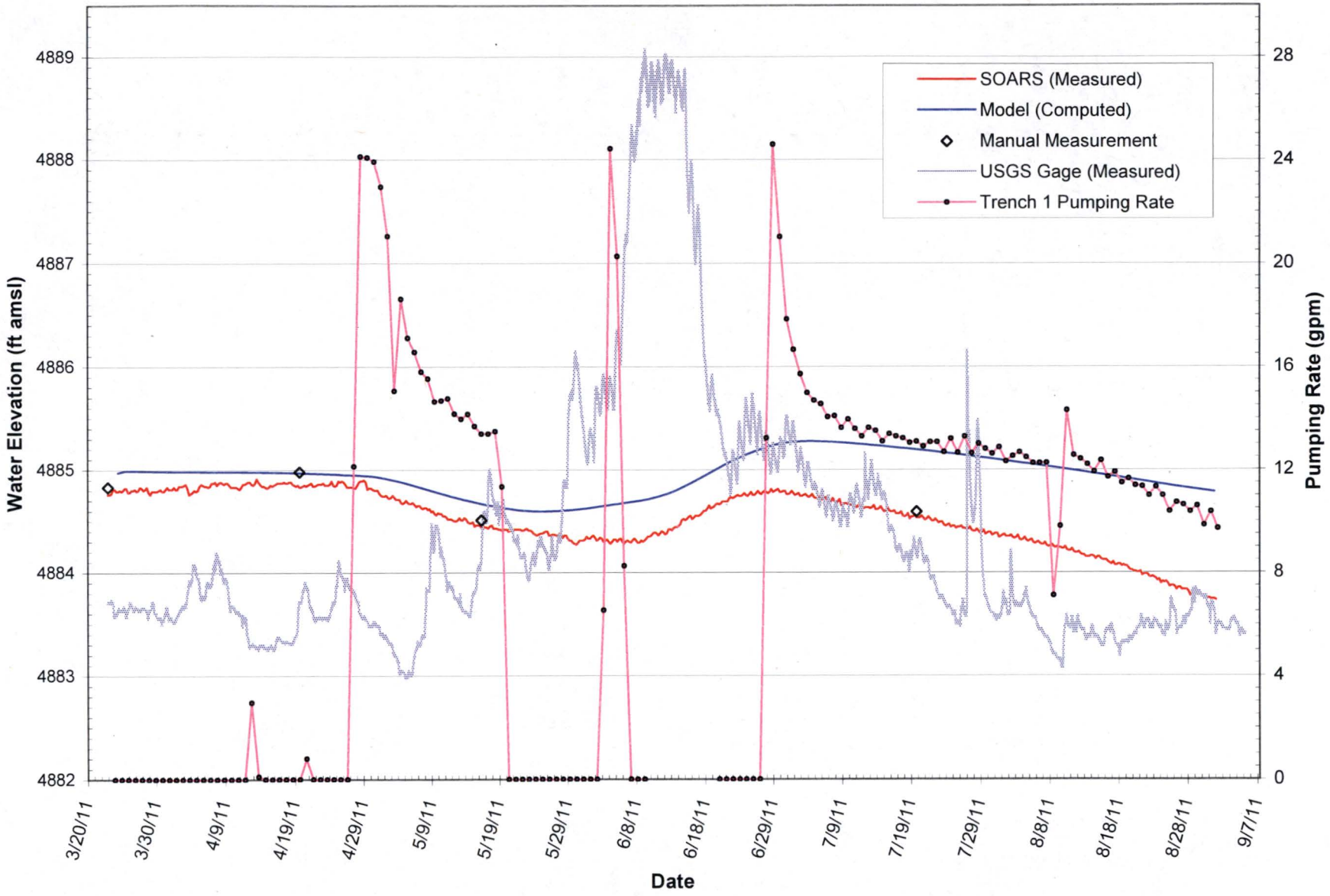

Figure 51. Observed and Computed Hydrographs at Well 1009

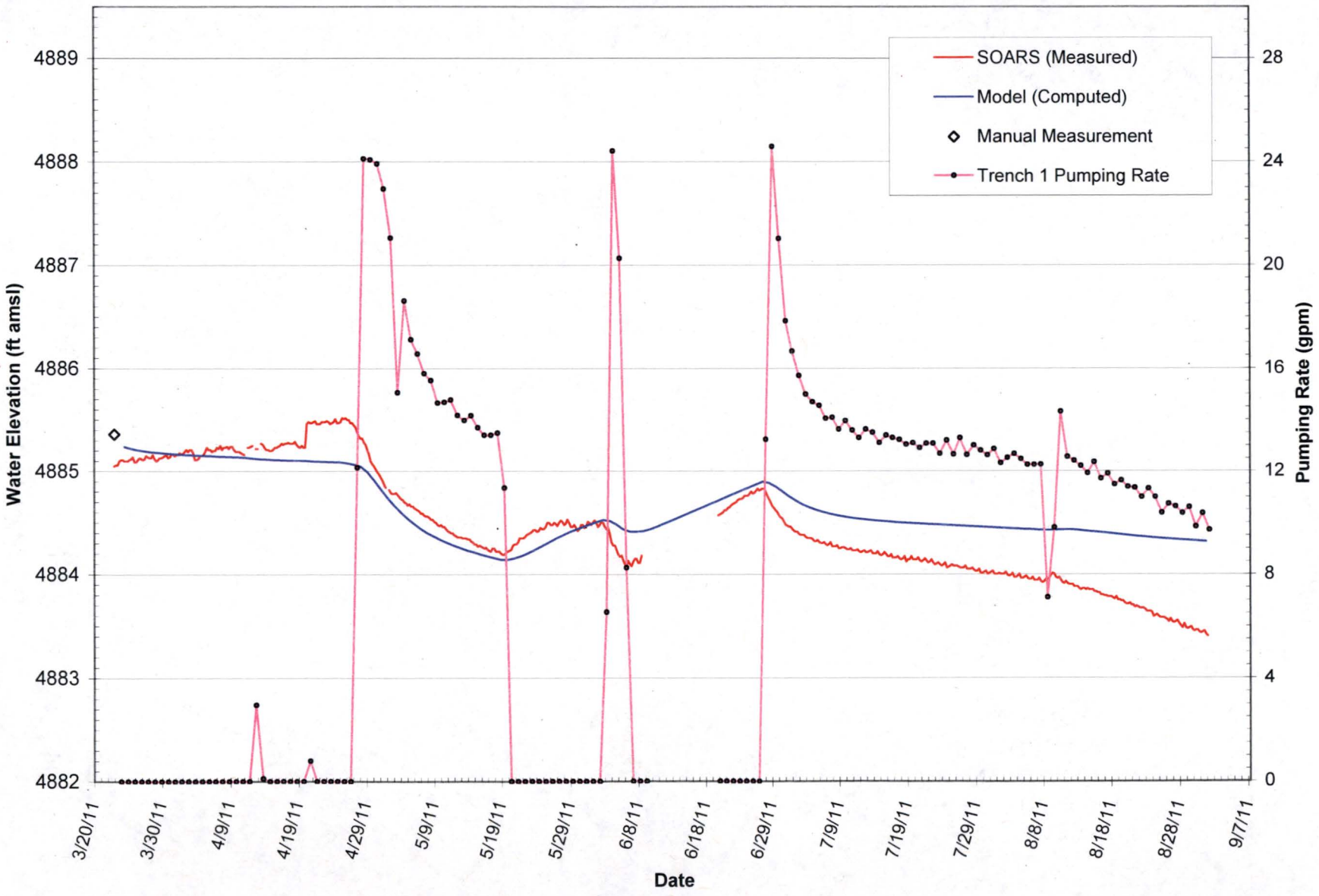

Figure 52. Observed and Computed Hydrographs at Well 1105

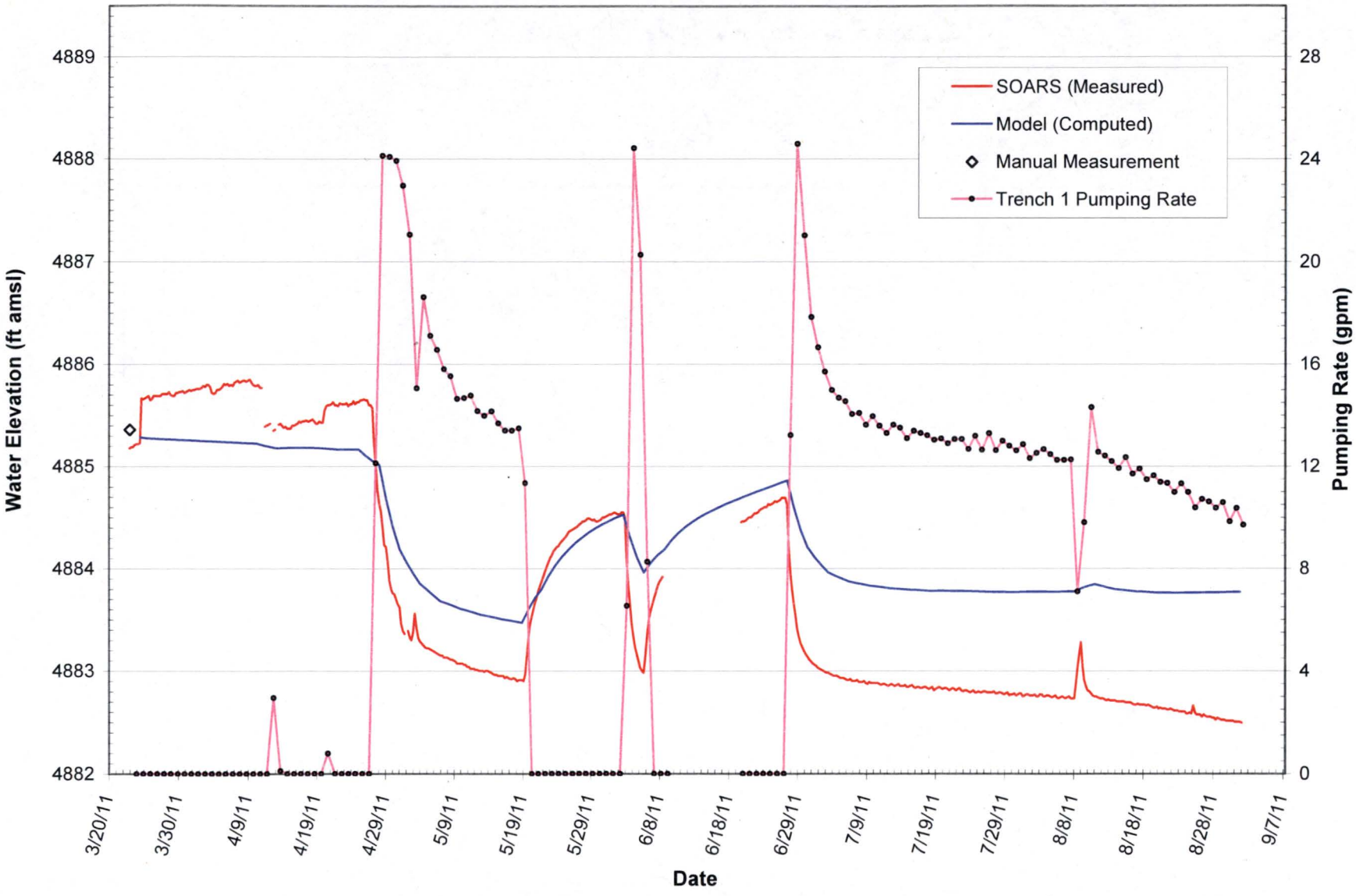

Figure 53. Observed and Computed Hydrographs at Well 1140

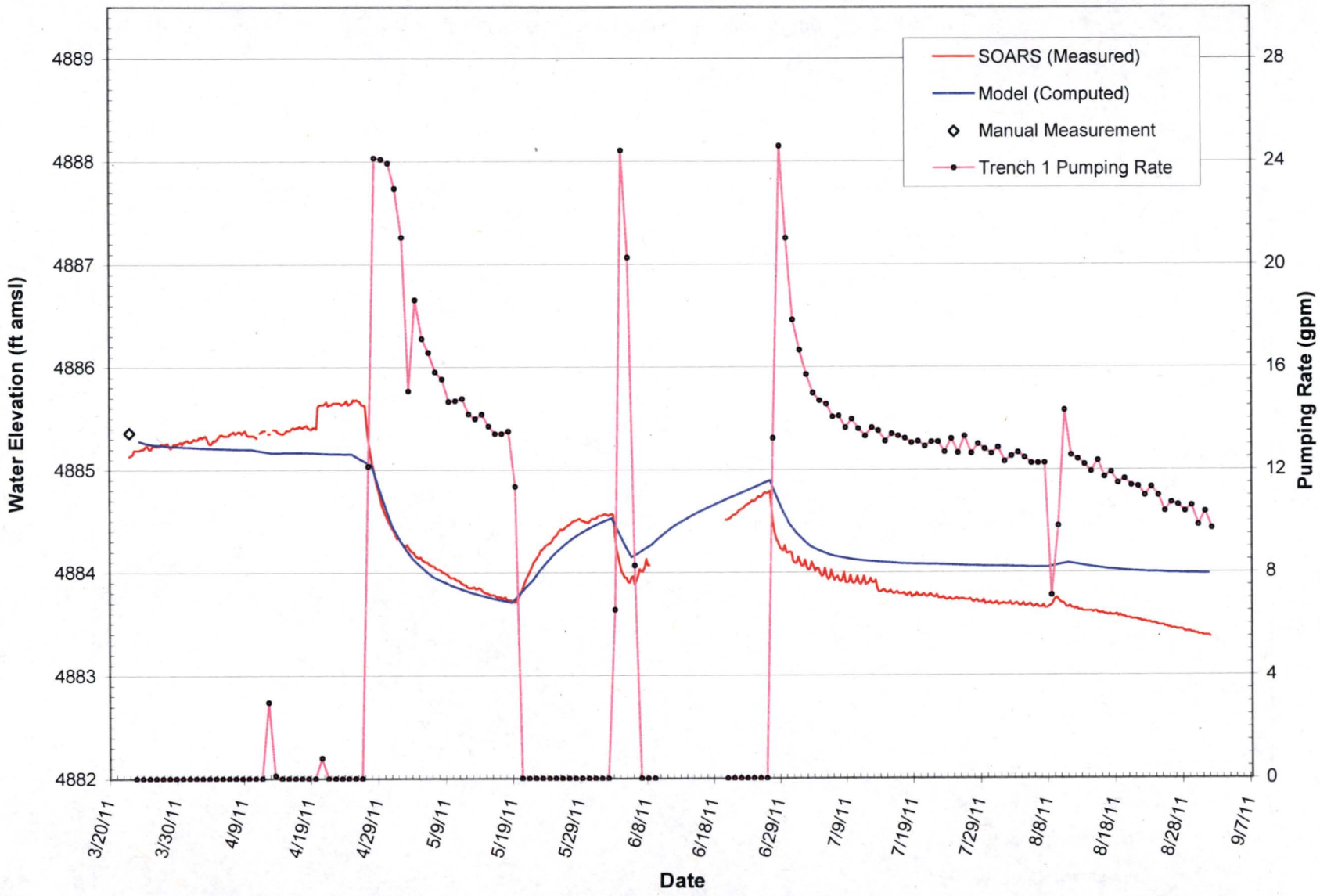

Figure 54. Observed and Computed Hydrographs at Well 1141

Computed groundwater elevations and flow vectors for June 13, 2011, at the base of the escarpment and about 400 ft south-southeast of the Highway 491 bridge (Figure 56) are noteworthy because they suggest this area acts as a zone of flow convergence, with groundwater flowing in from both the river and the mounding area. However, the flow vectors shown for this area in Figure 56 should not be interpreted to mean that local water is migrating from the alluvial aquifer into terrace groundwater, as the escarpment section between the mouth of Bob Lee Wash and the river is treated as a no-flow boundary in the model. The apparent flow convergence is necessarily a temporary phenomenon. Inspection of results from the transient simulation indicate that convergent flow behavior in this part of the aquifer is completely removed by June 24, or about a week and a half after the period represented by flow patterns shown in Figure 56.

The third map of computed hydraulic heads and flow vectors displays modeled flow conditions on June 28 (Figure 57), approximately 2 weeks after peak flow in the river. At this time, passage of the highest river elevations has begun to reverse the effects of bank storage, and the aquifer is now discharging to the river along most of the floodplain's total length. Nonetheless, remnants of the preceding river losses to the aquifer continue to be observed hundreds to thousands of feet from the river. This is particularly true in locales lying directly between the 1089/1104 area and the Trench 1 area, where flow vectors still indicate northwestward flow, parallel to the river and in the direction of floodplain's north end. This model result suggests that northwestward diversion of contaminated water away from portions of the plume lying between the two areas is persistent each year for multiple weeks after peak flow on the river. Similar phenomena have been observed in other shallow alluvial aquifers influenced by large changes in river elevation over relatively short time periods (e.g., Boutt and Fleming 2009).

7.4 Pumping Conditions in March 2010

The calibrated model was used to conduct an additional simulation of groundwater flow during a semiannual monitoring event that took place between March 23 and March 26, 2010. The main purpose of this simulation was to estimate flowpaths created by simultaneous pumping from all three components of the floodplain aquifer remediation system in a period of relatively stable river flow. The ability of the calibrated model to simulate drawdowns at monitoring wells in the vicinity of each of the pumping systems was also of interest. Because pumping rates remained relatively constant, and river levels fluctuated little during the 3 days of monitoring, the model was used to simulate assumed steady-state flow conditions.

The average river gage elevation during the March 2010 monitoring event was 4883.95 ft amsl, and the mean flow in the river was 943 cfs. Because the measured gage elevation slightly exceeded the elevation linked to the low-flow survey (4883.87 ft amsl), prescribed heads for each of the 679 model blocks used to represent the river profile at this time were computed using Equation (2). The average pumping rates during the monitoring event at well 1089 (6.53 gpm), well 1104 (1.44 gpm), Trench 1 (10.45 gpm), and Trench 2 (10.27 gpm) were assigned as prescribed flows in the model using techniques identical to those employed in the transient model runs (Section 7.3.2).

7.4.1 Flow Patterns

Figure 58 illustrates the computed groundwater elevations produced by the steady-state flow model along with associated flowpaths generated through particle tracking. The computed

flowpaths are virtually identical to those adopted in the existing conceptual model for remediation conditions (Figure 17), including the presence of a stagnation zone several hundred feet northeast of Trench 1. However, a discrepancy between the two sets of flowpaths is observed on the river side of the 1089/1104 area, where model results (Figure 58) suggest that the combined pumping rate from wells 1089 and 1104 is not large enough to induce seepage losses from the river. Given that available water-level data at three wells located between the river and well 1089 (wells 1137, 1138, 1139) indicated that groundwater extraction in this area was inducing flow from the river during the March 2010 monitoring event (Section 6.2.1), it is probable that the calibrated model does not accurately simulate aquifer conditions in the 1089/1104 area. Spatially variable hydraulic conductivity in the vicinity of pumping wells 1089 and 1104, which is unaccounted for in the numerical flow model, might explain the model's inability to simulate capture of river water by the pumping.

As suggested in the existing conceptual model, this simulation shows that simultaneous pumping from the Trench 1 and 1089/1104 areas creates a groundwater divide between the two areas (Figure 58). The computed flowpaths also comport with the existing conceptual model in that part of the contaminated subsurface is shown to escape capture by pumping in the Trench 1 and 1089/1104 areas. This occurs within a 300–600-foot-wide swath of aquifer (shaded area in Figure 58) that is a few hundred feet northeast of the simulated stagnation zone and includes well 618, where relatively high contaminant concentrations were observed in 2011 (Section 6.4.1). The model-computed flowpaths within the swath indicate that local contaminated groundwater is migrating northeastward and directly to the river, along a river section between the USGS gaging station and the 1089/1104 area.

The steady-state model results for March 2010 (Figure 58) confirm that groundwater extraction at each of the three pumping centers leads to convergent flows from surrounding locales. As a result, contaminant concentrations at wells affected by the pumping are expected to change over time (see Section 4.6). Contaminant concentrations that differ greatly between neighboring wells close to the pumping systems are also possible.

The flowpaths converging on Trench 1 (Figure 58) are similar in shape and extent to the estimated flowpaths ascribed to this part of the aquifer in the existing conceptual model (Section 4.6). In the model, groundwater extraction from this horizontal well induces river inflow about 1600 ft to the southeast of the trench footprint, and from the outlet of Bob Lee Wash, which is about 1000 ft northwest of the footprint. The March 2010 simulation also indicates that pumping at Trench 1 is capable of intercepting any contaminated bedrock groundwater discharging across more than 2500 ft of escarpment, again in agreement with the existing conceptual model (Figure 17).

7.4.2 Hydraulic Head Residuals

Measured water elevations at 50 monitoring wells were used as target elevations in the steady-state simulation of groundwater flow under remediation conditions in March 2010. The head residuals produced by the simulation, displayed in Figure 59, show several negative values (head overpredictions) of 0.5 ft or more, particularly at wells located in the 1089/1104 area and the Trench 1 area. This result signifies that the model is underpredicting groundwater drawdowns created by the pumping in these locations, suggesting that the 80 ft/day hydraulic conductivity value adopted in the floodplain-wide model is greater than the local hydraulic conductivity.

Unlike the 1089/1104 and Trench 1 areas, hydraulic head residuals in the Trench 2 area are relatively small, implying that the calibrated model performs well in simulating groundwater flow in the south third of the floodplain.

This page intentionally left blank

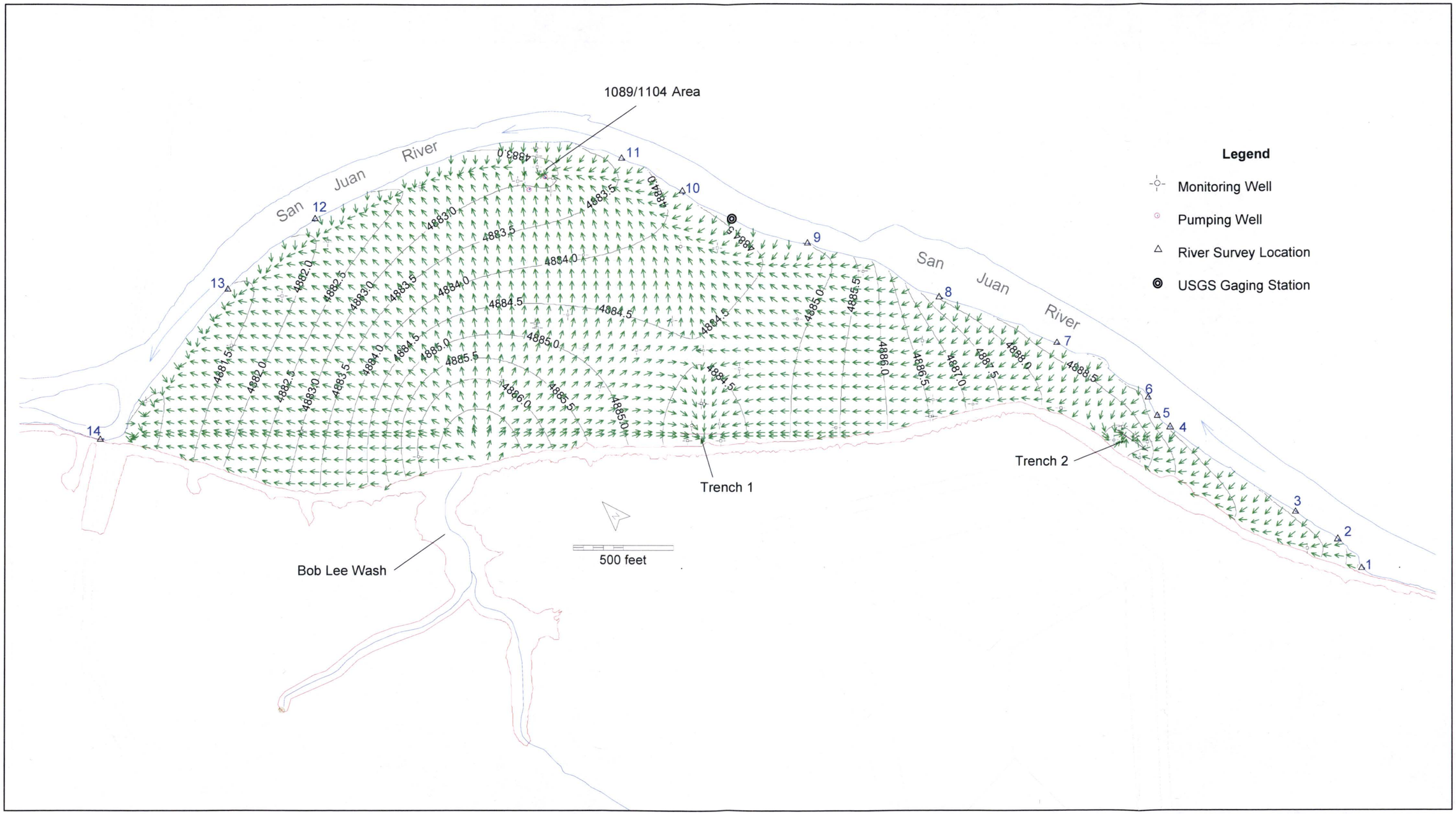

Figure 55. Computed Groundwater Elevations (ft amsl) and Flow Vectors, May 28, 2011

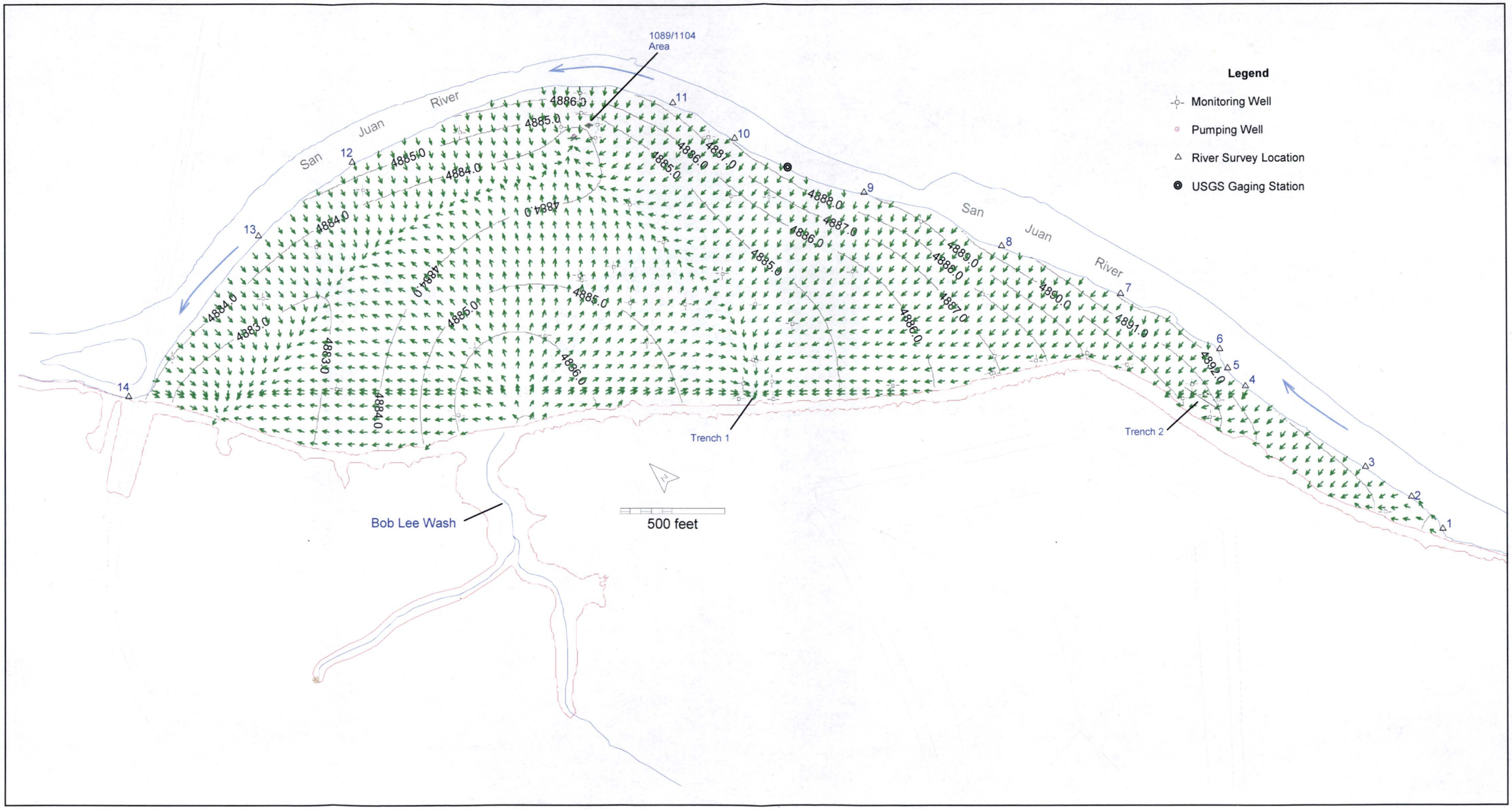

Figure 56. Computed Groundwater Elevations (ft amsl) and Flow Vectors, June 13, 2011

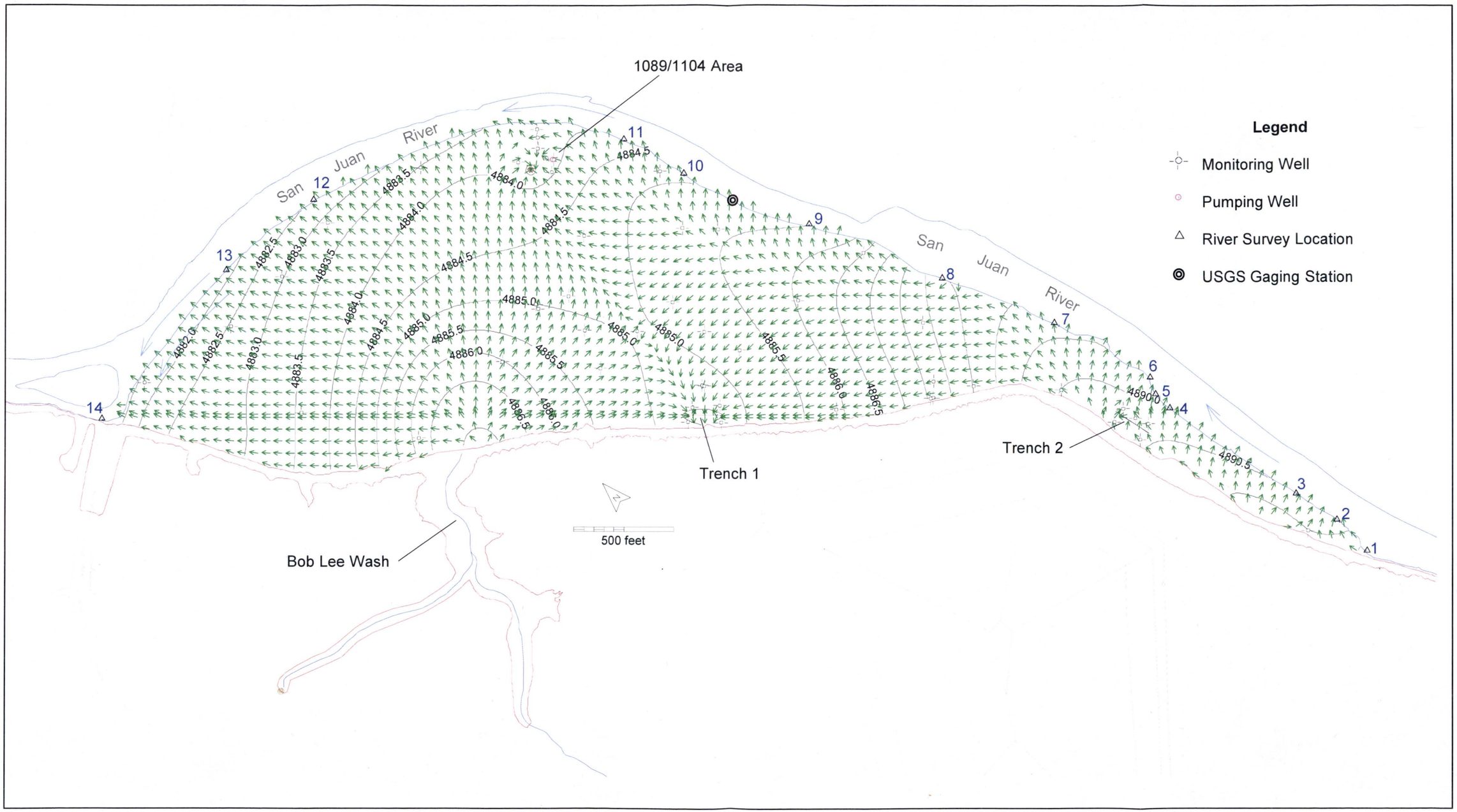

Figure 57. Computed Groundwater Elevations (ft amsl) and Flow Vectors, June 28, 2011

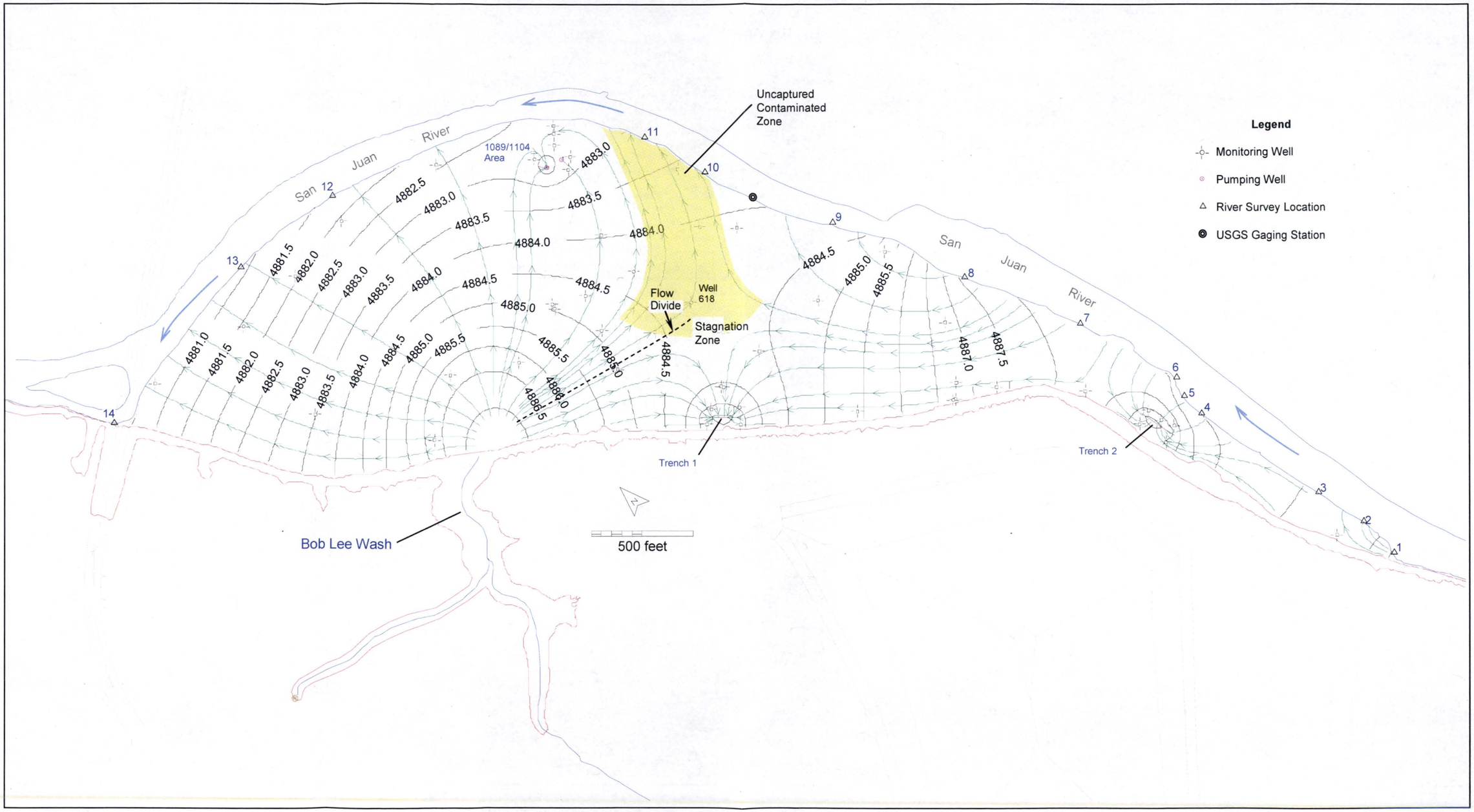

Figure 58. Computed Groundwater Elevations (ft amsl) and Flowpaths in the March 2010 Model of Steady-State Flow

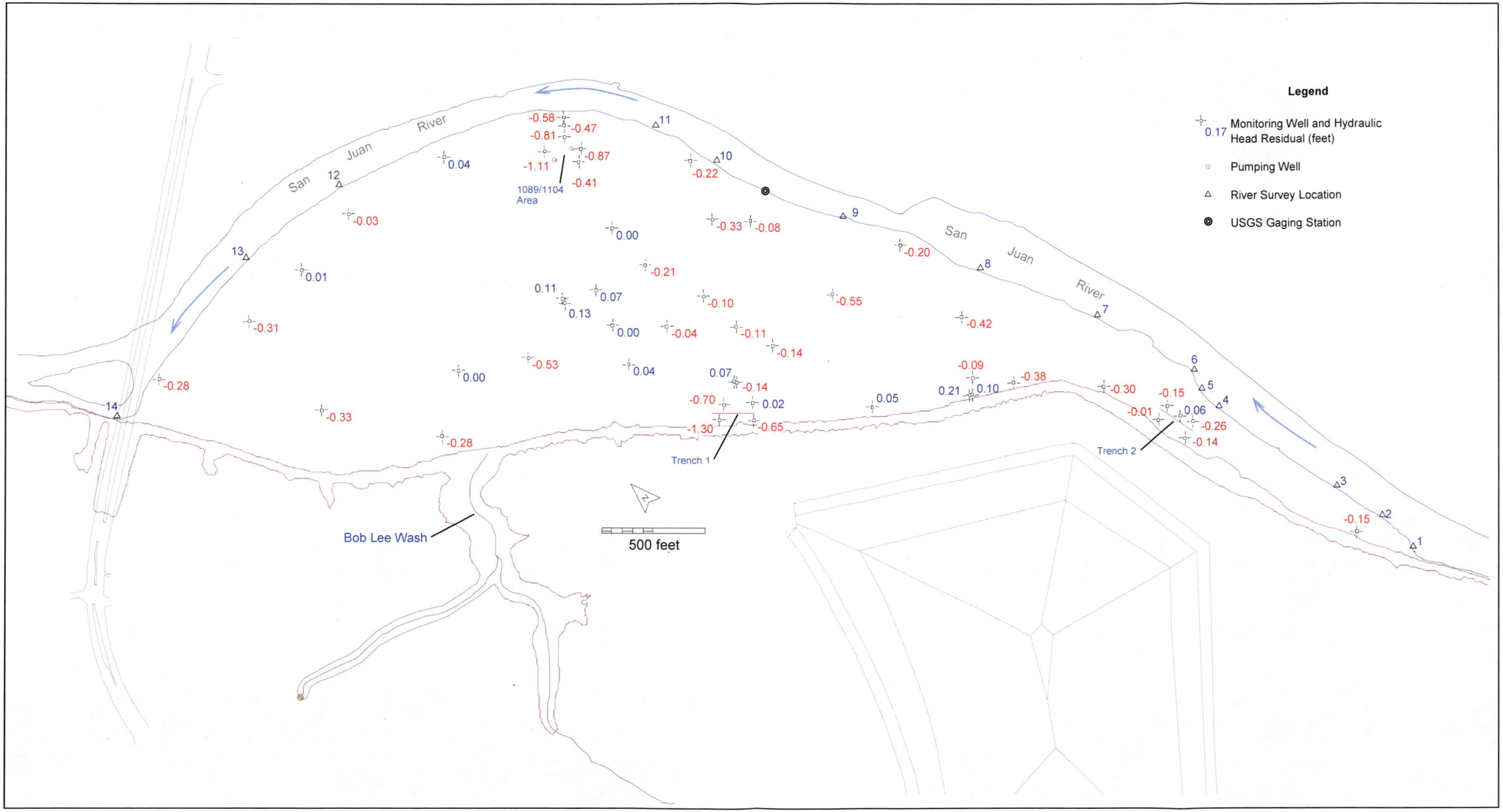

Figure 59. Computed Hydraulic Head Residuals in the March 2010 Model of Steady-State Flow

This page intentionally left blank

This page intentionally left blank

Other than the significant underpredictions of drawdown in the 1089/1104 and Trench 1 areas, computed head residuals in other portions of the model domain appear to be reasonably small (Figure 59). The mean value of the residuals at all 50 target wells is –0.236 ft, and the standard deviation of the 50 residuals is limited to 0.32 ft. The ratio of the standard deviation and the variation in observed target elevations (9.15 ft) is 0.035, a value that remains indicative of a reasonably good match between simulated and measured hydraulic heads.

7.4.3 Water Budget

Table 8 lists computed system inflows and outflows produced by the model of steady-state flow in March 2010. This water budget suggests that the total amount of water moving through the floodplain groundwater system in the spring and when all components of the remediation system are operating is 73.5 gpm (i.e., the sum of all inflows or all outflows), which is about 20 percent greater than that when no pumping occurs (61.9 gpm, Table 7). Most of the flow increase is attributed to enhanced seepage losses from the river induced by the remediation pumping. Of the three pumping centers, Trench 2 has the greatest impact on river losses because of its proximity to the river (~130 ft) and the relatively large pumping rates achieved at sump 1109 (10.3 gpm) during the March 2010 monitoring event). As indicated in Table 8, discharge of groundwater to the river (44.8 gpm) is reduced in comparison to the discharge occurring under baseline flow conditions (61.9 gpm, Table 7) because total groundwater pumping (28.7 gpm) (i.e., the sum of discharges from wells 1098 and 1104, and Trenches 1 and 2) is consuming a large portion (~40 percent) of the total aquifer inflow (73.5 gpm). The flowpaths produced by the model (Figure 58) suggest that combined pumping from the 1089/1104 and Trench 1 areas (18.4 gpm) is partly sourced by recharge attributed to infiltration of Bob Lee Wash flows (45.3 gpm).

Table 8. Computed Water Budget in the March 2010 Model of Steady-State Flow

Flow Component	(ft^3/day)	(gpm)	(%)
Inflow			
Seepage losses from the river	4,360	22.6	30.8
Recharge from Bob Lee Wash	8,720	45.3	61.6
Bedrock discharge	1,070	5.6	7.6
Outflow			
Discharge to the river	8,620	44.8	60.9
Well 1089 discharge	1,260	6.5	8.9
Well 1104 discharge	280	1.4	2.0
Trench 1 discharge	2,020	10.5	14.2
Trench 2 discharge	1,980	10.3	14.0

7.5 Pumping Conditions in September 2010

Despite the fact that insufficient information was available for developing an accurate model of groundwater flow in seasons influenced by ET processes, a simplified version of the calibrated model was used to gain insight into groundwater flow patterns induced by remediation pumping during a late-summer monitoring event. The monitoring event selected for this purpose took place from August 31 to September 2, 2010, during which time river gage elevations remained relatively steady at 4883.76 ft amsl, correlating to an average daily river flow of about 760 cfs.

Average daily remediation pumping rates over the 3-day monitoring period at Trench 1, Trench 2, well 1089, and well 1104 were 7.89, 21.9, 5.4, and 0.96 gpm, respectively.

The simplified model used for this purpose basically consisted of a short-duration, transient version of the calibrated model with all prescribed flow boundary conditions (i.e., bedrock discharge, remediation pumping) removed. Prescribed heads for the 679 model blocks representing the river profile were calculated using the average river gage elevation during the monitoring event (4883.76 ft amsl) and the algorithm in Equation (1). A field of initial water elevations was developed by entering into the model measured groundwater elevations at 48 monitoring wells during the event and allowing a data interpolation tool in Groundwater Vistas to fill in model starting elevations throughout the floodplain. The resulting model was then allowed to run for a total of 0.5 days, during which period starting water elevations evolved into a smoothed hydraulic head field that approximated flow conditions at the time of the monitoring.

A map view of contoured hydraulic heads resulting from this exercise along with associated groundwater flow vectors, shown in Figure 60, portrays a flow system that is noticeably different from the steady-state system associated with the monitoring event in March 2010 (Figure 58). The groundwater flow divide that separates the capture zones for Trench 1 pumping and pumping in the 1089/1104 is distinctly different in the respective simulations. Furthermore, the computed hyporheic flowpath associated with Riffle 4-Up and Riffle 4-Down in the March 2010 simulation (Figure 58) is no longer present in the computed flow field for September 2010 (Figure 60). As a result, Trench 1 is capturing surface water from a much larger section of the San Juan River in September than indicated for the March simulation, and the stagnation zone identified northwest of Trench 1 is not present in September 2010. Note also that a large capture zone is shown for the 1089/1104 pumping area in September that includes river losses from about 2000 ft of riverbank, including river seepage losses near the USGS gaging station.

The altered flow patterns discussed above appear to result from a combination of remediation pumping and lower groundwater elevations in late summer in comparison to elevations observed in colder months. Though previous analyses of seasonal changes in mean groundwater levels across the floodplain (Section 6.3 and Section 6.3.1) are on the order of 1–2 ft, comparison of the respective potentiometric surfaces illustrated in Figure 58 and Figure 60 suggests that local differences in seasonal elevations can be as great as 3 ft. This is the case at the mouth of Bob Lee Wash, where the combination of increased transpiration and bare-ground evaporation in September 2010 appears to result in mounding elevations in this area of about 4883.7 ft amsl, far short of the simulated elevation of 4886.7 ft amsl for this part of the floodplain in March 2010. Though remediation pumping in the Trench 1 and 1089/1104 areas affects the mound elevations in September 2010, groundwater drawdowns at the time at the Bob Lee Wash outlet are probably less than those created by groundwater extraction in March 2010. This is because the pumping rates in September at Trench 1 (7.89 gpm), well 1089 (5.4 gpm), and well 1104 (0.96 gpm) are decidedly less than comparable, respective rates during the preceding March (10.45, 6.53, and 1.44 gpm).

A steep head gradient from the river to the aquifer occurs between river survey locations 7 and 9 during the during the September 2010 monitoring event (Figure 60). Again, this appears to largely result from the presence of lower groundwater elevations in late summer, rather than possible higher water elevations in the river. Note that the average river flow in September 2010

was 760 cfs and the associated river gage elevation elevation was 4883.76 ft amsl, which are lower than the comparable river flow (943 cfs) and gage elevation (4883.87 ft amsl) in March 2010. As with the reduced groundwater elevations observed at the Bob Lee Wash outlet, the lower water levels in other parts of the aquifer in September 2010 appear to be caused by ET.

This page intentionally left blank

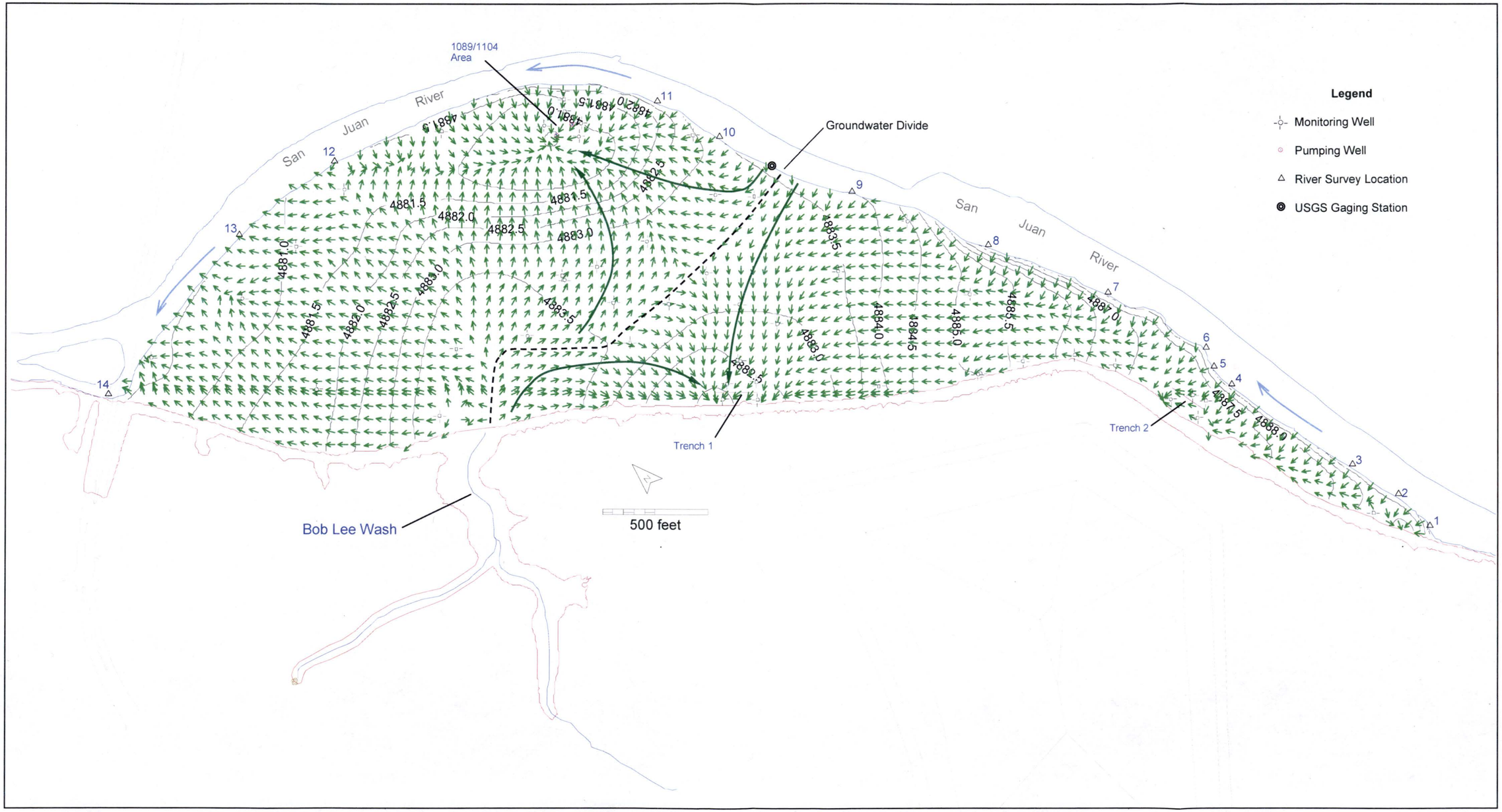

Figure 60. Estimated Groundwater Elevations (ft amsl) and Flow Vectors During the Monitoring Event in September 2010

This page intentionally left blank

8.0 Updated Conceptual Model

Most elements of the existing conceptual model of groundwater flow in the floodplain alluvial aquifer, described in Section 4, remain valid in this updated assessment of the floodplain groundwater system. However, this study has shown that some of the assumptions made under the existing conceptual model, particularly with regard to numerical models used to assess groundwater flow patterns and contaminant migration in the alluvial aquifer, are inapplicable during some parts of each year. This section draws from all data and modeling analyses presented in foregoing sections and proposes an updated conceptual model of groundwater flow in the floodplain alluvial aquifer. As part of the update, the following subsections point out where the existing conceptual model can be improved. In addition to highlighting differences between the existing and updated conceptual models, this report confirms the presence of many of the flow processes identified in the existing model and explains how modeling results and graphical illustrations have led to a greater understanding of them.

A large part of this updated assessment is based on groundwater-elevation data and river-elevation data collected during 2011 and groundwater modeling that made use of these data. Findings from two studies by the ESL (2011a, 2012) and investigations of vertical variations of concentration in alluvial-aquifer wells at the site (DOE 2014a, 2015b) are also incorporated in the conceptual model update.

The concepts presented here describe a flow system that is dynamic, the result of several interacting influences. It would be beneficial if the various influences were taken into consideration in any interpretation of data incorporated in annual remediation performance reports, modifications to the groundwater remediation system, and future studies of subsurface chemistry on the floodplain.

8.1 Naturally Dynamic Groundwater System

Though it has long been known that seasonally variable flows in the San Juan River impact groundwater elevations in the floodplain area, the existing conceptual model essentially treated groundwater flow in the alluvial aquifer as a steady-state process. All previously developed numerical models of groundwater flow in the floodplain system had assumed that flow patterns in the aquifer do not change between seasons and years. Accordingly, these earlier assessments of the alluvial aquifer assumed that one steady-state model can be used to represent the flow system during baseline (nonpumping) conditions and that a separate steady-state simulation manages to capture flow patterns under remediation (pumping) conditions.

Unlike the existing conceptual model, this study demonstrates that the floodplain groundwater system at the Shiprock site is dynamic, as changes in hydrologic processes affecting the floodplain cause groundwater flow patterns to vary noticeably with time. Temporal changes in groundwater conditions under nonpumping conditions are attributed primarily to increased flows in the San Juan River during snowmelt runoff months (May and June) and ET processes during the summer and early fall. Modeling groundwater flow in the alluvial aquifer as a steady-state process fails to capture the influence of temporally varying flow patterns on contaminant migration. Three different types of flow patterns generally associated with different times of the year are observed in floodplain groundwater under nonpumping conditions.

8.1.1 Winter and Spring (November–April)

Flows in the San Juan River during winter and early-spring months tend to be low and relatively stable, and transpiration of groundwater via floodplain vegetation is limited to nonexistent. As a consequence, river losses to the aquifer in river sections upstream from the USGS gaging station generate groundwater flow that mostly parallels the bedrock escarpment in the south half of the floodplain. The river losses mostly occur from river pools located upstream of three visually identified riffles on the river. Significant portions of the surface water lost to the aquifer appear to return to the river at short distances (tens to hundreds of feet) downstream from where the losses occur, creating distinct hyporheic zones in the aquifer. The remainder of the inflowing river water continues to flow northward and northwestward, much of it toward the Trench 1 area. Historically, discharge of Mancos Shale groundwater from beneath the terrace and across the bedrock escarpment (bedrock discharge) has also contributed to the northward-migrating groundwater in the south half of the floodplain, but the flows from this water source are relatively small in comparison to flows contributed by river losses.

Recharge of Bob Lee Wash outflow near the wash outlet produces groundwater mounding and wetland formation during winter and spring months. The source of the recharge is flowing artesian water discharging from well 648 on the terrace, a deep well screened in the Morrison Formation that underlies the Mancos Shale at the Shiprock site. The water mounding dominates groundwater flow in the north half of the floodplain and causes the recharged water from the wash to flow radially away from the wash outlet and mostly toward the river. Some of the recharged water flows toward the Trench 1 area where it diverts inflowing water from the south half of the floodplain toward the northeast, in the direction of wells 779 and 857, in the vicinity of the USGS gaging station.

Bedrock discharge from the terrace to the alluvial aquifer appears to occur year-round along 4500 ft of the escarpment between the south end of the floodplain and the mouth of Bob Lee Wash. As described in the existing conceptual model, bedrock discharge across the escarpment has been the primary source of the contamination currently in alluvial aquifer groundwater. It is uncertain whether this discharge persists or has greatly decreased since the SOWP (DOE 2000) was finalized. In the south half of the floodplain, the inflow of terrace water to the alluvial aquifer across the escarpment has historically caused groundwater flowpaths to gradually diverge from the escarpment alignment.

8.1.2 Early Summer (May–June)

During May and June of each year, snowmelt runoff in the San Juan Mountains causes flow in the San Juan River to increase substantially above the flows observed during preceding winter and spring months, and peak river runoff is typically recorded in late May or early June. The increased river levels cause groundwater elevations in the aquifer to increase as well. In the days leading to peak snowmelt runoff, surface water in the river seeps into the aquifer along the entire length of the floodplain, contributing relatively fresh water to the more saline groundwater system. Most of the surface water enters the aquifer as temporary bank storage, and nearly all the influent fresh water eventually returns to the river after the passage of the peak runoff period.

In addition to raising groundwater levels, high river discharges in the early summer cause groundwater flow patterns to noticeably diverge from predominant patterns in the preceding

winter and early spring. During early phases of the enhanced river loss, groundwater a few hundred feet from the river's bank tends to flow parallel to the river, with flowpaths of this kind extending thousands of feet. As surface-water elevations continue to rise prior to peak flow in the river, the river's influences on groundwater levels extend as much as 500 ft or more into the aquifer, leading to major changes in flow direction in some parts of the floodplain. These changes continue during and shortly after days of peak river flow. Portions of the floodplain aquifer that undergo particularly large changes in flow direction include an area about 600–700 ft long and a few hundred feet wide lying directly between the Trench 1 and 1089/1104 areas. There, the net effect of the elevated river's influence is to divert water and contaminant plumes from a northeastward flow direction to a more northwestward to westward flow. The hydraulic characteristics of the aquifer are such that changes in flow direction at locations more than 500 ft into the aquifer can persist for multiple weeks after passage of peak river flow.

Simultaneous to the onset of high river levels in May and June, ET processes on the floodplain begin removing groundwater from the subsurface at a more rapid rate than occurs in early spring, resulting in groundwater elevations generally lower than those that would occur if ET were not taking place. Because rising river elevations in May and June dominate groundwater elevation changes, the effects of early-summer ET are difficult to discern. Nevertheless, the reduced groundwater levels caused by ET help to increase hydraulic gradients from the river to the aquifer, thereby increasing river seepage losses and causing the altered flow patterns caused by high river levels to persist even longer.

The degree of hydraulic connection between the river and the alluvial aquifer varies along the 7300 ft long reach of river bordering the floodplain, such that the rising river's influence on groundwater elevations a few hundred feet from the river's west bank can vary greatly depending on location. In late May and early June 2011, spatially variable hydraulic connection between the river and the aquifer created a distinct reversal in respective groundwater elevations at two wells located west and south of the USGS gaging station, which in turn caused local groundwater that normally flowed to the north to begin migrating more to the southeast. This finding indicated that increased river levels in early summer months also had the potential to divert contamination at some locations in the north half of the floodplain in multiple directions.

8.1.3 Midsummer to Fall (July–October)

After passage of high-river flows in the early summer and a return to average river levels common in winter and spring months, ET processes in the floodplain can affect groundwater flow patterns. Increased ET in warm summer months near the outlet of Bob Lee Wash, in the form of bare-ground evaporation above the shallow water table plus transpiration from local vegetation, reduces net recharge of Bob Lee Wash surface water emptying onto the floodplain. As a result, groundwater levels across the floodplain can be 1–2 ft lower than comparable levels observed in winter and spring, and local decreases in groundwater elevation, such as in the groundwater mounding area at the mouth of Bob Lee Wash, can approach 3 ft or more.

Though available data regarding ET processes on the floodplain are insufficient for quantitatively describing (modeling) their influence on the groundwater system, their general effects on flow patterns can be discerned. The most apparent effect in late summer and early fall is that the river tends to lose water to the aquifer for several days at a time along portions of the 7300 ft river length adjacent to the floodplain (see Section 6.3.2). If remediation pumping occurs

in the 1089/1104 area and at the two trenches between midsummer and fall, ET processes at the time increase the length of river from which each of these systems induce seepage into the aquifer.

During periods when remediation pumping is not occurring, ET-induced flows from the river to the aquifer likely change flow patterns within hyporheic zones identified in the south half of the alluvial aquifer. As a result, flowpaths within the hyporheic zones change and mixing of contaminated water with fresh water from the river is enhanced. The existing conceptual model, which essentially represents flow conditions in winter and early spring, does not account for such phenomena.

8.2 Contaminant Movement and Distribution

8.2.1 Contaminant Migration Under Baseline (Nonpumping) Conditions

8.2.1.1 Influence of Transient Groundwater Flow

Historically, some of the highest contaminant concentrations in the north half of the floodplain were observed within a 300–600 ft wide strip of groundwater connecting the Trench 1 area to the 1089/1104 area. Though the cores of contaminant plumes extending from the bedrock escarpment to the river have been observed along this strip, relatively high contaminant concentrations have also been observed on both sides of the plume cores. In the existing model, the cause of apparent lateral spreading of contamination on the sides of the plume cores is limited to transverse dispersion induced by aquifer heterogeneity because groundwater flow is assumed to be in a steady state.

In contrast to the existing conceptual model, this study has shown that the apparent spreading of contamination in lateral directions is at least partly caused by temporally variable flow patterns in the alluvial aquifer, particularly the seasonal changes in groundwater flow direction that occur each year. Contaminant spreading between the escarpment and the river in the north half of the floodplain is more likely a form of effective, or apparent, transverse dispersion (e.g., Cirpka and Attinger 2003, Goode and Konikow 2000) created by transient flow conditions in the alluvial aquifer.

Aside from extensive plume spreading, seasonal changes in groundwater flow direction help to explain how some of the greatest contaminant concentrations historically observed in the north half of the alluvial aquifer ended up in the 1089/1104 area. In effect, the transient changes appear to produce irregular flow paths between the Trench 1 area and the river, with groundwater being subject to flow in one direction during several months of each year followed by flow in a direction largely perpendicular to the previous one in remaining months. This distinctive change in flow direction is partly revealed using particle tracking in conjunction with a transient model of flow conditions from January 2011 through August 2011 (Section 7.3.2).

Figure 61 illustrates the manner with which changing flow directions apparently led to the high concentrations observed in the 1089/1104 area. The irregular flowpath in this figure indicates that groundwater flow in winter and spring in the area between the Trench 1 and 1089/1104 areas is generally to the northeast, but flow in early summer, in response to high-river flows, turns more to the north and northwest. As suggested in Figure 61, repetition of these seasonal flow

patterns for multiple decades resulted in sulfate- and uranium-plume cores that appeared to extend directly to the north from the Trench 1 area during the years 1999–2001 (Figure 14 and Figure 15).

Some lateral spreading of contamination from plume cores reflects the fact that river flow conditions change from year to year as well as seasonally. During years when peak snowmelt runoff in the river is mild and short-lived, northeastward flow likely dominates contaminant migration. This helps to explain why relatively high contaminant concentrations have traditionally been observed at wells 779 and 857, in the vicinity of the USGS gaging station. In years of very high and extended snowmelt runoff, the tendency toward northwestward flow and contaminant migration in midsections of the plume cores is probably enhanced. As a result, the contamination periodically spreads farther to the northwest (Figure 61), producing relatively high contaminant concentrations in areas bordering the river on the north end of the floodplain (e.g., well 736). This latter phenomenon might also explain why historical contaminant concentrations in the Trench 1 and 1089/1104 areas appear to be greater than corresponding concentrations at wells located midway between the two areas (see Figure 14 and Figure 15).

In addition to the influences of temporally varying flows, relatively high contaminant concentrations in areas bordering the river on the north end of the floodplain are potentially the remnants of contamination that reached this part of the aquifer prior to the drilling of terrace well 648 in 1961 and the delivery of its artesian discharge to the floodplain. The mill and appurtenant features (e.g., tailings ponds, raffinate ponds) had been present at the site since 1954. Thus, about 7 years passed during which mill-related contamination possibly migrated to the floodplain and moved uninterrupted northwestward toward the river. Similarly, another 15 or more years passed before the flowing artesian water was diverted to Bob Lee Wash, providing additional time for mill-related contamination to migrate north and west. Subsequent recharge of Bob Lee Wash flows near the wash outlet migrated in a radial pattern toward the river, helping to flush some of the contamination that might have continued to reside in alluvium on the north end of the floodplain. It is plausible that the concentrations of sulfate and uranium observed near the floodplain's north end in 2011 (Figure 34 and Figure 35) are simply the remnants of mill-related contamination that migrated to the area between the mid-1950s and the late 1970s and was subsequently subjected to multiple decades of flushing by relatively fresh water.

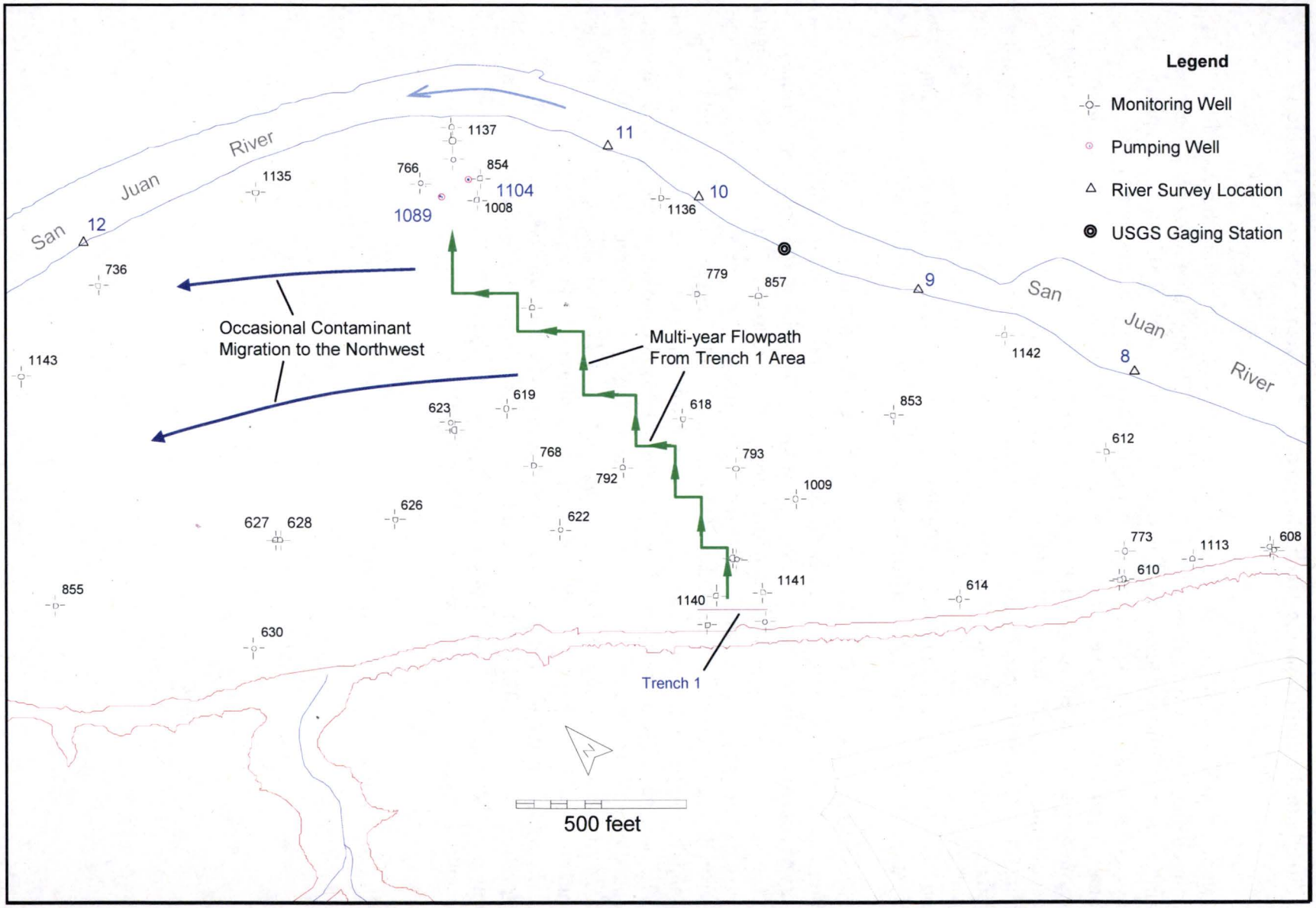

Figure 61. Flow Mechanisms for Distributing Contamination Northward and Northwestward from the Trench 1 Area

The exact causes of observed contaminant concentrations on the north end of the floodplain near the river are uncertain. Nonetheless, it does appear that sulfate and uranium levels in this part of the floodplain were at one time higher than those observed during the years 1999–2001. The previously mentioned study of floodplain hydrochemistry (Sections 6.3) in the late 1980s (DOE 1987) showed that sulfate concentrations in alluvial groundwater on the north end of the floodplain (from west to east) ranged from about 37,000 mg/L near the current location of well 856 to about 7400 mg/L near the current location of well 736 and to about 18,500 mg/L in the current 1089/1104 area. Similarly, uranium concentrations at these same locales in the late 1980s were approximately 4.3, 0.5, and 1.2 mg/L, respectively (DOE 1987). Comparison of these latter concentrations with values for sulfate and uranium during the years 1999–2001 (Figure 14 and Figure 15) suggests that groundwater originating near the Bob Lee Wash outlet has contributed greatly to the attenuation of these constituents in the vicinity of wells 856 and 736.

8.2.1.2 Additional Contributions to Plume Spreading and Variable Flow Patterns

Though transient flow conditions caused by changing river flows and pumping appear to cause much of the plume spreading occurring in the alluvial aquifer (Sections 6.2.2, 6.2.3, 7.3.2, and 8.2.1.1), two additional processes likely contribute to the spreading. One of these consists of the changing flow directions that apparently take place in the aquifer during mid-to-late summer and fall months (Sections 6.3, 6.3.2, and 7.5) because groundwater levels are frequently lower than nearby surface-water elevations in the San Juan River, causing river losses to the aquifer. Though the exact cause of the comparatively lower groundwater elevations has not been fully identified, the updated conceptual model attributes them to groundwater losses via ET. The computation of temporally variable flow directions over short intervals (e.g., 15 minutes) using three-point estimators of local magnitude and orientation of the hydraulic gradient (e.g., McKenna and Wahi 2006) would help determine whether flow directions in late summer and early fall change from those observed in other parts of the year and if the changes stem from ET.

Groundwater salinity has also contributed to plume spreading in the alluvial aquifer during earlier years at the site. With TDS concentrations exceeding 10,000 mg/L in many parts of the aquifer, density-driven advection (e.g., Zhang and Schwartz 1995) on both sides of the plumes caused them to spread laterally, much in the same manner that transverse horizontal dispersion causes spreading. It is unclear whether density-dependent groundwater flow is still a significant contributor to contaminant spreading because salinity levels in the aquifer have been greatly reduced since 2006, when Trench 1 and Trench 2 began removing contaminant mass from the subsurface.

In addition to enhancing plume spreading, the density-dependent flow driven by high aquifer salinity has probably helped to divert flows emanating from the Trench 1 area to more of a northward direction as opposed to the northeastward direction indicated by the groundwater flow modeling (see Section 7.3.1.1 and Figure 48). This is because the equivalent freshwater heads associated with the high-TDS groundwater historically observed in the Trench 1 area were distinctly higher than the freshwater head associated with recharged water near the Bob Lee Wash outlet. The resulting freshwater-head gradient between the two types of water likely pushed the higher-salinity, and more contaminated, water more to the north than northeast, in a fashion similar to that of the density-driven advection (e.g., Zhang and Schwartz 1995) mentioned in the previous paragraph. Under this conceptualization, the contaminant plume lobes

connecting the Trench 1 and 1089/1104 areas (Figures 14 and 15) would appear to be caused by a combination of seasonally variable flow directions (Section 8.2.1.1) and density-dependent effects.

8.2.1.3 Well 618 Area

The updated conceptual model allows for the possibility that year-to-year changes in flow conditions in the alluvial aquifer may have noticeably increased contaminant concentrations in a portion of the aquifer that lies about 600 ft northeast of the Trench 1 footprint. The area in question is centered on well 618, which in 2011 exhibited sulfate and uranium concentrations that were about double their measured values at this location during the years 1999–2001. Examination of the temporal history of uranium concentrations at well 618 (Figure 36) indicates that the concentration increases from their observed levels in 2011 occurred during 2002, and that the higher concentrations attained here in 2003 remained relatively constant through 2011. Because remediation pumping did not begin until spring 2003, and the pumping at the time was limited to the 1089/1104 area (the trenches began operating in 2006), any flow phenomena leading to the local concentration increases were likely created under baseline flow conditions. Changes in river flow from year to year or between multiyear periods provide possible explanations for the high concentrations observed at well 618 between 2003 and 2011. It should be noted that sulfate and uranium concentrations at well 618 began decreasing in 2013, apparently in response to continued remediation pumping. However the uranium concentration at well 618 as of March 2014 (DOE 2014b) remained above the UMTRA maximum concentration limit (MCL) of 0.044 mg/L.

Phenomena contributing to the high contaminant concentrations in the well 618 area between 2003 and 2011 remain uncertain. However, examination of sampling records strongly suggests that the increase in uranium concentrations observed here in 2002 is an artifact of a change in water sampling procedures during that year, from a high-flow, well-purging method to a low-flow sampling method. This finding is supported by a recent investigation of variations in constituent concentrations with depth in Shiprock-site wells (DOE 2014a, 2015b). The variation study revealed that specific conductance concentrations during 2012 in the well-618 casing increased steadily from about 9000 µS/cm at the top of the well screen to about 18,000 µS/cm near the bottom of the well, supporting the hypothesis that high salinity in alluvial-aquifer wells has led to density-dependent flow in the aquifer (Section 4.5.2) and sinking of the more dense water to the bottom of the aquifer. In addition, the uranium concentrations in the well casing increased steadily from about 0.5 mg/L at the top of the well screen to about 1.9 mg/L near the well bottom (DOE 2014a, 2015b). The combination of steadily increasing specific conductances and uranium concentrations with depth in the well casing with the higher uranium concentration measured at well 618 during semiannual monitoring events since 2002 (Section 6.4.1) suggests that the samples collected using low-flow techniques are representative of water from deeper parts of the well, whereas samples collected in earlier years using high-flow methods were representative of mixed water from multiple depths in the well.

8.2.2 Effects of Remediation Pumping

Under the existing conceptual model, the floodplain remediation system has been viewed as effective in intercepting contamination emanating from the bedrock escarpment area as well as reducing contaminant concentrations and total contaminant mass in the alluvial aquifer. These

findings were made during the preliminary Trench 1 evaluation (ESL 2011b) and became apparent from numerous annual performance reports prepared for the site (DOE 2007, 2008, 2009a, 2010, 2012, 2013, 2014b). Information presented in this updated assessment of the floodplain, including the results of groundwater flow modeling representative of pumping conditions, demonstrates why the remediation system has been effective in removing contamination from the alluvial aquifer.

This study uses aerial views of contaminant distribution at two separate times to help assess the progress of remediation pumping in removing contaminant mass. Large-scale maps (1 inch = 500 ft) containing color-flood plots of sulfate, uranium, and nitrate concentrations in the alluvial aquifer around the turn of the century (1999–2001) and again in 2011 clearly reflect large reductions of total contaminant mass in the respective plumes.

8.2.2.1 Trench 1 and Trench 2

As concluded in the Trench 2 evaluation (DOE 2009b) and assumed in the existing conceptual model, groundwater extraction using the horizontal well in Trench 2 has been successful in preventing that contamination from discharging to nearby reaches of the San Juan River. The trench has the capacity to capture virtually all discharge of contaminated terrace groundwater across the escarpment to the alluvial aquifer in the southernmost quarter of the floodplain. As illustrated in the 2011 color-flood plot for sulfate (Figure 34), the pumping at Trench 2 has induced a large amount of surface-water seepage from the river into the aquifer and, as a result, created a large zone of fresh water between the trench and the river. The color-flood map of sulfate concentrations during late March 2011 (Figure 34) shows that three monitoring wells on the river side of the trench, after pumping at the trench had been shut off for a period of more than a month, ranged from 154 to 342 mg/L, whereas concentrations at the time at two wells on the escarpment side of the trench were 6910 and 10,000 mg/L. These values are all lower than sulfate concentrations measured during 1999–2001 in what is now the Trench 2 area, which ranged from about 12,250 to 15,500 mg/L (Figure 14).

Measured uranium levels during 2011 (Figure 35) illustrate how remediation pumping from Trench 2 impacted this contaminant's distribution in the southern third of the floodplain in a manner similar to that for sulfate. Uranium concentrations in 2011 at the three monitoring wells on the river side of the trench ranged from 0.01 to 0.022 mg/L, which were much lower than concentrations of 1.1 and 1.49 mg/L at the two wells on the escarpment side of the trench at the time. Uranium concentrations in the vicinity of the Trench 2 footprint during the years 1999–2001 ranged from 1.23 to 1.98 mg/L (Figure 15).

Pumping from Trench 1 has been particularly effective at reducing contaminant concentrations and total contaminant mass in the alluvial aquifer because the flowpaths it creates sweeps a large part of the alluvial aquifer, preventing northward migration of a large portion of contaminated plumes connecting the Trench 1 and1089/1104 areas. Similar to Trench 2, Trench 1 has the capacity to intercept any discharge of contaminated groundwater from the terrace across thousands of feet of escarpment located both south and north of the trench. These findings are supported by flowpaths generated using the calibrated model developed for this study and by the color-flood plots of contaminant concentrations in the aquifer in 2011, as compared to plots reflective of conditions during the years 1999–2001. The largest decreases in contaminant concentration between these two times that are at least partly attributable to pumping at Trench 1

are observed in locales lying midway between the Trench 1 footprint and the 1089/1104 area, along what used to be the core of a contaminant plume lobe that connected the two areas. Whereas sulfate concentrations in this area during 1999–2001 appeared to fall in a range of 10,000 to 15,000 mg/L (see color-flood plot in Figure 14), concentrations in the area in 2011 (Figure 34) were predominantly on the order of 4000 to 8000 mg/L. Similarly, uranium concentrations in this area that ranged from 1 to 2.5 mg/L during 1999–2001 (Figure 15) were observed in 2011 to vary between 0.2 and 0.8 mg/L (Figure 35).

Strictly from the perspective of groundwater flow, pumping at Trench 1 appears to have a larger beneficial impact on the alluvial aquifer than does Trench 2 pumping or groundwater extraction at wells 1089 and 1104. The area of the capture zone created by pumping at Trench 1 appears to be more than double the size of the capture zone generated by groundwater extraction at Trench 2 and approximately 1.75 times the capture zone created by 1089/1104 pumping (see Figure 58 and Figure 60). In the model developed for this study, groundwater extraction from Trench 1 induces river inflow about 1600 ft to the southeast of the trench footprint, and from the outlet of Bob Lee Wash, which is about 1000 ft northwest of the footprint. In comparison, the capture zone created by Trench 2 pumping extends about 1200 ft to the south of the trench footprint and 300 ft to the north of it. A model run representative of groundwater flow conditions in March 2010 (Figure 58) indicates that pumping at Trench 1 intercepts contaminated water flowing into the alluvial aquifer as bedrock discharge across 2800 ft of escarpment, whereas the model shows Trench 2 and the pumping from wells 1089 and 1104 intercepting discharge from about 1400 and 200 ft of escarpment, respectively. These observations comport with estimates presented in the existing conceptual model derived without the benefit of model simulation. The apparent advantages provided by groundwater extraction at one of the pumping centers versus extraction at other locations within the remediation system highlight the importance of using flow models to help design and operate groundwater pump-and-treat systems.

8.2.2.2 Effects of Simultaneous Pumping in the Trench 1 and 1089/1104 Areas

Simulations conducted with the calibrated groundwater flow model developed for this updated assessment show that simultaneous pumping from the Trench 1 and 1089/1104 areas creates a groundwater divide between the two pumping centers (Figure 58 and Figure 60). As demonstrated by the modeling, the position and shape of the divide varies depending on the time of year that pumping is occurring and the type of river–aquifer exchange that is taking place at the time. The groundwater divide created in late summer and fall months follows a multiangle path that extends from the mouth of Bob Lee Wash to near the USGS gaging station on the river. Flowpath analyses conducted for the preliminary Trench 1 evaluation (ESL 2011b) showed the presence of a similar groundwater divide for pumping conditions in the alluvial aquifer in September 2010 (Figure 60).

Because the existing conceptual model effectively assumed that the groundwater flow patterns created by remediation pumping are those of a steady-state system, it did not take into consideration how the groundwater divide might take on different shapes and lengths depending on the season. This study suggests that the modeling described in the SOWP (DOE 2000) was developed for conditions typically seen during winter and spring months, when a lack of ET from the alluvial aquifer allows Bob Lee Wash recharge to create a flow-dominating groundwater mound at the mouth of the wash.

Flow modeling in this study reflective of winter and early spring conditions also predicted that the simultaneous pumping from the Trench 1 and 1089/1104 areas in combination with flow in a large hyporheic zone southwest of the USGS gaging station would create a stagnation zone in the aquifer about 400 ft northeast of Trench 1 and 200 ft southwest of well 618. Though evidence of such a zone was not investigated in the preliminary Trench 1 evaluation (ESL 2011b), its presence had been surmised in the existing conceptual model. The stagnation zone is considered an important feature of the flow system during winter and early spring months, as it signifies slow movement of groundwater within and near the zone. As a consequence, contaminants occurring locally in the aquifer at relatively high levels, such as at well 618, may be less susceptible to flushing by fresh water flowing into this area in response to remediation pumping.

Another phenomenon associated with the formation of a stagnation zone is the creation of a 300–600 ft wide swath of contaminated aquifer that escapes capture by pumping in the Trench 1 and 1089/1104 areas during winter and early spring (Figure 58). Well 618 lies in the south-central portion of the uncaptured swath of aquifer, and the contaminated water in it migrates toward a section of the river between the USGS gaging station and the 1089/1104 area.

8.2.2.3 1089/1104 Area

Pumping from wells 1089 and 1104 is very effective at reducing contaminant concentrations and total contaminant mass in the alluvial aquifer near the San Juan River. The color-flood plots of sulfate and uranium concentrations in 2011 (Figure 34 and Figure 35, respectively) in the 1089/1104 area reveal that local levels of these contaminants have decreased by as much as two-thirds from values observed 11 to 12 years earlier (Figure 14 and Figure 15). Pumping from the two wells also appears to prevent local contamination from discharging to the river. Measurement of water levels in a series of three wells (1137, 1138, 1139) lying between the pumping wells (1089 and 1104) and the river at six separate times indicated that pumping in the area induces inflow from the river. It was uncertain in the existing conceptual model whether the pumping rates achieved in wells 1089 and 1104 were sufficiently high to exceed a critical rate needed to induce flow from the river. The hydraulic head data examined in this study remove that uncertainty.

8.3 Aquifer Parameters

Calibration of the numerical model used to simulate floodplain-wide groundwater flow at the site indicates that a uniform hydraulic conductivity of 80 ft/day performs well in representing general flow processes in the alluvial aquifer. This value is of the same general magnitude as the conductivities derived from calibration of other models of floodplain groundwater, which ranged from 35 ft/day (DOE 1995a) to 85 ft/day (DOE 2009b) and 100 ft/day (DOE 2000).

Model calibration steps taken in this study using a transient version of the flow model indicated that a specific yield of 0.25 can be used uniformly throughout the alluvial aquifer domain to simulate general flow behavior. This value implies that the alluvial aquifer responds to pumping stresses over periods of several days as if it were an unconfined aquifer with a porosity of 25 percent. It was assumed in the existing conceptual model that the alluvial aquifer comprises an unconfined system, but quantitative evidence of such a response was unavailable prior to the transient model calibration conducted under this updated assessment.

The calibrated model for the floodplain system underpredicts pumping-induced drawdowns at some monitoring wells in the 1089/1104 and Trench 1 areas. This suggests that local hydraulic conductivities in these areas are less than 80 ft/day. Given that an aquifer test conducted in floodplain well 858 (~1200 ft southeast of Trench 1) in support of the SOWP (DOE 2000) indicated that the hydraulic conductivity of alluvium in the vicinity of the well is 110 ft/day, it is also likely that hydraulic conductivities greater than 80 ft/day are applicable to some portions of the aquifer. These observations suggest that future model simulations of groundwater flow in the alluvial aquifer would benefit from treating the aquifer as a heterogeneous medium and from using objective, automated calibration techniques (e.g., Doherty et al. 2010; Doherty and Hunt 2010) to discern the spatial distribution of hydraulic conductivity in the floodplain subsurface.

8.4 Water Budgets

8.4.1 Flow Rates Under Baseline (Nonpumping) Conditions

Flow rates and aquifer water budgets under preremediation conditions in the updated conceptual model can be compared with corresponding values in the SOWP model (DOE 2000). However, detailed comparisons with the water budget produced by the Knight Piesold (2002) model are not possible because most budget components were not provided in either the Knight Piesold report or the GCAP (DOE 2002). It is known that the Knight Piesold model assumed that recharge from Bob Lee Wash flows was 64 gpm, the same value used in the SOWP model, and that recharge from infiltration of precipitation on the floodplain was about 1.1gpm.

Under hydrologic conditions typically seen in winter and spring months (i.e., low, stable river flows and high, net recharge at the mouth of Bob Lee Wash), the groundwater flow model in this study indicates that about 60 gpm is circulating through the floodplain groundwater system. This value, which is about 60 percent of the total system throughflow identified in the SOWP model, results mostly from the fact that the recharge rate from Bob Lee Wash outflow is limited to about 45 gpm in the current model as compared to 64 gpm in the SOWP model (DOE 2000). Aerial recharge from infiltration of precipitation on the floodplain is assumed in this study to be an insignificant component of the alluvial aquifer's annual water budget partly because the final model used in the GCAP (DOE 2002) was limited to a very small value (1.1 gpm, Knight Piesold 2002). The SOWP model assigned a value of 13.5 gpm to this budget component.

The rate of bedrock discharge adopted in the model for this study (~5.6 gpm) is also of interest because it is less than 30 percent of the bedrock inflow rate used in the calibrated model developed for the SOWP (18.7 gpm, DOE 2000). Though the value for discharge of bedrock water across the escarpment in the Knight Piesold (2002) model is not available, it was assumed in this study that it was considerably less than the value derived in the SOWP because the value used for hydraulic conductivity of the weathered Mancos Shale in the later model was an order of magnitude lower than the conductivity in the earlier model, and the value used for unweathered shale was almost 2 orders of magnitude lower. The GCAP (DOE) reported that the discharge of terrace groundwater across the escarpment between the south end of the floodplain and about 500 ft south of Bob Lee Wash ranged between 3 and 5 gpm, values that are less than a third of the bedrock inflow in the SOWP model (DOE 2000).

The steady-state flow model in the SOWP (DOE 2000) indicated that the total recharge rate for the floodplain alluvial aquifer from river losses was 18.7 gpm, or about 16 percent of the total inflow to the aquifer. The comparable value in this study, estimated for conditions during winter and early spring months, is about 11 gpm, or approximately 18 percent of total aquifer inflow. No information is available regarding river losses in the Knight Piesold (2002) model.

A representative water budget for groundwater flow under baseline conditions during summer and fall was not developed in this study. Should sufficient information become available to model groundwater flow processes during these times of the year, the resulting water budget would probably show ET as comprising a large percentage of total system outflow. It would be useful to develop defensible estimates of the ET rates and volumes during summer and fall months and to help identify areas on the floodplain where ET is dominant, as the groundwater losses attributed to this process appear to induce seepage inflows from the river that not only impact groundwater flow directions but can influence aqueous chemistry, too. Whereas the updated conceptual model recognizes that ET processes strongly affect flow rates in the alluvial aquifer during summer and fall months, neither the SOWP (DOE 2000) model nor the Knight Piesold (DOE 2002) model directly accounts for the influences of ET.

8.4.2 Remediation Pumping Impacts

Groundwater extraction in the three pumping centers on the floodplain impacts the alluvial aquifer's water budget by increasing seepage losses from the river. Most of the water captured by the Trench 2 system comes from the river, and the pumping rates at this trench mostly vary between 10 and 20 gpm. In winter and early-spring months, pumping in the 1089/1104 and Trench 1 areas captures a large portion (~40 percent) of the recharge attributed to infiltration of Bob Lee Wash flow. As with Trench 2, a large portion of the water collected in Trench 1 comes from induced flow from the river, and the length of river contributing to the capture zone created by Trench 1 pumping varies between seasons. Because the flow modeling conducted for the SOWP (DOE 2000) and the GCAP (Knight Piesold 2002) did not account for pumping from Trench 1, Trench 2, or wells 1089 and 1104, the existing conceptual model did not contain quantitative estimates of the flows and water budget components associated with remediation pumping.

8.5 Inflow of Contaminated Terrace Groundwater

Prior to this study, all high constituent concentrations in floodplain alluvium have been attributed to contamination derived from former mill processes, and the discharge of high-salinity terrace groundwater in Mancos Shale across the escarpment to the floodplain has been considered a primary delivery mechanism. In models prepared for the SOWP (DOE 2000) and by Knight Piesold (2002), the assumed origin of the contaminated water in the transport simulations was spatially limited to an area approximating the footprint of the disposal cell. The updated conceptual model allows for the possibility that physical and chemical processes in the shale influence constituent concentrations in floodplain alluvial groundwater.

This investigation takes into account collective findings in the SOWP (DOE 2000) and the natural contamination report (ESL 2011a) to conclude that some contamination in alluvial-aquifer groundwater could be caused by the leaching of Mancos Shale beneath the terrace. With this possibility, the updated conceptual model assumes that contamination in floodplain

groundwater could have resulted from one or more of the following processes in the shale: (1) conservative (nonreactive) transport of mill-related constituents from the terrace to the floodplain; (2) discharge of naturally occurring contamination from the terrace to floodplain groundwater; and (3) reactive transport of mill-related constituents whose concentrations are modified while in the shale.

If inflow of naturally contaminated groundwater to the floodplain groundwater system takes place, it most likely occurs along portions of the escarpment between the Bob Lee Wash outlet and the San Juan River near Highway 491. Seepage of artesian water from terrace well 648 in a tributary to Bob Lee Wash represents a potential source of groundwater that flows to floodplain alluvium northwest of the wash outlet. Principles of groundwater flow suggest that any contaminated terrace groundwater that historically migrated northwestward from the former mill area likely discharged to the wash, which incises the terrace multiple tens of feet, rather than discharging to floodplain alluvium north of the wash.

The numerical flow and transport models developed for the SOWP (DOE 2000) and by Knight Piesold (2002) predicted that remediation processes on the terrace would eventually reduce contaminant discharge from the terrace to the floodplain such that remediation of the alluvial aquifer could succeed. Evidence that this discharge has decreased since the commencement of remediation in 2003 is not apparent. Groundwater-elevation data at terrace bedrock wells and floodplain alluvial wells close to the Mancos Shale escarpment do little to identify and quantify groundwater flow from the terrace to the floodplain. However, an ESL (2012) investigation of water chemistry at terrace wells near the disposal cell in conjunction with the chemistry of alluvial-aquifer wells at the foot of the escarpment does suggest that terrace groundwater contaminated by mill processes has been flowing to the floodplain in recent years. Rebound of specific conductance in near-escarpment wells in the vicinity of Trench 1 indicate that ongoing flow from the terrace to the floodplain is possible, but temporal histories of specific conductance at the near-escarpment wells do not confirm that the flow is still occurring.

The histories of sulfate and uranium concentrations and salinity (as indicated by specific conductance) in 10 alluvial-aquifer wells at the foot of the escarpment indicate that remediation pumping from Trench 1 and Trench 2 since spring 2006 has been successful in reducing contaminant concentrations at the base of the escarpment, but the data neither confirm nor refute the possibility that the flow of terrace groundwater to the floodplain across the escarpment is decreasing with time. The various types of data that can be used as evidence that continued discharge of contaminated terrace water to the alluvial aquifer is feasible are insufficient for accurately quantifying the discharges if they are present. Volumetric flows of contaminated terrace groundwater to the floodplain remain uncertain, and readily available technologies for estimating the magnitude of the flows appear incapable of greatly reducing the uncertainty. Prediction of when successful remediation of the floodplain alluvial aquifer will be achieved remains a challenge.

9.0 Predictive Simulations

A limited number of predictive simulations were conducted with the calibrated model of groundwater flow in the alluvial aquifer. Findings from these simulations can be used to make specific recommendations regarding future management of the alluvial aquifer and the floodplain remediation system.

9.1 Elimination of Bob Lee Wash Recharge

9.1.1 Baseline (Nonpumping) Conditions

The influence of recharge from Bob Lee Wash on contaminant migration has been a topic of discussion in previous years because of concerns that artesian water discharging from terrace well 648 might be terminated in future years. These concerns were addressed by conducting steady-state flow simulations with the calibrated model under the assumption that Bob Lee Wash recharge would be eliminated in the next few years.

An initial simulation examined flow patterns in the aquifer assuming that pumping would not occur after flows from well 648 were stopped. When the steady-state model that was calibrated from groundwater levels measured during the March 2011 sampling (Section 7.3.1) is used for the simulation, the resulting groundwater levels and flowpaths (Figure 62) depict a system dominated by flow parallel to the bedrock escarpment. Because flow is no longer diverted toward the river in the vicinity of the USGS gaging station and the 1089/1104 area, this flow system would be expected to push contamination between the Trench 1 and 1089/1104 areas in a northwestward direction, where it would eventually discharge to the river on the floodplain's north end. Elimination of recharge from the wash would also make it possible for an additional small hyporheic zone to develop in the vicinity of Riffle 5 (Figure 62), about 800 ft upriver from the 1089/1104 area.

Assuming that contamination remaining in and immediately south of the 1089/1104 area eventually was flushed from the aquifer while bedrock discharge continued to feed contaminated water to the alluvial aquifer, contaminant plumes beneath the floodplain would ultimately be confined to a band of aquifer material that hugs the escarpment. The width of these long-term, legacy plumes would be expected to increase along each plume's length. Nevertheless, a large portion of the floodplain groundwater system would remain unimpacted by the contamination, since the water feeding it would originate as river losses along the south half of the floodplain (Figure 62).

The water budget for the steady-state simulation that omits recharge from the flow of well 648 at the mouth of Bob Lee Wash is of interest because it is expected to come close to representing inflow and outflow rates for the alluvial aquifer as it naturally occurred during winter months when human activity had little impact on the aquifer. The resulting budget, shown in Table 9, suggests that the quantity of water migrating through the floodplain subsurface during winter months prior to the 1950s (~19 gpm) was small in comparison to the total groundwater flow rate in winter under baseline flow conditions today (~62 gpm, Table 7). Moreover, the budget suggests that river losses to the aquifer constitute about 70 percent of the aquifer inflow, as the model represented by groundwater levels and flowpaths shown in Figure 62 assume no recharge from precipitation on the floodplain.

The rate of bedrock inflow across the escarpment adopted in the model is identical to that invoked in the March 2011 steady-state model (~5.5 gpm, Section 7.3.1). Though this assumed inflow rate is probably greater than that which would have existed in years before human development affected the terrace, no data exist with which to test this possibility. This latter observation highlights the fact that the recharge on the terrace, whether from precipitation, anthropogenic water uses (e.g., irrigation, septic discharge), seepage losses in Bob Lee Wash, or all of the above, is an uncertain water budget component in the hydrogeologic conceptual model for the Shiprock site as a whole.

Table 9. Computed Water Budget in the Model That Omits Bob Lee Wash Recharge

Flow Component	(ft^3/day)	(gpm)	(%)
Inflow			
Seepage losses from the river	2,560	13.3	70.5
Bedrock discharge	1,070	5.6	29.5
Outflow			
Discharge to the river	3,630	18.9	100

Because ET losses from floodplain groundwater are poorly understood and have never been quantified, the budget presented in Table 9 is not representative of the alluvial aquifer during periods of low-river flow in late summer and early fall months. However, ET may have never been an important form of groundwater discharge from the alluvial aquifer prior to the 1950s, as vegetation was relatively scarce on the floodplain before human sources of water began affecting the terrace area and perhaps parts of the floodplain. Moreover, because large overbank flows from the river frequently scoured the floodplain before the Navajo Dam was constructed in 1963, removing local vegetation in the process (Section 3.1), ET outflow attributed to plants and trees growing on the floodplain was probably minimal.

9.1.2 Remediation (Pumping) Conditions

In a second simulation of steady-state flow unaffected by Bob Lee Wash recharge, the impacts of remediation pumping on the groundwater system were examined. This model run was performed by incorporating the steady pumping rates employed in the model of flow during March 2010 (Section 7.4) in the calibrated model for March 2011 conditions (Section 7.3.1). Though the potentiometric surface and flowpaths predicted by this model run (Figure 63) indicate that Trench 1 will continue to capture groundwater inflowing from the San Juan River upstream of the USGS gaging station, the trench's ability to capture groundwater from the direction of Bob Lee Wash is severely hampered. In fact, the flowpaths from this simulation suggest that contamination as little as 500 ft northwest of the trench would escape capture and would instead migrate toward the river. Unless a new pumping well or trench was installed closer to the mouth of Bob Lee Wash, this latter result suggests that contaminated water between Trench 1 and the 1089/1104 area would eventually impact a large section of the floodplain's north half.

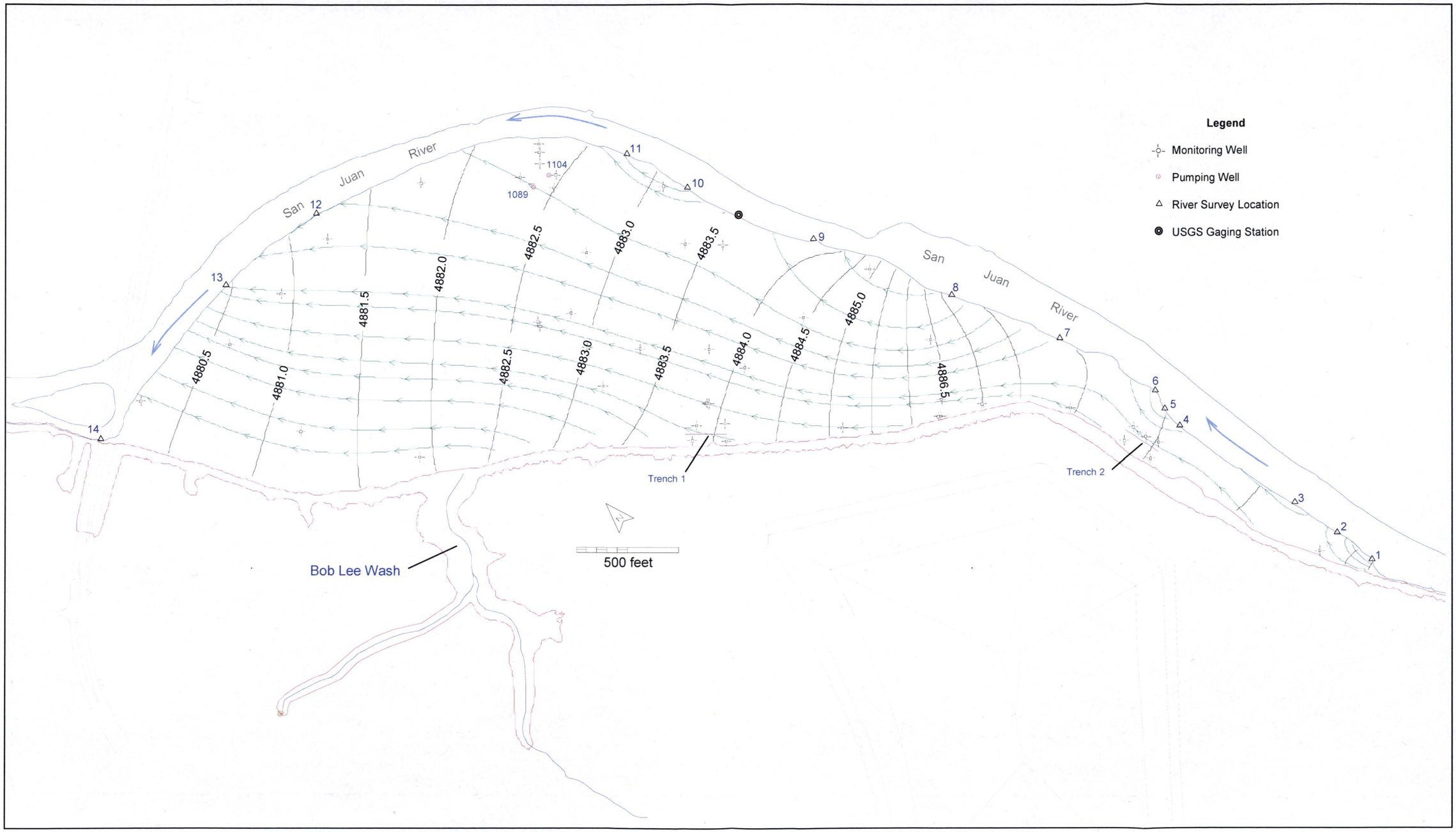

Figure 62. Computed Groundwater Elevations (ft amsl) and Flowpaths when Bob Lee Wash Recharge Is Eliminated

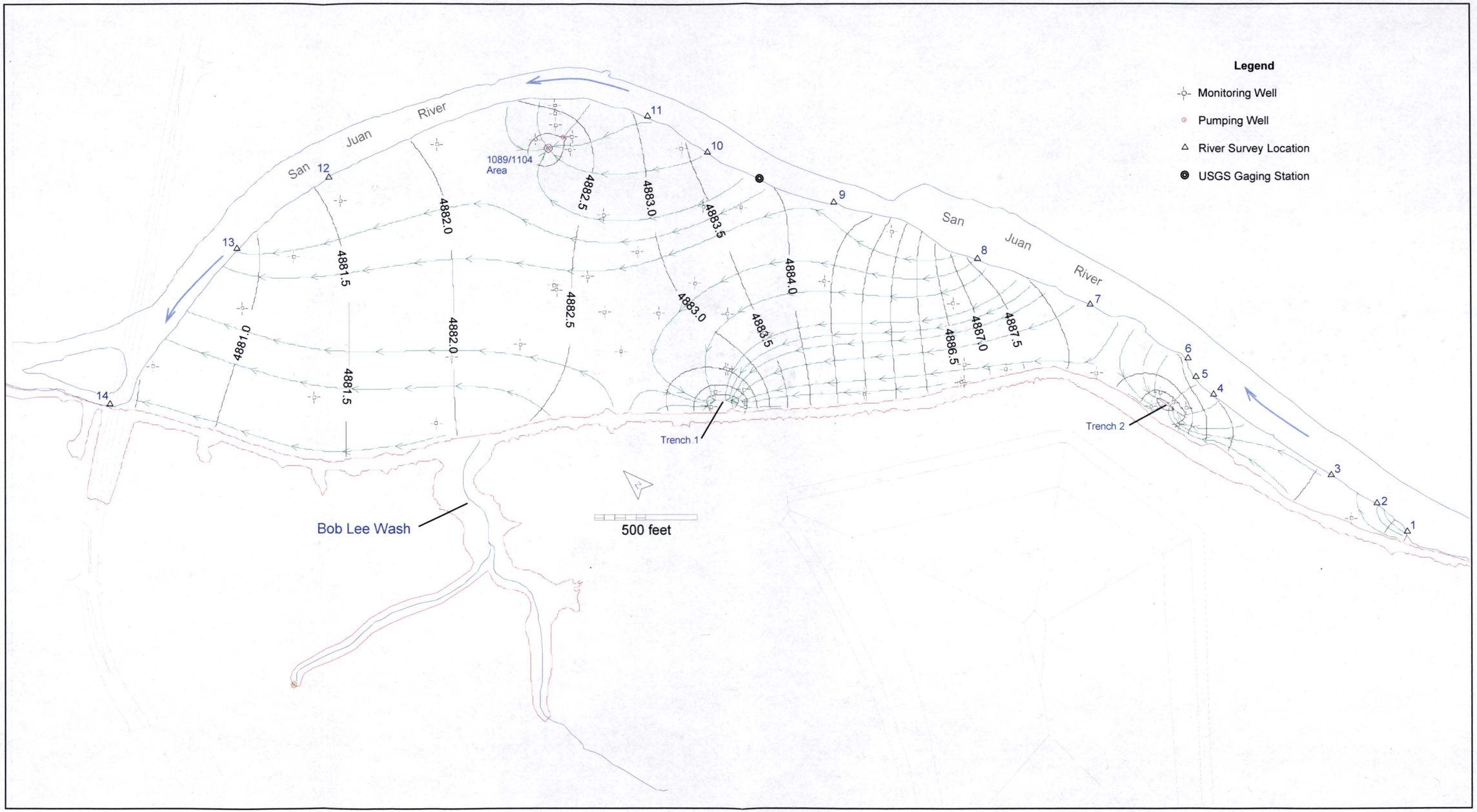

Figure 63. Computed Groundwater Elevations (ft amsl) Assuming No Bob Lee Wash Recharge and Full Remediation Pumping

9.2 Additional Pumping Locations

Two steady-state flow simulations were performed to determine whether groundwater cleanup would benefit from the addition of new pumping locations within and near the well-618 area. The motivation for installing new pumping components stems from the fact that contamination in this part of the aquifer currently escapes capture by the existing remediation system (Figure 58) during winter and early spring. Both simulations were conducted using the model developed to assess groundwater flow in response to pumping during the March 2010 sampling event (Section 7.4), at a time when recharge from Bob Lee Wash outflow was present. The average pumping rates at the time from well 1089, well 1104, and Trench 1 were 6.53, 1.44, and 10.45 gpm, respectively. Average flow in the San Juan River during the semiannual monitoring event was 943 cfs, and the river gage elevation (4883.95 ft amsl) was slightly above the gage elevation linked to the low-flow survey (4883.89 ft amsl).

The first simulation assumed that a 200-foot-long horizontal well similar to the water extraction systems in Trenches 1 and 2 would be installed about 150 ft of northeast of well 618, or approximately 700 ft northeast of Trench 1. The constant pumping rate assigned to the new trench was 10.45 gpm, the same pumping rate ascribed to Trench 1 in the March 2010 model. Groundwater elevations and flowpaths produced by this simulation (Figure 64) indicate that the proposed trench would be very successful in removing residual contaminant mass between well 618 and the USGS gaging station (Figure 34 and Figure 35). Furthermore, the new trench would induce additional inflow from the river in the vicinity of the gaging station (rather than allowing discharge to the river), thereby creating a large zone of fresh water in areas that have tended to remain contaminated over the past 10 years.

Given the apparent advantages provided by the installation of a new trench northeast of well 618, a less expensive alternative that would generally accrue the same benefits provided by the trench was considered. In particular, a steady-state simulation was performed to examine flow in response to two new extraction wells, each pumping 4 gpm, in the area between wells 618 and 779. The results of this latter model (Figure 65) suggest that accelerated cleanup of residual contamination in the vicinity of wells 618, 779, and 857 can also be accomplished with a smaller combined pumping rate from two wells, compared to that which might be achieved with a single trench. Installation of two vertical wells presents an attractive alternative to construction of a trench system not only because the costs are less but also because it provides much more flexibility with regard to possible pumping locations. Both alternatives would require the installation of additional piping to convey the additional pumped water to the evaporation pond (Figure 2).

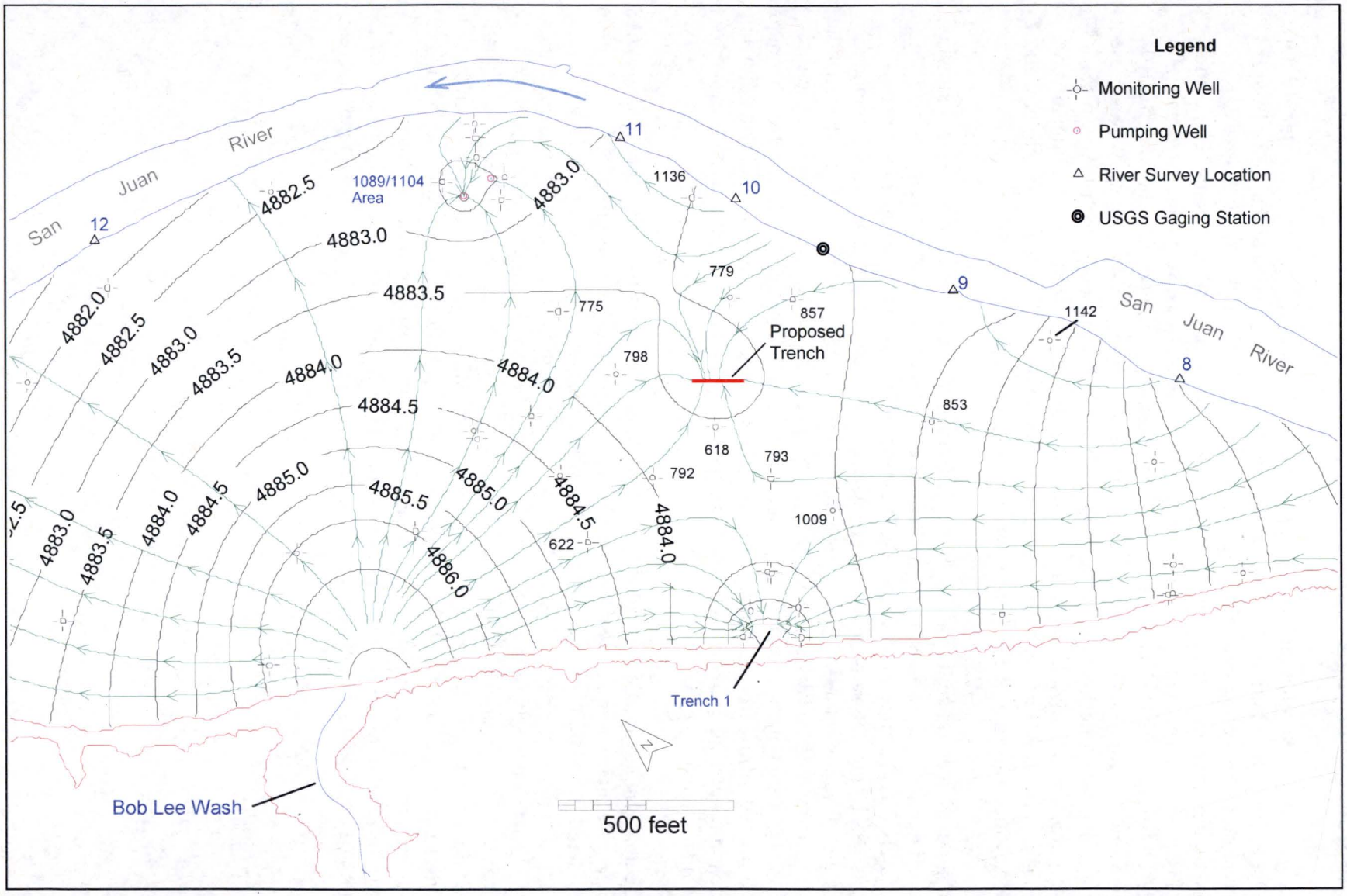

Figure 64. Computed Groundwater Elevations (ft amsl) and Flowpaths in Response to Pumping from a New Trench

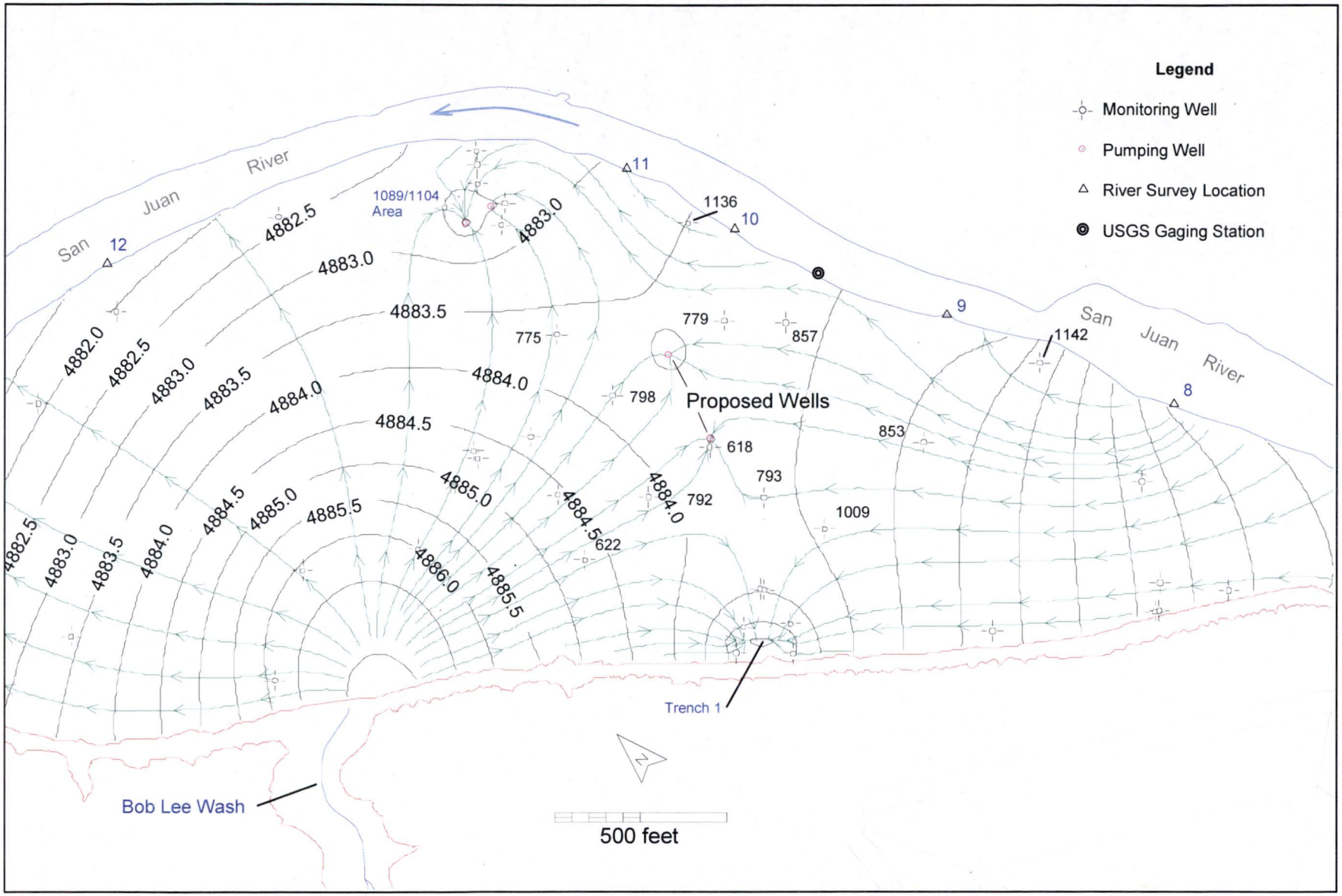

Figure 65. Computed Groundwater Elevations (ft amsl) and Flowpaths in Response to Pumping from Two New Wells

This page intentionally left blank

10.0 Summary and Conclusions

This study used numerous information sources to develop an updated assessment of groundwater flow processes in the floodplain alluvial aquifer at the Shiprock, New Mexico, site. Site information examined during the study included several DOE reports dating back to the mid-1980s and groundwater-level and water-chemistry data from more than 50 wells installed in the aquifer.

Special attention was given in this study to understanding interactions between alluvial aquifer groundwater and a 7300 ft long reach of the San Juan River that abuts the floodplain at the Shiprock site. This effort resulted in the identification of specific river sections adjacent to the south half of the floodplain that typically lose surface water to the aquifer under baseline (nonpumping) conditions as well as sections that commonly gain in flow due to groundwater discharges. The study showed that some of the river seepage returns to the river within relatively short distances (e.g., tens of feet to 400 feet) from where the river losses take place, creating hyporheic zones. This report also describes river–aquifer interactions under remediation (groundwater pumping) conditions, changes in aquifer flow patterns brought on by high-river flows in early summer due to snowmelt runoff, and potential resulting impacts on contaminant plumes.

A numerical model of groundwater flow was developed for the entire floodplain area. In addition to providing defensible estimates of various components of inflow and outflow to the alluvial aquifer, the model was helpful in identifying changes in flow patterns in response to seasonal changes in river flows. Modeling also facilitated more precise delineation of capture zones created by pumping from two vertical remediation wells (wells 1089 and 1104) and two horizontal wells (Trenches 1 and 2). The results from both steady-state and transient model simulations were combined with observations made regarding historical and recent contaminant plume configurations to develop an updated conceptual model of the floodplain groundwater system. With a few important exceptions, such as findings made regarding transient flow phenomena in the alluvial aquifer, the updated conceptual model was similar to an existing conceptual model. Enhancements of the existing conceptual model derived from this updated assessment of floodplain groundwater flow can be used to better manage remediation of the alluvial aquifer.

Multiple recharge and discharge processes influence flow directions and magnitudes in floodplain groundwater. Though some uncertainty is associated with each of the processes, the uncertainty of recharge from the inflow of terrace groundwater via the Mancos Shale bedrock is perhaps the most significant because it determines whether remediation pumping at the site will ultimately achieve full cleanup of the alluvial aquifer. Discharge of terrace groundwater in Mancos Shale to the floodplain appears to have been the greatest source of contamination in the alluvial aquifer stemming from activities at the former uranium mill site. With the use of both hydraulic and water-chemistry information, attempts were made to identify the ongoing inflow of terrace groundwater to the aquifer across the escarpment. Available information indicates that continued discharge of bedrock contamination is possible, but the data are insufficient for accurately quantifying the contaminant discharge.

Conclusions drawn from this study include:

- Groundwater flow processes in the floodplain alluvial aquifer are dynamic, with significant changes in groundwater flow patterns occurring between seasons and years.
- Seasonal variations in groundwater flow patterns are attributed primarily to changes in river surface elevations between seasons and to groundwater outflows in the summer via ET processes.
- Under baseline conditions, river flows during winter and early-spring months are generally low, and mounding due to recharge at the mouth of Bob Lee Wash dominates groundwater flow in the north half of the aquifer. Radial flow originating at the wash's outlet causes most of the recharged water to migrate northwestward to northward; remaining recharged water flows eastward and southeastward and diverts groundwater in the Trench 1 area northeastward toward the USGS gaging station on the river.
- High-river flows in early summer associated with seasonal snowmelt runoff contribute surface water to the floodplain groundwater system along the entire length of the floodplain in the form of bank storage; changing groundwater flow patterns during this period produce northwestward flow in contaminated areas located between the Trench 1 and 1089/1104 areas and, as a consequence, temporarily divert contamination to the northwest.
- Evapotranspiration from mid-summer to early fall, some of which occurs as bare-ground evaporation where the water table is shallow near the mouth of Bob Lee Wash, produces floodplain groundwater elevations that are typically 1–2 ft lower than elevations in the spring, despite the fact that river elevations during these two seasons are generally about the same.
- Floodplainwide reductions in groundwater elevation during summer and fall months are probably caused by ET losses, which may induce aquifer inflows from the river in the south half of the floodplain.
- ET-induced inflows from the river during summer and fall likely alter groundwater flow directions, leading to convoluted flowpaths and enhanced mixing of contaminated water in the aquifer with fresh water from the river.
- Seasonal changes in groundwater flow patterns and other temporally variable flow processes lead to contaminant spreading around the cores of plumes linking the Trench 1 and 1089/1104 areas. Before groundwater remediation pumping began in spring 2003, resulting spatial distributions of contaminants were reflective of plumes affected by effective, or apparent, transverse dispersion induced by transient flows.
- Density-dependent flow in areas of high groundwater salinity (density-driven advection on both sides of the plumes) and changes in flow direction in response to decreased water levels in the aquifer during late-summer and fall contribute to spreading of the contaminant plumes.
- Pumping from the horizontal well in Trench 1 removes significant quantities of contamination from the alluvial aquifer and successfully intercepts plume contamination originating as bedrock discharge of groundwater across 2800 ft of the Mancos Shale escarpment. The trench pumping prevents northwestward and northward contaminant migration from the Trench 1 area and a large portion of the escarpment toward the river.

- Strictly from the perspective of groundwater flow, pumping at Trench 1 has a greater beneficial impact on the alluvial aquifer than does pumping at either Trench 2 or the 1089/1104 well combination.
- Combined pumping from vertical wells 1089 and 1104 prevents contaminated water in the 1089/1104 area from discharging to a nearby reach of the river.
- Historical pumping from all components of the floodplain remediation system, particularly since spring 2006 when pumping was initiated at Trenches 1 and 2, has reduced contaminant concentrations and plume mass throughout the floodplain. The estimated percentage of reduction between 1999–2001 and 2011 for the respective contaminant plumes ranges from 40 to 71 percent.
- Monitoring well 618, about 600 ft northeast of Trench 1, showed sulfate and uranium concentrations through 2011 that were about double the concentrations measured at this location in 1999–2001, despite the initiation of groundwater remediation in 2003 and pumping from Trench 1 since 2006. Sulfate and uranium concentrations at the well began decreasing in 2013, apparently in response to continued remediation pumping, but the uranium concentration as of March 2014 remained above the UMTRA MCL of 0.044 mg/L.
- Available data indicate that the apparent increase in concentrations at well 618 probably resulted from a change in sampling technique during 2002 from high-flow, well-purge methods to low-flow sampling near the bottom of the well and continued low-flow sampling through at least 2011.
- Calibration of the floodplainwide groundwater flow model using steady-state and transient simulations indicates that 80 ft/day and 0.25 (dimensionless) are representative values of hydraulic conductivity and specific yield, respectively, for the alluvial aquifer.
- The alluvial aquifer behaves as an unconfined system in response to hydrologic stresses that last for several days or more, such as increases in river elevation and remediation pumping. As a result, groundwater flow patterns in the interior of the floodplain induced by elevated river flows during May and June of each year may persist for multiple weeks after passage of the peak river flow.
- Discharge of contaminated terrace groundwater to the alluvial aquifer might be decreasing with time, but this flow component remains uncertain.
- A study by the ESL revealed that leaching of Mancos Shale by fresh water can produce naturally elevated concentrations of multiple inorganic constituents, notably sulfate, uranium, and nitrate, leading to the possibility that some saline groundwater discharging to the floodplain alluvial aquifer from Mancos Shale is unrelated to historical mill operations at the Shiprock site.
- Elimination of recharge at the mouth of Bob Lee Wash, which is fed by artesian flows from terrace well 648, would greatly reduce the efficacy of the floodplain remediation system. If the artesian flows were terminated, pumping from Trench 1 would no longer capture much of the contaminated groundwater between the trench and Bob Lee Wash, and pumping in the 1089/1104 area would no longer capture much of the contamination located between the Trench 1 and the 1089/1104 areas.

- Installation and operation of two new vertical pumping wells between 700 ft northwest of Trench 1 and the USGS gaging station would intercept contaminated groundwater that, during winter and early spring months, evades capture by the existing remediation pumping. A horizontal well in the same area with length and construction similar to that of the horizontal well in Trench 1 would probably accomplish the same objective, but would likely cost more than the two vertical wells.

11.0 References

Bencala, K.E., M.N. Gooseff, and B.A. Kimball, 2011. "Rethinking hyporheic flow and transient storage to advance understanding of stream-catchment connections," *Water Resources Research*, 47(1): W00H03.

Bencala, K.E., 2011. "Stream-Groundwater Interactions," in *Treatise on Water Science,* Vol. 2, Peter Wilderer (ed.), 537–546.

Boutt, D.F., and B.J. Fleming, 2009. "Implications of anthropogenic river stage fluctuations on mass transport in a valley fill aquifer," *Water Resources Research*, 45(4): W04427.

Cardenas, M.B., J.L. Wilson, and V.A. Zlotnik, 2004. "Impact of heterogeneity, bed forms, and stream curvature on subchannel hyporheic exchange," *Water Resources Research*, 40(8): W08307.

Chow, V.T., 1959. *Open-Channel Hydraulics,* McGraw Hill.

Cirpka, O.A., and S. Attinger, 2003. "Effective dispersion in heterogeneous media under random transient flow conditions," *Water Resources Research*, 39(9): SBH 9-1–9-19.

DOE (U.S. Department of Energy), 1987. *Hydrogeochemical Conditions Within the Floodplain Alluvium, Shiprock Uranium Mill Tailings Site, San Juan County, New Mexico*, UMTRA-DOE/AL, Albuquerque, New Mexico, December.

DOE (U.S. Department of Energy), 1991. *Escarpment Seeps at Shiprock, New Mexico*, UMTRA-DOE/AL 350214.0000.

DOE (U.S. Department of Energy), 1994. *Baseline Risk Assessment of Ground Water Contamination at the Uranium Mill Tailings Site at Shiprock, New Mexico*, DOE/AL/62350-48F, Rev. 1, Albuquerque, New Mexico, January.

DOE (U.S. Department of Energy), 1995a. *Status of the Ground Water Flow Model for the UMTRA Project Shiprock, New Mexico, Site*, DOE/AL/62350-166, Rev. 0, Albuquerque, New Mexico, January.

DOE (U.S. Department of Energy), 1995b. *Site Observational Work Plan for the UMTRA Project Site at Shiprock, New Mexico*, DOE/AL/62350-158, Rev. 0, Albuquerque, New Mexico, July.

DOE (U.S. Department of Energy), 1996. *Geophysical Surveys at the UMTRA Project Shiprock, New Mexico, Site*, DOE/AL/62350-231, Rev. 0, prepared by Geraghty and Miller, Inc. for the U.S. Department of Energy, Albuquerque Operations Office, Albuquerque, New Mexico, March.

DOE (U.S. Department of Energy), 1998. *Work Plan for Characterization Activities at the Shiprock UMTRA Project Site*, MAC-GWSHP 1.8, prepared by the Albuquerque Operations Office.

DOE (U.S. Department of Energy), 2000. *Final Site Observational Work Plan for the Shiprock, New Mexico, UMTRA Project Site*, GJO-2000-169-TAR, Rev. 2, Grand Junction Office, Grand Junction, Colorado, November.

DOE (U.S. Department of Energy), 2002. *Final Ground Water Compliance Action Plan for Remediation at the Shiprock, New Mexico, UMTRA Site*, GJO-2001-297-TAR, Grand Junction Office, Grand Junction, Colorado, September.

DOE (U.S. Department of Energy), 2003a. *Baseline Performance Report for the Shiprock, New Mexico, UMTRA Project Site*, GJO-2003-431-TAC, Grand Junction Office, Grand Junction, Colorado, September.

DOE (U.S. Department of Energy), 2003b. *Semiannual Performance Report, February 2003 through August 2003 for the Shiprock, New Mexico, UMTRA Project Site*, GJO-2003-490-TAC, GJO-GWSHP 13.2, Grand Junction Office, Grand Junction, Colorado, September.

DOE (U.S. Department of Energy), 2004. *Semiannual Performance Report, September 2003 through March 2004 for the Shiprock, New Mexico, UMTRA Project Site*, DOE-LM/GJ725-2004, Office of Legacy Management, Grand Junction, Colorado, September.

DOE (U.S. Department of Energy), 2005a. *Annual Performance Report, April 2004 Through March 2005 for the Shiprock, New Mexico, Site*, DOE-LM/GJ933-2005, Office of Legacy Management, Grand Junction, Colorado, July.

DOE (U.S. Department of Energy), 2005b. *Refinement of Conceptual Model and Recommendations for Improving Remediation Efficiency at the Shiprock, New Mexico, Site*, GJO-2004-579-TAC, Office of Legacy Management, Grand Junction, Colorado, July.

DOE (U.S. Department of Energy), 2006. *Annual Performance Report, April 2005 Through March 2006 for the Shiprock, New Mexico, Site*, DOE-LM/GJ1212-2006, Office of Legacy Management, Grand Junction, Colorado, July.

DOE (U.S. Department of Energy), 2007. *Annual Performance Report, April 2006 Through March 2007 for the Shiprock, New Mexico, Site*, DOE-LM/1461-2007, Office of Legacy Management, Grand Junction, Colorado, June.

DOE (U.S. Department of Energy), 2008. *Annual Performance Report, April 2007 Through March 2008 for the Shiprock, New Mexico, Site*, LMS/SHP/S04378, Office of Legacy Management, Grand Junction, Colorado, September.

DOE (U.S. Department of Energy), 2009a. *Annual Performance Report, April 2008 Through March 2009 for the Shiprock, New Mexico, Site*, LMS/SHP/S05575, Office of Legacy Management, Grand Junction, Colorado, September.

DOE (U.S. Department of Energy), 2009b. *Evaluation of the Trench 2 Groundwater Remediation System at the Shiprock, New Mexico, Legacy Management Site*, LMS/SHP/S05037, Office of Legacy Management, Grand Junction, Colorado, March.

DOE (U.S. Department of Energy), 2010. *Annual Performance Report, April 2009 Through March 2010 for the Shiprock, New Mexico, Site,* LMS/SHP/S06815, Office of Legacy Management, Grand Junction, Colorado, September.

DOE (U.S. Department of Energy), 2011. *Preliminary Evaluation of the Trench 1 Collection Drain, Floodplain Area of the Shiprock, New Mexico, Site*, LMS/SHP/S07374, June.

DOE (U.S. Department of Energy), 2012. *Annual Performance Report, April 2010 Through March 2011 for the Shiprock, New Mexico, Site,* LMS/SHP/S07834, Office of Legacy Management, Grand Junction, Colorado, January.

DOE (U.S. Department of Energy), 2013. *Annual Performance Report, April 2012 Through March 2013 for the Shiprock, New Mexico, Site,* LMS/SHP/S10301, Office of Legacy Management, Grand Junction, Colorado, November.

DOE (U.S. Department of Energy), 2014a. *Technical Task Plan, Variation in Groundwater Aquifers*, TTP No. 2014-001, June.

DOE (U.S. Department of Energy), 2014b. *Annual Performance Report, April 2013 Through March 2014, for the Shiprock, New Mexico, Site,* LMS/SHP/S12021, Office of Legacy Management, Grand Junction, Colorado, October.

DOE (U.S. Department of Energy), 2015a. "Second Five-Year Plan to Address Uranium Contamination in the Navajo Nation," *Office of Legacy Management (LM) Program Update, January–March 2015.*

DOE (U.S. Department of Energy), 2015b. *Applied Studies & Technology – Variation in Groundwater Aquifers: Results of 2013–2014 Phase I Field Investigations-Final Draft*, LMS/ESL/S 12811, ESL-RPT-2015-02, September.

Doherty, J.E., M.N. Fienen, and R.J. Hunt, 2010. *Approaches to Highly Parameterized Inversion: Pilot-Point Theory, Guidelines, and Research Directions,* U.S. Geological Survey, Scientific Investigations Report 2010-5168.

Doherty, J.E., and R.J. Hunt, 2010. *Approaches to Highly Parameterized Inversion: A Guide to Using PEST for Groundwater-Model Calibration,* U.S. Geological Survey, Scientific Investigations Report 2010-5169.

Domenico, P.A., and F.W. Schwartz, 1998. *Physical and Chemical Hydrogeology*, John Wiley and Sons, Inc., New York.

Driscoll, F.G., 1989. *Groundwater and Wells*, 2nd ed., Johnson Filtration Systems, Inc., St. Paul, Minnesota.

ESI (Environmental Simulations, Inc.), 2001. *Guide to Using Groundwater Vistas,* Version 4, Herndon, Virginia.

ESL (Environmental Sciences Laboratory), 2011a. *Natural Contamination from the Mancos Shale*, LMS/S07480, ESL-RPT-2011-01, prepared for the U.S. Department of Energy Office of Legacy Management, Grand Junction, Colorado, April.

ESL (Environmental Sciences Laboratory), 2011b. *Preliminary Evaluation of the Trench 1 Collection Drain, Floodplain Area of the Shiprock, New Mexico, Site,* LMS/SHP/S07374, ESL-RPT-2011-03, prepared for the U.S. Department of Energy Office of Legacy Management, Grand Junction, Colorado, April.

ESL (Environmental Sciences Laboratory), 2012. *Multivariate Statistical Analysis of Water Chemistry in Evaluating the Origin of Contamination in Many Devils Wash, Shiprock, New Mexico,* LMS/SHP/S09257, ESL-RPT-2012-03, prepared for the U.S. Department of Energy Office of Legacy Management, Grand Junction, Colorado, December.

Fleckenstein, J.H., R.G. Niswonger, and G.E. Fogg, 2006. "River-Aquifer Interactions, Geologic Heterogeneity, and Low-Flow Management," *Ground Water*, 44(6): 837–852.

Freeze, R.A., and J.A. Cherry, 1979. *Groundwater*, Prentice-Hall Inc., Englewood Cliffs, New Jersey.

Goode, D.J., and L.F. Konikow, 2000. "Apparent dispersion in transient groundwater flow," *Water Resources Research*, 26(10): 2339–2351.

Harbaugh, A.W., and M.G. McDonald, 1996. *User's Documentation for MODFLOW-96, an Update to the U.S. Geological Survey Modular Finite-Difference Ground-Water Flow Model*, U.S. Geological Survey Open-File Report 96-485.

Harvey, J.W., and B.J. Wagner, 2000. "Quantifying Hydrologic Interactions Between Streams and their Subsurface Hyporheic Zones," Chapter 1 in *Streams and Ground Waters,* J.B. Jones and P.J. Mulholland, eds., Academic Press, San Diego, California.

Henry, E.J., 1995. *Groundwater modeling of gradient manipulation and barrier location for remediation at a Uranium Mill Tailings Remedial Action (UMTRA) site,* Master's Thesis, University of New Mexico, Albuquerque.

Huff, G.F., 2004. *Simulation of Ground-Water Flow in the Basin-Fill Aquifer of the Tularosa Basin, South-Central New Mexico, Predevelopment through 2040*, U.S. Geological Survey Scientific Investigations Report 2004-5197.

Huntington, J.L., and R.G. Niswonger, 2012. "Role of surface-water and groundwater interactions on projected summertime streamflow in snow dominated regions: An integrated modeling approach," *Water Resources Research*, 48: W11524.

Kennedy, E.J., 1984. "Discharge Ratings at Gaging Stations," Chapter A10 in *Techniques of Water Resources Investigations of the United States Geological Survey*, Book 3, *Applications of Hydraulics*, U.S. Geological Survey.

Knight Piesold (Knight Piesold and Company), 2002. *Results of Groundwater Modeling, Shiprock UMTRA Site,* prepared for the Navajo Nation, Navajo AML/UMTRA Department, Window Rock, Arizona, February.

McCutcheon, S.C., J.L. Martin, and T.O. Barnwell, Jr., 1992. "Water Quality," Chapter 11 in *Handbook of Hydrology*, D.R. Maidment, Editor in Chief, McGraw Hill, Inc.

McKenna, S.A., and A. Wahi, 2006. "Local Hydraulic Gradient Estimator Analysis of Long-Term Monitoring Networks," *Ground Water*, 44(5): 723–731.

Mosley, M.P., and A.I. McKerchar, 1992. "Streamflow," Chapter 8 in *Handbook of Hydrology*, D.R. Maidment, Editor in Chief, McGraw Hill, Inc.

Newsom, J.M., and J.L. Wilson, 1988. "Flow of Ground Water to a Well near a Stream—Effect of Ambient Ground-Water Flow Direction," *Ground Water*, 26(6): 703–711.

Packman, A.I., and K.E. Bencala, 2000. "Modeling Surface-Subsurface Hydrological Interactions," Chapter 2 in *Streams and Ground Water,* J.B. Jones and P.J. Mulholland, eds., Academic Press.

Pollock, D.W., 1989. *Documentation of Computer Programs to Compute and Display Pathlines Using Results from the U.S. Geological Survey Modular Three-Dimensional Finite-Difference Ground-Water Flow Model,* U.S. Geological Survey Open File Report 89-391.

Stonestrom, D.A., and J. Constantz, 2003. *Heat as a Tool for Studying the Movement of Ground Water near Streams*, U.S. Geological Survey Circular 1260.

Tsosie, B.B., 1997. *Hydrogeologic Characterization of the Floodplain That Lies Below the Uranium Mill Tailings Remedial Action Site at Shiprock, New Mexico*, Master's Thesis, New Mexico Institute of Mining and Technology, Socorro, New Mexico.

USPHS (U.S. Public Health Service), 1962. *Stream Surveys in Vicinity of Uranium Mills, IV, Area of Shiprock, New Mexico, November 1960*, U.S. Department of Health, Education, and Welfare, Denver, December.

USPHS (U.S. Public Health Service), 1963. *Shiprock, New Mexico Uranium Mill Accident of August 22, 1960*, U.S. Department of Health, Education, and Welfare, Denver, January.

Wilson, J.L., and W.R. Linderfelt, 1991. *Groundwater Quality in Pumping Wells Located near Surface Water Bodies*, New Mexico Water Resources Research Institute, Technical Completion Report No. 261.

Winter, T.C., J.W. Harvey, O.L. Franke, and W.M. Alley, 1998. *Ground Water and Surface Water, a Single Resource*, U.S. Geological Survey Circular 1139.

Zhang, H., and F.W. Schwartz, 1995. "Multispecies contaminant plumes in variable density flow systems," *Water Resources Research*, 31(4), 837–847.

This page intentionally left blank